MONTANUNIVERSITÄT LEOBEN

MASTER THESIS

Hydrochemical Characterisation of Groundwater Systems in Upper Austria

Author:
Irene Hartl, BSc.

Supervisor:
Assoz. Prof. Dipl.-Ing. Dr. mont.
Doris Groß

A thesis submitted in fulfillment of the requirements
for the degree of Diplomingenieur

at the

Chair of Petroleum Geology
Department Applied Geosciences and Geophysics

September 16, 2018

Declaration of Authorship

I declare in lieu of oath, that I wrote this thesis and performed the associated research myself, using only literature cited in this volume.

Signed:

_____

Irene Hartl, BSc.

Abstract

The North Alpine Foreland Basin in Upper Austria holds a manifold geogene potential. Shallow sedimentary aquifers are used for water supply, whereas Jurassic Carbonates (Malm) and Oligocene Linz Sands bear thermal waters utilised as a source of energy and for balneological purposes. Additionally, hydrocarbons are recovered from different stratigraphic horizons and gases are stored, respectively. In order to characterise different aquifers in this region and to identify zones of potential mixing between deep geothermal and shallow meteoric groundwater, water samples from different aquifers were investigated. The analytical programme consisted of measurements of the hydrochemical composition, the stable isotopic composition of the water, an investigation of the gas content coupled with a determination of the isotopic signature of these gases. Moreover, ^{14}C and ^{13}C contents of selected water samples were measured. In total, 32 waters were sampled from two springs and one well in the Bohemian Massif, Quaternary deposits (2 samples), Ottnangian sediments south of the Bohemian Massif outcrop (Ottnangian Sandstone: 10 samples; Ottnangian Schlier: 6 samples; Atzbach Sands: 3 samples), Linz Sands (4 samples), Rupelian Sands (1 sample) and from Malmian Carbonates (3 samples).

Based on the measured parameters, the water samples can be categorised into four different groups: Group I contains waters from the Bohemian Massif and one sample from the Atzbach Sands which is characterised by a low mineralisation and presumably recharged from the Bohemian Massif. The total mineralisation of the Ca-Mg-HCO_3-type waters ranges between 55-222 mg/l. The samples summarised in Group II are of the same type as Group I, however, their amount of total dissolved solids is increased (204-507 mg/l). Variations in the measured ion contents of this group are probably caused by facial differences and anthropogenic influences. The samples of Group III are characterised by cation exchange and assigned as Na-HCO_3-type. The dissolved mineral content ranges between 395-436 mg/l, similar to the waters of Group II. The samples from Group III show higher water temperatures and lower contents in ^{14}C, though. Moreover, stable isotope measurements imply an entry into the aquifer during a glacial period. These characteristics could indicate a mixture with Malmian thermal water. The ion concentration of Na-HCO_3-(Cl) waters assigned to Group IV varies between 961-1409 mg/l (Malm) and 526-648 mg/l (Linz Sands, Rupelian), respectively. One water sample of this group originates from a shallow well in Andorf. The stable isotope values of the waters suggest a Pleistocene infiltration into the aquifer. The observed mixture with thermal waters in Andorf shows that the existing thermal aquifer model needs to be revised.

The analysed gas samples contain traces of methane in the Innviertel Group (Group II

and III) and Linz Sands (Group III). The thermal water samples and the water in Andorf are characterised by significantly higher amounts of methane (Group IV). Additionally, higher hydrocarbons were detected in four water samples. The isotopic signatures suggest a biogenic origin of the methane of shallow strata whereas the Malmian gases are composed of a mixture between thermogenic and biogenic natural gas. Upper Austria as well as Bavaria could serve as provenance areas for these thermogenic hydrocarbons.

Zusammenfassung

Das Nordalpine Vorlandbecken in Oberösterreich birgt ein vielfältiges geogenes Potential. Seichtliegende Aquifere werden für die Grundwasserversorgung genutzt, während jurassische Karbonate (Malm) und die oligozänen Linzer Sande Thermalwasser für Energiegewinnung und Badezwecke beinhalten. Zudem werden aus verschiedenen stratigraphischen Horizonten Kohlenwasserstoffe gefördert bzw. Gase gespeichert. Um nun Wässer verschiedener Aquifere in dieser Region zu charakterisieren und auch Mischungsprozesse zwischen tiefen Thermalwässern und seichten meteorischen Wässern zu erkennen, wurden Wasserproben aus unterschiedlichen Aquiferen in Oberösterreich genommen und untersucht. Das Analyseprogramm umfasste die Messung der hydrochemischen Zusammensetzung, der stabilen Isotope des Wassers, eine Gasanalyse und die Bestimmung der Gasisotopien. Darüber hinaus wurden Messungen der ^{14}C und ^{13}C Gehalte ausgewählter Brunnen vorgenommen. Die 32 Wasserproben stammen aus zwei Quellen und einem Brunnen der Böhmischen Masse, aus quartären Ablagerungen (2 Proben), aus Sedimenten des Ottnangs südlich des Ausbisses der Böhmischen Masse (Ottnang Sandsteine: 10 Proben; Ottnang Schlier: 6 Proben; Atzbach Sande: 3 Proben), aus den Linzer Sanden (4 Proben), dem Rupel (1 Probe) sowie den Malmkarbonaten (3 Proben).
Die Messergebnisse zeigen, dass sich die untersuchten Wässer in vier verschiedene Gruppen einteilen lassen: Gruppe I beinhaltet Wässer der Böhmischen Masse und eine gering mineralisierte Probe der Atzbacher Sande, die vermutlich aus der Böhmischen Masse gespeist wird. Die Gesamtmineralisation dieser Ca-Mg-HCO_3 Wässer beträgt 55-222 mg/l. Vom selben Typus sind auch die Wässer der Gruppe II, jedoch sind sie durch einen höheren Gehalt an gelösten Stoffen gekennzeichnet (204-507 mg/l). Variationen der untersuchten Ionen sind in dieser Gruppe wahrscheinlich auf fazielle Unterschiede und anthropogene Einflüsse zurückzuführen. Die Wässer der Gruppe III sind durch Kationenaustausch gekennzeichnet und gehören dem Na-HCO_3-Typ an. Ihre Gesamtmineralisation beträgt, ähnlich wie in Gruppe II, 395-436 mg/l, allerdings zeigen die Proben der Gruppe III teilweise erhöhte Temperaturen und geringe Gehalte an ^{14}C an. Zusätzlich legen die stabilen Isotope ein kaltzeitliches Bildungsalter nahe. Diese Indizien könnten auf eine Beimischung von Thermalwasser aus dem Malm hindeuten. Die Ionenkonzentrationen der Na-HCO3-(Cl) Wässer aus Gruppe IV liegen zwischen 961-1409 mg/l (Malm) bzw. 526-648 mg/l (Linzer Sande, Rupel). Eine Probe dieser Gruppe stammt aus einer seichten Bohrung in Andorf. Die stabilen Isotope des Wassers dieser Proben legen eine pleistozäne Infiltration in den Aquifer nahe. Die Beimischung von Thermalwasser in Andorf zeigt, dass das bestehende Strömungsmodell des Thermalwasserkörpers einer Revision unterzogen werden muss.

Die analysierten Gasproben zeigen Spuren von Methan in der Innviertler Serie (Gruppe II und III) und den Linzer Sanden (Gruppe III). Die Proben der Geothermiebohrungen und aus Andorf weisen deutlich erhöhte Methangehalte auf (Gruppe IV). Zusätzlich wurden in vier Proben auch Spuren höherer Kohlenwasserstoffe entdeckt. Die Isotopenzusammensetzung dieser Gase lässt auf einen rein biogenen Ursprung des Methans in den seichteren Formationen schließen, während die Gase des Malm aus einer Mischung von thermischem und biogenem Gas bestehen. Als Herkunftsgebiet dieser thermischen Kohlenwasserstoffe kommen Oberösterreich, aber auch das benachbarte Bayern in Frage.

Acknowledgements

First of all, I would like to thank my parents, Johann and Helga, for enabling me my whole education and their support and patience during all this time.
I would also like to express my gratitude to Univ.-Prof. Mag. rer. nat. Dr. mont Reinhard Sachsenhofer and assoz. Prof. Dipl.-Ing. Dr. mont. Doris Groß for the opportunity to write this thesis and their guidance and help during the whole process. I am thankful for the helping hands whenever needed and advice in many different aspects of this topic.
Lukasz Pytlak was also a very important person for this thesis. Thank you for showing me all the laboratory devices and steps for a correct sample treatment and investigation in the laboratory and for the good company during all the field trips. I would also like to thank Dipl.-Ing. Christian Benold and Leopold Pöppel for their company and assistance in the field and for investigating the samples in their laboratory at the Geological Survey of Austria together with Hofrat Mag. Dr. Gerhard Hobiger. Ao. Univ.-Prof. Dr. phil. Walter Prohaska, who did the ICP measurements for Iodide and Bromide has to be mentioned here as well. Thank you for your assistance and contribution to the success of this project!
Thank you to Dr. Florian Eichinger for giving me the opportunity to visit the laboratories of Hydroisotop GmbH to get to know the analysing and sampling procedure of water samples, especially geothermal water samples. I would also like to mention Dr. Stefan Wechner, Johanna Gandorfer and Martin Niedermeier, they made me feel like part of the team for my entire stay and were willing to share all their experience and knowledge with me.
I am very grateful to all the private people, municipal employees, mayors and operators of the geothermal plants in Upper Austria for their help and time in order to take all the samples for this thesis. Without the assistance and cooperation of all these people, this whole project would not have been possible. Therefore, thank you for your time, patience and support!
A special thank you goes to the team of the Chair of Petroleum Geology. I enjoyed my time at this chair while working on my thesis very much. You all made me feel like part of a family and I would like to say thank you for a few very nice months, full of scientific and non-scientific conversations, very entertaining coffee and lunch breaks and good advice for many different situations.
Last, I would like to thank Thomas Schifko for his endless patience and putting up with all of my moods. You were a very important support for me during all this time and therefore I am very thankful.

πάντα ῥεῖ - Heraclitus

Contents

List of Figures

List of Tables

List of Symbols

K_H	Henry's constant	atm/mol
P_{Gas}	Partial pressure of gas	atm
χ_{Gas}	Quantity of gas	mol
C_{total}	Total aqueous gas concentration of Headspace sample	mg/l
C_{HS}	Aqueous gas concentration in headspace after equilibration	mg/l
C_W	Aqueous gas concentration in water after equilibration	mg/l
V_{total}	Sample volume	l
V_{HS}	Headspace volume	l
C_{GC}	Measured gas concentration (Gas Chromatograph)	ppmv $* 10^6$
MW	Molecular weight of gas	g/mol
T_{sample}	Temperature of Headspace sample	°C
δ^{13}C	Deviation of ^{13}C concentration compared to standard	‰
δD	Deviation of D/^{2}H concentration compared to standard	‰
δ^{18}O	Deviation of ^{18}O concentration compared to standard	‰

1 Introduction and Motivation

The North Alpine Foreland Basin (NAFB) forms an intensively used area for hydrocarbon production and for gas storage. Deep groundwaters in the Upper Jurassic (Malm) aquifer and in deeper sections of the Oligocene Linz-Melk Formation are utilized for energetic and balneological use. Furthermore, deep groundwaters tapped by wells with a depth of up to 500 m are used for drinking water purposes in municipal and private supplies. Hydrocarbons have been recovered (partly from the same formations) in the NAFB for decades (e.g. Reischenbacher and Sachsenhofer, 2011). In order to allow a juxtaposition of the individual interests and to secure a sustainable usage of the basin´s resources, detailed knowledge of the basin structure, its hydrogeological units and the interactions of the different systems within, is essential.

Several hydrostratigraphic units can be defined in Upper Austria. Those units differ in their chemical and isotopic composition (Andrews et al., 1985; Goldbrunner, 1984). However, it is assumed that these hydrostratigraphic units are not strictly separated but subjected to mixing processes. The aim of this thesis is to obtain more information about the interaction of these hydrostratigraphic units, especially the mixing of thermal water with water from shallower aquifers. Therefore, 32 samples from different aquifers, ranging from springs to thermal wells, were collected and analysed. The resulting chemical and physical properties of these samples are used to characterise the investigated aquifers and identify possible mixtures of these waters. Moreover, the free and dissolved gases of the water samples were analysed to supplement the hydrochemical results. The base of these measurements is, that the hydrocarbon deposits in Upper Austria have experienced various alteration processes, e.g. biodegradation or water washing (e.g. Pytlak et al., 2017; Pytlak et al., 2016b). Water washing is a process which transfers light aromatic, water-soluble components, e.g. benzene, toluene, ethylbenzenes and xylenes (summarised as BTEX) into the water enabling their transport with water currents in the subsurface (Lafargue and Barker, 1988). The composition of the associated gases could give more information about the interaction between the hydrostratigraphic and the petroleum system in the area of investigation.

Fig. 1.1 shows a map with the sampling locations, accompanied by a small inset of Upper Austria and its main geologic units, where the sampling area is framed in red. The main geologic groups present in this area are the Bohemian Massin and the Alpine Foreland Basin.

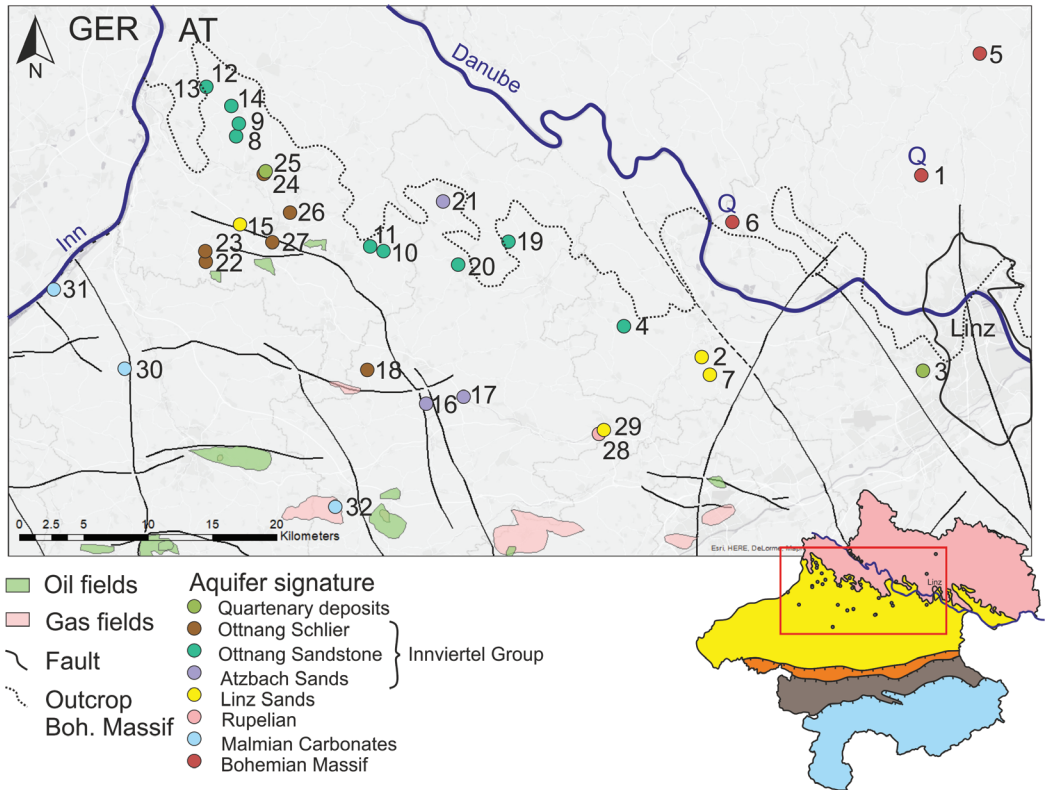

FIGURE 1.1: Investigation area with sampling locations (coloured by aquifer) and oil and gas fields in this area (marked in green and pink); The bottom inset shows a simplified geological map of Upper Austria with the sample points and the investigation area framed in red. The geological units are (in north-south direction): Bohemian Massif (pink), Molasse Zone (yellow), Imbricated Molasse (orange), Flysch and Helvetic (brown) and Northern Calcareous Alps (blue).

2 Geological Overview

2.1 Bohemian Massif

The Bohemian Massif is located in the northern part of Upper and Lower Austria. It acts as a basement of the Alpine Foreland Basin and is divided into the Moldanubian and the Moravian units which are intersected by granitic intrusions, summarised as the South-Bohemian Plutonite. The Moldanubian and Moravian units are characterised by the appearance of gneisses, quartzites, mica schists, phyllites and marbles (Fuchs and Matura, 1976). The sampling locations of the samples 1, 5 and 6 are situated within the Weinsberg granite, a subdivision of the Bavarian unit, which forms a part of the South-Bohemian Plutonite. Due to the intrusion of neighbouring granite bodies, the formation became subjected to contact metamorphism. Therefore, paragneisses can be encountered along with the granites (Fuchs and Matura, 1980).
The Bohemian Massif is intersected by numerous faults which are oriented in northwest-southeast and northeast-southwest direction. One of them, the northeast-southwest oriented, sinistral "Rodl Fault" (Fuchs and Matura, 1980), is located to the west of the sampling point no. 1. The sampling point no. 5 is situated in the vicinity of this fault.

2.2 Alpine Foreland Basin

The Alpine Foreland Basin in Austria overlies the southern part of the Bohemian Massif and extends to the imbricated sediments and Helvetic nappes of the Alpine orogen (Fig. 1.1). It is characterised by an increase of sediment thickness towards the south. Post-variscian Paleozoic and Mesozoic sediments, which form the lowermost strata of the basin are overlain by alpidic molasse sediments of Cenozoic age (Wessely, 2006). A stratigraphic chart of the basin infill is visible in Fig. 2.1, Fig. 2.2 shows the variation of the observed formations in Upper Austria and Fig. 2.3 shows a north-south cross-section through the basin.

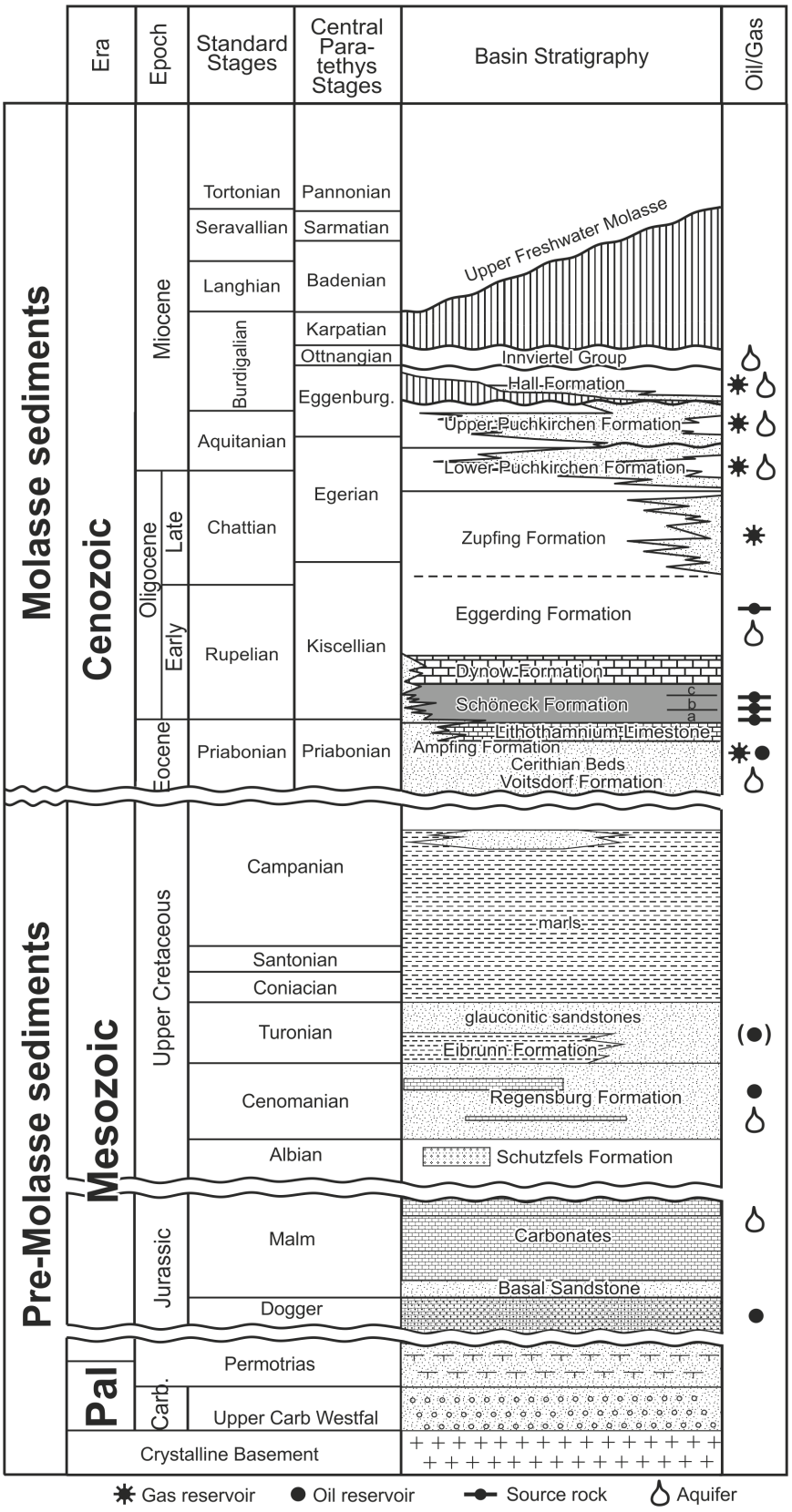

FIGURE 2.1: Stratigraphic chart of the Pre-Molasse and Molasse Strata of the Alpine Foreland Basin in Upper Austria (modified after Wagner, 1996; Andrews et al., 1985; Groß et al., 2015; Pytlak et al., 2017)

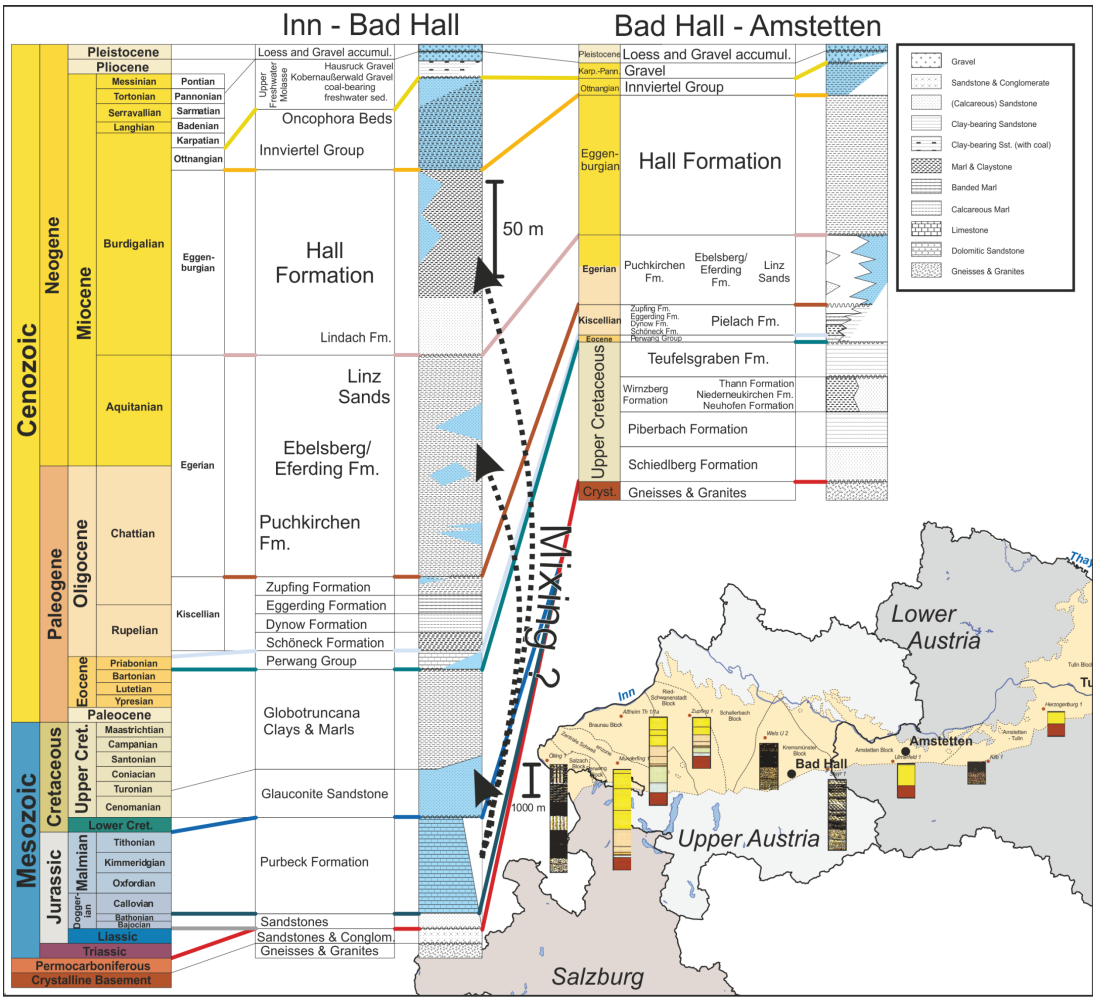

FIGURE 2.2: Stratigraphic chart of the formations occurring in the Upper Austrian part of the Alpine Foreland Basin and their regional extent (modified after Pfleiderer et al., 2016), aquifers are coloured in light blue, the arrows indicate possible mixing processes between the Malmian aquifer and aquifer on the hanging wall of this formation

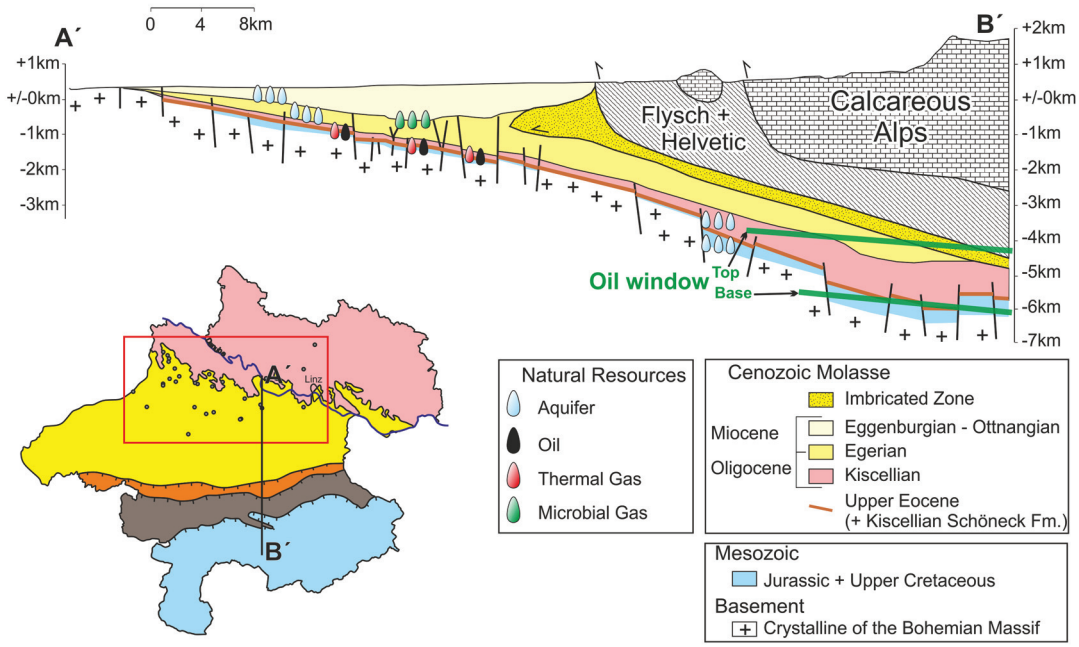

FIGURE 2.3: Cross-section through the Alpine Foreland Basin (modified after Wagner, 1996; Pytlak, 2017, the top and bottom of the oil window are marked in green, occurrences of natural resources (water, oil, thermal and microbial gas) are marked as drops in different colours

2.2.1 Pre-Molasse Strata

The lowermost strata deposited in the Pre-Molasse stage of the NAFB consist of quartz-arenites and dark shale layers with thin coal layers of Carboniferous age. They are overlain by Permian metadiabase and volcanoclastics. The Paleozoic sediments only appear in narrow Graben structures in the southwestern margin of the Central Swell Zone (Fig. 3.1).

During the Mesozoic and Eocene, sediment deposition mainly occurred in a passive continental margin setting of the northern Tethyan shelf adjacent to the Bohemian Massif and was therefore controlled by the prevailing tropical, shallow marine conditions (Wagner, 1998; Grunert, 2011; Bachmann et al., 1987; Wagner, 1996; Groß et al., 2018). The Jurassic sediments comprise of Doggerian sandstones, their depositional environment ranges from braided fluvial to shallow marine. Coal seams can be found within these sandstones. The siliciclastics are overlain by carbonates of Malmian to lower Cretaceous age. They are characterised by a facies transition from deep to shallow marine environment from the southwest towards the north (Nachtmann and Wagner, 1987; Wagner, 1996). The boundary between the Jurassic carbonates and the late Cretaceous deposits is marked by an unconformity. The early Cretaceous is characterised by a phase of uplift and erosion in Upper Austria, which lead to a karstification of the carbonates. In the northeastern part of the Alpine Foreland Basin, the karst crevasses are filled with light-grey to white, fluvial, coarse-grained sandstones. This infill is called "Schutzfels Beds". Towards the southwest, a major Cenomanian transgressional phase approaching from this direction

led to the deposition of a shallow marine sediment succession (Groß et al., 2018; Nachtmann and Wagner, 1987). The base of this succession is comprised of coal-bearing marls (Wagner, 1996) rapidly transitioning to shallow marine, storm-dominated, glauconitic sandstones (Groß et al., 2018; Nachtmann and Wagner, 1987; Regensburg Formation according to Niebuhr et al., 2009). These depositions directly overlie the carbonates in this area (Nachtmann and Wagner, 1987). In between the fluvial and shallow marine sediments, a narrow northwest-southeast directed zone of immature beachsands, running nearly parallel to the erosional rim of the Jurassic carbonates, can be encountered (Wagner, 1996). The sedimentary succession is conformably continued by early Turonian marls formed in deeper-water conditions due to continuous subsidence (Groß et al., 2018) in the lower and glauconite-bearing storm deposits in the upper section. At the late Turonian stage, the deposition mainly consists of mudstones again. During the late Campanian, approximately 300 m thick sandstones cover the basin northwest of the Central Swell Zone shaling out towards the southwest. However, a subsequent uplift caused an erosion of these Mesozoic strata on paleogeographic highs, affecting the southern margin of the Bohemian Massif and the Central Swell Zone (Wagner, 1996).

2.2.2 Molasse Strata

The deposition of the alpine Molasse sediments starts in the Eocene, after a phase of basin inversion during the late Cretaceous and Paleocene resulting in an erosional phase marked by an unconformity. This natural interface separates the Molasse from the Pre-Molasse strata. Eocene fluvial to shallow marine transgressive siliciclastics form the lowermost section of the Molasse sediments, followed by Lithothamnium limestone (Nachtmann and Wagner, 1987).
At the beginning of the Oligocene, a deepening and widening of the Molasse Basin (Sissingh, 1997) led to the deposition of deep-water sediments, rich in organic compounds. These organic-rich marls and shales, known as the Schöneck Formation, serve as the main source rock for the oil and thermal gas deposits within the basin. They are overlain by the Dynow, Eggerding and Zupfing formations, which are comprised of marls with intercalated limestone layers, pelites with sandstone occurrences towards the northern basin margin and dark grey hemipelagites with integrated layers of gravitational mass movements i.e. slumpings and turbidites (Sachsenhofer and Schulz, 2006). The Eggerding Formation is characterised by an average thickness of 35-45 m (Groß et al., 2018). However, during the deposition of this formation, periodically occurring north-south oriented, submarine mass movements caused a relocation of the sedimentary material coupled with an erosion of lower Oligocene strata. Therefore, the thickness of Oligocene strata is significantly reduced in parts of the basin (Sachsenhofer and Schulz, 2006; Sachsenhofer et al., 2010; Groß et al., 2018). The reworked material, gathered at the southern basin slope is summarised under the term "Oberhofen facies" (Sachsenhofer and Schulz, 2006).
Towards the hanging wall of the basin fill, the deep marine sedimentary succession is

continued by the Lower and Upper Puchkirchen formations and the basal Hall Formation, which were deposited during late Oligocene to early Miocene (Fig. 2.1). The deposition of those formations and their sediment distribution is mainly controlled by a deep marine channel system, which is located close to the Alpine thrust front (de Ruig, 2003). The sediment stratification along this eastward propagating sinuous channel system is impacted by its depositional environments. Conglomerates and sandstones are found within the main channel, whereas the overbank strata holds fine-grained material as silt- and mudstones. The sediment supply is controlled by debris and slurry flows from the Bavarian region, west to northwest of the Austrian part of the Molasse Basin (e.g. de Ruig and Hubbard, 2006; Bernhardt et al., 2012). A time equivalent to the Puchkirchen Channel sediments are well-sorted, aeolian sandstones, the so-called Linz and Melk Sands, which were deposited at the northern edge of the Upper Austrian Molasse Basin (Fig. 2.2; Wagner, 1998; Kuhlemann and Kempf, 2002). Their provenance area is, as opposed to the Puchkirchen silicilastics, located in the Bohemian Massif (Roetzel et al., 1983). Between the Linz and Melk sandstones in the north and the Puchkirchen strata, further contemporaneous deposits, the Ebelsberg and Eferding formations, can be found (Fig. 2.2). They are mainly composed of pelitic sediments which are partly bituminous and non-calcareous and occasionally bear fish remnants (Wagner, 1998).

The Eggenburgian basal Hall Formation, holding greenish-grey marls and micaceous pelites with layers of sandstone and conglomerates, is separated from the Puchkirchen units by unconformities, a result of submarine erosions and sediment relocations (Wagner, 1998; Grunert et al., 2013). Sub- and intertidal shallow marine sediments (Fig. 2.4) were deposited during Ottnangian times. The occurring formations are composed of glauconite-bearing silt- and sandstones. In the central part of the Molasse Basin, these formations are summarised under the term Innviertel Group (Wagner, 1998). Fig. 2.5 shows a detailed stratigraphic chart of the Ottnangian subdivision. The "Robulus Schlier" formation is characterised by its abundance in the eastern and central Molasse Basin. These micaceous pelites can be seen as a facial continuation of the Hall Formation due to their similar properties. Towards the west of Upper Austria, these pelites become interspersed with sand layers (Vöckla Beds). A similar trend can be observed towards the hanging wall of these beds. The Atzbach Sands are fine- to medium-grained glauconitic sandstones with frequently occurring coarser layers. The depositional environment of this up to 100 m thick formation is interpreted as intertidal shallow-marine (Faupl and Roetzel, 1987; Schubert, 2015). The Ottnang Schlier is located above the Atzbach Sands (Fig. 2.5). This formation consists of clayey marls with thin sandstone layers. Towards the northern basin margin, the Ottnang Schlier interfingers with the Enzenkirchen, Phosphorite and Fossil-rich Coarse Sands, which are, again, mainly composed of quartz-rich, glauconitic sandstones with reworked Phosphorite nodules. The transition between the Ried Beds and the "Rotalienschlier" is defined by the occurrence of the foraminifera "Rotalia". The only litological difference which can be observed between those formations is a slight increase in interspersed sandstone layers from north to south. The uppermost shallow-marine sediments are summarised as Glauconitic Series. The sediments of

this series share similar characteristics in comparison to the footwall formations of the Innviertel Group. The description of the individual sand bodies refer to their local abundance. The Sand and Gravel Group (Wachtberg Formation after Schubert, 2015; Wagner, 1998) is comprised of detrital material from the Paleo-Salzach and mainly restricted to the south-western part of the Ottnangian Strata. The Oncophora Formation on top of the marine sediment is characterised by the occurrence of the eponymous mollusk indicating a brackish environment (Schubert, 2015). Therefore, this formation marks the transition from shallow marine over brackish to terrestrial conditions (Kuhlemann and Kempf, 2002). This marine regression causes an exposure of the sedimentary deposits leading to weathering of these strata. The remaining unconformity marks the boundary between the Innviertel Group and the Upper Freshwater Molasse (Schubert, 2015). Within the terrestrial fluviatile sediments, coal seams can be found (Wagner, 1998).

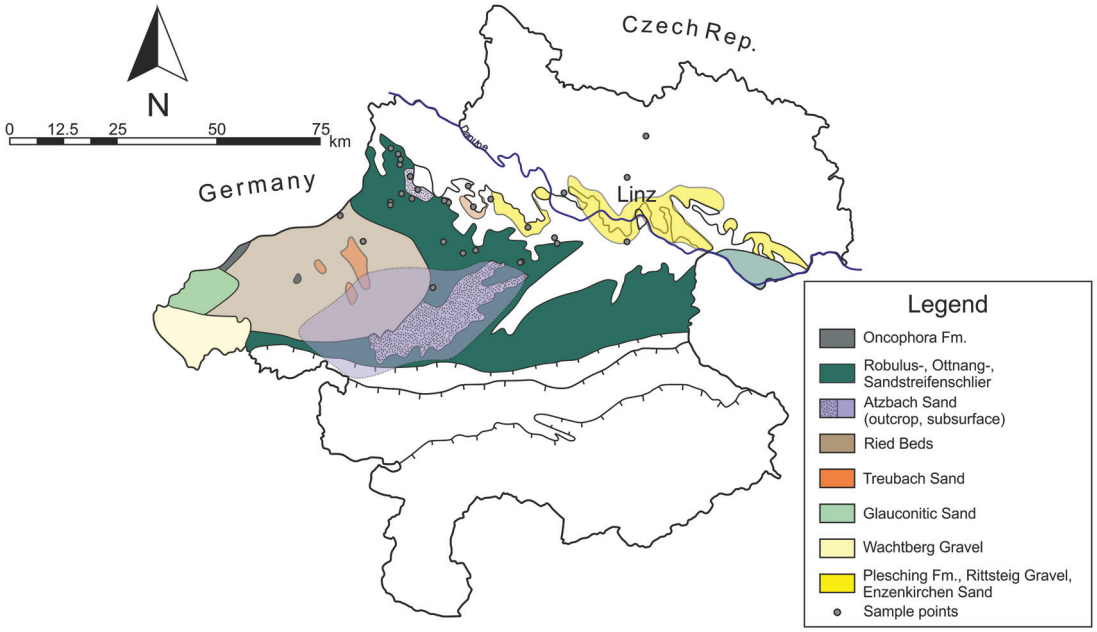

FIGURE 2.4: Occurrence and extent of Ottnangian formations (modified after Wagner, 1998)

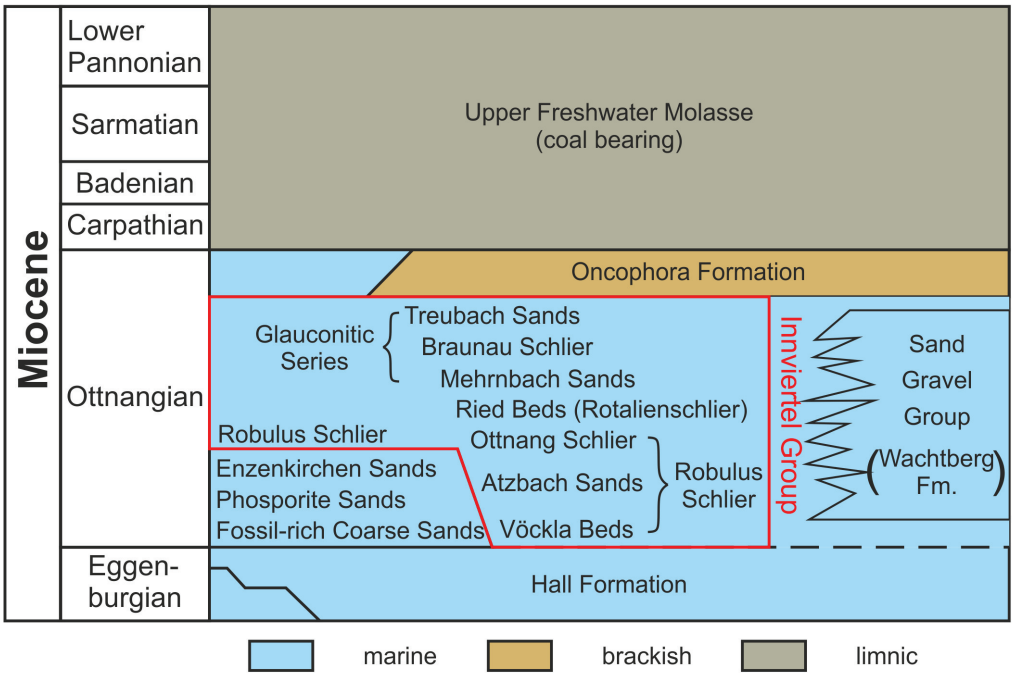

FIGURE 2.5: Stratigraphic chart of the Miocene Molasse strata (modified after Faupl and Roetzel, 1987 and Lengauer et al., 1987); the Ottnangian formations (framed in red) in the central part of the basin are summarized as Innviertel Group

2.2.3 Tectonic Evolution

The Alpine Foreland Basin is intersected by several fault systems (Fig. 2.6). Two conjugate strike-slip fault sets are north(north)west-southeast and northeast-southwest oriented. They are supplemented by east-west trending normal faults. The north(north)west and northeast trending ruptures were developed in the Paleozoic as a result of the Variscian orogeny and reactivated as a result of extensional processes at later stages of the basin evolution in the Mesozoic and Paleocene. During the early Oligocene, overthrusting of the Alpine nappes caused a downbending of the European plate which led to the development of the east-west oriented faults and the reactivation of the formerly developed northnorthwest-oriented fracture zones (Wagner, 1996; Sissingh, 1997; Groß et al., 2018). The main phase of this tectonic activity was in the Oligocene, however, some of those ruptures remained active until Miocene times (Groß et al., 2018; Pytlak et al., 2016a).

Due to the northward movement of the Alpine nappes, Molasse sediments deposited on the European plate became overthrusted and partly incorporated into the Alpine nappe stack (Kuhlemann and Kempf, 2002). These imbricated parts are referred to as Allochtonous Molasse, whereas the strata covering the European plate are known as Autochtonous Molasse.

The Central Swell Zone forms the southeast extension of the Landshut-Neuöttingen High (Fig. 3.1) and was developed in the Paleozoic. During the Cretaceous, a reactivation of

the pre-existing faults in this area led to an uplift of this paleotopographic high. As a result, the erosion of Mesozoic strata can be observed in this region (Nachtmann and Wagner, 1987; Wagner, 1998).
During the Miocene, the ongoing transpression from the south led to a lateral eastward oriented extrusion of the Eastern Alps (Wagner, 1998), contemporaneously earlier developed faults of the North Alpine Foreland Basin were reactivated (Nachtmann and Wagner, 1987; Wagner, 1998).

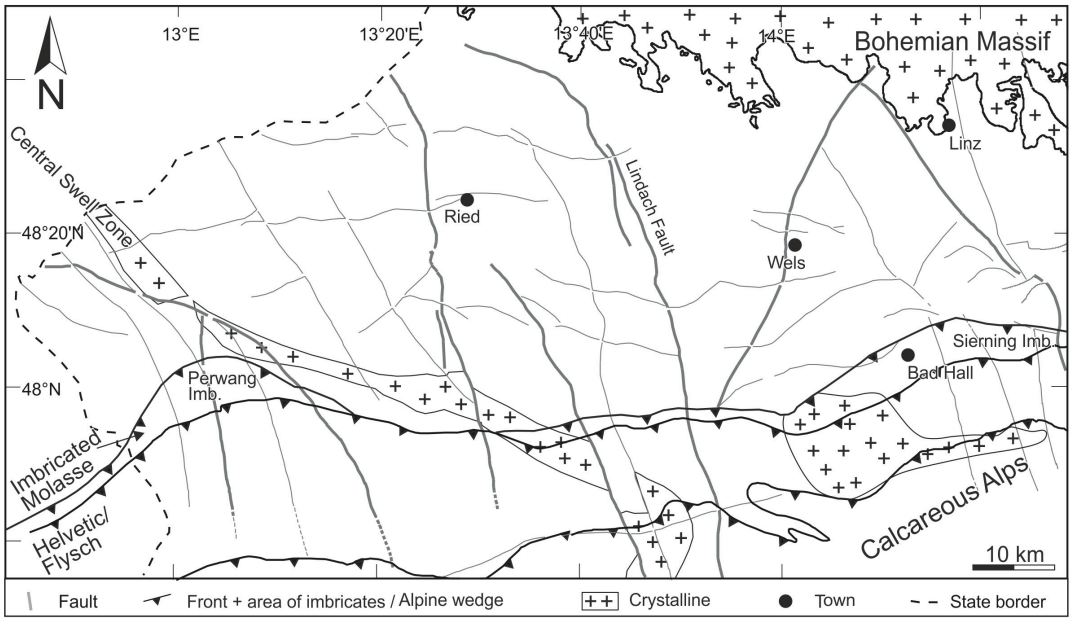

FIGURE 2.6: Map of the Upper Austrian part of the North Alpine Foreland Basin depicting the occurrence of the most prominent fault sets of this region and the Central Swell Zone (modified after Pytlak et al., 2016b; Groß et al., 2018); the north(north)west-southeast and northeast-southwest trending fracture zones were developed in the Paleozoic, the east-west trending faults were formed in the Oligocene due to overthrusting of the Alpine nappes

2.2.4 Hydrocarbons in the Alpine Foreland Basin

The Alpine Foreland Basin hosts numerous oil and gas deposits. According to Wagner (1996), two different petroleum systems can be distinguished, a Mesozoic to lower Oligocene system containing oil and thermal gas and an upper Oligocene to Miocene, biogenic gas system. These two systems were assumed to be separated, with local mixing (e.g. Sachsenhofer and Schulz, 2006). However, investigations of Reischenbacher and Sachsenhofer (2011) and Pytlak et al. (2016b) showed, that mixing of thermal and microbial gas can be observed in an extensive area of the Molasse Basin and that it is feasable to distinguish several groups with variable gas composition.
The main thermogenic hydrocarbon source rocks are situated in the Oligocene Schöneck, Dynow and Eggerding formations (Schulz et al., 2002; Sachsenhofer and Schulz, 2006; Sachsenhofer et al., 2010). Two different facies zones of these organic-rich formations can

be distinguished in Upper Austria. The western part is characterised by the occurrence of the "Oberhofen facies" (Groß et al., 2018), describing lower Oligocene strata which were relocated with submarine mass movements (Sachsenhofer and Schulz, 2006; Sachsenhofer et al., 2010) and overthrusted during the Alpine orogeny (Linzer and Sachsenhofer, 2010). In contrast, the "normal facies" of the source rocks is located in the eastern part of Upper Austria. Both facies types show variations in their geochemical parameters (e.g. Schulz et al., 2002; Sachsenhofer and Schulz, 2006) which may be responsible for the generation of different oil types found in Upper Austrian deposits (Gratzer et al., 2011).
Basal Eocene sandstones and carbonates, along with Mesozoic and Oligocene strata serve as the main hydrocarbon reservoirs. The Cenomanian reservoirs are sealed by Upper Cretaceous shales and marls (Wagner, 1996), however, in some areas of the basin, these strata became eroded, leading to a connection of Cenomanian with Eocene sandstones (Groß et al., 2018). Pelitic Eocene layers locally prevent hydrocarbons in this formation from migrating further upwards. Oligocene and Miocene shales act as regionally widespread seals for the Upper Austrian deposits, though. Local thickness variations due to erosional processes lead to local decrease in seal integrity, enabling mixtures of biogenic and thermogenic hydrocarbons in the shallower reservoirs (Groß et al., 2018).
Investigations of Gusterhuber et al. (2013) showed, that thermogenic hydrocarbon generation was triggered by Miocene overthrusting of the deposited source rocks by the Alpine nappe stack and migration processes started contemporaneously. In the Late Miocene, hydrocarbon generation ceased due to uplift and erosion processes and favoured biodegradation of already formed oil and gas (Gusterhuber et al., 2012).
Biogenic gas is a result of degradation activity of microorganisms during diagenesis (up to 60 °C), whereas thermogenic gas is formed by thermal cracking of higher hydrocarbon-chains in the stages of katagenesis (60-225 °C) and metagenesis (from 200 °C onwards). However, secondary microbial gas may evolve due to biodegradation of hydrocarbons. Microorganisms reprocess the oil stored in the reservoir and generate dry gas as a metabolite. Since the involved microbes consume n-alkanes first, the remaining oil in the deposit developes a characteristic composition, moreover, API gravity decreases while sulfur content increases (Ladwein and Schmidt, 1993).
Both processes occurred in the Alpine Foreland Basin. These are located within the Upper Oligocene and Miocene strata, the Upper Puchkirchen and Hall formations in particular (Sachsenhofer and Schulz, 2006; Groß et al., 2018). For the primary microbial gas, these sediments hold a dual function as source (pelitic layers; Schulz et al., 2009; Schulz and van Berk, 2009) and reservoir rocks (siliciclastic layers, e.g. Puchkirchen channel ; de Ruig and Hubbard, 2006). The primary microbial gas was generated shortly after sediment deposition and fixed in gas hydrates which became decomposed during Miocene and trapped in stratigraphic pinch-outs and compaction anticlines (Groß et al., 2018). Mixing of this natural gas with thermogenic and biodegraded hydrocarbons is frequently observed and investigated by Pytlak (2017).
In addition to biodegradation, thermogenic hydrocarbons were also affected by other

alterations such as water washing. In the course of this process, formation waters, circulating in the vicinity of hydrocarbon reservoirs, are able to incorporate benzene, toluene, ethylbenzenes and xylenes (BTEX). These components are carried away with the water currents in the subsurface (Lafargue and Barker, 1988). Recent analysis of hydrocarbon and water samples in Upper Austria have shown, that some Cenomanian and Eocene fields have experienced this alteration (Pytlak, 2017).

3 Hydrogeological Overview

3.1 Main Aquifers

3.1.1 Bohemian Massif

The granitic intrusions of the Bohemian Massif are characterised by low discharge values (generally < 5 l/s). Due to the low permeability of the formations in this geological section, water can only be produced from alluvial sediments or fractures dissecting the weathered upper section of the Bohemian granites (Goldbrunner, 1984; Goldbrunner, 2000).

3.1.2 Malmian Carbonates

The Malmian Carbonates depict the most important thermal aquifer in the Bavarian and Upper Austrian Molasse Basin (e.g. Andrews et al., 1987). Karstification processes during marine regression phases led to the development of deep groundwater flow pathways. These karst structures, together with faults and fractures in the formation control the permeability of the aquifer (Goldbrunner, 1984; Goldbrunner, 2000). Therefore, these carbonates are considered as inhomogenous in terms of its aquifer properties, the transmissive sections are concentrated around zones of tectonic activity (Goldbrunner, 1984).
The aquifer extent in Upper Austria is bordered by the Central Swell Zone in the south and southeast, where the carbonates have been eroded, and by the outcropping crystalline rocks in the Bavarian Forest and the Sauwald region in Upper Austria in the north and northwest (Goldbrunner, 2000).
The Global Meteoric Water Line (GMWL) is a regression line which states the average worldwide ratio between ^{2}H and ^{18}O for meteoric waters (Craig, 1961a). Waters from the Malmian aquifer show a slight deviation from the GMWL regarding their stable isotopic composition. This deviation could result from mixing of meteoric waters with formation waters of limited mobility (e.g. Puchkirchen Formation waters), since their position is located at the mixing line of these water types (Goldbrunner, 2000). In terms of its chemical composition, the water recovered from the Malmian carbonates is considered as $Na-HCO_3-Cl$-Type. The amount of dissolved solids is on average 1.0-1.2 g/l (Elster et al., 2016).
In 1981, oil was encountered in the Upper Jurassic (Polesny, 1983), indicating a connection between this aquifer and the oil-bearing Cenomanian. This is supported by the findings of Pytlak et al. (2017), who stated that connate waters in the overlying Cenomanian

and Eocene reservoirs were partly replaced by water resembling the chemical composition of Malmian water.

3.1.3 Upper Cretaceous

Most of the Upper Creataceous sediments are considered as impermeable, for which reason they are often declared as a cap rock of the Malmian carbonates (Goldbrunner, 1984). However, transmissive Cenomanian and Santonian to Lower Campanian sandstone beds have been drilled locally (Goldbrunner, 1984). Well log interpretation (Weber, 1980; Goldbrunner, 1984) and chemical investigations (Pytlak et al., 2017) have shown that these Cenomanian beds are locally hydraulically connected to the Malmian aquifer, resulting in mass transfer processes.

3.1.4 Lower and Upper Puchkirchen Formation & Linz Sands

The Lower and Upper Puchkirchen formations play an important role as a gas reservoir parallel to the Alpine front in the southern Molasse Basin. Despite to their hydraulic conductivity and their depth, an assessment of the geothermal potential of these strata came to the result, that they are only suitable for geothermal use to a minor extent (GeoMol Team, 2015).
However, the time-equivalent Linz Sands consisting of quartz sand with high permeabilities and porosities (Goldbrunner, 2000) represent an important aquifer for shallow and deep groundwater in the northern and northeastern part of the Molasse Basin (Andrews et al., 1987).
The Na−Cl-Type formation waters from the Lower and Upper Puchkirchen formations are characterised by a high mineralisation (up to 15-17 g/l). Due to the structural setting of the basin, deep groundwaters from the south ascend towards their northern discharge area at the Danube infiltrating the Linz Sands. This results in an increased geothermal gradient of up to 6.5 °C in the convection areas of the Innviertel region. The convection transports higher mineralized deep groundwater into shallow areas near the Danube where mixing with meteoric water occurs (Goldbrunner, 2000).
Investigations of the stable isotope composition of Puchkirchen Group waters show a strong enrichment in ^{2}H and ^{18}O compared to the Malmian waters. Moreover, an offset from the GMWL is observed, presumably caused by a lack of recharge by meteoric waters and stagnant conditions in the aquifer (Goldbrunner, 1988). The isotopic composition shows different characteristics compared to the Malmian carbonates and therefore contradicts a recharge via the "leaky-aquifer" principle. According to this principle, transmissive sediments are recharged by water seeping from shallow strata to aquifers in greater depth (Goldbrunner, 1984).

3.1.5 Hall Formation

The Hall Formation is an important stratigraphic unit in the petroleum system of the Upper Austrian Alpine Foreland Basin since its porous sand horizons serve as a reservoir

rock for natural gas deposits. However, its aquifer properties are hardly investigated (Goldbrunner, 1984).
The Hall Formation waters are highly mineralised (similar to the Puchkirchen Formation waters) and do not reach the northern basin margin, which leads to the assumption, that their hydrodynamic activity is limited (Goldbrunner, 1988) and that there is no exchange of these formation waters and meteoric waters (Goldbrunner, 2000). These assumptions are supported by stable isotope data which range in a similar span than the Puchkirchen Group waters (Goldbrunner, 2000).
However, investigations of Pytlak (2017) have shown, that Eocene oil reservoirs in the northeastern part of the NAFB in Upper Austria, which are located directly under or in the vicinity of the Hall strata are affected by water washing (section 2.2.4). Moreover, the investigated water samples showed a low mineralisation, which stands in contrast to the expected stagnant conditions. The occurrence of condensates in the Hall Formation suggests a diffusion of thermal hydrocarbons from the Eocene to these shallower formations (Pytlak, 2017). Therefore, an upwards migration of these lower mineralised waters from the Eocene to the Hall Formation could be possible.

3.1.6 Innviertel Group

The Innviertel Group occurs in the western part of Upper Austria (near Ried and Braunau). The transmissive sandstone layers are widely overlain by impermeable silty and clayey sediments, which lead to the formation of artesian groundwater deposits. The recharge area for this aquifer is assumed in the topographically higher Kobernaußerwald region in the south. The water flows northwards through the Innviertel Group to its discharge area in the Salzach and Inn river (Andrews et al., 1985; Goldbrunner, 1984). However, some formations of the Innviertel Group located near the outcrop of the Bohemian Massif are presumably infiltrated from the north (Goldbrunner, 1984).
The formation waters are characterised by their low mineralisation (TDS $< 0.5\,g/l$). According to stable isotope investigations, the recharge of the flow system presumably happened during the young Pleistocene (Goldbrunner, 2000). This is supported by piezometric and hydraulic conductivity observations, which gave a groundwater residence time from the recharge to discharge area of approximately 30000 to 40000 years (Andrews et al., 1985).

3.1.7 Upper Freshwater Molasse

The sedimentary strata of the Upper Freshwater Molasse hold artesian groundwater deposits (Goldbrunner, 1984). The coal-bearing fine grained layers in the Hausruck region serve as local aquicludes, whereas the gravel and sand layers are transmissive and discharge at numerous springs. Prior to the coal mining activities in this area, the aquifer discharge took place at the interface of the sand and gravel layers ("Hausruckschotter") and the footwall clay sediments ("Ampflwang Formation"). However, the longwall coal

mining in those fine-grained sediment deposits created new groundwater flow pathways and drainage systems in the subsurface (Kolmer, 2011).

3.1.8 Alluvial and Glacial Sediments

The Quaternary alluvial and glacial sediments form an important regional aquifer. Due to their good hydraulic conductivity, the glacial terraces and fluvial deposits of interglacial episodes have excellent aquifer properties and play an important role for groundwater recharge and private as well as municipal and industrial water supply (Gattinger, 1980).

3.2 Hydrodynamical Characteristics

Several attempts have been made, to analyse and characterise the flow behaviour of deep groundwaters in Upper Austria and Bavaria (e.g. Bayerisches Landesamt für Wasserwirtschaft, 1999; Schubert, 1996; Goldbrunner, 1984). In order to achieve a holistic and comprehensive result, Upper Austria and Bavaria have been working together on a project with the main focus on the Malmian thermal water aquifer. In Fig. 3.1, a Malmian thickness map with arrows indicating the flow directions within the thermal aquifer, is displayed. The cross-section in Fig. 3.2 illustrates the water currents in the subsurface.
The movement of thermal water in the Malmian carbonates is bound to faults, joints and karstified areas within the formation. Over the majority of the area, where this aquifer is present, it is covered by 10-40 m thick, porous Cenomanian sandstones. These two formations are hydrodynamically coupled. Towards the central part of Upper Austria a thinning of the Malmian carbonates is observed and the role of the thermal aquifer is taken over by the Rupelian and Linz Sands up to the Danube, where the discharge area of this groundwater system is located.
Hydrochemical and isotopic composition may indicate groundwater origin and flow directions. Therefore, results of chemical and isotopic groundwater investigations are used to derive the flow paths of the water throughout its migration from the aquifer recharge to its discharge area. The recharge area, located at the northwestern margin of the thermal aquifer model south of the Bavarian Forest (assigned as "Bayerischer Wald" in Fig. 3.1), is characterised by a low total mineralisation with relatively high contents of Ca^{+}, Mg^{2+} and $HCO_3{}^{-}$. Tritium, which became emitted in the 1950's and is only traceable in groundwaters formed afterwards, can be detected in these waters. Altogether, this leads to the assumption, that water influx from the Bavarian Forest feeds the thermal aquifer system (Bayerisches Landesamt für Wasserwirtschaft, 1999).
In Upper Austria, the regeneration area of the thermal aquifer is assumed in the Sauwald region. Due to its increased hydraulic potential (Fig. 3.1, isolines of hydraulic potential are coloured in purple) compared to the Malmian aquifer, waters from the crystalline basement and Innviertel Formation in this region infiltrate strata of hydraulically lower potential towards the south (Goldbrunner, 1984). Contemporaneously, groundwater ages increase towards the basin center (Bayerisches Landesamt für Wasserwirtschaft, 1999).

Groundwaters, descending from the Sauwald area, are characterised by a low total mineralisation. According to their chemical composition, they can be described as Ca-(Mg)-HCO_3^- Type waters. With increasing residence time in the aquifer, calcium and magnesium is replaced by sodium in the course of cation exchange of clay minerals (Goldbrunner, 1984).
West of Linz, the discharge of the thermal aquifer is supported by the observation of ascending Pleistocene waters in the Linz Sands. According to their chemical composition, these discharging thermal waters mix with autochtonous, younger waters which leads to a decrease in total mineralisation towards the Danube.
The southern part of the Malmian aquifer holds highly mineralised waters shaded in yellow in Fig. 3.1, which leads to the assumption, that these waters are hardly participating in the hydrodynamic system and have only little to no exchange with groundwaters from other aquifers (Bayerisches Landesamt für Wasserwirtschaft, 1999).
Although this hydrodynamic model is quite established, it is based on rather sparse and heterogeonous data. In comparison to Bavaria, the amount of wells drilled into Malmian carbonates is low and especially in the southern part of the Upper Austrian Malm occurrence, data is missing. Therefore, the border between high salinity and low salinity waters in the Jurassic carbonates is mainly assumed and not exactly verified by well data. An integration of well data from hydrocarbon wells could improve the data situation and aid to obtain new insights into the hydrodynamic characteristics of deep aquifers in Upper Austria.

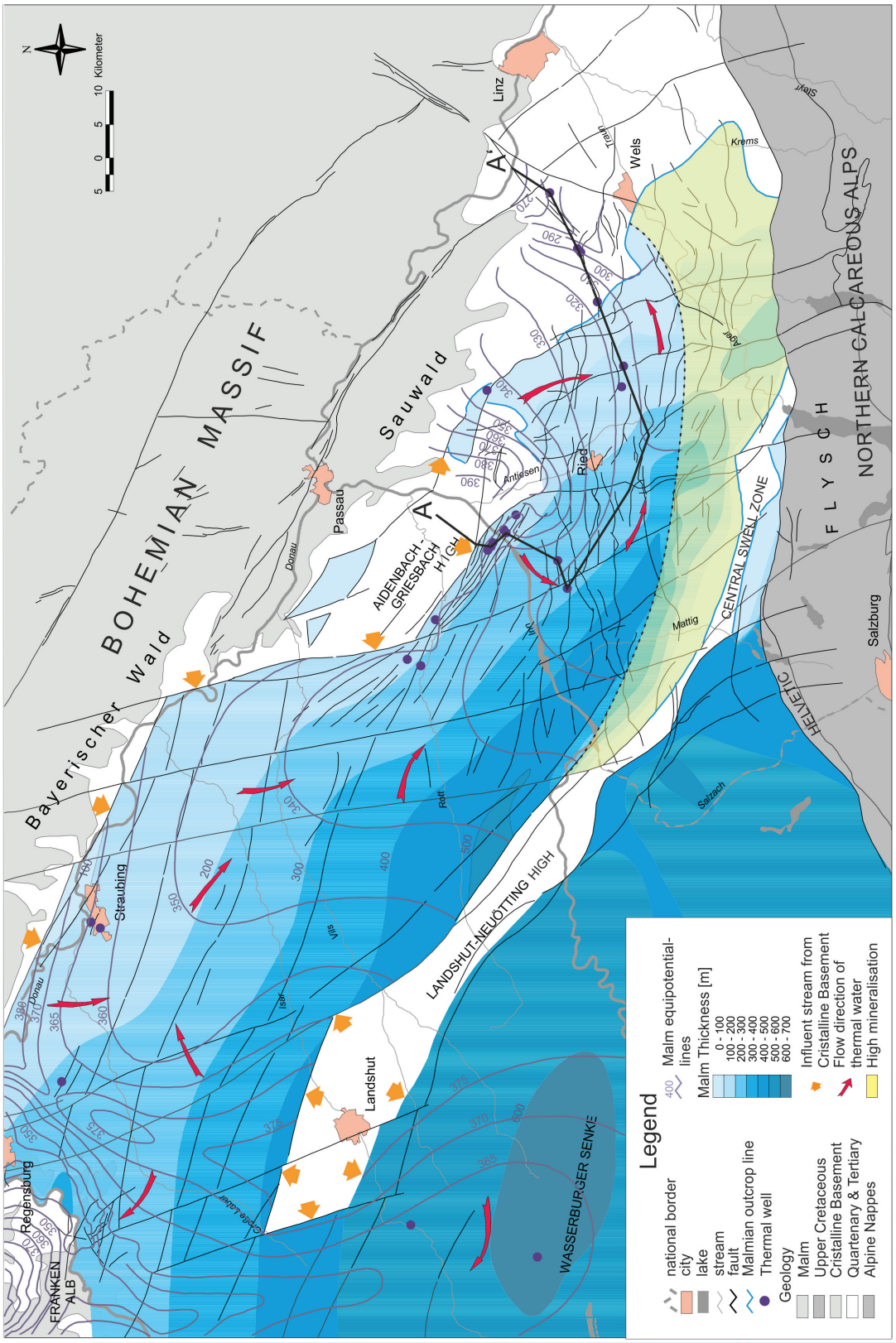

FIGURE 3.1: Malmian thickness map (modified after Bayerisches Landesamt für Wasserwirtschaft, 1999 and Pytlak et al., 2017) with groundwater potential lines of this formation (purple lines) and flow directions of thermal water within the aquifer perpendicular to these potential lines (red arrows), recharge areas from the crystalline basement are marked with yellow arrows. The area of highly mineralised, stagnant waters is bordered by a black, dashed line and marked in yellow. The profile visible in Fig. 3.2 is marked with a black line (A-A')

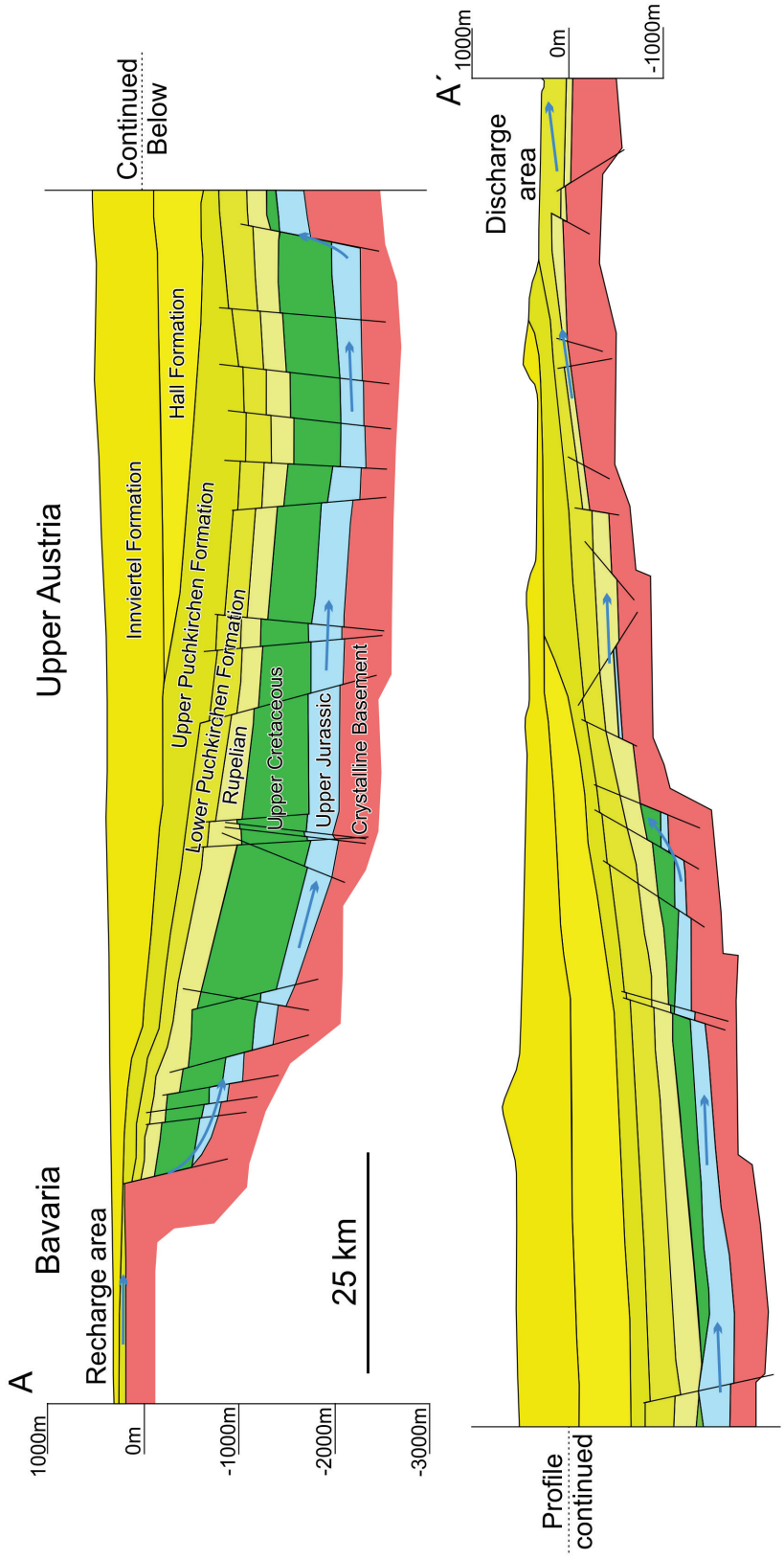

FIGURE 3.2: Profile through a section of the Bavarian and Upper Austrian Alpine Foreland Basin (modified after Goldbrunner, 2000 and Pytlak et al., 2017), the course of the cross-section is marked in Fig. 3.1, thermal water flow directions are shown with blue arrows

4 Principles of Hydrochemistry

4.1 Hydrochemical Processes

In order to understand a hydrological system as well as the behaviour and composition of its different components, a profound knowledge about the regeneration (e.g. from precipitation or surface runoff), the water supply and the geochemical processes, mainly controlled by rock-fluid interaction in the subsurface, is of great importance. These processes allow to draw conclusions about the provenance and migration pathways of the water. However, due to the huge variability of influencing factors, the interpretation of water composition has to be handled with care (Matthess, 1990).

4.1.1 Dissolution and Precipitation

The dissolution of minerals is a mechanism mainly influenced by chemical weathering. The redox-potential (Eh), pH and temperature serve as the physical boundary conditions controlling dissolution and precipitation. Moreover, the contact area between rocks and water within an aquifer is of great importance as it determines their extent. The larger this area of interaction is, the greater the impact on the water propagating through the aquifer. The same principle can be applied to the factor time. The larger the transmission coefficient of an aquifer, the smaller the influence of the water on the rock mass and vice versa. Therefore, a high mineralised water is more likely found in a porous aquifer, characterised by small grain size and pores, resulting in a higher groundwater residence time. The depth of an aquifer is another aspect which should be considered, since dwell time is increased with increasing aquifer depth as well as the aquifer temperature. This results, again, in a higher content of dissolved minerals (Matthess, 1990). Examples for these conditions are found in the vicinity of hydrocarbon deposits (oilfield brines, Rogers, 1917; Schoeller, 1956) or crystalline basement (Frape and Fritz, 1987; Pekdeger and Balderer, 1987; Nurmi et al., 1988).
Due to the fact, that the major amount of dissolved solids results from the dissolution of Ca- and Mg-carbonates or evaporites, the main ion content is composed of Ca^{2+}, Mg^{2+}, Na^{+}, Cl^{-}, $SO_4{}^{2-}$ and $HCO_3{}^{-}$. With increasing circulation time of the water in the subsurface, the ion proportions undergo changes, mostly in relation with groundwater depth. The zonation of anions (equation 4.1) and cations (equation 4.2) with increasing depth from left to right (Matthess, 1990) is stated below:

$$\begin{aligned} HCO_3^- \longrightarrow HCO_3^- + SO_4^{2-} \longrightarrow SO_4^{2-} \longrightarrow SO_4^{2-} + Cl^- \longrightarrow \\ \longrightarrow Cl^- + SO_4^{2-} \longrightarrow Cl^- \end{aligned} \tag{4.1}$$

$$Ca^{2+} \longrightarrow Ca^{2+} + Mg^{2+} \longrightarrow Na^+ \tag{4.2}$$

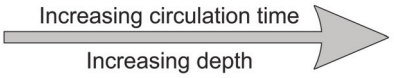

If the concentration of dissolved solids rises, an exceedance of the solubility product of specific substances (usually hardly soluble compounds) occurs, leading to their precipitation. This means, that the supply of one or more compounds is higher than the maximally soluble amount in the water. The excess quantity cannot be dissolved and remains as precipitate in the water (Matthess, 1990).

4.1.2 Adsorption and Ion exchange

If groundwater flows across specific solid layers in the earth's crust, organic and anorganic substances are bound and released, changing the composition of the water. The most important sorbents in the subsurface are clay minerals, zeolithes, iron-, aluminium- and manganese-hydroxides and -oxidhydrates (Krauskopf, 1956) as well as organisms and organic compounds such as microbes, plants and humic substances.
Clay minerals (e.g. glauconite, according to Schoeller, 1962) mainly sorb cations along their interfaces replacing H^+-ions aiming for charge equalisation. This procedure is commonly known as cation-exchange. But also anions are absorbed instead of OH^--ions. Organic substances show similar characteristics regarding their material exchange properties (Matthess, 1990).

4.1.3 Mixing Processes

Mixing of different waters from different aquifers often results in dissolution and precipitation leading to different characteristics and an overall change of the mineral content. Especially, if an excess of specific ions is present, the solubility product acts as a boundary condition for the maximum amount of this element to be dissolved. The amount, exceeding this parameter, precipitates. If, e.g. $CaCl_2$-containing water is blended with $CaSO_4$- or $Ca(HCO_3)_2$-rich groundwater, a precipitation of gypsum or calcite may occur. In particular, the carbonate balance (section 4.2.1) is sensitive to mixing processes. It is not only affected by changes in the chemical composition, but also by variations in pH and temperature. These changes may lead to precipitation of carbonate, but also other compounds can be withdrawn from the water if their solubility product is exceeded. If specific ions are able to replace others in a mineral structure (e.g. Sr^{2+} is able to replace Ca^{2+}) they may coprecipitate as a result of these mixing processes as well.

Indications, whether a sampled water has undergone mixing, can be derived from a comparison of the equivalent sum of Ca^{2+} and Mg^{2+} with $HCO_3{}^-$ of the water. If the hydrocarbonate content is higher than the sum of Ca^{2+} and Mg^{2+}, a replacement of Ca^{2+} with Na^+ is likely to have occurred, indicating a mixing process (Matthess, 1990).

4.2 Anions and Cations

4.2.1 Anions

Hydrocarbonate - $HCO_3{}^-$

Carbon is an important element in all organic substances. Kaustobiolithes (e.g. coals) and carbonates host a major amount of bound carbon in the lithosphere, but it can be enriched in sediments as well. Its occurrence in water is mainly controlled by the system listed below:

$$CO_2 + H_2O \rightleftharpoons H_2CO_3 \rightleftharpoons HCO_3{}^- + H^+ \rightleftharpoons CO_3{}^{2-} + H^+ \tag{4.3}$$

The source of the different carbonate forms in water are carbonate rocks and free carbon dioxide. Carbon dioxide occurs in its free form (as dissolved CO_2 and undissociated H_2CO_3) and bound as hydrocarbonate-ions ($HCO_3{}^-$) and carbonate-ions ($CO_3{}^{2-}$, Matthess, 1990). The occurrence of these carbonate forms is driven by the pH, pressure and temperature conditions. The diagram in Fig. 4.1 shows the percentage of CO_2-species which are present in the water with varying pH and temperature. For naturally occurring groundwaters, ranging between 6 and 8 pH (Fig. 4.1), the dominating carbonate species are hydrocarbonate-ions and undissociated carbonic acid (H_2CO_3). In acidic conditions, this composition shifts towards a larger amount of carbonic acid and in basic environments, carbonate ions tend to dominate in comparison to other CO_2-species(Hem, 1985).

The supply of free CO_2 in water is either controlled by the solution of this gas from the atmosphere or its release in the course of diagenetic and metamorphic processes, especially diagenesis of organic matter. Moreover, it is formed as a product of anaerobic or aerobic metabolic activity, by combustion of fossil fuels and the reaction of acids with carbonates.

Two important parameters are closely linked to the amount of carbonate in water: alkalinity and acidity. Alkalinity is a measure of the water's ability to neutralise acids, whereas acidity is the measure of the fluid's ability to neutralise bases. Since carbonic acids and hydrocarbonate-ions are the most commonly occurring buffer systems in water, these two parameters can be set equal to their abundance. They are usually determined by titration with specific indicators, methyl-orange (end point at pH 4.3) for alkalinity and phenolphtalein (end point at pH 8.2) for acidity (Hem, 1985). Waters containing higher concentrations of weak acids (e.g. silicic, phosphoric or organic acids) form an exception regarding the rule mentioned above, since the occurrence of those acid's ions may lead to a misinterpretation of the carbonate content if they were neglected. This

applies especially for oil field brines or waste disposal sites (Badecker and Back, 1979; Golwer et al., 1976; Fresenius et al., 1977).

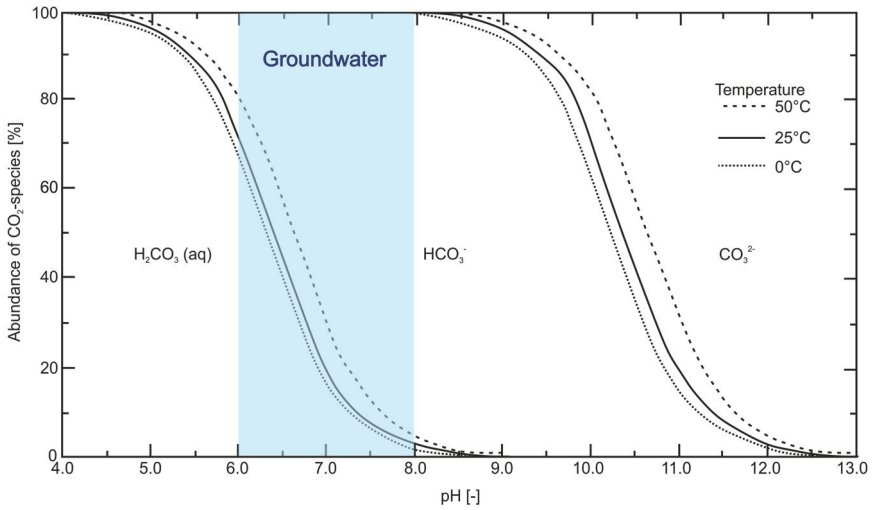

FIGURE 4.1: Percentage of dissolved CO_2-species as a function of pH, temperature at 101.324 kPa/ 1 atm (roughly 1 bar) (only valid for diluted solutions, Hem, 1985); the area shaded in blue illustrates the usual pH range for groundwaters

Groundwaters usually contain 10-20 mg/l of H_2CO_3, if the content exceeds 250 mg/l the water is named acidulous. The concentration of HCO_3^- in rain water is below 10 mg/l, sometimes even below 1 mg/l. Its content in groundwaters is between 50 and 400 mg/l, in the presence of high amounts of CO_2, caused by endogene or diagenetic processes, HCO_3^- concentrations above 1000 mg/l may occur in waters low in earth alkalines (Foster, 1950).

Chloride - Cl^-

The major part (> 75 %) of the naturally occurring chloride is dissolved in seawater. It originates from volcanic gases which were released during eruptions in the early stages of the earth's atmosphere and hydrosphere development.
Nowadays, although there is still volcanic activity which transfers chloride-bearing chemical compounds to the earth's crust, most of the chloride supply originates from dissolution of evaporite deposits. To a minor extent, anthropogenic contamination may be caused by the usage of fertilizers or road salt (Matthess, 1990; Zötl and Goldbrunner, 1993).
Transmissive layers contain less chloride than rocks with lower porosity and permeability. In these clay layers, the chloride content is increased. This presence may be caused by the relative size of chloride-ions and clay membrane effects, which prevent its emission from these strata (Hem, 1985).

Sulfate - SO_4^{2-}

Naturally occurring sulfur is assumed to originate from degassing of magma (Ricke, 1960) and can be found in seawater, sedimentary and evaporitic rocks (e.g. gypsum or anhydrite) today. These are the main sources for sulfate in groundwater, where its content is normally limited to few mg/l and may increase in the vicinity of formations with a higher amount of sulfate. Moreover, decomposition of sulfur bearing minerals (e.g. pyrite or marcasite) as well as its presence in lignite and swamps may contribute to the sulfate supply. A lack of oxygen combined with microbial activity may lead to a conversion of sulfate to gaseous hydrogen sulfide. Acid rain, fertilisers and landfill are sources of sulfate created due to human influence (Matthess, 1990; Zötl and Goldbrunner, 1993).

Nitrate - NO_3^-

Nitrate is a chemical compound which is mainly formed due to biogenic activity. In the presence of oxygen, organically bound nitrogen is oxidised to amino acids and ammonia which is later reduced to nitrite and nitrate after oxygen consumption. This nitrate reduction usually takes place in the uppermost layers of the subsurface during early diagenesis and provides a natural nitrate source for groundwaters (Wisotzky, 2012). However, agricultural activity has caused a severe influence onto the nitrate content, because it is contained in fertilisers. Nowadays, especially shallow groundwaters bear excessive, anthropogenically induced nitrate (Matthess, 1990; Zötl and Goldbrunner, 1993).

Fluoride - F^-

Compared to chlorine, fluorine can be found in larger quantities in magmatites. But its abundance in the earth's hydrosphere is considerably smaller. Fluoride can be bound to mineral surfaces, replacing OH^--ions, but with increasing pH, this effect is reversed. If the pH is low, fluorine attaches to H^+-ions, forming HF as a product. Moreover, this element tends to build complex compounds, especially with Al, Be and Fe^{3+} (Matthess, 1990). Fluorine can be enriched in carbonates due to precipitation as calcium fluoride in seawater during carbonate development (Michel, 1997).
The fluoride content of fresh waters is typically below 1 mg/l (Matthess, 1990). According to Zötl and Goldbrunner, 1993, fluorine bearing chemical compounds ascend from great depths.

Iodide - I^-

Iodine is a rare element in the litho- and hydrosphere. Its anion, iodide, occurs in waters flowing through salt deposits (Zötl and Goldbrunner, 1993). Iodine is biophile, living organisms accumulate this element. In the course of degradation and transformation of organic material, the bound iodine is transferred into the surrounding environments (e.g. formation waters in organic rich sediments, Matthess, 1990). Thus, an enrichment in iodide is observed in waters which have been in contact with hydrocarbons. Therefore,

the iodide content may be related to the occurrence of natural gas or oil in the Austrian Foreland Basin (e.g. Kölbl, 1958; Schröckenfuchs, 1975). Thermal waters recovered in Bad Hall represent a well-known example for iodide-rich waters in Upper Austria (Zötl and Goldbrunner, 1993).

Bromide - Br^-

Similar to chloride, the origin of bromide is volcanic emanation. Its content in seawater is approximately 7.3 mg/l which is significantly higher than its content in volcanic rocks (Behne, 1953). Traces of bromide can be found in rainwater, compared to seawater, the Br/Cl ratio is increased (Matthess, 1990). Thus, the Br/Cl ratio decreases with increasing chloride content. Moreover, bromide is preferentially adsorbed by organic compounds and released during their decompostion, therefore the abundance and processing of organic matter is an additional drive mechanism for the Br/Cl ratio (Gerritse and George, 1988). Similar to iodide, bromide is a characteristic component of oilfield brines or waters related to hydrocarbon deposits (Zötl and Goldbrunner, 1993).

4.2.2 Cations

Sodium - Na^+

Sodium is an important element in magmatites, where it mostly occurs in different types of plagioclase (e.g. Albite). To a minor extent, sodium may also be included in other silicates. Sediments (e.g. sand and clay) contain it as well, whereas sodium is not enriched in carbonates. This element is liberated in the course of weathering processes and due to its excellent solubility, it is one of the principal constituents in mineralised water. Sodium is mainly enriched in sea water and evaporitic deposits and reaches its highest concentration in the presence of chloride (Matthess, 1990; Zötl and Goldbrunner, 1993). Compared to other cations, an enrichment in sodium can be observed in deep groundwaters. Ion exchange processes are held responsible for this augmentation of the sodium content with increasing depth (Elster et al., 2016). Adsorptive forces and membrane effects of clay minerals cause an accumulation of e.g. calcium, while sodium is released into the groundwater (Matthess, 1990).

Potassium - K^+

Potassium can be found to a slightly minor degree than sodium in magmatic rocks. As opposed to sodium, which is bound in plagioclase, potassium occurs in potash feldspars (e.g. orthoclase and microcline). Mica and other silicates also contain this element. Similar to sodium, this element is released by weathering, but it can be absorbed and bound by clay minerals on its way through the subsurface. This and its inferior chemical mobility accounts for its lower abundance in waters (especially sea water) compared to sodium. Exceptions are undrained basins and mineral waters (Matthess, 1990; Zötl and Goldbrunner, 1993). Increased potassium contents are also observed in oil-field brines (Elster et al.,

2016). Potassium deposits of commercial relevance can be found in evaporitic sequences and as saltpetre.
The usage of fertilizers on agricultural land may cause an increase in the potassium content of groundwaters as a concomitant. Therefore, this anthropogenic influence must be taken into account when interpreting analytic results (Matthess, 1990; Zötl and Goldbrunner, 1993).

Calcium - Ca^{2+}

The major amount of calcium is contained in carbonates (bound in calcite, aragonite and dolomite) and sulfates (gypsum and anhydrite). This element is essential for many living organisms, who need it for building shells or bones. But it can also be found as a component of plagioclase in magmatic rocks (e.g. Anorthite) and may occur in amphiboles, pyroxenes, garnets, fluorite and apatite.
Small amounts of calcium are brought into the groundwater with rainfall, they yield from seawater salts, dust from weathered carbonate containing rocks or industrial emissions. Since it is a component of agricultural fertilizing products, anthropogenic contaminations of the natural calcium content of groundwater can be observed (Hem, 1985).
The calcium concentration of fresh waters, where it is the most common cation, is controlled by the carbonate balance. At 20 °C temperature, 14 mg/l of calcite can be dissolved in distilled water (D'Ans and Lax, 1967), contemporaneously, the pH of the fluid rises with increasing dissolution. In the presence of CO_2, hydrocarbonate-ions are formed and the evolving H^+-ions favour this process (Matthess, 1990). This sequence of activities is commonly known as carstification (Zötl and Goldbrunner, 1993). If gypsum or anhydrite is present in the system, the amount of Ca^{2+} is controlled by the solubility equilibrium of these minerals.
The content of Ca^{2+}-ions in waters flowing in siliciclastic environment is usually below 100 mg/l. In carbonates, it can reach a multiple of this value due to the increased presence of CO_2 (Hem, 1985).

Magnesium - Mg^{2+}

The element magnesium is mainly included in minerals of the olivine, pyroxene and amphibole group. It also occurs in mica, cordierite, talc, serpentine, chlorite and clay minerals. Although magnesium is present in many different minerals and is characterised by a high solubility, its content in fresh water is usually lower than the calcium content of the water. This is probably caused by the lower abundance of this element in the earth's crust. Groundwaters flowing in olivine-basaltic, dolomitic or serpentinitic aquifers form an exception. These environments are favourable for magnesium enrichment. Normally, fresh water contains up to 40 mg/l of Mg^{2+} (Matthess, 1990; Zötl and Goldbrunner, 1993).

Iron - Fe^{2+}

Iron is one of the most important elements included in magmatic rocks, especially in dark minerals (e.g. pyroxene, amphibole, biotite, magnetite, garnet and olivine). Iron-bearing chemical compounds, which are released in the course of weathering, are mostly oxides and hydroxides. These are characterised by their poor solubility and low mobility. Quantitatively, clay layers hold the major part of iron minerals in sediments, followed by sandstones and carbonates.
Iron is involved in biochemical processes. Microorganisms oxidise it to Fe^{3+} under aerobic conditions or reduce it in the absence of oxygen to Fe^{2+}. The content of Fe^{2+} is normally limited to 1 mg/l, only under reducing conditions higher concentrations can be found in water. Additionally, iron often occurs in combination with manganese (Matthess, 1990).

Strontium - Sr^{2+}

Strontium is an element, which occurs in magmatic rocks due to its similar chemical characteristics compared to calcium and potassium resulting in an ability to replace them. It can be enriched in felsic to intermediate igneous rocks (e.g. granite or syenite) and sediments. Despite its higher abundance in those rocks, its content does not exceed a relation of Sr/Ca of 1/1000 (Matthess, 1990). Another aspect of this element is, that it indicates an origin from or contact with a deep groundwater system (Zötl and Goldbrunner, 1993).

4.3 Trace Elements

Elements which occur in very small amounts in groundwater are summarised as minor and trace elements. These components may aid in provenance analysis of groundwaters or prospection of ore deposits (Gundlach et al., 1981; Rose et al., 1979; Ginsburg, 1963). Examples for trace elements are: lithium, rubidium, beryllium, aluminium and copper. Some of those elements are mostly associated with certain ions in the water, e.g. Li and Na are paired, so do Rb and K (Michel, 1997).

4.4 Water Classification

There are different ways to classify waters, either according to their genetic origin, their hydrological characteristics or chemical parameters. One way to distinguish groundwater types is to assign them with the terms deep or superficial/shallow. According to Goldbrunner (1984), deep groundwaters can be characterised by a lack of oxygen. This property results from long residence times in the subsurface combined with very limited to no infiltration of meteoric waters from the surface.
A very simple classification, regarding the concentration of total dissolved solids in water is suggested by Davis and de Wiest (1967) and listed in table 4.1:

TABLE 4.1: Classification of waters regarding their concentration of total dissolved solids (Davis and de Wiest, 1967)

Type of Water	**Concentration of total dissolved solids [mg/kg]**
fresh water	0 - 1000
brackish water	1000 - 10000
seawater	10000 - 100000
brine	> 100000

However, mixtures of high and low salinity waters are not considered in this categorisation. A subdivision of water types according to their chemical composition offers a greater variability and may also give indications about the formation and origin of the water. Palmer (1911) recommended to assign weights to the individual measured ions, taking their individual mass into account. The result is a sum of 100 % including proportional shares of the contained ions in meq%. If an ion fraction exceeds 20 % of the overall content, it is assigned to the watertype (e.g. Ca-HCO_3 type, anions before cations, Elster et al., 2016).

In order to improve the differentiation of water types, a wide range of display methods for hydrochemical data exist. A very widely used plot is the Piper-Plot (after Piper, 1944). The data sets are plotted in two ternary diagrams, one for anions, the other one for cations. These ternary systems are combined in a diamond-shaped plot which allows the sampled water to be classified according to its principal components. One option of such a characterisation scheme, according to Furtak and Langguth (1967) is displayed in Fig. 4.2. A major advantage of this form of data presentation is, that apart from identifying data clusters, it allows to see mixtures between these different water types. Another method for visualisation of water compositions is via a pie diagram (e.g. Hem, 1985). By colour-coding the individual components, differences in the elementary distribution of individual samples are quickly recognized.

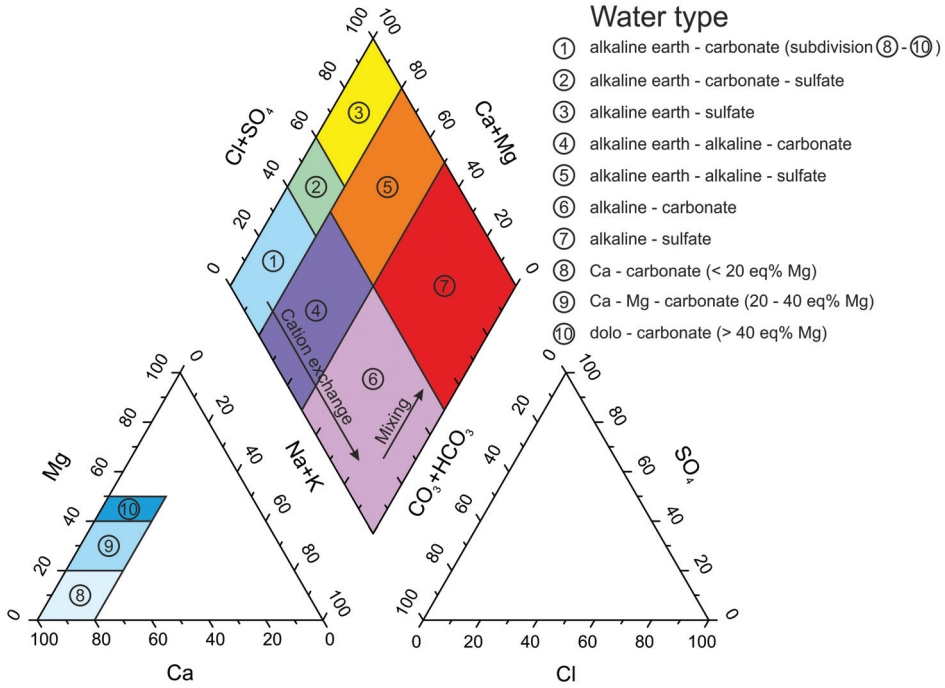

FIGURE 4.2: Classification scheme of a Piper diagram (modified after Piper, 1944 and Furtak and Langguth, 1967)

The term mineral and thermal water is subject to legal restrictions in Austria. In Table 4.2, the element-specific threshold values for descriptions added to a water source are listed according to the BGBl. II Nr. 309/1999 (1999). Additionally, a water is classified as thermal water when constantly exceeding a temperature of 20 °C (LGBl. OÖ Nr. 47/1961, 1961).

TABLE 4.2: Element-specific threshold values for descriptions of mineral or thermal waters (BGBl. II Nr. 309/1999, 1999)

Specification	**Criteria**
Low mineralisation	The amount of TDS is < 500 mg/l.
Very low mineralisation	The amount of TDS is < 50 mg/l.
High mineralisation	The amount of TDS is > 1500 mg/l.
Bicarbonate bearing water	The amount of HCO_3^- is > 600 mg/l.
Sulfate bearing water	The amount of SO_4^{2-} is > 200 mg/l.
Chloride bearing water	The amount of Cl^- is > 200 mg/l.
Calcium bearing water	The amount of Ca^{2+} is > 150 mg/l.
Magnesium bearing water	The amount of Mg^{2+} is > 50 mg/l.
Fluoride bearing water	The amount of F^- is > 1 mg/l.
Ferrous water	The amount of Fe^{2+} is > 1 mg/l.
Acidulous water	The amount of free CO_2 is > 250 mg/l.
Sodium bearing water	The amount of sodium is > 200 mg/l.

4.5 Dissolved and Free Gases

The major amount of gases occurring with groundwaters is composed of oxygen O_2, nitrogen N_2, carbon dioxide CO_2 and hydrogen sulfide H_2S. They are either chemically bound, physically dissolved or mechanically added. With increasing depth and overburden pressure, respectively, the ability of the water to absorbe gases is increased and vice versa (Zötl and Goldbrunner, 1993). Therefore, gases of ascending thermal waters are liberated during recovery.
Deep groundwaters are depleted in O_2, actively circulating waters in carstic aquifers are an exception to this rule. N_2 finds its way into the water through contact with air (Zötl and Goldbrunner, 1993). However, most of the nitrogen dissolved in water is related to biogenic activity in the course of the nitrogen cycle. Anthropogenic activities (e.g. combustion of fossil fuels, usage of fertilizers) also have a considerable influence on the nitrogen content in the water (Hem, 1985). The amount of CO_2 is closely related to the pH, temperature and pressure (as mentioned in section 4.2.1). If the CO_2 content exceeds 250 mg/l (for drinking purposes) and 1000 mg/l (for balneological purposes), respectively, the water receives "acidulous" as an additional term (Elster et al., 2016). Similar to CO_2, the presence of H_2S is closely related to pH and temperature conditions. Additional control factors are O_2- and dissolved CO_2-contents as well as the presence of microorganisms. These microbes produce H_2S as a result of biochemical reduction. Another possibility for H_2S-generation is by thermal reduction. The threshold of H_2S detection by its scent is around 0.1 ppm, therefore even amounts below the detection limit can be recognized by the human sense of smell (Michel, 1997). Biodegradational anaerobic processes also form CH_4 (Matthess, 1990). However, in the presence of hydrocarbon deposits, CH_4 may also be supplied from these deposits (Humez et al., 2016 and references therein). Whether the methane occurrence is of biogenic or thermogenic origin, can be evaluated by isotope investigations (e.g. Schoell, 1988).

4.6 Isotopes

4.6.1 ^{14}C

^{14}C is a naturally occurring carbon isotope. The main source of this isotope is the transformation of ^{14}N to ^{14}C as a result of the neutron bombardment of the upper atmosphere caused by cosmic rays (Sigg and Stumm, 1989; Langmuir, 1997). This isotope is absorbed by living organisms by photosynthesis or nutrition. During their lifetime, the amount of ^{14}C in these organisms remains constant, but it starts to decrease after their death (Langmuir, 1997) with a half life of approximately 5720 years (Sigg and Stumm, 1989). The amount of ^{14}C in the sample indicates its age. Due to its half-life, this dating method is applicable up to an age of approximately 40000 years. The ^{14}C content in the atmosphere has experienced slight anthropogenically induced variations due to the consumption of fossil fuels (Langmuir, 1997).
The amount of ^{14}C in groundwater varies between 50 and 100 pmC (per cent modern

Carbon; Münnich et al., 1967). Due to the reaction of limestones/carbonate rocks (which are considered as ^{14}C-free due to their age) with atmospheric CO_2 (where the amount of ^{14}C ranges at approximately 100 pmC), HCO_3^--ions with a ^{14}C content of 50 pmC are dissolved in water. This number is increased by the amount of free CO_2 in the water (Matthess, 1990), by ion exchange with carbon dioxide (Münnich et al., 1967) and by carbonates with a remaining quantity of ^{14}C incorporated (Geyh, 1970). Regenerated groundwater usually contains around 85 pmC, this amount naturally decreases with increasing groundwater residence time. However, a carbonate-CO_2 reaction with CO_2 from endogenous or diagenetic processes (free of ^{14}C) may distort this process of natural decay and yield a lower percentage of radioactive carbon as a result (Matthess, 1990). Moreover, isotope exchange with carbonates present in the aquifer may be a source of errors as well (Thilo and Münnich, 1970). Therefore, a determination of the Dissolved Inorganic Carbon (DIC) and ^{13}C should be done in combination with ^{14}C-dating in order to avoid misinterpretations (Pearson and Hanshaw, 1970; Fritz and Fontes, 1980; Reardon and Fritz, 1978).

4.6.2 ^{13}C

The stable isotope ^{13}C is used to determine the source of carbon dissolved in water and supports the ^{14}C isotope analysis. High values of ^{13}C indicate either isotope exchange effects or fossilized carbonates as an origin for this element. This method achieves good results in siliciclastic aquifers, but carbonate dissolution and precipitation within a carbonate-bearing hydrostratigraphic unit may distort the measurement outcome (Elster et al., 2016).

4.6.3 Stable Isotopes - ^{2}H and ^{18}O

The stable isotopes deuterium (D or ^{2}H) and ^{18}O are measured as ‰-deviation from a seawater standard (Standard Mean Ocean Water - SMOW; Craig, 1961b). Both, ^{2}H and ^{18}O, are depleted in rain water with increasing inland distance from the ocean (continental effect) and altitude (altitude effect, Fig. 4.3). This isotopic fractionation is the result of evaporation and condensation processes (Ehhalt and Knott, 1965). For ^{18}O the altitude decrease can be quantified as 0.2-0.3 ‰ per 100 m, for ^{2}H it is 1.6-2.4 ‰ per 100 m (Siegenthaler, 1979; Siegenthaler, 1980). Since the altitude effect is based on a temperature decrease with increasing height, a diminished stable isotope concentration may be an indicator for climatic conditions. For instance, Holocene deep groundwaters (^{2}H= -75 ‰ and ^{18}O= -10.0 ‰) in the South-Bavarian Molasse Basin are less depleted in stable isotopes than their Pleistocene equivalents (^{2}H= -92 ‰ and ^{18}O= 12.4 ‰; Andres, 1983). This is of great relevance, not only for the interpretation of paleowaters, but also for the estimation of seasonal variations in shallow aquifers.

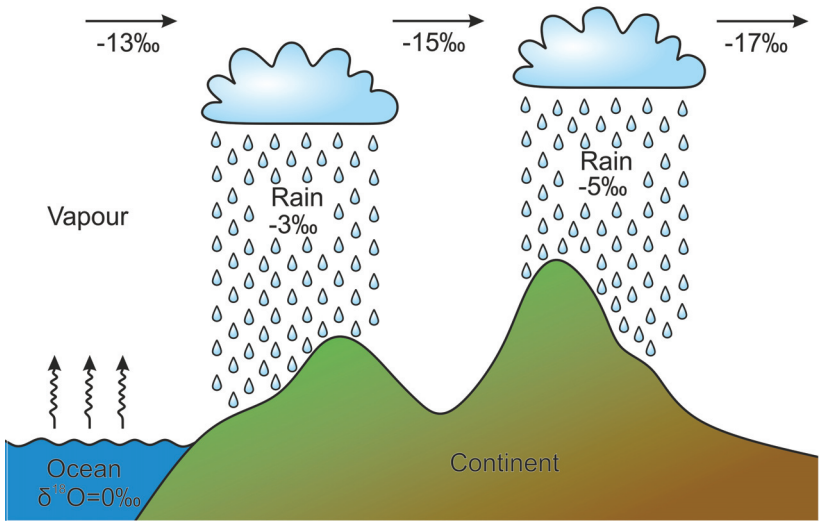

FIGURE 4.3: Schematic depiction of ^{18}O-fractionation in the hydrological cycle (modified after Siegenthaler, 1979)

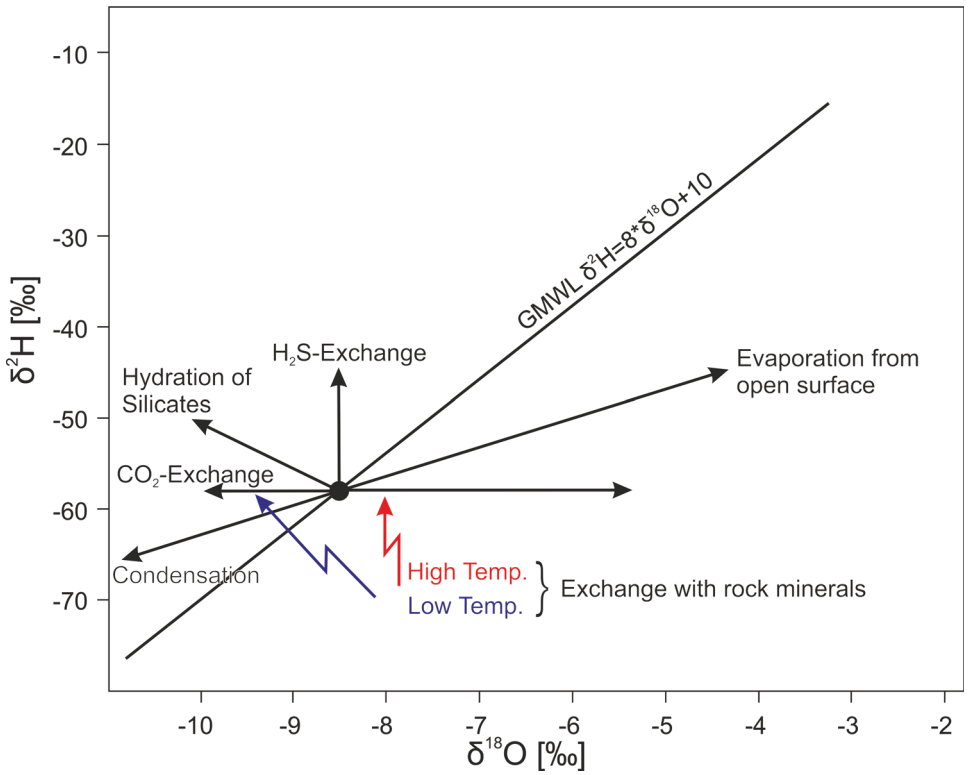

FIGURE 4.4: Schematic plot of ^{18}O vs. ^{2}H, environmental effects and their according change of position within the diagram are marked with arrows (IAEA, 1981; IAEA, 1983)

5 Methodology

5.1 Sampling of Water Wells

Before sampling of the water, field parameters are measured at the site of investigation (Fig. 5.1). The field parameters which were measured at every sampling point are: Temperature, pH, Conductivity and Eh of the water. Additionally, a titration using methylorange as an indicator was carried out to determine the acid capacity at a pH of 4.3. In order to enable parameter determination at the geothermal well sites, the water had to be cooled to at least 55 °C since the measuring devices are not able to handle higher temperatures. Afterwards the water designated for Inductively coupled Mass Spectometry (ICP-MS) measurements was filtered and sampled in flasks of polyethylene.
The water used for the investigation of dissolved gases via headspaces was sampled in glass flasks according to a procedure proposed by Capasso and Inguaggiato (1998) as well as Caruso and Santoro (2014). Therefore, the designated flasks were put into a vessel filled with the sample water. Then they were completely filled with water and crimped in the water-filled container in order to prevent any atmospheric contamination.
A device, developed by Łukasz Pytlak was used to sample the free gas of selected investigation sites. This construction is based on the same principle as desribed by Michel (1997) and depcited in Fig. 5.3. The sampling facility consists of a plastic pipe with an outlet valve, mounted at the bottom of the pipe. The inlet valve is placed on the opposite side of the pipe bottom and connected to a small tube placed in the center of the pipe and mounted along the pipe rotation axis. The first step in the free gas sampling procedure is, to fill the pipe with sampling water. Then, a cloche is placed above the small tube to collect the gas escaping from the water. Therefore, the water flow rate should be moderately in order to enable a sufficient amount of gas to escape. This is done, until a certain amount of gas has been collected under the cloche (Fig. 5.2 and Fig. 5.3). The collected gas is transported into the water-filled gas collecting tube via a water-filled hose. The gas volume replaces the water volume in the collecting tube and is then ready to be transported for further laboratory investigation.

FIGURE 5.1: Measurement of field parameters (Temperature, pH, Conductivity and Eh at a sampling site (courtesy of Łukasz Pytlak)

FIGURE 5.2: Gas sampling with a sampling device developed by Łukasz Pytlak (courtesy of Łukasz Pytlak)

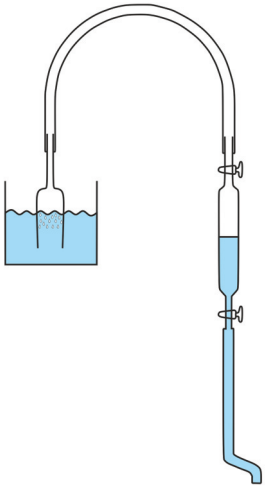

FIGURE 5.3: Schematic illustration of the free gas sampling device (modified after Michel, 1997)

5.2 Inductively Coupled - Mass Spectometry (ICP-MS)

A technique coupling ICP and MS (schematic setting in Fig. 5.4) was applied to analyse the selected water samples. A plasma is used to ionise the sample components in combination with a quadrupole mass spectrometer to analyse the constituents. The sample is inserted into the measuring device via a nebuliser and transported together with a carrier gas (Ar in most cases) to the high-frequency generated plasma. The next step, the ion-extraction, starts with an ion transfer to an intermediate storage from where they are sampled by a skimmer and induced into the mass spectrometer. Behind the skimmer, four ion lenses are mounted in a vacuum environment. The spectrometer's transition as well as the mass resolution of ions is regulated by the voltage applied to these lenses. The term quadrupole refers to the four columns placed in front of the detection unit. Detection is carried out with electron multiplication and scintillation counting. An advantage of the ICP-MS method is the device's ability to analyse individual components of a sample simultaneously. Moreover, the detection limit is very low (1 ppb or even lower, Schwedt, 1992).

The ion measurements (except for iodide and bromide) were performed at the geochemical department of the Geological Survey of Austria. Iodide and bromide concentrations were measured at the Chair of Economic Geology by Ao. Univ.-Prof. Dr. phil. Walter Prohaska. The used ion chromatography system at the Chair of Economic Geology was a DIONEX ICS-3000. Bromide concentrations (detection limit: 0.1 ppb) were measured by a conductivity detector using sulfuric acid with external suppression as an eluent. Iodide (detection limit: 1 ppb) was investigated by amperometric detection with a sodium-hydroxide eluent (pers. comment W. Prohaska, 2018).

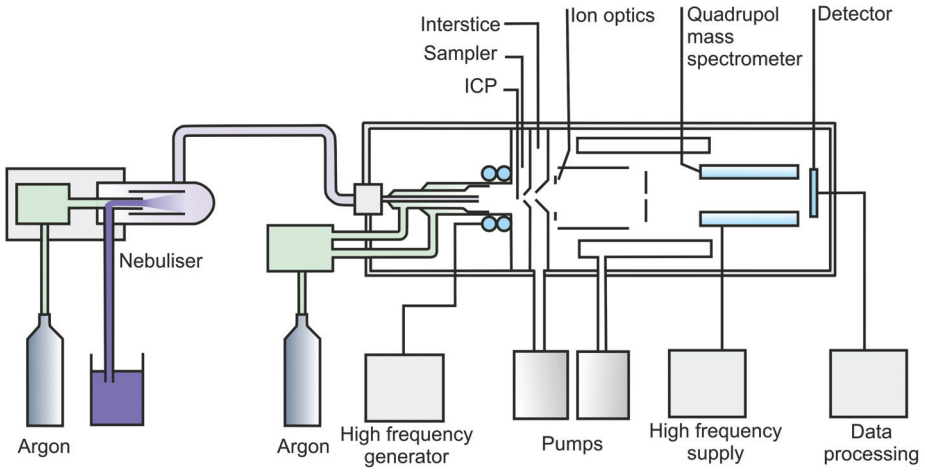

FIGURE 5.4: Schematic illustration of an ICP-MS measuring device setting (modified after Schwedt, 1992)

5.3 Molecular Composition of Dissolved Gas

5.3.1 Headspace Preparation

In order to investigate the composition of the dissolved gas, headspace samples were taken in the field. The sampling procedure is listed in Chapter 5.1.
In the laboratory a headspace sample was prepared, following a description by Capasso and Inguaggiato (1998). Fig. 5.5 shows the schematic procedure of headspace preparation in the laboratory. It is of great importance to determine the mass and temperature at each step of the preparation procedure in order to be able to perform the volume calculations correctly.
First, a water volume of 10 ml was taken out of the sample flask and replaced by helium (Fig. 5.5a). Then, the flasks were stored overnight at constant temperature to enable the development of a gas equilibrium. Afterwards, the gas in the head of the sample was slowly taken out by an injection, while this volume was replaced by hydrochloric acid (Fig. 5.5b). Finally, the obtained gas samples were analysed in a gas chromatograph.

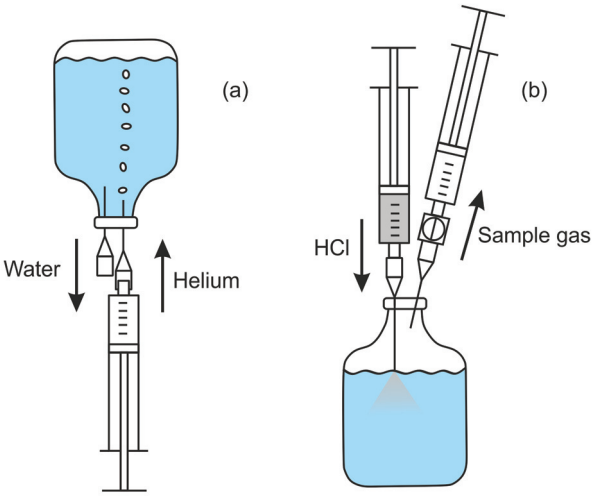

FIGURE 5.5: Schematic depiction of Headspace preparation (modified after Capasso and Inguaggiato, 1998); (a) shows the replacement of a certain water volume (10 ml) by helium, (b) depicts the withdrawal of the sample gas in the headspace after equilibration, the sample gas volume is replaced by injected hydrochloric acid

5.3.2 Gas Chromatography (GC)

The molecular gas composition of the headspace and free gas samples was measured with a gas chromatograph equipped with three different columns and corresponding detectors. Helium was used as a carrier gas for all channels. FID was used to detect hydrocarbons on a 30 m Rtx-Alumina capillary column (i.d. 0.53 mm; filling Na_2SO_4, 10 µm film thickness). Other gases (e.g. O_2, CO_2 or N_2) were resolved on two packed columns: HayeSep Q (2 m x 1/8″ OD) and MolSieve 5A (2 m x 1/8″ OD). TCD was used for detection. The FPD detector was used to identify sulfur components such as H_2S. The column is an Rtx-sulfur packed column (2 m x 1/8″ OD).

The columns described above were assembled into an oven. The measuring sequence was programmed to hold at 50 °C for 4.3 minutes and to increase to 165 °C using a gradient of 10 °C/min. This temperature was set to hold for 0.5 minutes.

In order to identify the detected peaks, the retention times of the individual peaks were compared to the retention times of the calibration gas peaks. The component concentration was calculated by comparing the area under the calibration gas peaks (where the concentration is known) to the area of the sample gas peaks. A prerequisite for this method is, that all constituents which could be detected in the investigated samples are included in the calibration gas mixture (Pytlak, 2017). Each gas sample was split to analyse its composition twice. The results of these two measurements were averaged.

5.3.3 Calculation of Dissolved Methane

Henry's law states that at chemical equilibrium and constant temperature, a specific quantity of a gas (χ_{Gas}) which is in contact with a known volume of a liquid, dissolves into the liquid. The quantity is proportional to the gas' partial pressure (P_{Gas}) (Henry, 1803). The proportion factor is called Henry's constant (K_H, equation 5.1).

$$K_H = P_{Gas}/\chi_{Gas} \quad \text{(atm/mol)} \quad (5.1)$$

K_H varies according to the temperature and the amount of Total Dissolved Solids (TDS). This principle was applied in this study to calculate the amount of dissolved methane in the collected samples. In order to calculate the total gas concentration (C_{total}) in the headspace sample, the following formulae were applied (Jurek, 2015):

$$C_{HS} = \frac{V_{HS}}{V_{total} - V_{HS}} * C_{GC} * \frac{MW}{22.4} * \frac{273}{273 + T_{sample}} * 10^3 \quad \text{(mg/l)} \quad (5.2)$$

$$C_W = 55.5 * \frac{C_{GC}}{K_H} * MW * 10^3 \quad \text{(mg/l)} \quad (5.3)$$

$$C_{total} = C_{HS} + C_W \quad \text{(mg/l)} \quad (5.4)$$

In order to obtain the correct K_H for the according temperature, the formula below is used for methane (Jurek, 2015):

$$K_{H-\mathrm{CH_4}} = 748.33 * T_{sample} + 22738 \quad \text{(mg/l)} \quad (5.5)$$

5.4 Isotopes

5.4.1 ^{14}C - Radiocarbon Dating

The ^{14}C dating method was applied to selected water samples in order to determine the age of its last participation in the hydrological cycle. Therefore, 120 litres of water were taken from these wells (Fig. 5.6). The water was mixed with NaOH and $BaCl_2$ in the field. NaOH is used to lower the pH of the sampled water, $BaCl_2$ has the purpose to precipitate the dissolved CO_2 in the water as $BaCO_3$. The sample was left overnight to let all dissolved CO_2 precipitate, afterwards the remaining water was siphoned off and the precipitate was kept for further analysis.
The analysis was performed by Hydroisotop GmbH in Schweitenkirchen (Germany). The collected $BaCO_3$ was transferred into CO_2 in the laboratory and remaining traces of atmospheric gases were removed from the sample. This CO_2 was then resublimated to its solid phase in order to ensure that the sample only contained CO_2. Afterwards, the solid CO_2 was dissolved in a solvent mixture and stored for several weeks. This time is needed to remove all possible contaminations by naturally occurring ^{222}Ra ($\tau = 3.8$ days according to Sigg and Stumm, 1989).

In order to date the water sample, the ^{14}C is not detected directly, but measured by LSC (Liquid Scintillation Counting). This method measures the number of decays per minute and calculates the amount of ^{14}C in the sample based on the decay rate. 13.57 ^{14}C-decays per minute per gram C is the atmospheric decay rate. This value indicates 100 per cent modern carbon (pmC). The older the water sample and its last participation in the hydrological cycle, respectively, the smaller is the amount of ^{14}C in the water.

FIGURE 5.6: Sampling of water for ^{14}C dating (courtesy of Łukasz Pytlak)

5.4.2 Stable Isotopes - ^{13}C, ^{2}H and ^{18}O

The stable isotope measurements of the collected samples were performed by Hydroisotop GmbH in Schweitenkirchen. The analysing technique which was applied is Isotope Ratio Mass Spectrometry (IRMS).
GC-IRMS (IRMS system coupled to a gas chromatograph) or LC-IRMS (IRMS system coupled to a liquid chromatograph) are commonly used for the analysis of complex compounds. These devices allow a component separation before the actual isotope ratio analysis. A prerequisite for a precise measurement is a steady gas stream (e.g. CO_2). Isotope ratios of light-weighted elements are determined in a GC-IRMS. The sample elutes from the GC column into an oxidation chamber, an aluminium tube containing three wires (made of Copper, Nickel and Platinum) which is normally located at the side of the GC oven. The sample is combusted and integrated into a gas mixture (e.g. CO_2, NO_x and H_2O). Then it is transferred to the reduction chamber, where nitrogen oxides are reduced to nitrogen. The excess O_2 is removed. H_2O removal is accomplished with a semipermeable membrane where the analyte is passed through and separated with a dry Helium counter-flow. This step is important due to the risk of H_2O protonating into the mass

spectrometer source causing a signal adulteration. Since a constant flow of the gas sample stream is essential, the stream velocity is constantly monitored and controlled (Muccio and Jackson, 2009). The next step of the analysis is the introduction into the mass spectrometer, which operates as described in section 5.2. The measured isotope ratios are always expressed in relation to a component-specific standard (δ-notation, Equation 5.6, 5.7 and 5.8), for carbon-isotopes a marine carbonate standard is utilised (Vienna Pee Dee Belemnite - VPDB, Craig, 1957; Hoefs, 2009), for hydrogen- and oxygen-isotopes VSMOW (Vienna Standard Mean Ocean Water) is chosen (Hoefs, 2009).

$$\delta^{13}\mathrm{C} = \frac{(^{13}\mathrm{C}/^{12}\mathrm{C})_{Sample} - (^{13}\mathrm{C}/^{12}\mathrm{C})_{VPDB}}{(^{13}\mathrm{C}/^{12}\mathrm{C})_{VPDB}} * 1000 \quad (‰) \quad (5.6)$$

$$\delta\mathrm{D} = \frac{(\mathrm{D}/\mathrm{H})_{Sample} - (\mathrm{D}/\mathrm{H})_{VSMOW}}{(\mathrm{D}/\mathrm{H})_{VSMOW}} * 1000 \quad (‰) \quad (5.7)$$

$$\delta^{18}\mathrm{O} = \frac{(^{18}\mathrm{O}/^{16}\mathrm{O})_{Sample} - (^{18}\mathrm{O}/^{16}\mathrm{O})_{VSMOW}}{(^{18}\mathrm{O}/^{16}\mathrm{O})_{VSMOW}} * 1000 \quad (‰) \quad (5.8)$$

5.4.3 Stable Isotopes (^{13}C and ^{2}H) - Free Gas samples

A Trace GC-ultra gas chromatograph coupled to a ThermoFisher Delta-V isotope ratio mass spectrometer (IRMS) with a combustion and high temperature reduction interface (GC Isolink, ThermoFisher) was used to perform the stable isotope measurements of C and H on the collected free gas samples. The gas chromatograph contained a 25 m PoraPlot capillary column (i.d. 0.32 mm; 0.10 μm film thickness). Helium served as a carrier gas. The measurement configuration was set to increase the oven temperature from 30-180 °C by 5 °C/min and to hold it at 180 °C for 5 minutes.
The calibration measurements, performed before and after each sample analysis, were conducted using an in-house standard gas (CO_2 or H_2). Another calibration gas, containing C_1-C_6 hydrocarbons and CO_2 with a known isotopic signature, was used to secure reproducibility via control measurements on a regular basis. The isotopic sample composition is reported as $^{2}\mathrm{H}/^{1}\mathrm{H}$ (relative to VSMOW) and $^{13}\mathrm{C}/^{12}\mathrm{C}$ (relative to VPDB) ratios (Pytlak, 2017). Similar to the analysis of the dissolved gas composition, each sample was split to perform to measuring sequences.

5.5 Geothermometers

Geothermometers are commonly used to evaluate hydrothermal systems with a special emphasis to receive the temperature of the water within the geothermal reservoir. Since this temperature cannot always be determined, either because no geothermal well has been drilled yet or due to temperature losses during thermal water recovery, geothermometry is used to derive this property from the chemical composition of the water. Hence, this technique is often applied in geothermal exploration. An equilibrium state of the multicomponent system reservoir rock - water - gas within the observed aquifer is a

prerequisite for this method (e.g. Wishart, 2015; Can, 2002; Michel, 1997). Because of the individual properties and conditions in the underground, depending on the occurring formations and their structural setting, most of the proposed formulae for geothermometers are based on empirical measurements and regional calibrations. However, there are a few prerequisites, which have to be met in order to obtain meaningful results (Michel, 1997; Fournier et al., 1974; Michard, 1979):

- Long contact duration of thermal water and the homogenous aquifer formation
- Dissolution of ions and molecules from the formation into the water resulting in a temperature-dependent, thermodynamic equilibrium state
- Due to the abundance of dissolvable mineral components, the equilibrium is controlled by the temperature-dependent saturation of the thermal water
- Long groundwater residence time to reach this equilibrium
- Rapid ascension of thermal waters to prevent a variation of the equilibrium during water cooling
- No mixture of thermal waters and shallow or superficial groundwaters
- An oversaturation of specific mineral components in recovered thermal waters, this oversaturation enables an estimation of the reservoir temperature in the subsurface

Several Alkali-geothermometers (Na/K, K/Mg and Na/Li) have been calculated for selected samples. The equations which were used for these calculations are listed below. They were derived from the following publications: Fournier (1979), Arnórsson et al. (1983), Nieva and Nieva (1987), Giggenbach (1988), Verma and Santoyo (1997), Can (2002) and Drever (2005). The ion concentrations are given in mg/l.

$$T_{Fournier} = \frac{1217}{\log(Na/K) + 1.483} - 273.15 \quad (°C) \quad (5.9)$$

$$T_{Arnórsson\ et\ al.} = \frac{1319}{\log(Na/K) + 1.699} - 273.15 \quad (°C) \quad (5.10)$$

$$T_{Nieva\&Nieva} = \frac{1178}{\log(Na/K) + 1.239} - 273.15 \quad (°C) \quad (5.11)$$

$$T_{Giggenbach1} = \frac{1390}{\log(Na/K) + 1.750} - 273.15 \quad (°C) \quad (5.12)$$

$$T_{Verma\&Santoyo} = \frac{1289}{\log(Na/K) + 1.615} - 273.15 \quad (°C) \quad (5.13)$$

$$T_{Can} = \frac{1052}{1 + e^{1.714 * \log(Na/K) + 0.252}} + 76 \quad (°C) \quad (5.14)$$

$$T_{Giggenbach2} = \frac{4410}{14 - \log(K^2/Mg)} - 273.15 \quad (^{\circ}\text{C}) \quad (5.15)$$

$$T_{Drever} = \frac{1590}{0.776 + \log(Na/Li)} - 273.15 \quad (^{\circ}\text{C}) \quad (5.16)$$

6 Results and Discussion

6.1 General Data

In total, 32 samples were taken from springs, municipal water supply wells, private water wells and thermal wells either utilised for balneological or energy supply purposes. These samples can be categorised into different aquifer horizons (Fig. 1.1): two samples were taken from springs in the Bohemian Massif and one from a well in this group, two samples from Quaternary deposits, ten samples from Ottnangian Sandstones (either described as Ottnangian Sandstone, fossil-rich coarse sands (Ottng.) or Natternbach Sands), six samples from Ottnangian Schlier, three samples from the Atzbach Sands, four samples from the Linz Sands, one sample from the Rupelian and three samples from Malmian carbonates. The samples were taken in five campaigns between September 2017 and January 2018.

General data of the sample locations (visible in Fig. 1.1) are summarised in Table 6.1. Well depth and total depth of the samples corrected to sea level are listed in two separate columns. The aquifer information was either provided by the owners of the according water wells or derived from literature data. For data security reasons, the well names were anonymised.

Due to the lack of well data for several of the selected sampling points, the drilled aquifers had to be reconstructed on the base of literature data. This was applied to the sample points no. 4, 15, 20, 22, 24 and 25. Geological surface maps and borehole data of wells drilled near the sample points 4, 20 and 22 (according to Land Oberösterreich, 2018) served for the reconstruction of aquifer data for these locations. A study conducted by Lengauer et al. (1987) provided sufficient information to assign an aquifer to the corresponding well location and depth. Fig. 6.1 and 6.2 show cross-sections of the publication with the inserted sample points of this thesis.

TABLE 6.1: Sample number, well depth (true vertical depth is listed in column 2 and corrected depth above sea level is listed in column 3) and aquifer of collected samples

Sample No.	Well Depth [m]	Above Sea Level [m]	Aquifer
1	0	843	Spring in Bohemian Massif
2	88	192	Linz Sands
3	26	257	Glacial Terraces
4	34	278	Ottnangian Sandstone*
5	65	645	Bohemian Massif
6	0	360	Spring in Bohemian Massif
7	200	89	Linz Sands
8	160	236	Fossil-rich Coarse Sands (Ottng.)
9	51	319	Fossil-rich Coarse Sands (Ottng.)
10	71	333	Fossil-rich Coarse Sands (Ottng.)
11	120	280	Fossil-rich Coarse Sands (Ottng.)
12	125.5	305	Fossil-rich Coarse Sands (Ottng.)
13	124	312	Fossil-rich Coarse Sands (Ottng.)
14	66.5	306	Fossil-rich Coarse Sands (Ottng.)
15	166	194	Linz Sands*
16	220	160	Atzbach Sands
17	140	215	Atzbach Sands
18	180	228	Ottnangian Schlier
19	50	332	Natternbach Sand
20	72	323	Ottnangian Sandstone*
21	55	375	Atzbach Sands
22	87	369	Ottnangian Schlier*
23	85	340	Ottnangian Schlier
24	158	177	Ottnangian Schlier*
25	9	326	Alluvial and Glacial deposits*
26	60	284	Ottnangian Schlier
27	65	285	Ottnangian Schlier
28	646	-326	Rupelian
29	479	-173	Linz Sands
30	2214	-1799	Cenomanian/Malmian/Doggerian
31	1560	-1228	Malmian
32	2056	-1489	Malmian/Doggerian

* Aquifer derived from literature

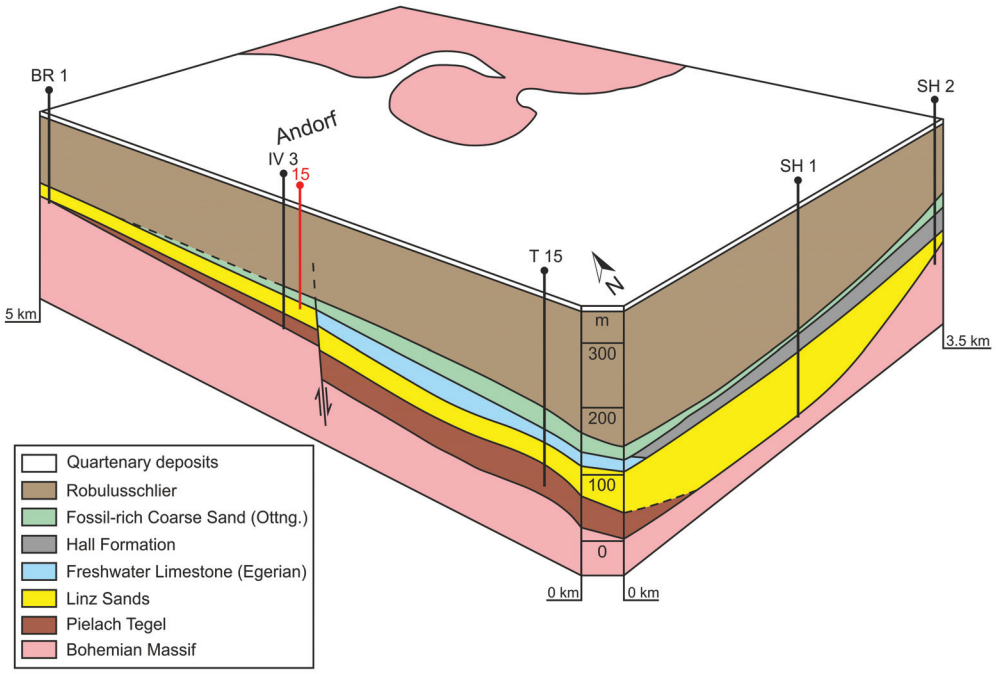

FIGURE 6.1: Three-dimensional subsurface model of the southern Taufkirchen Bay south of Leoprechting; the cross-section was reconstructed according to the formation tops of wells drilled in this area, well abbreviations BR 1 - Braunau 1; IV 3 - Innviertel 3; T 15 - Taufkirchen 15; SH 1 - Siegharting 1; SH 2 - Siegharting 2; 15 - Sample no. 15 (modified after Lengauer et al., 1987)

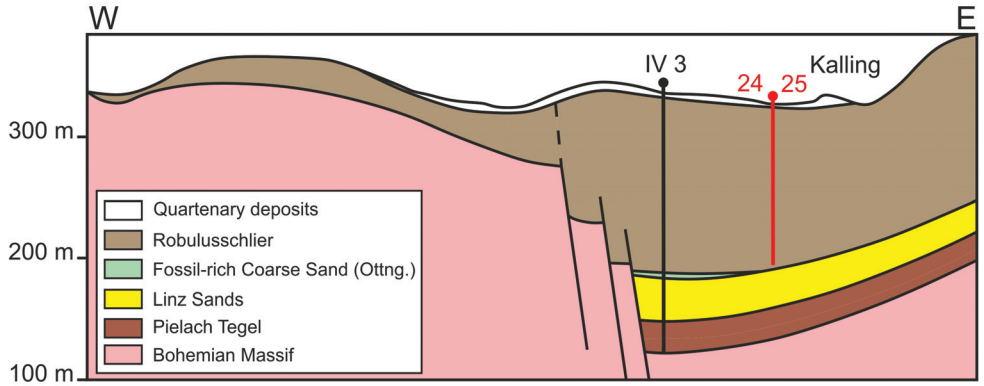

FIGURE 6.2: Cross-section across the Taufkirchen Bay near Kalling, well abbreviations IV 3 - Innviertel 3; 24 - Sample no. 24; 25 - Sample no. 25 (modified after Lengauer et al., 1987)

TABLE 6.2: Physical parameters of collected samples (field measurements)

Sample No.	Depth [m]	Temperature [°C]	pH [-]	Redox Potential [mV]	Conductivity [µS/cm]	O_2 [mg/l]
1	0	8.0	6.14	360	75	8.80
2	88	16.4	8.38	-295	460	0.04
3	26	12.9	7.15	270	867	11.25
4	34	11.7	6.70	130	360	0.49
5	65	8.1	6.76	34	160	0.01
6	0	11.4	7.13	59	282	0.21
7	200	19.7	8.34	-248	467	2.50
8	160	11.7	7.57	24	378	0.17
9	51	10.8	7.53	45	534	6.30
10	71	10.9	7.75	-124	322	0.01
11	120	11.8	7.68	-85	317	0.02
12	125.5	10.8	7.56	-98	468	0.16
13	124	10.6	7.53	-150	476	0.01
14	66.5	11.4	7.60	-133	410	0.10
15	166	13.2	8.29	93	703	2.50
16	220	12.2	8.76	-173	460	0.04
17	140	12.5	8.64	-213	480	0.03
18	180	11.4	8.61	-149	471	0.06
19	50	10.1	7.38	-18	544	0.27
20	72	10.7	6.59	75	511	0.07
21	55	10.5	6.44	175	154	8.39
22	87	10.0	7.44	-	571	-
23	85	9.7	7.48	-168	605	0.50
24	158	12.0	7.89	16	440	5.17
25	9	8.8	7.29	141	254	10.25
26	60	11.0	7.41	20	577	2.47
27	65	9.1	7.77	-57	460	2.55
28	646	36.6	8.34	-315	558	0.01
29	479	38.3	8.59	-303	827	0.01
30	2214	27.1*	7.25	-190	1428	1.92
31	1560	51.4*	6.93	-310	1431	0.04
32	2056	49.2*	7.72	-80	2010	2.29

* Water temperature after cooling

6.2 Hydrochemical Characteristics

6.2.1 Physical Parameters

The field parameters, which were measured at the sampling site, are listed in table 6.2. The O_2 content is supposed to be close to zero for the deep groundwater samples. However, due to the sampling conditions this value could not always be achieved.

All samples show pH values in a range of 6 to 9. According to investigations of Kralik et al. (2005), this range is common for water samples in Austria. Sample no. 1 shows the lowest pH, plotting between values of rain water and waters hosted by fractured aquifers. This is explained by the sampling location, a spring within the Bohemian Massif which results in a high influx of meteoric water. Sample no. 21 is also characterised by

a low pH value. Although this well recovers water from the Atzbach Sands, its location is close to the Bohemian Massif. The highest pH values are encountered in the samples located in the Rupelian, Linz and Atzbach Sands. The thermal water samples do not show a deviation compared to the shallower waters.
Eh values indicate environmental conditions regarding the supply of oxygen. Positive values are linked to oxidising conditions and contact of water with O_2, negative values are the result of oxygen depletion and therefore reducing environments. Mostly, these negative Eh values appear in combination with the occurrence of CH_4 and H_2S (Wisotzky, 2012). Most of the collected samples show values in accordance with this description. While deeper wells are characterised by negative Redox potentials, positive values were measured in the shallow waters and springs. Samples 15 and 24 show a positive Eh although their well depth would suggest, that these waters originate from reducing environments. Since both waters were only accessible via a tap, this facility could have caused a contamination of oxygen during the measurements. The same effect could have also caused the different Redox potential in sample 32 compared to the other Malmian waters. Sample 6, a spring in the Bohemian Massif shows a significantly lower Eh than expected for a spring sample.

In comparison to the other wells, the conductivity of the Malmian thermal water samples is highly increased. They range between 1428-2010 μS/cm, which is more than double as the other results. The samples from the Bohemian Massif form the lower end of the conductivity scale with values between 75-282 μS/cm. The waters from wells 21 and 25 fit into this range as well. Although sample 3 was also recovered from shallow strata, its value is significantly increased. Waters from the Innviertel Group and Linz Sands (except for the samples 15 and 29) are characterised by conductivities between 317-605 μS/cm. Surprisingly, sample 28 does not show an increased value, although it is recovered from a geothermal well in the Rupelian.
In order to visualise possible correlations of physical parameters of the water samples, pH was plotted against Eh (Fig. 6.3) and electrical conductivity (Fig. 6.4). The crossplot in Fig. 6.3 is also used to derive information about the activity of specific compounds (e.g. Fe; Matthess, 1990). The water samples from this study are located in the range of natural groundwaters. A group of samples in the bottom right corner shows high pH values coupled with low Eh. This indicates reducing and anaerobic surrounding conditions. Waters sampled from the Malm aquifer also originate from anaerobic environments, nevertheless, their pH values are significantly lower than the pH values of the siliciclastic deep groundwaters.

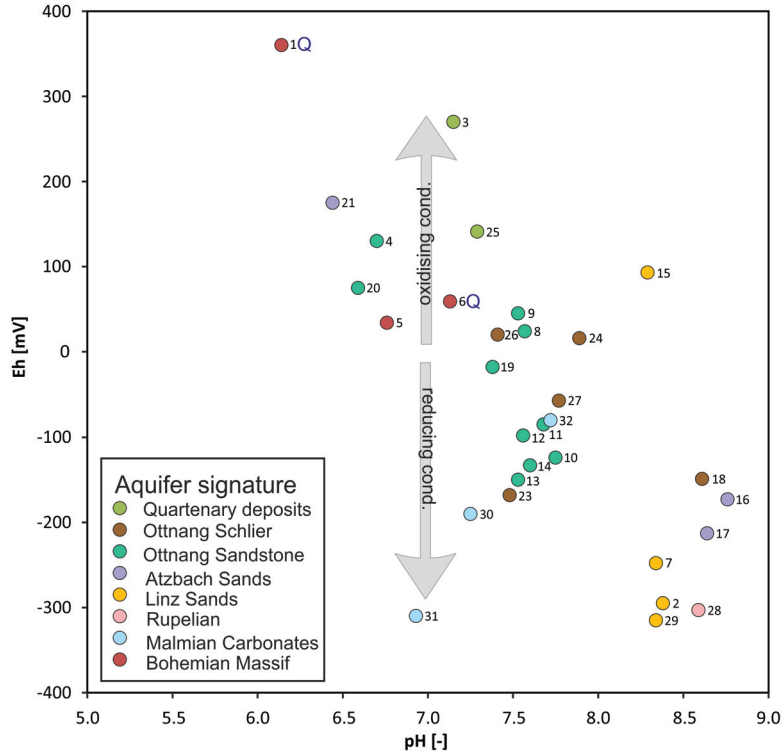

FIGURE 6.3: Crossplot of pH vs. Eh of collected samples, the grey shaded arrows indicate the trends of values in oxidising and reducing conditions

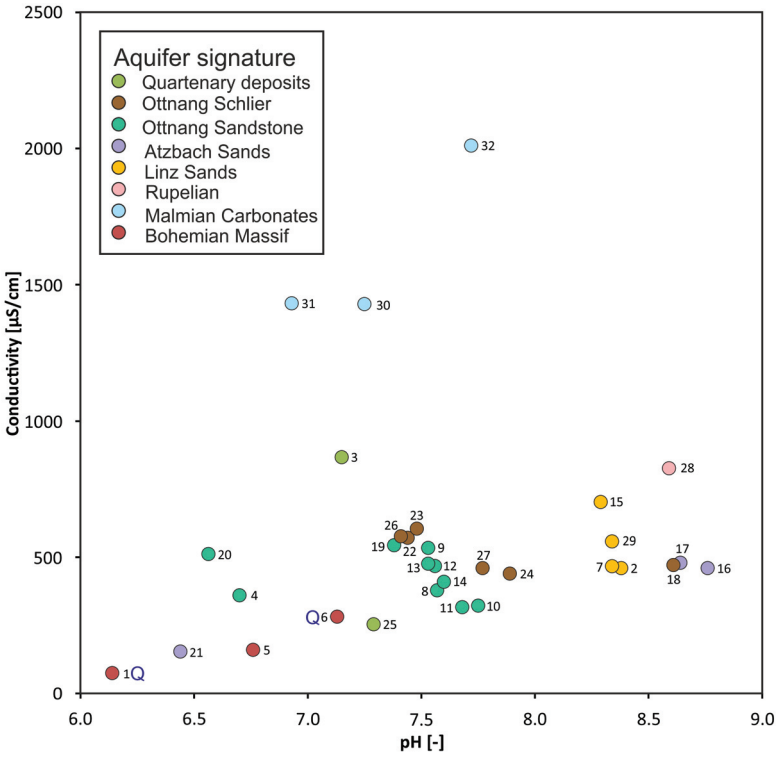

FIGURE 6.4: Crossplot of pH vs. Conductivity of collected samples

Fig. 6.4 could indicate a correlation for those samples which do not recover Malmian water. An increase in pH occurs in combination with an increase in the electrical conductivity of the samples. The samples of the crystalline basement are located in the bottom left part of the plot. Samples (between 88-646 m depth) from the Linz and Atzbach Sands and the samples 18 and 28 form a group at the right part of the plot. Sample 3 is characterised by an offset from the other groundwater samples induced by a higher electrical conductivity. This parameter is mainly influenced by the amount of dissolved solids in the water. Since the total mineralisation is significantly augmented in sample 3 as well as the Malmian water samples, they do not fit into this correlation.

Geothermal use of water resources is strongly connected with the temperature in the subsurface. Geothermal wells are usually drilled in regions with an elevated geothermal gradient, a phenomenon that is observed in the Alpine Foreland Basin. Fig. 6.5 shows the measured temperature of the water samples. Due to cooling of the thermal water during the sampling procedure, the original subsurface temperature of the samples 30, 31 and 32 could not be determined. Therefore, literature values from Elster et al. (2016) were used for this graph.

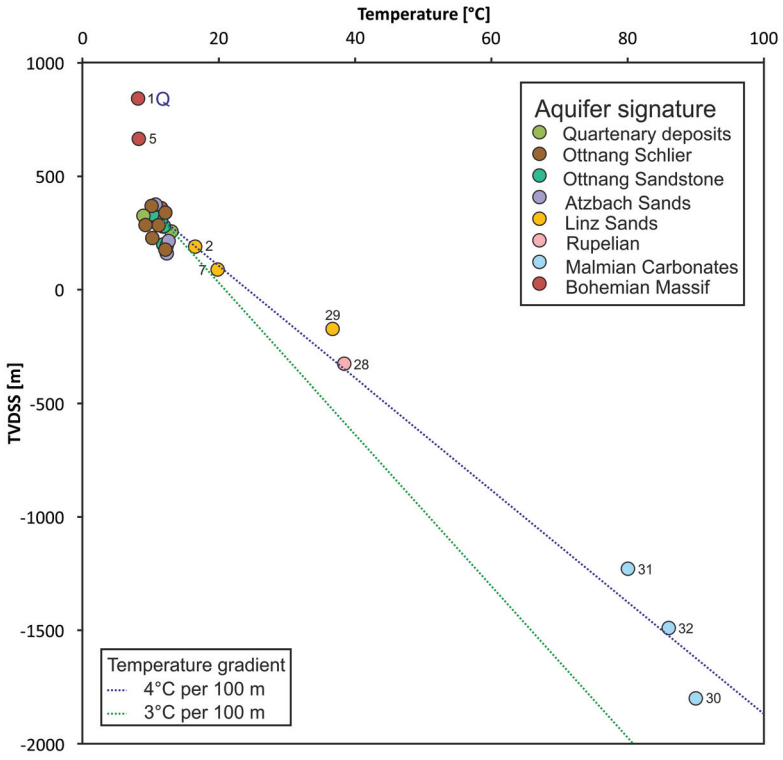

FIGURE 6.5: Crossplot of water temperature of collected samples vs. well depth (corrected to sea-level), the geothermal gradients of 3 °C and 4 °C are marked in green and blue, water temperatures for the samples 30, 31 and 32 were taken from Elster et al. (2016)

Most of the samples plot in a temperature range of 10 °C-15 °C. Apart from three samples, the well depths are greater than 15 m. In moderate climate zones, this is considered as a boundary for the influence of seasonal temperature variations on subsurface temperatures (Matthess, 1990). Sample 1 and 5 show a similar temperature compared to the large sample cluster in the plot, however, their offset position in the graph is explained by their elevation in reference to sea level. Moreover, the temperature value of the spring (sample 1) corresponds to the surface temperature of the sampling date.
The geothermal well samples as well as two samples from the Linz Sands (2 and 7) are clearly distinguishable from the others due to their increased temperature. They follow roughly the trendline of the 4 °C geothermal gradient (Fig. 6.5). Especially sample 2 and 7 show a significant temperature difference despite their similar depth compared to the major part of the other samples. This could indicate that the recovered water arises from greater depths. In terms of the reaction rate, this ascension process proceeds probably faster than the time which would be necessary to reach a temperature balance. This effect is also visible for the samples 28 and 29. The neighbouring wells are drilled in two juxtaposed fault blocks characterised by an offset of approximately 150 m. The distinct elevation of the temperature of sample 29 in relation to the geothermal gradient trendline is a second indication for this northward drainage of deep groundwater.

6.2.2 Chemical Parameters

The chemical elements and compounds which were analysed in this study are summarised in the tables below (6.3, 6.4 and 6.5). The last column in table 6.5 lists the water types assigned to the samples according to their chemical composition as suggested by Palmer (1911) and Elster et al. (2016).

A ternary diagram system after Piper (1944) summarises the most important ions of the individual samples in a graph (Fig. 6.6). Two different sample populations can be distinguished in this plot. A cluster of samples, characterised by an increased amount of Ca_2^+ and Mg_2^+ is located at the left corner of the diamond plot. The second cluster is concentrated around the bottom corner of the diamond plot. These samples show a higher amount of Na^+, the thermal waters (samples 30, 31 and 32), which form a part of this second group indicate a movement in direction towards the corner at the right side of the diamond plot. This movement is connected to an increase in the amount of dissolved chloride in the samples (table 6.5).

TABLE 6.3: Chemical parameters of collected samples

Sample No.	Ca^{2+} [mg/l]	Mg^{2+} [mg/l]	Na^{+} [mg/l]	K^{+} [mg/l]	Sr^{2+} [mg/l]	Ba^{2+} [mg/l]	Li^{+} [mg/l]	Rb^{+} [mg/l]	Cs^{+} [mg/l]	Fe^{2+} [mg/l]	Mn^{2+} [mg/l]
1	4.7	2.4	5.00	2.00	0.054	0.011	0.002	0.0006	< 0.0001	0.002	0.0005
2	5.7	1.1	106.20	1.50	0.103	0.009	0.023	0.0020	< 0.0001	0.000	0.0054
3	122.2	31.1	13.80	2.70	0.208	0.075	0.003	0.0007	< 0.0001	0.002	0.0017
4	45.0	12.6	6.50	1.40	0.123	0.028	0.005	0.0013	< 0.0001	0.047	0.0214
5	16.5	4.7	6.60	2.60	0.114	0.047	0.010	0.0010	< 0.0001	1.284	0.1178
6	32.1	9.3	8.60	3.40	0.121	0.119	0.016	0.0016	< 0.0001	0.670	0.0997
7	9.3	1.4	99.60	1.30	0.146	0.013	0.022	0.0020	< 0.0001	0.013	0.0058
8	53.9	16.7	4.84	1.07	0.310	0.026	0.016	0.0015	< 0.0001	0.019	0.0055
9	87.5	19.8	3.11	1.29	0.327	0.018	0.019	0.0015	< 0.0001	0.112	0.0266
10	47.3	11.9	4.02	1.03	0.109	0.009	0.007	0.0011	< 0.0001	0.312	0.0384
11	46.4	10.0	3.98	0.72	0.124	0.007	0.006	0.0008	< 0.0001	0.425	0.0490
12	74.9	13.5	3.11	0.75	0.222	0.009	0.010	0.0017	< 0.0001	0.029	0.0040
13	79.5	13.3	2.71	0.73	0.229	0.006	0.010	0.0020	< 0.0001	0.027	0.0029
14	60.1	16.0	3.30	0.81	0.251	0.017	0.012	0.0014	< 0.0001	0.083	0.0048
15	6.4	3.0	160.51	1.46	0.143	0.011	0.056	0.0015	< 0.0001	0.014	0.0039
16	3.3	1.1	100.25	2.38	0.085	0.030	0.084	0.0011	< 0.0001	0.003	0.0018
17	3.1	1.0	107.43	2.42	0.060	0.039	0.084	0.0014	< 0.0001	0.013	0.0036
18	3.7	1.9	110.51	1.75	0.107	0.012	0.076	0.0005	< 0.0001	0.010	0.0030
19	86.8	21.1	3.61	1.26	0.221	0.016	0.016	0.0004	< 0.0001	0.231	0.0315
20	61.3	17.6	20.90	1.79	0.204	0.027	0.017	0.0025	< 0.0001	0.138	0.8829
21	20.5	3.0	4.24	0.72	0.036	0.035	0.003	0.0001	< 0.0001	0.001	0.0038
22	70.6	26.0	6.60	1.80	0.375	0.039	0.030	0.0009	< 0.0001	1.857	0.0659
23	74.7	28.4	6.70	4.80	0.647	0.055	0.032	0.0012	< 0.0001	0.677	0.0357
24	55.8	18.6	20.70	1.60	0.944	0.046	0.036	0.0024	< 0.0001	0.268	0.0044
25	33.3	5.3	4.70	8.00	0.130	0.008	0.002	0.0017	< 0.0001	0.101	0.0029
26	78.5	21.3	6.70	1.80	0.295	0.026	0.016	0.0011	< 0.0001	0.069	0.0258
27	63.4	16.8	3.30	1.30	0.190	0.008	0.011	0.0019	< 0.0001	0.250	0.0546
28	2.9	0.7	139.10	1.50	0.050	0.006	0.027	0.0022	< 0.0001	0.005	0.0063
29	0.9	0.2	192.30	1.40	0.017	0.002	0.031	0.0021	< 0.0001	0.021	0.0019
30	9.9	1.5	263.50	14.70	0.369	0.063	0.247	0.0339	0.0016	0.014	0.0011
31	12.5	2.0	292.20	16.30	0.408	0.062	0.243	0.0377	0.0017	0.013	0.0035
32	9.6	1.7	399.60	17.60	0.381	0.394	0.272	0.0351	0.0024	0.039	0.0026

TABLE 6.4: Chemical parameters of collected samples (continued); calculated HCO_3^- concentrations are marked in red

Sample No.	HCO_3^- [mg/l]	Cl^- [mg/l]	SO_4^{2-} [mg/l]	NO_3^- [mg/l]	F^- [mg/l]	I^- [mg/l]	Br^- [mg/l]	Cu [mg/l]	Zn [mg/l]	Pb [mg/l]
1	20.86	1.60	8.4	9.6	< 0.05	< 0.0001	0.0103	0.0011	0.0101	< 0.0001
2	284.95	6.20	5.6	0.0	0.270	0.0181	0.0501	0.0002	< 0.0001	< 0.0001
3	435.08	39.40	36.1	29.1	0.120	0.0001	0.0337	0.0024	0.0272	0.0002
4	137.84	13.10	39.6	13.4	0.140	0.0003	0.0142	0.0013	0.0181	< 0.0001
5	83.96	1.10	9.8	< 0.5	0.070	0.0008	0.0036	0.0013	0.0030	< 0.0001
6	142.05	4.50	20.3	0.6	0.230	0.0017	0.0121	0.0003	0.0016	< 0.0001
7	285.36	7.90	3.6	-	0.250	0.0232	0.0635	0.0003	< 0.0001	< 0.0001
8	241.01	0.81	15.6	< 0.5	0.126	0.0014	0.0053	0.0011	< 0.0001	< 0.0001
9	341.69	0.92	24.2	< 0.5	0.226	0.0011	0.0033	0.0005	< 0.0001	< 0.0001
10	213.56	0.70	6.3	< 0.5	0.145	0.0022	0.0051	0.0013	< 0.0001	< 0.0001
11	207.45	0.76	6.4	< 0.5	0.136	0.0007	0.0051	< 0.0001	< 0.0001	< 0.0001
12	247.11	5.38	45.7	< 0.5	0.112	0.0006	0.0079	0.0003	< 0.0001	< 0.0001
13	253.22	5.70	47.8	< 0.5	0.084	0.0006	0.0109	0.0005	< 0.0001	< 0.0001
14	241.01	2.10	29.6	< 0.5	0.133	0.0007	0.0056	0.0002	< 0.0001	< 0.0001
15	375.25	46.70	< 0.5	< 0.5	0.576	0.1915	0.4712	0.0016	0.0747	< 0.0001
16	268.47	5.57	13.6	< 0.5	0.159	0.0561	0.0185	0.0005	0.0070	< 0.0001
17	286.78	2.48	18.3	< 0.5	0.135	0.0234	0.0079	0.0017	0.0163	< 0.0001
18	317.28	0.47	0.3	< 0.5	0.328	0.0121	0.0062	0.0003	0.0274	< 0.0001
19	347.79	2.99	25.1	1.6	0.089	0.0078	0.0006	0.0007	0.0073	< 0.0001
20	244.06	19.14	44.4	< 0.5	0.113	0.0226	0.0047	0.0016	0.0199	< 0.0001
21	67.13	1.79	3.8	15.5	0.069	0.0091	< 0.0001	0.0007	0.0119	< 0.0001
22	335.59	7.30	21.8	< 0.5	0.100	0.0025	0.0125	< 0.0001	0.0404	< 0.0001
23	356.90	6.30	27.8	< 0.5	0.110	0.0019	0.0082	0.0004	0.0055	< 0.0001
24	298.00	0.60	17.8	< 0.5	0.530	0.0018	0.0069	0.0010	0.0326	< 0.0001
25	134.24	2.30	4.4	11.2	0.100	< 0.0001	0.0025	0.0095	0.1303	0.0002
26	323.38	4.10	28.8	< 0.5	0.190	0.0015	0.0047	0.0015	0.1147	< 0.0001
27	259.32	2.60	21.4	< 0.5	0.130	0.0008	0.0075	0.0015	0.6885	0.0004
28	353.89	21.10	6.3	< 0.5	0.490	0.1631	0.5445	0.0007	0.0012	< 0.0001
29	369.15	76.90	6.4	< 0.5	0.920	0.0438	0.1502	0.0014	0.0132	0.0001
30	524.74	134.40	5.9	< 0.5	5.610	0.4144	0.8288	0.0013	0.0096	< 0.0001
31	533.04	169.80	4.5	< 0.5	6.010	0.4152	0.8415	0.0003	0.0070	0.0001
32	676.06	252.20	43.6	< 0.5	7.240	0.5222	1.2848	0.0010	0.0049	< 0.0001

TABLE 6.5: Chemical parameters of collected samples (continued)

Sample No.	Cd [mg/l]	Al [mg/l]	As [mg/l]	Cr [mg/l]	Ni [mg/l]	U [mg/l]	Co [mg/l]	Mo [mg/l]	V [mg/l]	TDS [mg/l]	Water Type
1	< 0.0001	0.0027	< 0.0001	0.0002	0.0013	< 0.0001	< 0.0001	< 0.0001	0.0004	55	Na-Ca-Mg-HCO_3-SO_4
2	< 0.0001	0.0019	< 0.0001	< 0.0001	< 0.0001	< 0.0001	< 0.0001	< 0.0001	< 0.0001	412	Na-HCO_3
3	< 0.0001	0.0017	0.0002	0.0014	0.0005	0.0012	< 0.0001	0.0002	0.0005	710	Ca-Mg-HCO_3
4	< 0.0001	0.0020	0.0009	< 0.0001	0.0009	0.0020	0.0001	0.0013	0.0003	270	Ca-Mg-HCO_3-SO_4
5	< 0.0001	0.0019	< 0.0001	< 0.0001	< 0.0001	< 0.0001	< 0.0001	0.0004	< 0.0001	127	Ca-Mg-HCO_3
6	< 0.0001	0.0015	< 0.0001	< 0.0001	< 0.0001	< 0.0001	< 0.0001	0.0013	< 0.0001	222	Ca-Mg-HCO_3
7	< 0.0001	0.0022	< 0.0001	< 0.0001	0.0003	< 0.0001	< 0.0001	< 0.0001	< 0.0001	409	Na-HCO_3
8	< 0.0001	0.0014	0.0001	< 0.0001	0.0007	< 0.0001	< 0.0001	0.0011	< 0.0001	334	Ca-Mg-HCO_3
9	< 0.0001	0.0015	0.0002	< 0.0001	< 0.0001	< 0.0001	< 0.0001	0.0006	< 0.0001	479	Ca-Mg-HCO_3
10	< 0.0001	0.0022	0.0015	< 0.0001	0.0003	< 0.0001	< 0.0001	0.0004	< 0.0001	285	Ca-Mg-HCO_3
11	< 0.0001	0.0010	0.0000	< 0.0001	< 0.0001	< 0.0001	< 0.0001	0.0004	< 0.0001	277	Ca-Mg-HCO_3
12	< 0.0001	0.0011	0.0005	< 0.0001	< 0.0001	< 0.0001	< 0.0001	0.0010	< 0.0001	391	Ca-Mg-HCO_3
13	< 0.0001	0.0013	0.0004	< 0.0001	0.0008	< 0.0001	< 0.0001	0.0010	< 0.0001	403	Ca-Mg-HCO_3
14	< 0.0001	0.0010	0.0002	< 0.0001	< 0.0001	< 0.0001	< 0.0001	0.0009	< 0.0001	353	Ca-Mg-HCO_3
15	< 0.0001	0.0014	0.0000	< 0.0001	< 0.0001	< 0.0001	< 0.0001	0.0005	< 0.0001	594	Na-HCO_3
16	< 0.0001	0.0019	< 0.0001	0.0002	< 0.0001	< 0.0001	< 0.0001	0.0003	< 0.0001	395	Na-HCO_3
17	< 0.0001	0.0027	< 0.0001	0.0003	0.0002	< 0.0001	< 0.0001	0.0003	< 0.0001	422	Na-HCO_3
18	< 0.0001	0.0015	< 0.0001	0.0002	< 0.0001	< 0.0001	< 0.0001	0.0002	< 0.0001	436	Na-HCO_3
19	< 0.0001	0.0016	0.0011	0.0002	0.0001	0.0009	0.0002	0.0006	< 0.0001	491	Ca-Mg-HCO_3
20	< 0.0001	0.0028	0.0014	0.0003	0.0024	0.0004	0.0006	0.0023	0.0002	411	Ca-Mg-HCO_3
21	< 0.0001	0.0021	0.0002	0.0009	< 0.0001	< 0.0001	< 0.0001	< 0.0001	0.0003	117	Ca-HCO_3
22	< 0.0001	0.0008	0.0001	< 0.0001	< 0.0001	< 0.0001	< 0.0001	0.0008	< 0.0001	472	Ca-Mg-HCO_3
23	< 0.0001	0.0385	< 0.0001	< 0.0001	< 0.0001	< 0.0001	< 0.0001	0.0008	< 0.0001	507	Ca-Mg-HCO_3
24	< 0.0001	0.0049	< 0.0001	< 0.0001	< 0.0001	< 0.0001	< 0.0001	0.0002	< 0.0001	415	Ca-Mg-HCO_3
25	< 0.0001	0.0251	0.0015	0.0009	< 0.0001	0.0003	< 0.0001	0.0005	0.0013	204	Ca-HCO_3
26	< 0.0001	0.0040	0.0003	< 0.0001	0.0013	< 0.0001	< 0.0001	0.0005	< 0.0001	465	Ca-Mg-HCO_3
27	< 0.0001	0.0049	0.0032	< 0.0001	< 0.0001	< 0.0001	< 0.0001	0.0004	< 0.0001	369	Ca-Mg-HCO_3
28	< 0.0001	0.0079	< 0.0001	< 0.0001	< 0.0001	< 0.0001	< 0.0001	< 0.0001	< 0.0001	526	Na-HCO_3-Cl
29	< 0.0001	0.0242	< 0.0001	< 0.0001	< 0.0001	< 0.0001	< 0.0001	< 0.0001	< 0.0001	648	Na-HCO_3
30	< 0.0001	0.0135	0.0003	< 0.0001	0.0006	< 0.0001	< 0.0001	< 0.0001	< 0.0001	961	Na-HCO_3-Cl
31	< 0.0001	0.0090	0.0002	< 0.0001	0.0001	< 0.0001	< 0.0001	< 0.0001	< 0.0001	1037	Na-HCO_3-Cl
32	< 0.0001	0.0130	0.0001	< 0.0001	0.0002	< 0.0001	< 0.0001	< 0.0001	< 0.0001	1409	Na-HCO_3-Cl

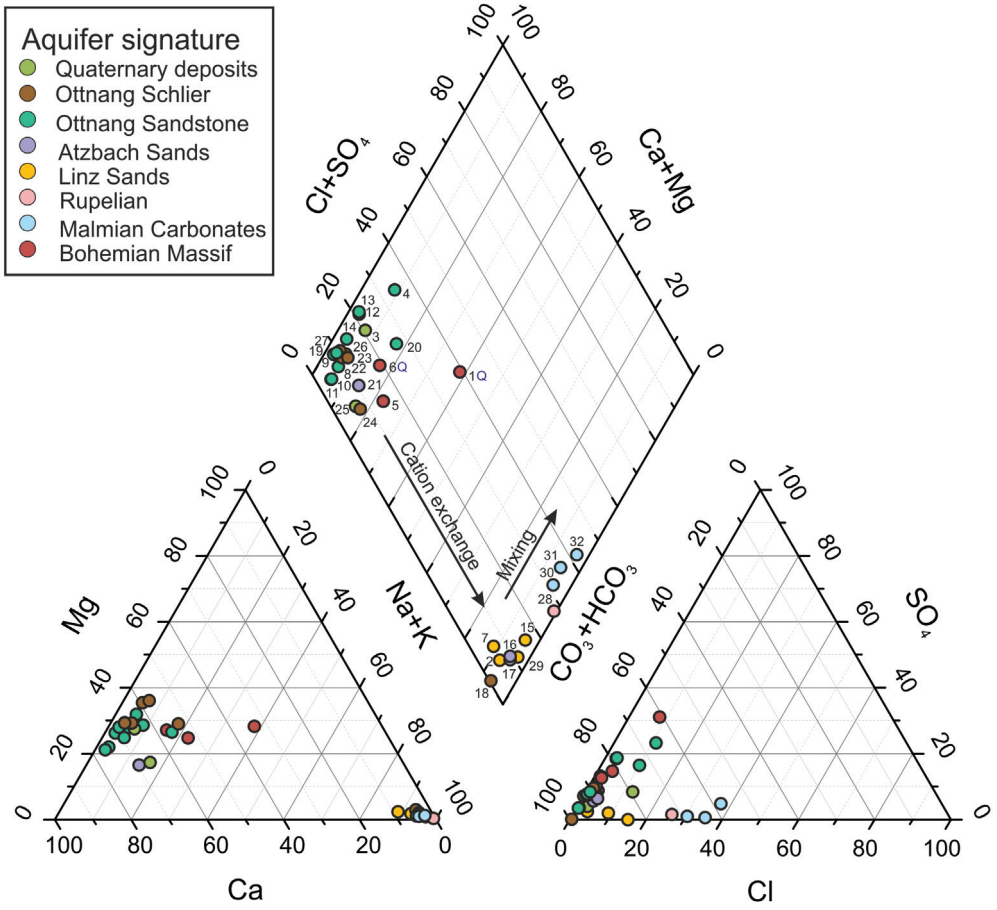

FIGURE 6.6: Ternary diagram (after Piper, 1944) of the collected samples. The movement of the sample points within the plot according to the physical processes (cation exchange according to Goldbrunner, 1988) are marked with arrows and labelled

The results of the sampled Ca-(Mg)-HCO_3 waters from this study are consistent with data published by Kralik et al. (2005), who investigated shallow water wells in Upper Austria. This could be an indication that most of the groundwater samples investigated in this study are neither in contact with the Malmian carbonate aquifer nor have they experienced mixing with this thermal water. Samples from the Malmian aquifer are similar to published data of Andrews et al. (1987) and Goldbrunner (1988). Waters showing similar characteristics to the Malmian samples and which plot in the vicinity of these thermal aquifer samples could be interpreted as waters characterised by an advanced cation exchange, the direction of movement within the plot during cation exchange is marked with an arrow (Fig. 6.23). A second process, which could lead to a further movement of the sample points towards the Malmian groundwaters is the increased thermal water influence due to mixing processes. This is illustrated by a second arrow (Fig. 6.23).

In Figure 6.7, a basemap of the study area with all sampling locations is shown. The chemical composition of the water samples is illustrated using pie diagrams showing the

main ions in different colours stated in the legend. The size of the pie diagrams reflects the overall mineralisation of the sample; large diagrams indicate a high mineralisation, whereas small circles stand for a low amount of Total Dissolved Solids. The dots marking the sampling sites are coloured according to the aquifer layer.

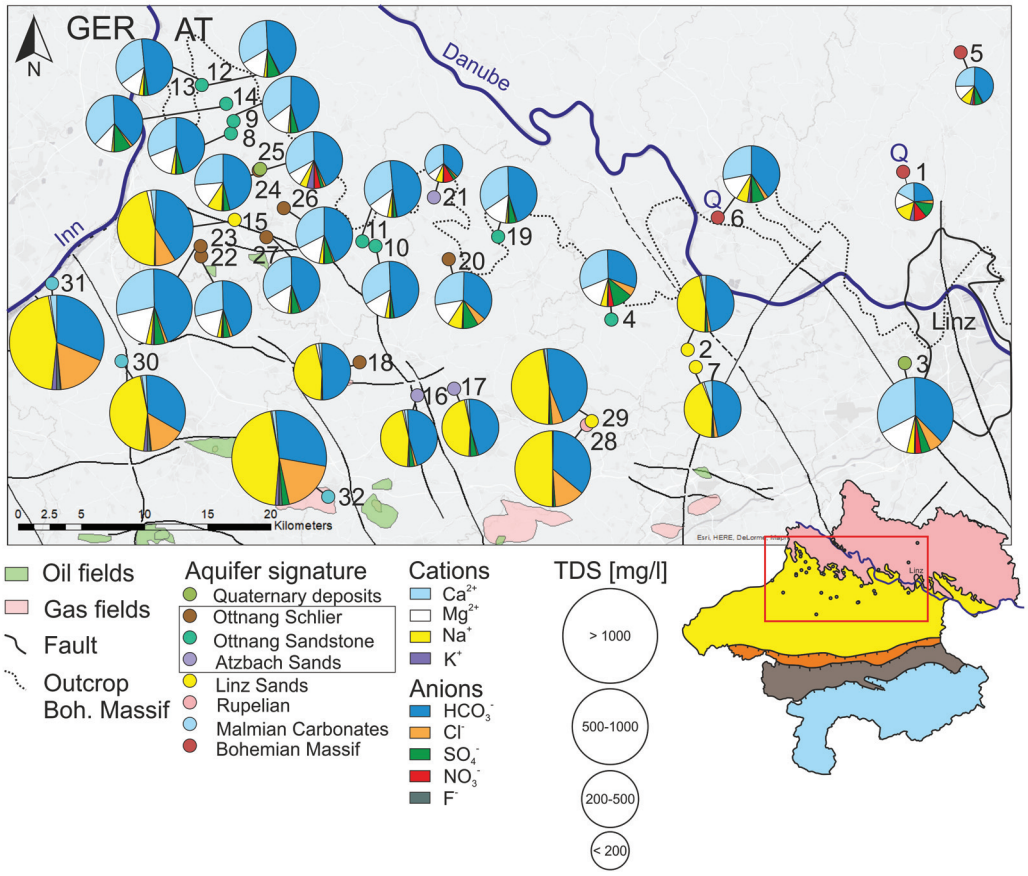

FIGURE 6.7: Basemap of Upper Austria with locations of the collected water samples, marked according to their aquifer (the aquifers which can be assigned to the Innviertel Group are framed with a black rectangle) and pie diagrams illustrating the percentual composition of the main ions.

The summary of all pie diagrams in one figure clearly shows, that the major part of the samples belong to the Ca-(Mg)-HCO_3-Type. These samples, mainly concentrated in the northern part of the study area, are included in the cluster on the left corner of the diamond diagram in Fig. 6.6. Seven samples (samples 2, 7, 15, 16, 17, 18 and 29) can be assigned to Na-HCO_3-Type, four to Na-HCO_3-Cl-Type waters (samples 28, 30, 31 and 32). The lowest mineralisation is observed in samples from the Bohemian Massif (samples 1, 5 and 6) and sample 21, which resembles the groundwater of the Bohemian Massif in its characteristics. Therefore, it can be assumed that the recharge area for this part of the aquifer is located in the crystalline basement. On average, the total mineralisation of samples 1, 5, 6 and 21 is 134 mg/l. The amount of dissolved solids from the shallow

porous strata of the Molasse Basin is on average 385 mg/l (table 6.5). The thermal waters recovered from the Malmian carbonates range between 961-1409 mg/l (table 6.5). A closer look at the regional distribution of these samples reveals that, with exception of sample 15, samples containing high amounts of sodium or chloride are preferably encountered in the southern part of the study area. The same waters can be found in the bottom cluster of the diamond graph in Fig. 6.6. Apart from the geothermal wells, the well depths of these samples mentioned (samples 2, 7, 15, 16, 17 and 18) do not greatly differ in their order of magnitude from the wells sampled in the north. However, the samples 15, 16, 17 and 18 are located in the vicinity of the Lindach fault and a conjugation of this fracture zone. This fault could maybe serve as a pathway for the upwards migration of thermal water. An increased groundwater residence time in the area of the samples 16, 17 and 18 could have also lead to the development of their hydrochemical characteristics.

Figures 6.8-6.23 show crossplots of different ions against the amount of dissolved solids of the individual samples. In Figure 6.8, **sodium** is plotted on the diagram ordinate. The plot shows, that the sodium concentration of the major part of the samples does not exceed 21 mg/l. Only the thermal water samples (samples 28-32) and a few other waters (samples 2, 7, 15, 16, 17 and 18) exceed this sodium content. Their amount of dissolved sodium ranges between 99-400 mg/l (table 6.3). These waters from the Malmian carbonates form a linear trendline with the waters from the Rupelian, Linz and Atzbach Sands.
Although sample 3 comes from a quaternary age aquifer, it has a higher mineralisation than all other waters, except the ones from the Malmian carbonates. This is probably caused by the sampling conditions and not by natural conditions. Since this sample was taken from a public pool facility, chloride is added to the water due to hygiene regulations. The sample was taken at a tap bearing untreated groundwater. However, the chloride is added in the vicinity of this tap. Since the chloride content of the sample is strongly increased in comparison to the other ions contained (Fig. 6.16) it is probably contaminated by the additive and hence, cannot give a reliable result regarding its total mineral content.

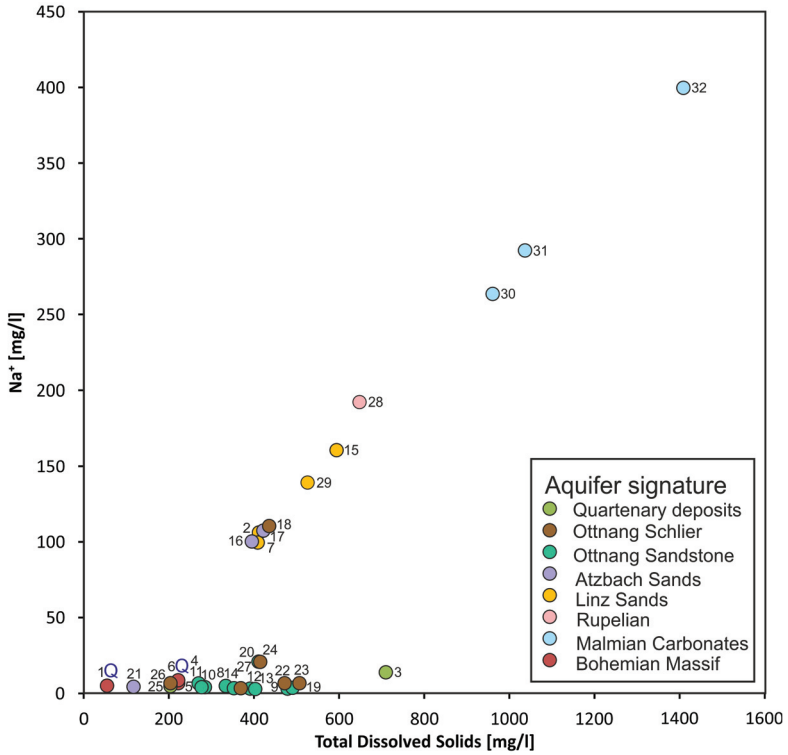

FIGURE 6.8: Crossplot of Na^+ vs. Total Dissolved Solids

The crossplot with K^+ on the diagram ordinate (Fig. 6.9) shows, similar to the major part of the other figures (Fig. 6.13, 6.15 and 6.16), that this element is enriched in the Malmian waters. The **potassium** content of the samples 30, 31 and 32 varies between 14 and 18 mg/l, whereas the amount contained in other waters does not exceed 5 mg/l. Sample 25 is the only exception, this water is characterised by a K^+-content of 8 mg/l (table 6.3). In contrast to the Malmian samples, the thermal wells producing from the Linz Sands and Rupelian do not show any significant differences in comparison to the shallower groundwater wells. This leads to the assumption, that potassium is not able to serve as an indicator for (ascending) deep groundwaters. Sample 25 also shows an increased potassium content. However, because this water originates from a shallow water supply source, this K^+-content may be a result of anthropogenic influence. Wastewater or agricultural fertilisers could be responsible for an enhanced potassium supply in groundwater (Matthess, 1990). Sample 1, 5 and 6 from the Bohemian Massif form a group with a slight offset from the other groundwaters. Thus, the reason for this observation is probably naturally conditioned. Feldspar is one of the major components of granite, especially in felsic granite, potassium-rich feldspar occurs frequently. Weathering processes decompose and dissolve these minerals. The released elements are then diluted into the surrounding groundwater causing an enrichment of certain ions. Moreover, an increase of this ion coupled to the amount of total dissolved solids is also observed within these three samples. For sample 23, a different reason for the increased potassium content is assumed. Since this well recovers water from the Ottnang Schlier, a clay-rich formation, a

higher circulation period within this formation could have lead to a concentration of this element because potassium forms a major component in clay minerals (Matthess, 1990).

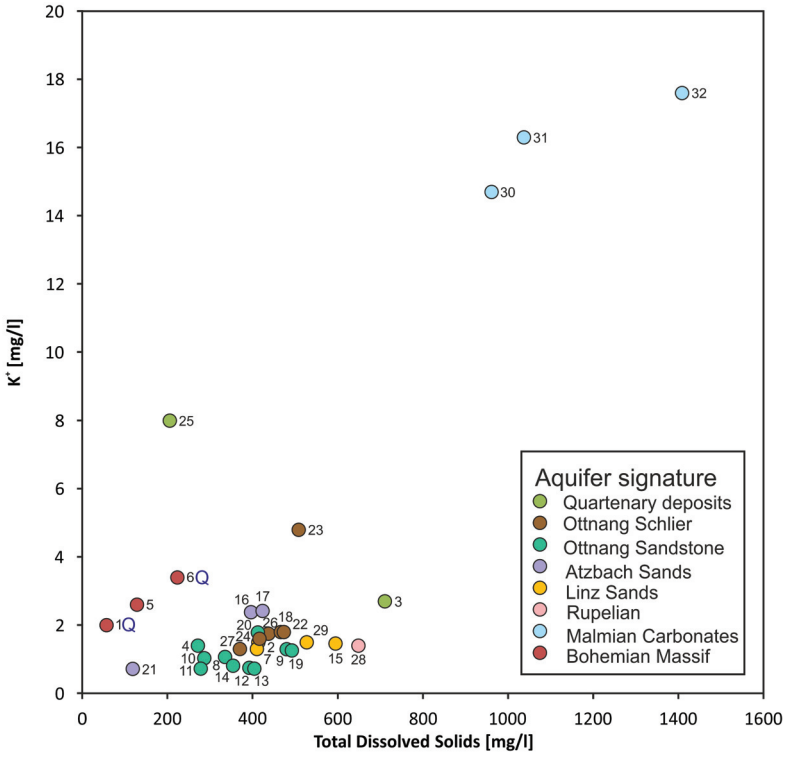

FIGURE 6.9: Crossplot of K^+ vs. Total Dissolved Solids

The figures 6.10 and 6.11 show the same overall trends, although the ion content of both differs slightly for individual samples. The difference between both diagrams is the order of magnitude of the ion concentrations. Whilst the **calcium** concentrations reach values up to 130 mg/l, the **magnesium** values range around a third of these Ca^{2+} values (table 6.3). Again, in both plots two different groups of samples exist. The first group is characterised by a linear increase in calcium and magnesium coupled to the increase of the total dissolved solids. The meteoric groundwaters of the springs and wells with shorter groundwater residence times form this group. In contrast, the population of deep groundwaters (samples 2, 7, 15-18 and 28-32) show a noticeable depletion in calcium as well as magnesium. This phenomenon is explained by the replacement of Ca^{2+} and Mg^{2+} by Na^+ with increasing depth and dwell time. The offset of the Malmian waters is caused by their increased mineral content. Fig. 6.8 therefore forms a counterpart to these plots, because in this previous plot, samples with increased Na^+-content are elevated, whereas in the figures 6.10 and 6.11 the same samples plot near the abscissa.

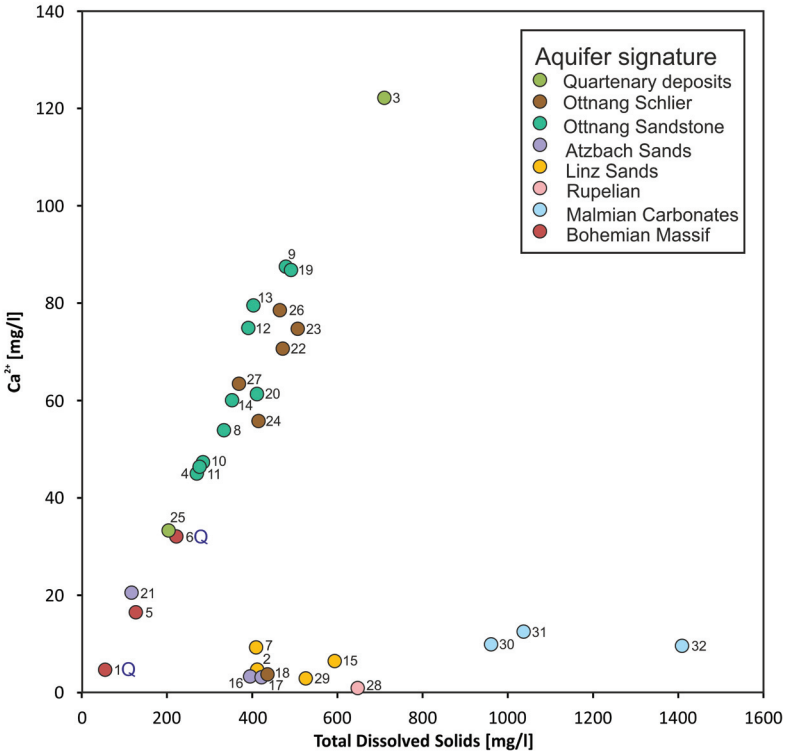

FIGURE 6.10: Crossplot of Ca^{2+} vs. Total Dissolved Solids

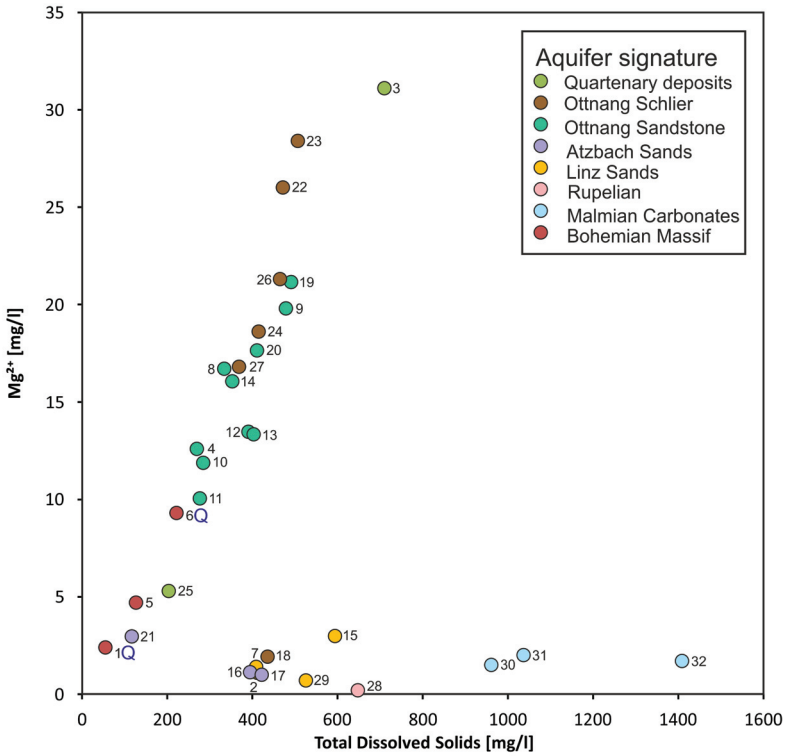

FIGURE 6.11: Crossplot of Mg^{2+} vs. Total Dissolved Solids

Sample 3 shows a significantly higher amount of calcium and magnesium, leading to its position outside of the normal range of the other shallow groundwaters. This could be a result of anthropogenic influence. Federal regulations specify the hygienic standards for public pool facilities (e.g. Umweltbundesamt, 2014). In order to meet these requirements, chemicals are added to the water, e.g. calcium hypochlorite. These additives would not only account for the amount of chloride in the water, but also for the calcium content. Hence, the results of the chemical analyses do probably not show the original water composition.

The diagram which plots **strontium** on the y-axis and total dissolved solids on the x-axis (Fig. 6.12), does not show clear trends regarding all samples. The strontium contents of all samples do not exceed 1 mg/l, they range between 0.017-0.944 mg/l (table 6.3). Due to their increased total mineralisation, the thermal water samples form a separate group, thus, their strontium content does not differ from the shallower groundwater samples. Zötl and Goldbrunner (1993) stated, that strontium is a trace element which can be used to identify deep groundwaters. However, this can not be confirmed for the samples of this study, quite the contrary is observed in the investigated waters. Sample 29, a geothermal well is characterised by the lowest strontium content of all samples in this study. The highest amount of this element is included in sample 24, a water well of 158 m depth. Therefore, strontium can be excluded to serve as a tracer element for Malmian groundwaters.
Although the contents are still in the usual range, higher strontium mineralisations could be observed at the sampling sites 23 and 24. Due to the ability of strontium to replace calcium, this element could be enriched in any mineral which includes calcium. This creates a broad variety of possible strontium sources. Therefore, a definite statement about the cause of the higher amount of strontium in those two samples cannot be made.
Even though the total strontium content does not deliver any significant results, an investigation of the isotope ratios of this element could give indications about the origin, age or mixing of groundwaters. Due to this reason, further investigations of the isotopic composition should be considered.

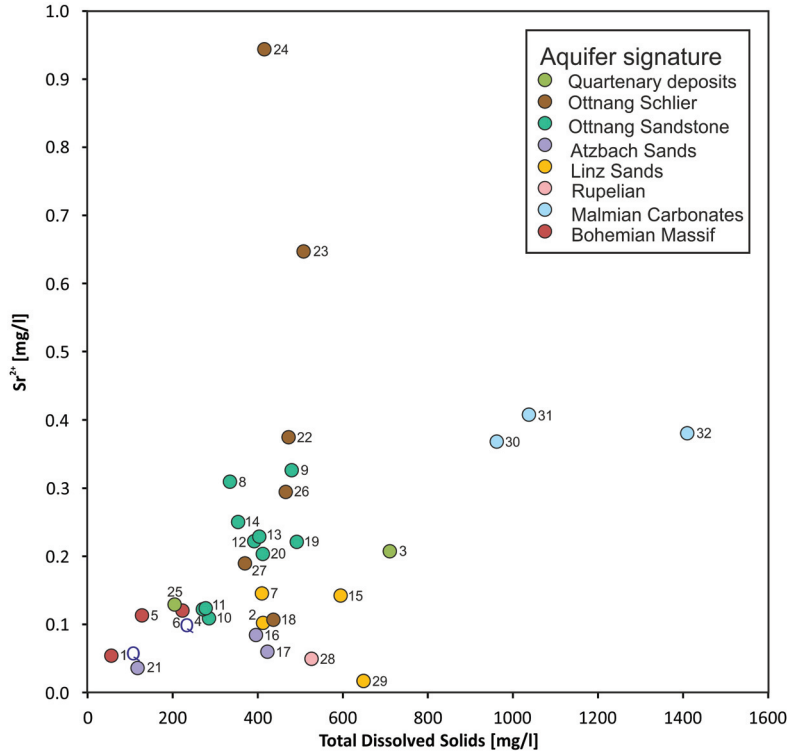

FIGURE 6.12: Crossplot of Sr^{2+} vs. Total Dissolved Solids

The amount of **barium** in the sampled wells is generally low and does not exceed 0.15 mg/l. Only sample 32 is characterised by an augmented portion of this element (table 6.3). An explanation for this observation could be found in the adjacent region. Matthess (1990) described higher barium concentrations in oilfield brines which are poor in or free of sulphate. The oilfield Trattnach is located at an adjacent fault block eastwards of the sampling point 32. This oil within the reservoir is characterised by a low sulfur content (Groß et al., 2015). Furthermore, Andrews et al. (1987) has mentioned the low salinity of the formation waters associated with this oilfield, indicating a hydrodynamic connection of the Cenomanian with the underlying Malm. Due to the proximity of this hydrocarbon deposit, a diffusion of contained compounds into the vicinity of the oilfield may provide a possible explanation for the barium supply of this water.
Another characteristic feature of the water from site 32 is the slightly increased mineralisation. Due to the connection of Malm and Cenomanian in this area, this higher value of dissolved solids may be explained. The geological setting of this area may also provide an explanation th the increased mineralisation. Since the well is located close to the Schwanenstadt fault, which forms part of the structured trap of the Trattnach oilfield, the impermeability of this discontinuity may cause a slight decrease in water circulation and therefore, provide a reason for the enrichment of dissolved solids.

For all samples, except the Malmian thermal waters (sample 30, 31 and 32), **lithium** contents between 0.002-0.084 mg/l were measured (table 6.3). In contrast, the Malmian

samples have increased amounts of this trace element (between 0.243-0.272 mg/l; Fig. 6.13). The amount of lithium contained in these waters is three times as high as in the shallow aquifers. Waters from sites 15, 16, 17 and 18 (encircled in red in Fig. 6.13) also show a slight elevation in this element. Both, Matthess (1990) and Zötl and Goldbrunner (1993), state that a raised lithium concentration is a characteristic feature of thermal waters. Due to this reason, the four shallow groundwater samples mentioned earlier could be the product of a mixing process of meteoric water with deep thermal groundwaters causing this alteration. However, temperature-dependant water-rock interactions coupled with ion exchange processes control the supply of this element. During diagenesis, illite-smectite is converted to illite and further to illite/muscovite. This results in an exchange of potassium (or sodium) by lithium which dissolves into the water flowing through the formation (Hoth et al., 1997). Because these processes preferably occur in siliciclastic sediments, the Malmian geothermal aquifer bears little amounts of lithium in comparison to other thermal waters. As opposed to that, the wells where increased temperatures were measured (Fig. 6.5) do not show any conspicuities in this plot.

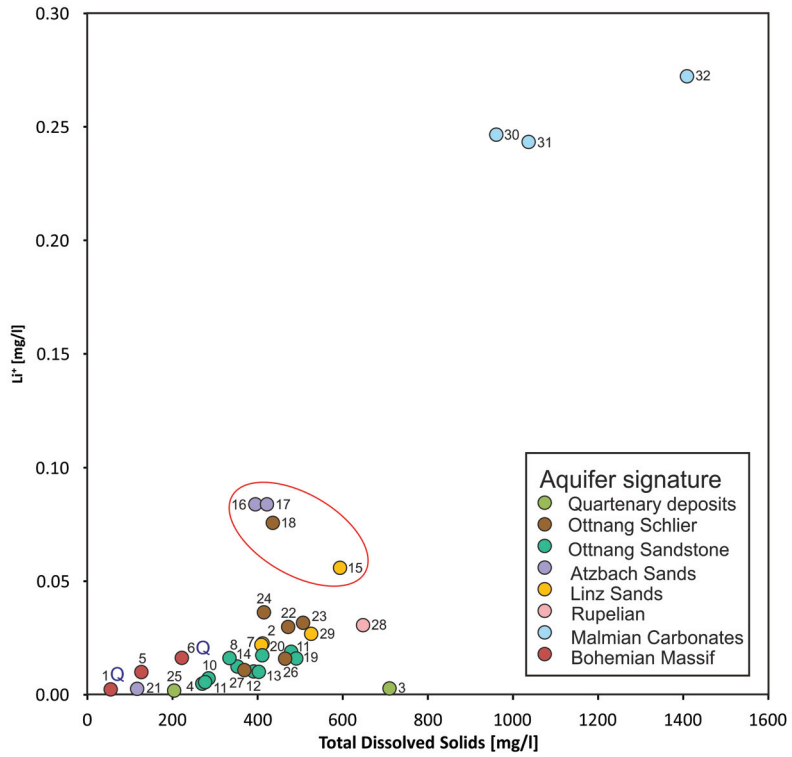

FIGURE 6.13: Crossplot of Li^+ vs. Total Dissolved Solids, the shallow groundwater samples 15, 16 17 and 18 (encircled in red) are characterised by an increased lithium content which could indicate mixing with thermal waters

In comparison to lithium, the **rubidium** contents in the samples are more than ten times lower with values between 0.0001-0.0025 mg/l (table 6.3). This range excludes

the Malmian samples, because, again, the contents in the three geothermal wells are enhanced (between 0.0339-0.0377 mg/l). The data which have been collected, suggest that this ion is characteristic for Malmian thermal waters, because all other samples have nearly no rubidium dissolved. Unfortunately, no additional former investigation of this element is published inhibiting comparison of the results with literature data.

The **iron** contents in the samples lie between 0.000-1.857 mg/l (table 6.3) and show no clear trend (Fig. 6.14). The only apparent feature which is visible is, that the deep groundwaters are concentrated in the lower section of the plot whereas the water located closer to the surface are characterised by a higher iron concentration. A reason for this distribution may be related to the aquifer specifications, the Malmian carbonates are presumably low in iron which decreases the provided dissolvable amount of this element, despite the fact that reducing, oxygen-poor conditions are favourable for iron dissolution (Matthess, 1990). In comparison to their total mineralisation, samples 5 and 6 show a high iron content. This characteristic is depicted in Fig. 6.14 where those two samples are located in the uppermost part of the graph. The increased iron supply of plutonites of the Bohemian Massif may be responsible for this elevated iron content. This increased iron content in sample 6 may also provide an explanation for the low redox potential measured in this spring (Fig. 6.3, table 6.2), since an augmented amount of this ion reduces the redox potential of water (Wisotzky, 2012). The samples 22 and 23 originate from the Ottnangian Schlier aquifer. These two waters show higher values of iron as well. Due to the proximity of both sampling wells, the higher iron content could result from an enrichment of iron-bearing sediments in this area.

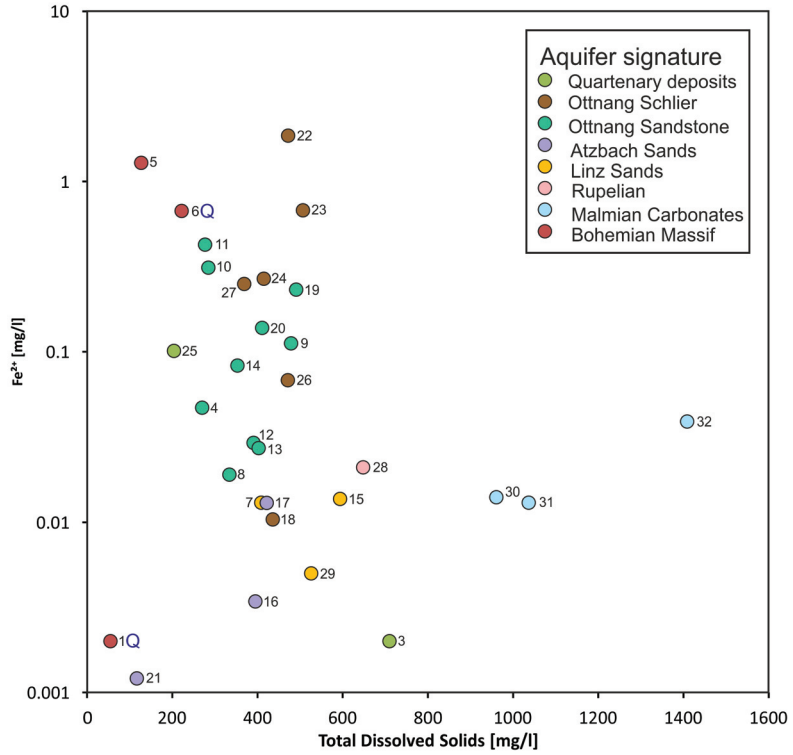

FIGURE 6.14: Crossplot of Fe^{2+} vs. Total Dissolved Solids

The trace element **manganese** (table 6.3) holds similar characteristics as iron, but its solubility is significantly lower. For this reason, its content in groundwater is reduced in comparison to iron (Matthess, 1990). Except for three samples, the manganese contents observed in the samples do not exceed 0.1 mg/l. The values of concentrations of samples 5 (0.118 mg/l) and 6 (0.0997 mg/l) are again slightly increased in this plot. The water from the sampling site 20 is noticeable due to its manganese content of almost 0.9 mg/l. However, since this phenomenon is neither observed in other samples of the same aquifer nor in the vicinity of the sampling location, its origin must be locally restricted.

The **hydrocarbonate** contents of the collected waters vary between 20.86-676.06 mg/l. Therefore, this compound, which takes up approximately half of the total dissolved solids, is the principal component of all samples. All samples range between pH values of 6-9. In this pH range, HCO_3^- is the main CO_2-species present in water (Fig. 4.1). Although the HCO_3^- content is supposed to decrease with increasing depth or groundwater residence time (equation 4.1), the observed decrease in the Malmian thermal water samples (30, 31 and 32) is very low. The water composition of the thermal water samples reflects their origin from a carbonate aquifer with an increased supply of HCO_3^-.
Fig. 6.15 shows the hydrocarbonate contents of the collected waters. After Matthess (1990), the hydrocarbonate range of common groundwaters lies between 50-400 mg/l. The sampling points characterised by a low mineralisation are situated at the lower end of the linear trend visible in the graph. The geothermal water samples form the other

end of the trendline due to their high amount of dissolved minerals resulting in a larger hydrocarbonate content. However, these water samples located at the top right part of the plot seem to follow a different trend characterised by a lower gradient compared to the shallow groundwater samples. An explanation for this development could be given by the increasing admixture of chloride in deep groundwaters (cf. equation 4.1). This anion takes up to a third of the total anion share of these samples and contemporaneously reduces the amount of HCO_3^-. The integration of sample 3 into this trend would confirm this assumption due to its high anthropogenically induced chloride content.

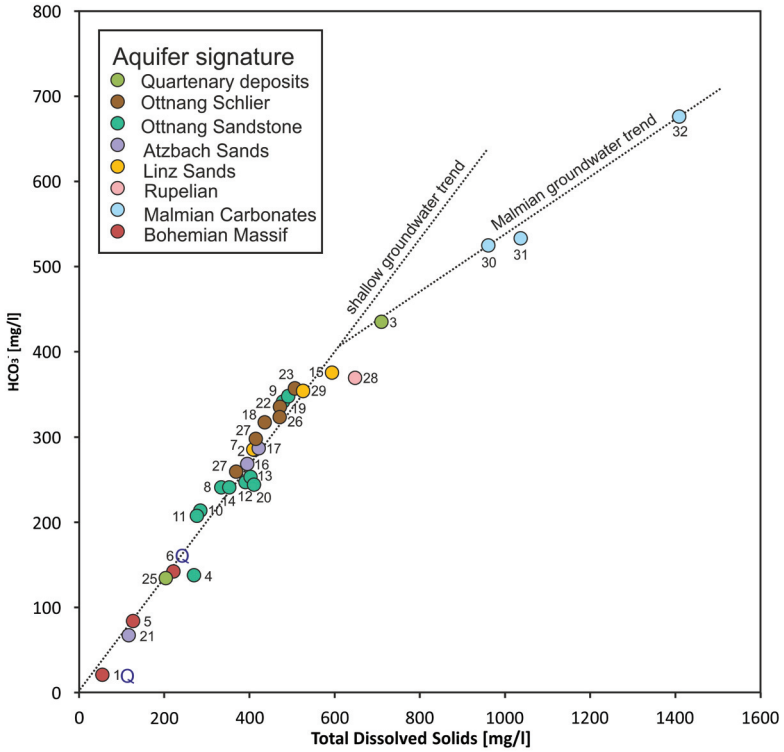

FIGURE 6.15: Crossplot of HCO_3^- vs. Total Dissolved Solids, the shallow groundwater trendline marks the trend for all samples, except 3 and 30-32, the trendline for the samples 30-32 is marked as Malmian groundwater trendline

A closer observation of the amount of **chloride** of the samples (Fig. 6.16) confirms the trend for the deep groundwater samples which was mentioned above. The waters recovered from deeper formations show a significantly increased amount in chloride in comparison to the shallow groundwater samples which are characterised by a chloride mineralisation which does not exceed 25 mg/l. For the deeper situated geothermal wells a chloride increase with rising amount of dissolved solids is observed. Sample 15 forms an exception to this description. Although its well depth is 160 m, it is situated between two samples taken from balneologically used geothermal wells and therefore, follows the deep groundwater trendline. This could be a clear sign that deep groundwaters ascend to shallow strata in this region.

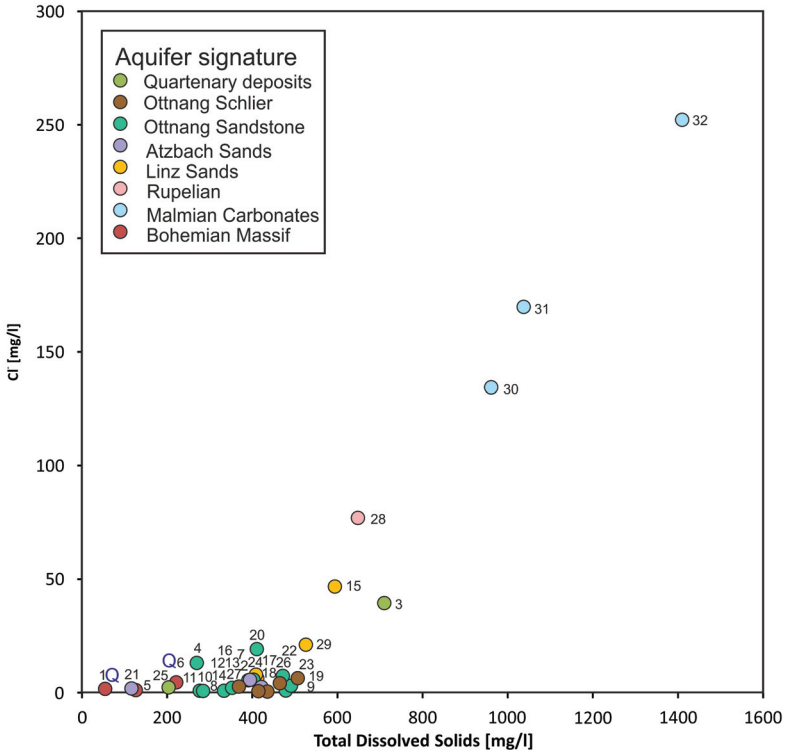

FIGURE 6.16: Crossplot of Cl^- vs. Total Dissolved Solids

Although the absolute **sulfate** contents of the samples 1 and 5 located in the Bohemian Massif as well as sample 21 are rather low (3.8-9.8 mg/l), their contents take up to 24 eq% of the overall anion share (Appendix). Most of the Ca-(Mg)-HCO_3 type waters show sulfate contents up to 22 eq% (4.4-47.8 mg/l). However, it remains questionable if these amounts are caused by natural processes or anthropogenically induced. Vohryzka et al. (1986) states, that the Bohemian Massif mainly composed of granite and gneiss is rich in sources of sulfide, but these hardly participate in the groundwater mineralisation of this aquifer. Maybe this is caused by the fact that the Bohemian Massif conducts water through fractures, which do not provide as much surface for water-rock interaction as porous aquifers. However, a dissolution of pyrite in these fractures should not be completely neglected and could maybe serve as a source for sulfate. Sample 6 (characterised by a sulfate content of 20.3 mg/l) is located in an area, where high sulfate contents are observed in groundwaters. These were either induced by fertilising products for agricultural purposes or industrial sulfur emissions. The content which is then taken up by groundwaters is mainly driven by the filter characteristics of the uppermost formations and its clay minerals (Vohryzka et al., 1986). However, a natural sulfate supply by dissolution of pyrite and markasite contained within the aquifer should not be excluded. An increased pyrite content and dissolution in the subsurface could also explain the augmented sulfate contents (44.4-447.8 mg/l) of the samples 12, 13 and 20.
A crossplot of sulfate content versus TDS (Fig. 6.17) does not show significant differences in shallow and deep groundwaters. This observation is opposed to the trends illustrated

in equation 4.1, which states that the sulfate amount takes up a major share in deeper located groundwaters. However, samples from the Linz Sands and Rupelian as well as two samples from the Malmian carbonates are characterised by a low sulfate content (4.5-6.4 mg/l). In contrast to these waters, the amount of sulfate measured in sample 32 (43.6 mg/l) is among the highest concentrations of all samples taken. An enrichment in this ion caused by limited water circulation and dissolution of sulphate from the carbonate aquifer is probably responsible for this higher content. A second argument for this theory is the comparably high mineralisation of this sample. A connection of the sulfate content with the oil deposit located in the vicinity of the sampling site can be excluded since this hydrocarbon deposit bears low amounts of sulfur (Groß et al., 2015). The sulfate depletion of the remaining deep groundwaters could be the result of microbial or thermogenic sulfate reduction. Thereby, sulfate is reduced to hydrogen sulfide, either by microorganisms under anaerobic conditions (biogenic sulfur reduction; Matthess, 1990) or by a reaction with gaseous hydrocarbons at temperatures between 100-180 °C (thermogenic sulfur reduction; Orr, 1974; Orr, 1977; Machel, 2001). Since many of the deep groundwaters were accompanied by the characteristic odour of hydrogen sulfide during sampling, this assumption is probably realistic.

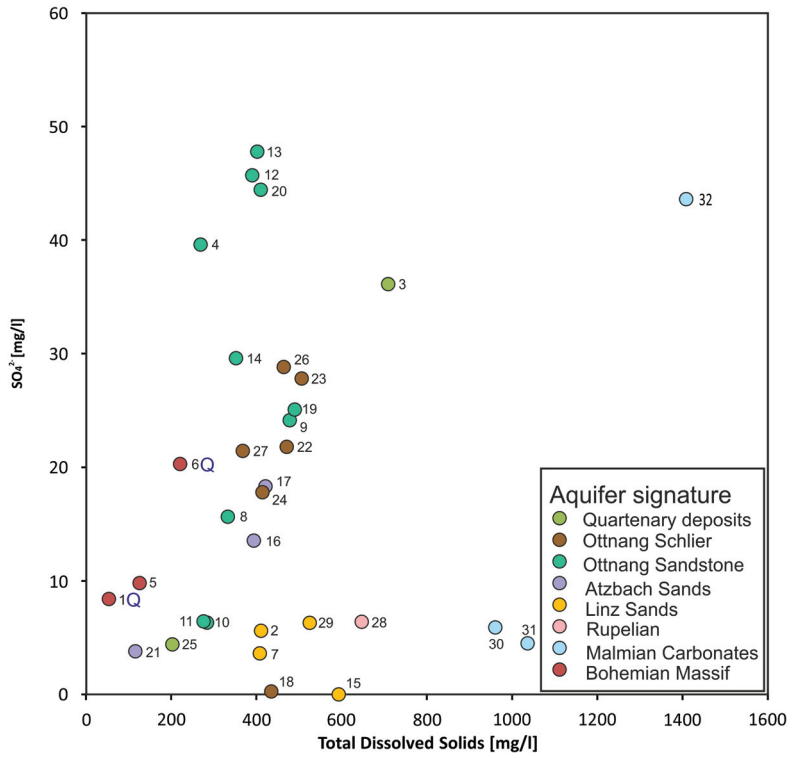

FIGURE 6.17: Crossplot of SO_4^{2-} vs. Total Dissolved Solids

Waters from the wells 15, 24, 28 and 29 are characterised by a **fluoride** content between 0.49-0.92 mg/l which is significantly different to the remaining shallow groundwaters. Their amount of dissolved fluoride does not exceed 0.35 mg/l. Only the thermal

water samples gave fluoride results of more than 5 mg/l. Therefore, according to BGBl. II Nr. 309/1999 (1999), "fluoride-bearing" can be supplementary added to the water type description of samples 30, 31 and 32. This ion content could be influenced by numerous factors. Zötl and Goldbrunner (1993) claims, that high amounts in fluoride occur in deep groundwaters which is the case for these geothermal samples. Michel (1997) proposes two different reasons: Firstly, due to the co-precipitation of CaF_2 during carbonate formation in marine conditions, the aquifer itself provides a potential source of this element. Secondly, the amount of fluoride is increased during ion exchange processes. This theory is supported by the increased pH of the samples 30-32, which is a side-effect of these reactions (Michel, 1997) and by the fact that samples 28 and 29 as well as 15 bear higher fluoride contents, too.

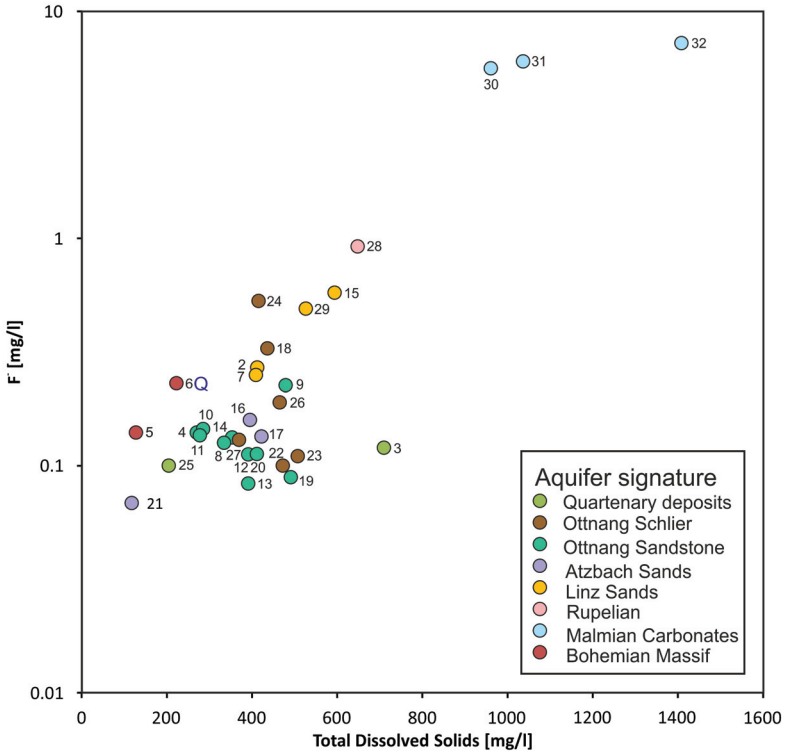

FIGURE 6.18: Crossplot of F^- vs. Total Dissolved Solids

Only a few water samples have yield a higher **nitrate** concentration than 0.5 mg/l. A common property of all these samples is their depth, they either originate from springs or shallow aquifers (samples 1, 3, 4, 21 and 25). Due to their position, the nitrate contamination is probably induced from the surface. The areas where samples 1 and 21 are located are partly covered by forests. These forests could have contributed to the nitrate concentrations measured (pers. comment F. Eichinger, 2017). Moreover, the spread of fertilizers is probably responsible for increased nitrate amounts as well.

As far as the other **trace elements** and metals which were investigated are concerned,

a major amount of the values was below the detection limit of the measuring device (tables 6.4 and 6.5). Therefore, none of these can be used as a trace element for the detection of thermal water or mixtures of groundwater and thermal water, because no regional trends or correlations can be identified. For the trace element Cadmium no results above the detection limit could be reached by any sample.

The inspection of the ratio between sodium and chloride of the samples (Fig. 6.19) reveals, that most of the shallow groundwater samples gather near the origin of the plot at a position along the Seawater Dilution Line (marked as Na:Cl=1:1). This implies that these waters have very small amounts of diluted NaCl, probably caused by the dissolution of minerals in the subsurface or contact with formation waters. Three samples are located close to the first group - but aside the Seawater Dilution Line. Sample 3 is influenced by its chloride additives as mentioned above. Samples 20 and 24 show a slightly increased sodium content. This could be interpreted as a sign for commencing cation exchange. During this process, the samples would move towards higher Na^+ values and thus, towards the second group displayed in the crossplot. The upper blue dashed trendline marks the trend of the waters most probably affected by cation exchange. The rise of the sodium content is a result of cation exchange. During this process, the chloride content of the water is not affected. However, after the termination of cation exchange, the amount of sodium and chloride increase contemporaneously with depth and overall mineralisation. Again, this plot shows, that the sample taken at location 15 clearly follows the trendline of the thermal waters and shares their characteristics. According to these observations, two different sample groups can be distinguished. The first group is concentrated at the Seawater Dilution Line near the plot origin and includes the major part of the shallow groundwaters. The second group plots aside the Seawater Dilution Line on a separate trend. This group contains thermal waters and shallow groundwaters which are probably affected by cation exchange.

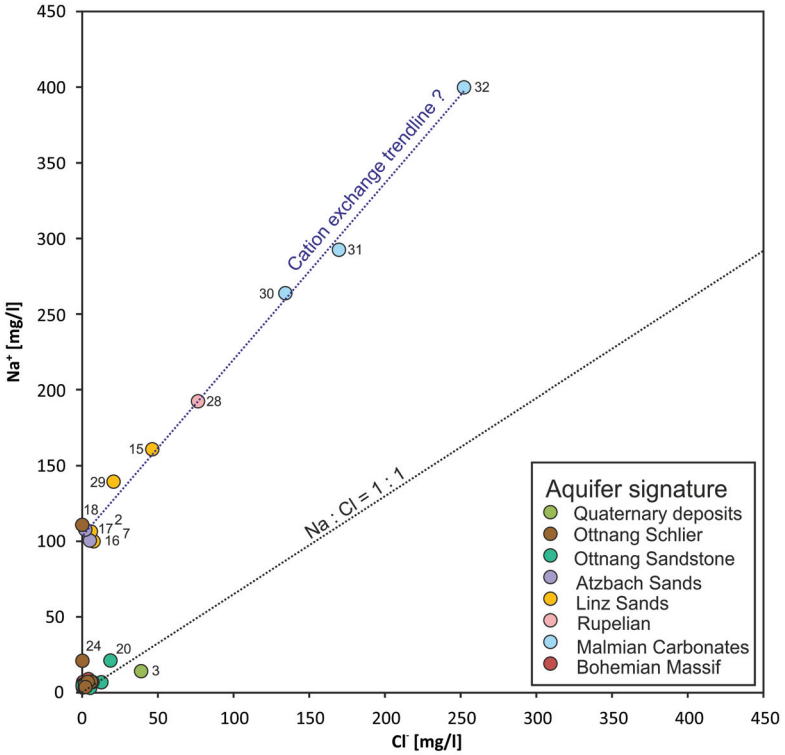

FIGURE 6.19: Crossplot of Na^+ vs. Cl^- with the black dashed Seawater Dilution Line (marked with Na:Cl=1:1) and the blue dashed trendline for the samples most probably affected by cation exchange (marked with "Cation exchange tendline ?")

Crossplots of chloride against bromide are used to identify the origin of salinity of a water (e.g. seawater origin, leaching of evaporites or anthropogenic effects; Alcalá and Custodio, 2008). The ratio of these two elements is very conservative, which means that it remains constant for natural waters with varying ion concentration. The reason for this consistency is, that both elements hardly participate in physical processes in the subsurface. Hence, it is even possible to reconstruct the origin of deep groundwaters with long subsurface residence times (Alcalá and Custodio, 2008; Davis et al., 1998). A prerequisite for this reconstruction is, that the investigated water originates from one source and is not a mixing product of waters from different sources. Mixing processes are able to influence and distort the Cl:Br ratio (Davis et al., 1998). Common chloride to bromide ratios of meteoric waters with chloride contents below 200 mg/l do not exceed 200. Halite is known for its high ratio in chloride to bromide (Davis et al., 1998). The dissolution of this mineral augments the amount of chloride and as a result the quotient of these two elements. Natural factors (flow through evaporitic strata or mixture with formation waters) may produce this alteration as well as human influence (e.g. industrial aerosols or road salt for de-icing in winter; Davis et al., 1998).

Generally, the ratios of chloride and bromide from the samples of this study vary between 39-5059. The crossplot of chloride versus bromide (Fig. 6.20) visualises that those water samples, which are geothermal waters as well as those which could be affected by

a mixture with geothermal waters show higher amounts of chloride and bromide and plot in the upper half of the plot. The Seawater Dilution Line (marked with Cl:Br=288 according to Stober and Bucher, 1999) is illustrated as a dashed line. This trendline reflects the Cl:Br ratio of seawater (similar to the Seawater Dilution Line in Fig. 6.19). Although the Malmian waters are located next to this line, their calculated chloride to bromide ratios vary considerably compared to the marine ratios (dashed line in Fig. 6.20). Their ratios range between 162 and 202. Although sample 32 possesses 252 mg/l Cl^-, its Cl:Br ratio remains at a value of 202. This admits the assumption that waters recovered from this carbonate aquifer are of meteoric origin, which is presumed for the samples located above the Seawater Dilution Line, too. Although the water below the Seawater Dilution Line are probably of meteoric origin as well, the Cl:Br ratio of these samples may have been influenced by the dissolution of halite. However, since no evaporitic formations occur in the study area, this option can be excluded. Therefore, an anthropogenic influence should be considered. Sample 25, which is probably affected by this influence (Fig. 6.20) is characterised by a Cl:Br ratio of 920. The well depth of this location is 9 m and the sampling occurred in January, when a snow cover had to be removed from a street, located near the well.

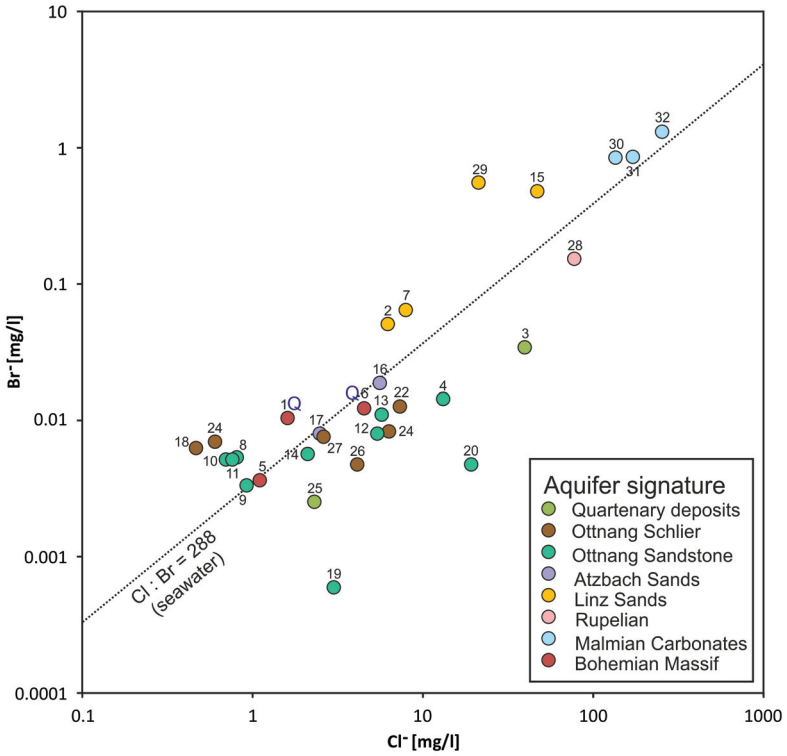

FIGURE 6.20: Crossplot of Cl^- vs. Br^- with the black dashed Seawater Dilution Line (indicating the Cl:Br ratio of seawater according to Stober and Bucher, 1999, marked with Cl:Br=288)

The ratio of chloride to iodide varies considerably between 38-394000. The highest value of this ratio is observed in sample 3 and distorted by the high amount of chloride. Iodine is a biophile element and becomes enriched in sediments bearing organic matter (Matthess, 1990). Therefore, waters which pass these organic-rich layers in the subsurface may become enriched in iodine. A crossplot of the chloride and iodide content of the collected samples (Fig. 6.21) shows a separation of the thermal groundwaters and samples which may be influenced by thermal waters (located in the upper half of the plot) from the rest of the wells (located in the lower half of the plot). The low amounts of iodide (approximately ≤ 0.01 mg/l) in the samples plotting at the lower section of the graph may be related to a shorter dwell time of these waters. During this time the samples did not get in touch with substances which could have increased their iodide content. However, the samples in the upper section (approximately ≥ 0.01 mg/l) are characterised by an increased groundwater residence time and may have flown through organic-rich strata causing an augmentation of the iodine content (pers. comment, Goldbrunner 2018).

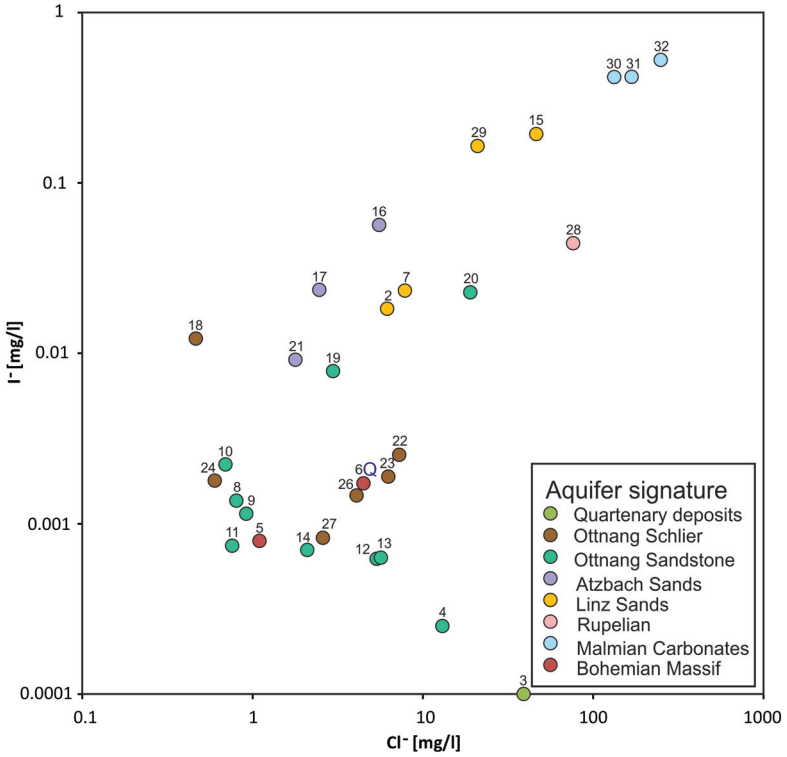

FIGURE 6.21: Crossplot of Cl^- vs. I^-

A comparison of iodide and bromide (Fig. 6.22) shows, that most shallow groundwaters occur as a cluster of similar characteristics. In contrast, the Malmian, Rupelian and Linz Sand groundwaters form a trendline, which links rising iodide contents with increasing bromide amounts. However, a connection of this trend with the overall sample mineralisation cannot be observed since sample 28 is characterised by a greater amount of dissolved solids than samples 15 and 29, which appear next to the Malmian waters. Five samples (samples 16, 17, 18, 19 and 20) can neither be associated with the shallow

nor with the deep groundwaters (Fig. 6.22). The higher iodide amount could be a result of an increased contact with organic matter. The depletion in bromide visible for sample 19 may be associated with anthropogenic effects. The other four samples show similar bromide contents than the shallow groundwaters, the shift occurs because of slightly higher I^- contents, which could be caused by a contact of these waters with organic-rich sediments.

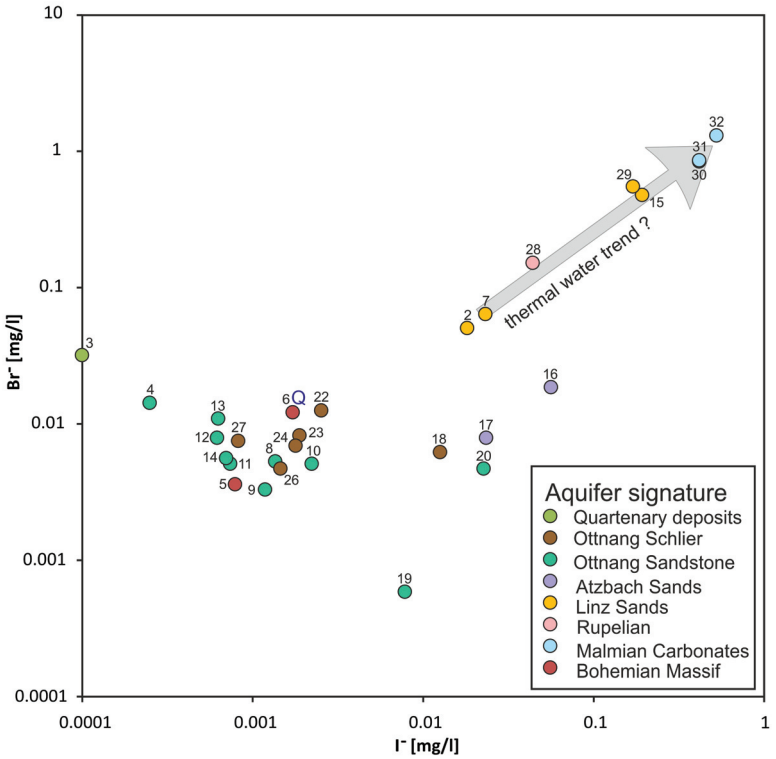

FIGURE 6.22: Crossplot of I^- vs. Br^-; the grey arrow indicates a possible trend of the thermal water samples

Various ion contents (e.g. Na^+, Li^+, Cl^-) could indicate an influence of Malmian thermal water on several water samples (e.g. 2, 7, 15, 16, 17, 18). Therefore, an attempt to create a mixing line was made to quantify the assumed influence of thermal waters of selected samples (Fig. 6.23). This mixing line is based on the comparison between the sum of cations and sodium content of the waters. The diagram shows that shallow Ca-(Mg)-HCO_3 waters aligned along the x-axis, whereas the samples containing an increased amount of sodium are set apart from these samples and located on a trendline (marked as a black dashed line in Fig. 6.23). As in Fig. 6.8, a linear trend among the sodium-rich waters is visible. To calculate the mixing ratios, a decision concerning the end-members of the mixing line were made. The upper end-member of this trendline is taken by the Malmian waters which are considered to be pure thermal waters in the Upper Austrian Foreland Basin. The lower end-member on the other side is formed by samples 1, 5 and 21. These samples were chosen due to their low mineralisation (on average 100 mg/l) and the fact that an influence by thermal waters can be entirely excluded. If an average

total mineralisation of 1167 mg/l is assumed for the Malmian samples, an average sum of cations of 15 meq/l and a sodium share of 14 meq/l can be expected, respectively. Taking these assumptions into account, a calculation for samples 28 and 29 would approximately result in a 30 % proportion of thermal water (pers. comment, G. Schubert 2018). The remaining water would be meteoric water. Since the samples 2, 7, 16, 17 and 18 are plotted on a similar position, a share of around 4 % of thermal water is calculated. The diagram also shows, that not only samples from the Linz Sands, where a mixture with Malmian waters has already been assumed, lie on this trendline, but also wells (16, 17 and 18) which do not show all characteristics of the deep carbonate groundwaters. Therefore, it still remains questionable if these waters are really influenced by the thermal water aquifer or if they are just the result of extensive cation exchange. However, sample 15 clearly shows thermal water influence, not only derived from this crossplot but due to its similarity in many different chemical characteristics. To illustrate the geographic position of the samples discussed before (encircled in red), a map of all sample points was inserted to display their spacial distribution (Fig. 6.23).

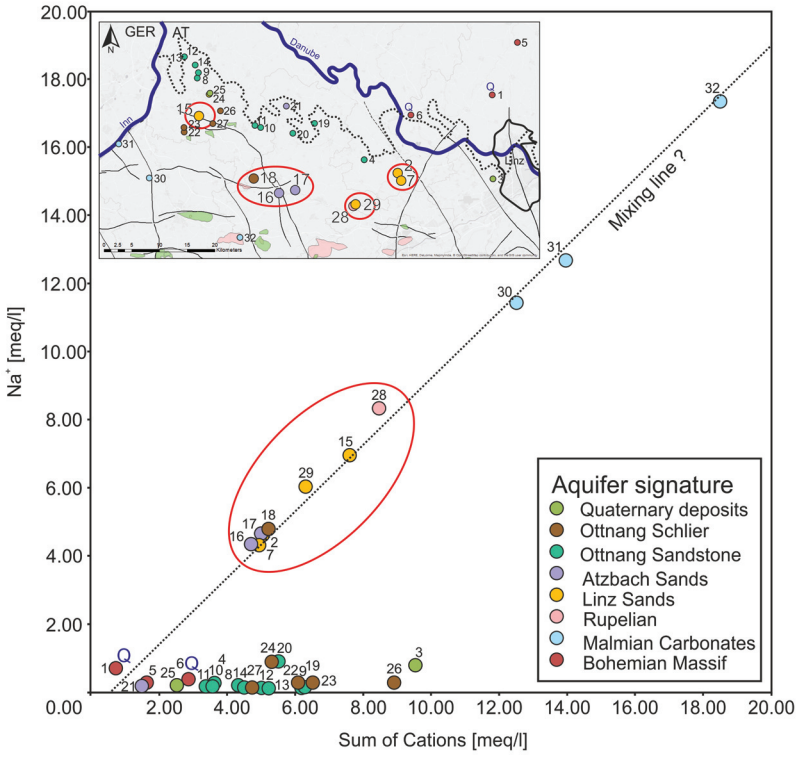

FIGURE 6.23: Crossplot of Na^+ vs. sum of cations, the samples encircled in red are marked in the map displayed at the top right corner of the plot

6.3 Isotopic Signature of water samples

The investigation of different isotopes in water was part of the analysis program. For all samples the ratios of δ^2H, δ^2H - excess and δ^{18}O were measured as part of the standard procedure, some samples were selected for additional investigations of δ^{13}C - DIC and δ^{14}C. All results received from these investigations as well as the results of the measured isotopic composition of the free gas samples taken from selected wells are summarised in table 6.6.

The stable isotope ratios of δ^{18}O and δ^2H were plotted in Fig. 6.24, in order to derive connections between individual samples and to draw conclusions about the formation conditions and connection between different aquifers. Most of the samples taken from shallow strata (quaternary deposits, Ottnang Schlier, Ottnang Sandstone and Bohemian Massif) show δ^{18}O values around -10.5 ‰ coupled with δ^2H values ranging from -72.0 to -76.0 ‰. These values fit to the results obtained by Goldbrunner (1988), who investigated samples from shallow aquifers in the Innviertel region as well. The range of isotopic ratios in these water samples of the Innviertel Group is marked as a red solid line within the graph (Fig. 6.24). All samples from this study which can be assigned to aquifers included in the Innviertel Group can be encountered within this zonal sector. Since the water samples from the Bohemian Massif as well as sample 4 taken from a well west of Linz, plot in this isotopic range, it can be assumed that this range of stable isotope ratios is probably not only valid for waters with comparably short residence times from the Innviertel Group but generally for shallow waters in the Upper Austrian area with short groundwater residence times.
The samples of the Malmian aquifer are located slightly apart from the other waters in the plot. They show values of δ^2H between -76.5 and -79.5 ‰ paired with δ^{18}O ranging from -9.8 to 10.6 ‰ (Fig. 6.24). Sample points 30 and 31 plot closely together at the Malmian regression line (marked in blue in Fig. 6.24) suggested by Goldbrunner et al. (2007), whereas point 32 is set to a value with a larger offset from the Global Meteoric Water Line (GMWL). Higher mineralisation of this sample may indicate a slightly increased evaporation leading to this effect (Mayrhofer et al., 2014). If this process of evaporation continues , the measured results would move upwards along the orange dashed line (after Elster et al., 2016 and Goldbrunner, 2000) with increasing evaporation as illustrated by the scheme in Fig. 4.4.
The deep groundwater samples (samples 2, 7, 15-18, 28 and 29) form a group in the stable isotope plot in the same manner as in many diagrams observing the chemical parameters of the samples before. The samples plot along the GMWL but they are characterised by lighter isotopic values. These depletions in δ^{18}O and δ^2H are the results of a climatic effect, during glacial periods the ratio of stable isotopes contained in water is reduced. Therefore, these values resemble the climatic conditions at the entry of the aquifer, probably Pleistocene. The shallow water samples serve as reference values for the isotopic ratio in warmer time spans like today.

TABLE 6.6: Isotope measurements of collected samples

	Water					Gaseous Hydrocarbons			
Sample No.	$\delta^{18}O$ [‰]	$\delta^{2}H$ [‰]	$\delta^{2}H$ - excess [‰]	$\delta^{13}C$ - DIC [‰]	$\delta^{14}C$ [pmC - %]	$\delta^{2}H$ - CH_4 [‰]	$\delta^{13}C$ - CH_4 [‰]	$\delta^{2}H$ - C_2H_6 [‰]	$\delta^{2}H$ - C_3H_8 [‰]
1	-10.58	-72.2	12.44						
2	-11.92	-84.9	10.46	-15.5	20.2 ± 1.7		-45.60		
3	-9.75	-70.3	7.70						
4	-10.57	-74.6	9.96						
5	-10.30	-72.7	9.70						
6	-10.57	-74.9	9.66						
7	-12.10	-84.7	12.10	-15.6	17.9 ± 1.4		-50.2		
8	-10.43	-71.0	12.44	-11.8	22.5 ± 1.5				
9	-10.65	-73.5	11.70						
10	-10.53	-72.7	11.54						
11	-10.64	-73.1	12.02	-13.7	34.3 ± 1.7				
12	-10.50	-72.4	11.60						
13	-10.55	-72.6	11.80						
14	-10.66	-73.5	11.78						
15	-12.10	-84.7	12.10			-232.48	-73.17		
16	-12.60	-88.7	12.10	-8.2	2.3 ± 1.1				
17	-12.87	-90.7	12.26						
18	-11.74	-82.1	11.82						
19	-10.78	-75.2	11.04						
20	-10.55	-73.6	10.80						
21	-10.90	-75.1	12.10						
22	-10.51	-73.2	10.88						
23	-10.46	-73.0	10.68						
24	-10.72	-74.8	10.96						
25	-12.45	-88.4	11.20						
26	-10.11	-71.3	9.58				-71.12		
27	-10.45	-73.4	10.20						
28	-11.46	-81.8	9.88			-222.61	-65.71		
29	-11.45	-79.5	9.70			-209.96	-65.37		
30	-10.46	-79.5	4.18			-235.13	-58.87	-27.00	-22.33
31	-10.57	-79.4	5.16			-233.15	-58.78	-27.05	
32	-9.84	-76.5	2.22	-6.0	5.0 ± 1.2	-226.08	-57.58	-29.07	-26.26

Sample 25 forms an exception in this study. The isotopic ratio of $\delta^{18}O$ and $\delta^{2}H$ is depleted. Therefore, this sample plots in a different area than the other shallow water samples. However, since this well has a well depth of 9 m and its hydrochemical characteristics can be assigned to the Ca-Mg-HCO_3 type, its isotopic ratios are expected to plot in the cluster of shallow wells. The explanation for this phenomenon is found in the date of the sampling campaign. Since the water sample was taken in January 2018, the shallow well was affected by the seasonal conditions during winter. A comparison of the isotopic signatures from this study with published data (e.g. Elster et al., 2016) shows similar results for the samples 2, 7, 28 and 29. This confirms that the measuring procedure was performed correctly.

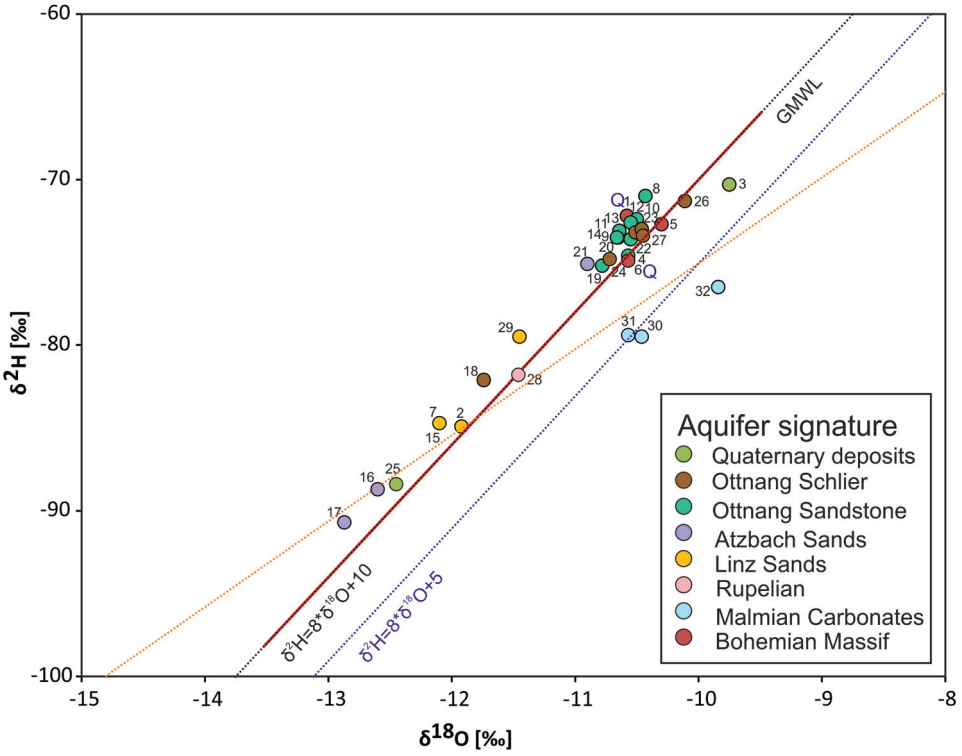

FIGURE 6.24: Stable isotope composition of collected samples, the black dashed trendline is the GMWL with the range of stable isotope values for waters from the Innviertel Group marked as a solid red line, the blue dashed trendline indicates the Malmian carbonate trendline and the orange dashed line marks the evaporation trendline of intermediate aquifers (e.g. Puchkirchen or Hall Formation, after Goldbrunner, 2000; Elster et al., 2016 and Goldbrunner et al., 2007)

In order to verify the infiltration times during the glacial period, an investigation of the ^{14}C content of the deep groundwater samples discussed above, was conducted. For this study, six different sampling locations were selected for analyses of ^{14}C and ^{13}C-DIC isotopes. Fig. 6.25 shows a map of all sampling locations. The results of the ^{14}C investigations are written next to the sampling points in purple. Moreover, results from previous investigations published by Elster et al. (2016) and Goldbrunner (1988), respectively, have

been added to the corresponding locations (orange colour in Fig. 6.25).

Fig. 6.26 depicts the assumed hydrodynamic concept of the Innviertel Group after Goldbrunner (1984) and Goldbrunner (1988). According to this model, the recharge area for waters in the Innviertel Group is located in the Kobernaußer Wald High. From this recharge area, the water propagates northwards through the aquifer towards the river Inn, where the discharge area of this flow model is assumed. This means, that older groundwaters in this aquifer should be located in the northern Innviertel region. However, the collected data show that the highest ^{14}C concentrations are situated in the northern part of the Molasse Basin, near the outcrop of the Bohemian Massif. Especially sample 11, characterised by more than 30 pmC suggests that this well contains a high portion of meteoric water. This young meteoric water could originate from the Bohemian Massif. Near the outcrop of this formation, this young waters infiltrating the Ottnangian strata are mixed with the older waters ascending from the south, creating the measured ^{14}C concentration. In the Taufkirchen Bay, where the sampling points 8, 9, 12, 13 and 14 as well as 24 and 25 are located, an investigation by Goldbrunner (1988) of a well in the vicinity of sample 14 gave a result of 28.2±1.8 pmC ^{14}C. Further to the south, sample 8 delivered a value of 22.5±1.5 pmC. These values and their decrease in the ^{14}C concentration towards the south support the argument of an infiltration from the Bohemian Massif in the northern Innviertel area.
The measured ^{14}C concentrations of samples 2 and 7 show a similar trend as observed in the Ottnangian formations further to the northeast, which could have resulted from a mixing process as well. These two wells, recovering water from the Linz Sands gave results of 20.2±1.7 and 17.9±1.4 pmC. In contrast to the Innviertel area, an influence of ascending Malmian waters and meteoric waters is supposed for these samples since they are located in the discharge area of the Malmian thermal aquifer model (Fig. 3.1). This is supported by the increased temperatures of the recovered samples (Fig. 6.5) and their chemical characteristics (tables 6.3, 6.4 and 6.5). Whereas samples 8, 11 and Rainbach 2 (cf. Goldbrunner, 1988; Fig. 6.25) can be described as Ca-Mg-HCO_3 waters, water of the Linz Sand aquifer (samples 2, 7 and 29) have experienced cation exchange and are therefore assigned to the Na-HCO_3-type. Moreover, the stable isotopic signature of the water suggest a Pleistocene infiltration age.
Further south of the sampling points 2 and 7, ^{14}C investigations were also performed on the waters from the locations 28 (646 m well depth) and 29 (479 m well depth; cf. Elster et al., 2016). The wells are drilled on both sides of a fault, well 28 in the south reaches the Rupel sediments on the footwall of this fault, well 29 in the north stops in the Linz Sands at the hanging wall. The thermal water originating from the Malm is thought to rise at this fault from the Rupel to the Linz Sands (e.g. Goldbrunner, 2000; Elster et al., 2016). The measured values of well 28 fit into this proposed concept, however, well 29 is characterised by a higher percentage of ^{14}C in the water. This contradicts the other three values (from the samples 2, 7 and 28). Therefore, another source of freshwater supply is assumed to feed the aquifer system in the area of this well, otherwise this result could

not be generated.
The ^{14}C concentration is surprisingly low in sample 16. Despite the sample depth of 220 m, the water hardly contains any ^{14}C. A closer examination of the contemporaneously measured ^{13}C gives a closer insight into the generation of the ^{14}C content in this sample. During exchange of calcium by sodium in this water it becomes undersaturated in calcite. To counteract this procedure, calcite contained in the host rock is dissolved to compensate the undersaturation. Usually, a ^{13}C isotope ratio of -22 ‰is measured in the subsurface, the ^{13}C ratio of carbonates formed in marine conditions reaches 0 ‰. The equilibrium state of waters in the subsurface would give a value of approximately -10 ‰(Goldbrunner, 1988). The ^{13}C content of sample 16 is -8.2 ‰. This indicates an oversaturation in calcite, probably induced by carbonate dissolution in the aquifer. The dissolved carbonate induces carbon without ^{14}C into the water system and therefore, distorts the original amount of ^{14}C. As a result, the measured amount of ^{14}C does not provide any information about the age of the water and should be verified by a different method of age determination. A similar effect was observed by Goldbrunner (1988) in samples which are classified as group 3 in this publication.
The ^{14}C isotope measurement at the sampling site 32 gave a result of 5.0$\pm$1.2 pmC. If this value is compared to literature data from sample 30 (cf. Elster et al., 2016), a slightly increased value can be observed. However, considering the supposed hydrodynamic behaviour of the Malmian carbonates (flow directions in Fig. 3.1), this should not be the case. An atmospheric contamination of the sample during the ^{14}C sampling procedure may have resulted in a slightly increased ^{14}C concentration. For further comparison, an unpublished report, provided by the owner of the geothermal plant was consulted. An earlier investigation resulted in a value of < 2 pmC (Hydroisotop GmbH, 2017b). This means, that the amount of ^{14}C contained in the sample was below the detection limit. For data security reasons, the reference title in the bibliography was slightly modified to guarantee anonymisation.
Apart from the ^{13}C-DIC value from sample 16, which has already been discussed above, the remaining investigation results (samples 2, 7, 8 and 11, between -11.8 and -15.6 ‰) are in a normal range for groundwaters (between approximately -20 and 0 ‰). Sample 32 is characterised by a ^{13}C-DIC isotopic ratio of -6 ‰, which is commonly observed in freshwater carbonates (between approximately -18 and +7 ‰; Clark and Fritz, 1998). This fits to the Malmian aquifer.

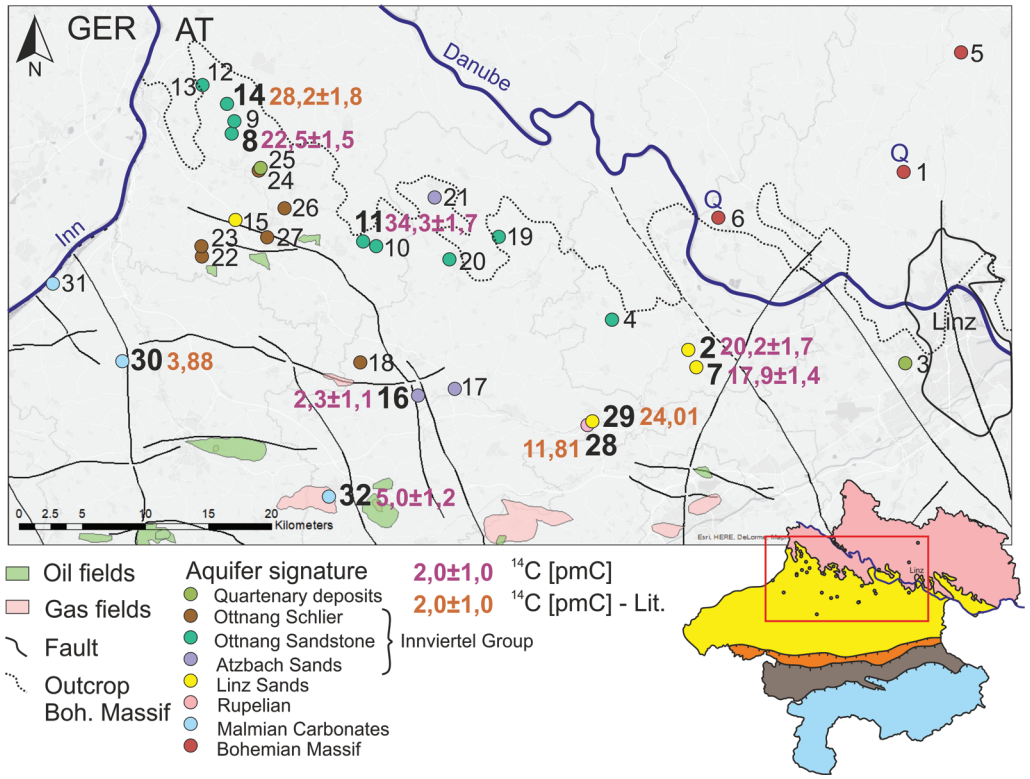

FIGURE 6.25: ^{14}C content of selected samples, the ^{14}C analyses which were taken for this study are written in purple, the brown values indicate literature data from Elster et al., 2016 and Goldbrunner, 1988 which were added to aid a holistic interpretation and comparison

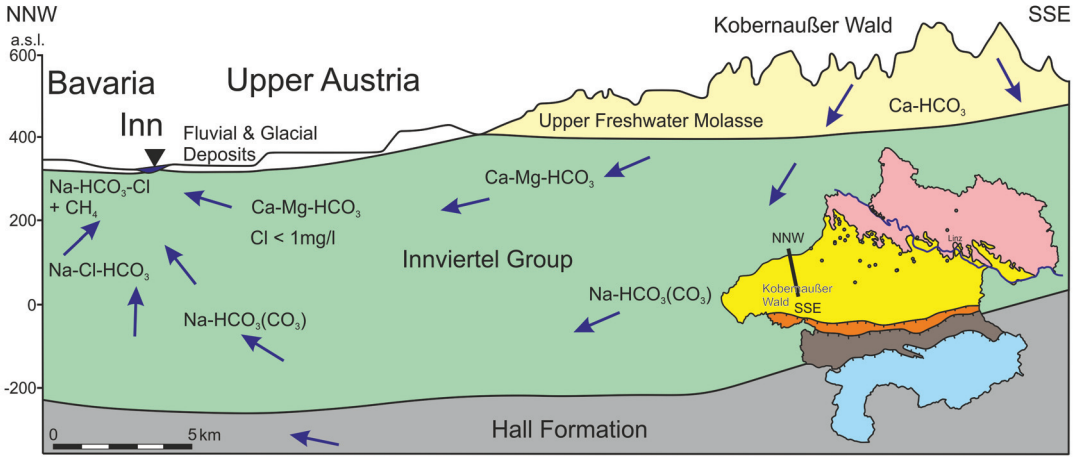

FIGURE 6.26: Cross-section through the shallow Innviertel strata with blue arrows indicating the hydrodynamic flow regime and chemical zonation of waters in this area (modified after Goldbrunner (1984) and Goldbrunner (1988))

6.4 Gas Composition and Isotopic Signature of gas samples

The results of free and dissolved gases associated with the sampled waters are listed in tables 6.7 and 6.8. Table 6.7 contains the results of detected concentrations of dissolved methane. A headspace sample was taken from every site of investigation. The main gas phase which was investigated in these samples was methane, other phases which were detected were oxygen, nitrogen, carbon dioxide and hydrogen sulfide. A free gas sample was taken from those wells, where a significant amount of free gas was noticed during sampling. Apart from the hydrocarbons detected in these samples and listed in table 6.8, the atmospheric gases mentioned before were encountered as well. Moreover, for some free gas samples which were taken from the wells, it was possible to determine the isotopic composition of the hydrocarbons within the gas samples (table 6.6).

TABLE 6.7: Methane concentrations of headspace samples

Sample no.	CH_4 [mg/l]	Sample no.	CH_4 [mg/l]
1	-	17	1.879
2	0.066	18	0.244
3	-	19	0.008
4	-	20	0.012
5	-	21	-
6	-	22	-
7	0.241	23	-
8	-	24	0.015
9	-	25	-
10	-	26	-
11	-	27	-
12	-	28	7.440
13	-	29	2.195
14	-	30	6.937
15	0.053	31	4.477
16	2.351	32	0.812

14 samples from this study contain dissolved methane in various amounts. Since methane is a common trace component in groundwaters and can be formed biogenically via acetate fermentation or CO_2 reduction under anaerobic conditions, its occurrence in small amounts in shallow groundwater systems is widely observed (e.g. Barker and Fritz, 1981; Coleman et al., 1988; Gooddy and Darling, 2005 and Grossman et al., 1989). Therefore, the small amounts of this gas which were observed in shallow groundwater wells were probably formed during metabolic processes of microorganisms in the aquifer. However, the headspace samples from geothermal wells are characterised by a methane content of 0.812-7.440 mg/l. In contrast to the other geothermal water samples, sample

32 contains less than one mg/l dissolved natural gas. This may result from the sampling procedure, as it was not possible to take the sample directly at the well head. The short cooling phase coupled with a pressure decrease after the withdrawal of the water could have lead to a degassing and phase transition of the methane from dissolved to free gas. To avoid any distortion in the gas composition of the free gas sample, this sample was not taken from the well head but from the heat exchanging device of the geothermal plant.
Fig. 6.27 illustrates the spatial distribution of the measured methane concentrations in the headspace samples. A decrease in methane concentrations from south to north is well visible in the graph. This trend is probably controlled by the well depth and drilled formations of the individual samples. The deepest wells selected are located in the south of the study area with well depths ranging between 479 and 2056 m. Due to the increased hydrostatic (and lithostatic) pressure acting on these deep aquifers, the water is able to dissolve a bigger gas volume compared to water located in shallow strata (Enns et al., 1965). The major part of the sampled wells are characterised by a depth of 0-220 m. Furthermore, a decline of the methane concentration from south to north is observed in the samples 28, 29, 7 and 2. A degassing of Malmian water during the migration from the Rupelian towards its discharge area in the Linz Sands south of the Danube could be responsible for this decrease in dissolved methane.
None of the headspace samples showed indications of higher hydrocarbons. To summarize, the analysis of dissolved gases via headspaces reveals quite useful results. However, a correct sampling procedure, if possible directly from the well head and without atmospheric contamination is crucial in order to receive realistic results. Secondly, this method depicts a good supplement of the free gas inspection.

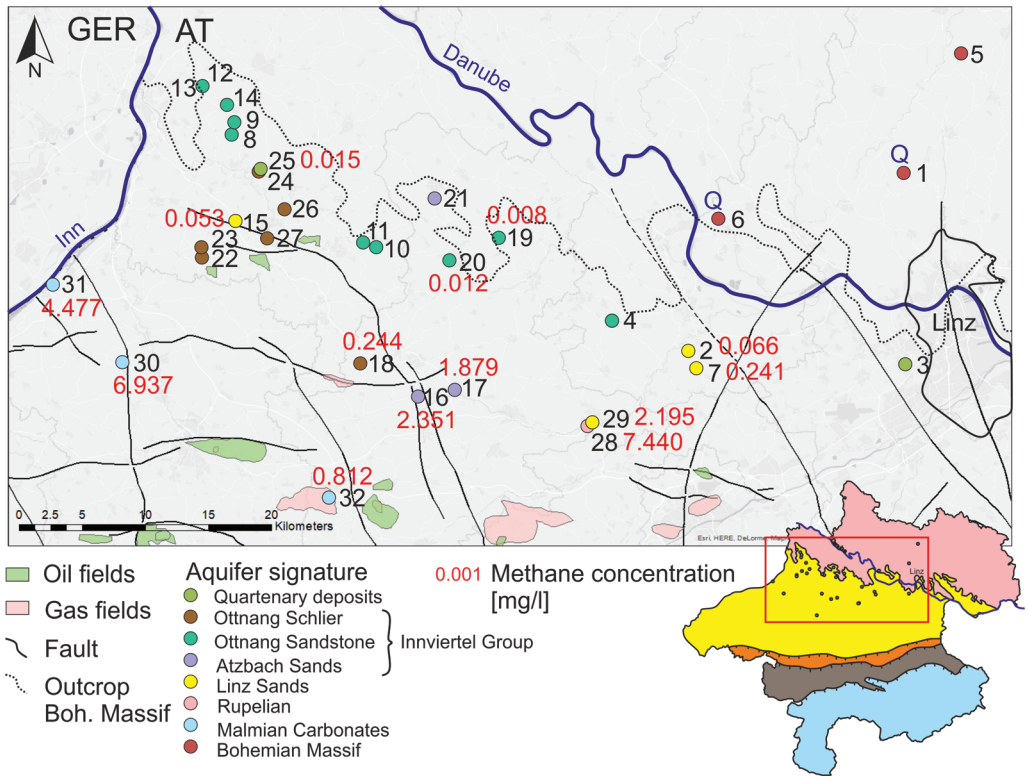

FIGURE 6.27: Calculated concentrations of methane from headspace samples

The analysis of free gas samples of the locations 2, 7, 22 and 26 gave results of methane concentrations below 1.5 %. Although all of these samples indicated a noticeable gas content during sampling in the field, the main components were atmospheric gases such as nitrogen, oxygen and carbon dioxide with only minimal amounts of methane (table 6.8). However, the investigation of the free gas samples of the geothermal wells (28-32) and sample 15 showed major amounts of methane (between 11.5 and 60.3 %). In the Malmian wells not only methane but also detectable amounts of higher hydrocarbons up to hexane were observed (table 6.8). Fig. 6.28 shows a gas chromatogram of sample 32, several peaks of different hydrocarbons and their isomers were identified and labelled. During sampling of the geothermal waters, a scent of hydrogen sulfide was noticed. However, these H_2S contents were below the gas chromatograph detection limit.

Sample 15 is characterised by a free methane concentration of around 30 % despite of its well depth of 166 m. Moreover, the gas chromatography detected traces of ethane as well. Due to these results, the sampled water shows similarities compared with the thermal wells. The observed gas composition in combination with the hydrochemical and isotopical characteristics provides a multitude of remarks for the ascension of Malmian water into the drilled aquifer at this location.

Unfortunately, a sampling of free gas of some wells which hold methane in their headspaces was omitted and should be considered for future campaigns and investigations.

TABLE 6.8: Gaseous content of free gas samples from selected wells, the left side shows the contents of CO_2, N_2 and O_2, the right side of the table lists the contents of gaseous hydrocarbons in the samples

Sample no.	**CO_2** [%]	**N_2** [%]	**O_2** [%]	**Total** [%]	**CH_4** [ppm]	**C_2H_6** [ppm]	**C_3H_8** [ppm]	**iso-C_4H_{10}** [ppm]	**C_4H_{10}** [ppm]	**iso-C_5H_{12}** [ppm]	**C_5H_{10}** [ppm]	**C_6H_{14}** [ppm]	**Total** [%]
2	0.15	88.24	2.28	90.67	12240								1.22
7	0.13	88.68	2.30	91.11	3642								0.36
15	0.37	64.54	6.74	71.65	317680	209							31.79
22	1.10	79.71	18.82	99.63	10								0.00
26	1.60	91.78	5.64	99.02	103								0.01
28	0.07	61.24	1.43	62.74	405009								40.50
29	0.18	86.97	1.91	89.06	115881								11.59
30	10.77	36.72	4.41	51.90	509015	1676	93	22	17	7	1		51.08
31	12.34	29.26	1.14	42.74	600486	2226	112	26	26	14	8	3	60.29
32	13.14	45.81	8.79	67.74	351401	2562	878	204	291	146	97	39	35.56

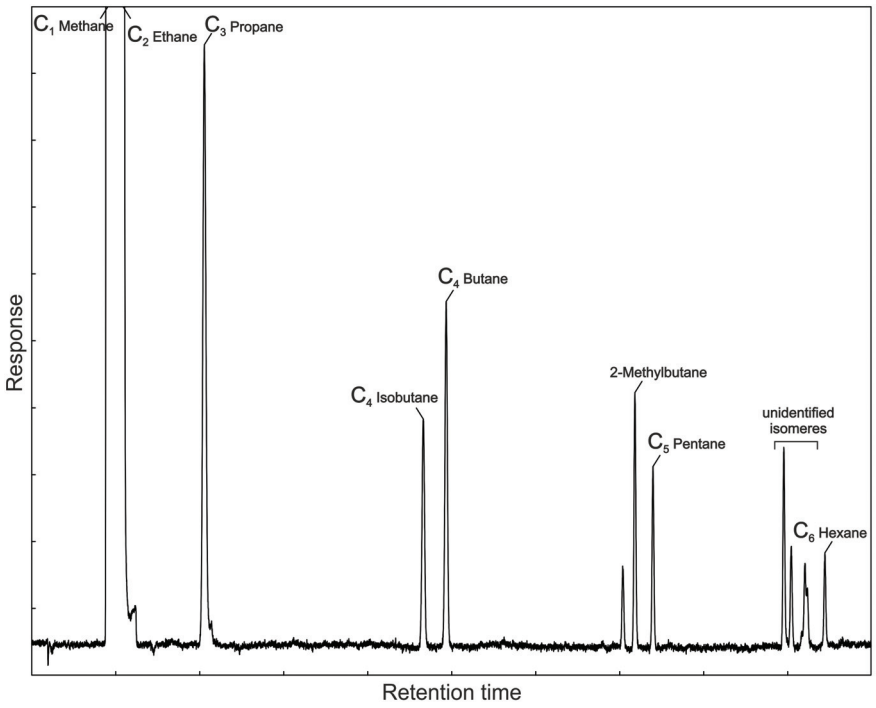

FIGURE 6.28: Magnified gas chromatogram of sample 32; in this sample methane and higher hydrocarbons and their isomers were detected additionally, the according peaks were labelled

The occurrence of higher hydrocarbons in samples of the Malm aquifer and sample 15 reveals a non-exclusive biogenic natural gas source. In order to support this hypothesis, the stable isotopic composition of these hydrocarbons was determined. The results are listed in table 6.6. Fig. 6.29 shows a diagram of δ^{13}C-CH_4 against the gas dryness, the proportion of methane to the sum of ethane, propane and butane (Bernard et al., 1978). The plot depicts that all four investigated gas samples contain dry gas, however, sample 32 contains a significant amount of C_{2+} components (dryness of sample 15: 1520, sample 30: 288, sample 31: 257, sample 32: 102). Especially sample 15 consists of nearly pure methane, only traces of ethane were measured. Furthermore, its methane isotopic ratio is lower compared to the other samples (-73 ‰). In contrast to this gas, the free gases of samples from the Malm aquifer still plot in the range of microbial gas, but a mixture with thermal gas or biodegradation of thermal gas by microorganisms resulting in a partly microbial signature cannot be excluded according to their location within the diagram. Regarding their isotopic composition, those samples are characterised by heavier isotopic ratios (between -57 and -59 ‰).

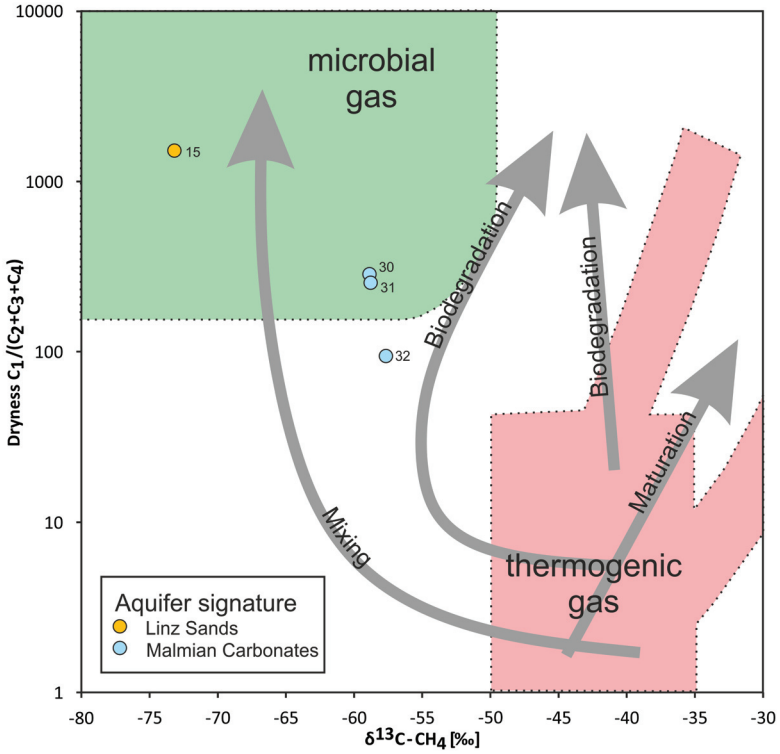

FIGURE 6.29: Differentiation of genetic origin of gas associated with water samples (modified after Bernard et al., 1978 and Pytlak et al., 2016b) Grey arrows indicate the impact of different processes on the gas composition (suggested by Milkov, 2011; Jones et al., 2008)

A different illustration plotting δD versus δ^{13}C-CH_4 of the gas samples is used to delineate the formation mechanisms of the different gases (Fig. 6.30). Samples 15 as well as 28 and 29 are located in the area of microbial CO_2 reduction whereas the gases of 30, 31 and 32 are displayed in the transition zone between thermal and microbial natural gas. This confirms the suspected mixing of thermal hydrocarbons with biogenic methane. However, the origin of biogenic methane in these samples is questionable due to various processes which could have lead to its generation.

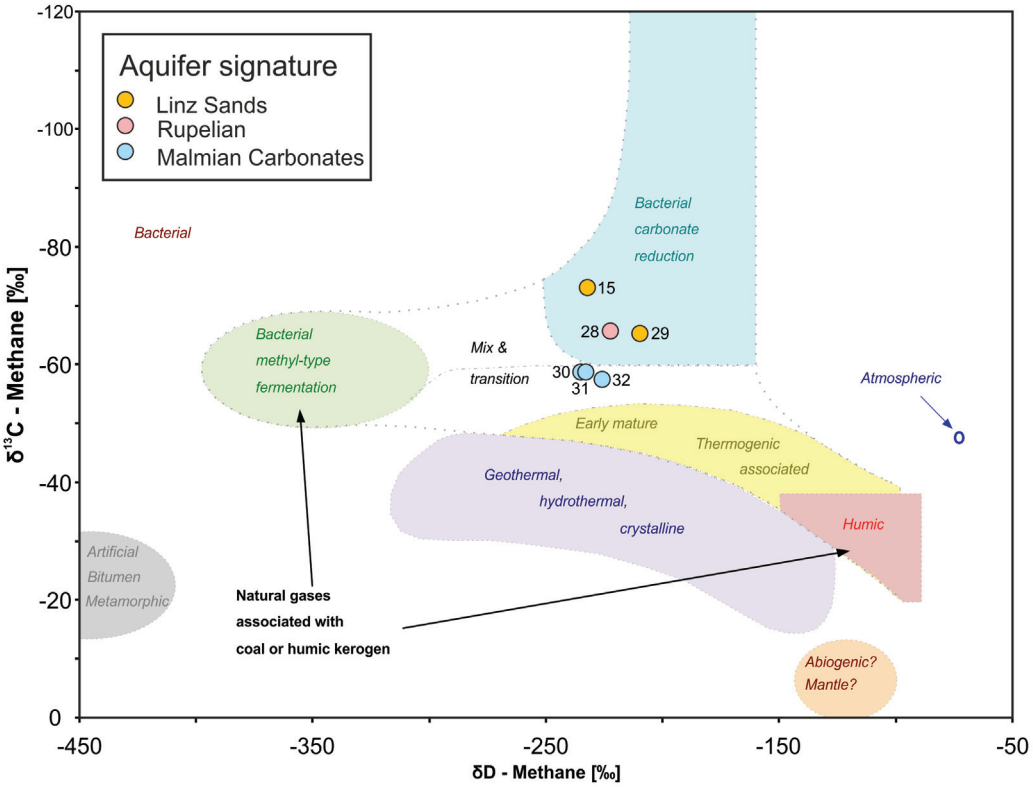

FIGURE 6.30: Isotopic crossplot of water-associated methane (modified after Whiticar et al., 1986 and Pytlak, 2017); different areas of isotopic composition indicate different genetic sources

Lower Oligocene strata (Schöneck and Eggerding formation) are considered to serve as the main source rocks for thermogenic hydrocarbons in Upper Austria (Sachsenhofer and Schulz, 2006; Sachsenhofer et al., 2010; Schulz et al., 2002). They became mature under the Alpine nappe stack in Miocene times (Gusterhuber et al., 2013) and were expulsed into Cenomanian and Upper Eocene reservoirs. Since the Cenomanian strata are directly underlain by Malmian carbonates, a migration of these thermally generated hydrocarbons into Jurassic layers could be possible. Microbial gas generation could have been feasable by reduction of CO_2 within the aquifer or by biodegradation of present thermal hydrocarbons. The isotopic signature results from mixing of those two hydrocarbon types. The reservoir temperature (table 6.2) may provide an argument against the hypothesis of biodegradation in the Jurassic carbonates because microbial activity is considered to cease at around 80 °C (Pytlak, 2017 and references therein). Thermal sulfate reduction may also provide an explanation for the occurrence of minor amounts of CH_4 in the Malm aquifer, since this gas may be produced as a by-product of this abiogenic process. Moreover, thermal sulfur reduction is observed at elevated temperatures (above 100 °C, preferably between 120 and 140 °C; Machel et al., 1995). A comparison with investigations performed by Pytlak et al. (2016a) reveals that sample 30, 31 and 32 appear in a similar area than the hydrocarbon accumulations in Oligocene and Miocene strata. These are also considered as mixtures of thermal and microbial gas. The origin of the

microbial gas components in these Oligocene/Miocene reservoirs seem to be different, since a downward migration of natural gas from Oligocene/Miocene to the Malm is unlikely.

A second theory to explain the presence of hydrocarbons in the Upper Austrian thermal aquifer implies that the natural gas was generated in Bavaria and transported through thermal water flux. The occurrence of hydrocarbon deposits in Mesozoic and Paleogeone reservoirs of the Bavarian part of the Alpine Foreland Basin supports this hypothesis. Several formations could serve as a source rock in the region east of Munich. According to Wehner and Kuckelkorn (1995), lower Oligocene, organic-rich sediments ("Sannois fish shale", a time equivalent of the Schöneck Formation) may have served as the main source rock for oil occurrences in eastern Bavaria. The oil was probably generated below the Alpine nappe stack. In the western part of Bavaria, Mesozoic strata may also serve as a source rock for hydrocarbon occurrences (Wehner and Kuckelkorn, 1995). Microbial gas could have been formed in the Sannois fish shale during early diagenesis and transferred into the Malm as a result of a Pliocene pressure decrease in the Jurassic carbonates which caused a downward migration of pore water. The microbial methane could have been carried downwards with these descending pore waters where it mixed with present thermogenic hydrocarbons (Lemcke, 1981; Hahn-Weihnheimer et al., 1979). Faults may also provide migration pathways for microbial gas from the Oligocene to the Malm (pers. comment, Groß 2018).

An analogue to the observed phenomenon in this study of the Upper Austrian Alpine Foreland Basin was described in Switzerland. The geothermal well St. Gallen GT-1 holds thermogenic gas. The gas composition of this well is characterised by a major amount of methane with traces of higher hydrocarbons. Isotopic investigations revealed a thermal gas generation process from a supposed Permo-Carboniferous origin. The vitrinite reflectance which is assumed for the generation of this kerogen type II/III gas is > 2 $\%R_o$, supporting its origin from Carboniferous coals or Autunian shales (Wolfgramm et al., 2015).

Although an oil deposit with associated gas is located in the vicinity of sample 32, it is unlikely that the gas found in the sampled waters originates from this hydrocarbon occurrence. According to Groß et al. (2015), the Cenomanian reservoir bears wet (Dryness $\leq$ 50) and isotopically light (δ^{13}C $\sim$ -70 ‰) gas. Both of these features cannot be confirmed in the geothermal well. It is assumed, that the gas of the Cenomanian reservoir was generated due to biodegradation of the trapped oil leading to its observed properties. Moreover, the oil from this deposit is undersaturated in gas (Groß et al., 2015).

A crossplot of δ^{13}C isotope ratios from ethane and propane together with a maturity trend derived from Pytlak (2017) gave a vitrinite reflectance of around 1.4 $\%R_o$ for sample 32. This could be an indication for an allochtonous origin (e.g. Bavaria) of the observed gas since model calculations of Gusterhuber et al. (2013) gave a maximum vitrinite reflectance of 1.0 $\%R_o$ for the Schöneck Formation below the Alpine nappe stack.

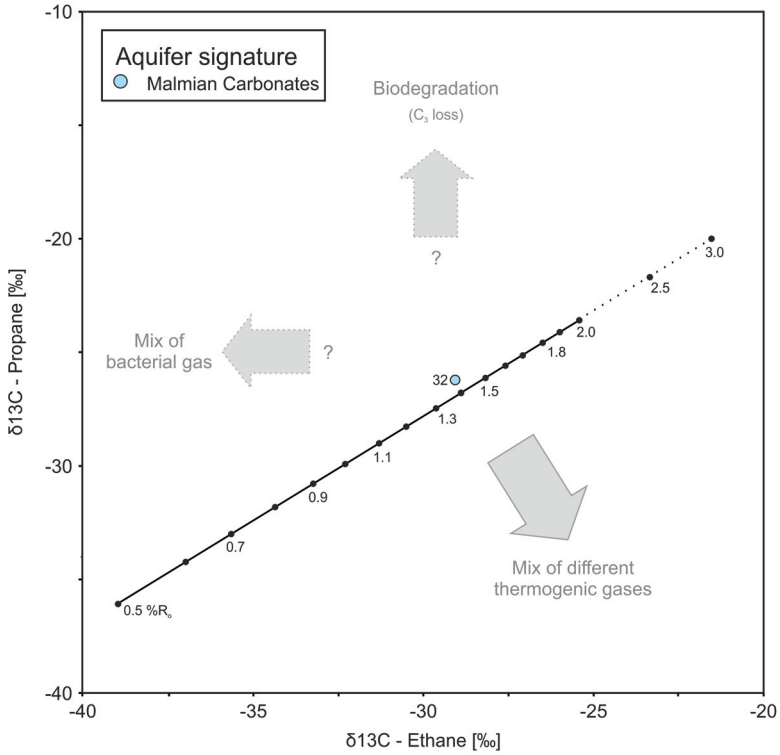

FIGURE 6.31: Estimation of gas maturity of the thermogenic gases contained in sample 32 by isotopic relations of δ^{13}C of ethane vs. δ^{13}C of propane (modified after Berner and Faber, 1996; Pytlak, 2017), the generalised maturity trend was taken from Pytlak (2017)

Wells 15, 28 and 29 hold solely biogenic gas. For the samples 28 and 29, either an autochtonous CO_2 reduction (Whiticar et al., 1986) in the drilled aquifers could have formed this methane. A combination of both versions should be considered, too. Sample 15 may be charged with biodegraded gas stemming from shallow oil deposits near this well (Fig. 1.1). Oil trapped at approximately 200 m depth in Leoprechting north of the sampling location is characterised by heavily biodegraded oil (Groß et al., 2015; Nachtmann, 2001). Moreover, a water well of around 300 m depth in the town Andorf near Schärding (close to the location of sample 15) encountered an oil film at the surface of the recovered water (pers. comment Sachsenhofer, 2018). Unfortunately, a sampling of this well is not possible, since this well collapsed years ago. Additionally, wells recovering water from the Innviertel Group carry methane according to Goldbrunner (1988). Therefore, an origin of the methane in Bavaria cannot be excluded. However, if this is the case, the hydrodynamic conditions of this aquifer should be reevaluated since the Inn is considered to form a major water discharge area in the Innviertel (Fig. 6.26, Goldbrunner, 1984; Goldbrunner, 1988).

6.5 Geothermometers

Alkali-geothermometers have been calculated for selected wells according to the formulae in section 5.5. The calculations were performed on the following samples: 2, 7, 15, 16, 17, 18, 28, 29, 30, 31 and 32. The results of the geothermometric calculations are listed in table 6.9. The second column in this table lists the water temperature which was measured in the course of sampling and derived from literature, respectively.

A comparison of the calculated geothermometer results in table 6.9 with the measured (or literature derived) water temperature clearly shows, that all results are remarkably higher than the temperature measured at the sampling sites. For those samples recovered from shallow water supply wells, temperatures between 39 °C and 139 °C were received, the values of the geothermal wells range from 98-199 °C. These data ranges also exhibit a great variation which leads to the assumption that the majority of calculated temperatures are not representative for the subsurface reservoir temperatures and cannot be considered as realistic. However, one column, listing the results of equation 5.15 gives values which could be considered as realistic for the water samples. For the shallower wells (samples 2, 7, 15, 16, 17 an 18) the results range between 39-60 °C, the two geothermal wells recovering water from the Rupelian and Linz Sands, achieved results of 66 °C (sample 28; Rupelian) and 54 °C (sample 29; Linz Sands). The calculated Malmian aquifer temperatures (samples 30, 31 and 32) yield results between 98-103 °C. Since these values are only slightly increased in comparison to the measured water temperatures and literature data from Elster et al. (2016), it could be realistic that the thermal waters of the Malm reached their equilibrium state at these temperatures and cooled down during their ascension within the aquifer (Fig. 3.2). During this ascension, an equilibrium state could not have been reached again resulting in the higher values for the geothermometer according to Giggenbach (1988). The temperature difference for the samples 2, 7, 15, 16, 17 and 18 is higher in comparison to the water samples from geothermal wells. This increased temperature difference could be caused by a mixing with meteoric waters. These mixing processes lead to a change of the initial ion concentrations and therefore, a distortion of the calculated reservoir temperatures.
In order to determine, whether water samples are suitable for the application of cation geothermometry, a ternary diagram developed by Giggenbach (1988) can be used (Fig. 6.32). Although this diagram was originally developed for a hydrothermal system influenced by magmatic activity, it is widely used to determine the maturity/equilibrium state of geothermal waters. The three corners display the relative proportions of potassium, sodium and magnesium. Isothermal lines as well as two curves, separating immature from partly equilibrated waters and indicating the state of full equilibrium are illustrated as well. If samples reach the line of full eqilibrium, it can be assumed that water-rock interactions have created balanced conditions and therefore the calculated geothermometry result can be considered as reliable. If this is not the case, the waters have not reached

TABLE 6.9: Alkali-geothermometers of selected samples according to different authors

Sample no.	Temperature [°C]	Fournier (1979)	Arnórsson et al. (1983)	Nieva & Nieva (1987)	Giggenbach 1 (1988)	Verma & Santoyo (1997)	Can (2002)	Giggenbach 2 (1988)	Drever (2005)
2	16.4	92	99	108	113	99	109	49	84
7	19.7	88	95	104	109	95	107	44	85
15	13.2	72	80	86	94	79	100	39	102
16	12.2	119	124	138	139	125	124	59	139
17	12.5	116	121	135	136	122	122	60	136
18	11.4	98	104	114	118	104	112	46	130
28	38.3	63	87	94	101	70	97	66	74
29	36.6	80	71	76	84	87	103	54	81
30	90.0*	172	174	199	190	176	163	99	145
31	80.0*	172	174	199	190	176	163	98	139
32	86.0*	156	159	181	174	161	150	103	130

* Sample temperature from Elster et al. (2016)

this state yet, which could be due to various influencing factors, e.g. mixing with shallow or superficial waters, short residence time in the aquifer, low aquifer temperatures (diminishing the reaction velocities).
The samples taken during this study are plotted in Fig. 6.32. The plot illustrates that none of the investigated samples is in equilibrium state. All samples are immature, except three waters from wells 28, 29 and 32. They are located in the area of partial equilibrium at low temperatures. The samples 30 and 31 plot very close to the boundary between immature and partly equilibrated waters, therefore it can be assumed that they are in the transition of these two states. Most of the shallow samples are concentrated around the bottom right corner, where magnesium is depicted. This clustering phenomenon can be explained by the higher magnesium content. This element can be dissolved in cooler waters providing an adequate groundwater residence time.
The samples characterised by a higher amount of dissolved sodium are located in the vicinity of the boundary between immature and partly equilibrated waters. This shows, that the increased retention time in the aquifer has already resulted in mineral-water interaction processes and therefore, in a movement in direction of an equilibrium state.
Due to the low temperature of all sampled wells, the groundwater residence time has to be appropriate to enable a balance approach between the individual components in the aquifer. However, this amount of time has not been reached in these samples yet. According to Giggenbach (1988) geothermometric formulae containing the sodium concentration of the water are not suitable for disequilibrated samples, but K-Mg-Geothermometers could still deliver useful results if the water is not acidic. Therefore, most of the calculated cation-geothermometer values can be discarded and should not be used for further interpretation in this case. The values received by equation 5.15 gave the lowest temperature values for the investigated samples and therefore, confirm the observations of Giggenbach (1988). Moreover, these values are closer to the measured water temperatures leading to the assumption that those results could be realistic.
Cation geothermometers are commonly compared to silica geothermometers in order to verify the obtained results because both methods are able to calculate the same property by using independent variables. Unfortunately, this parameter has not been analysed so far. A determination of the silica content of the collected samples is highly recommended to cross-check the reservoir temperatures received for the cation-geothermometers. Furthermore, since most of the waters seem to have undergone mixing processes during their flowpath in the subsurface, a numerical approach by simulation of different mixing models could give new insights into the behaviour of the Malmian water during its residence time in the underground and its ascension into shallower strata.

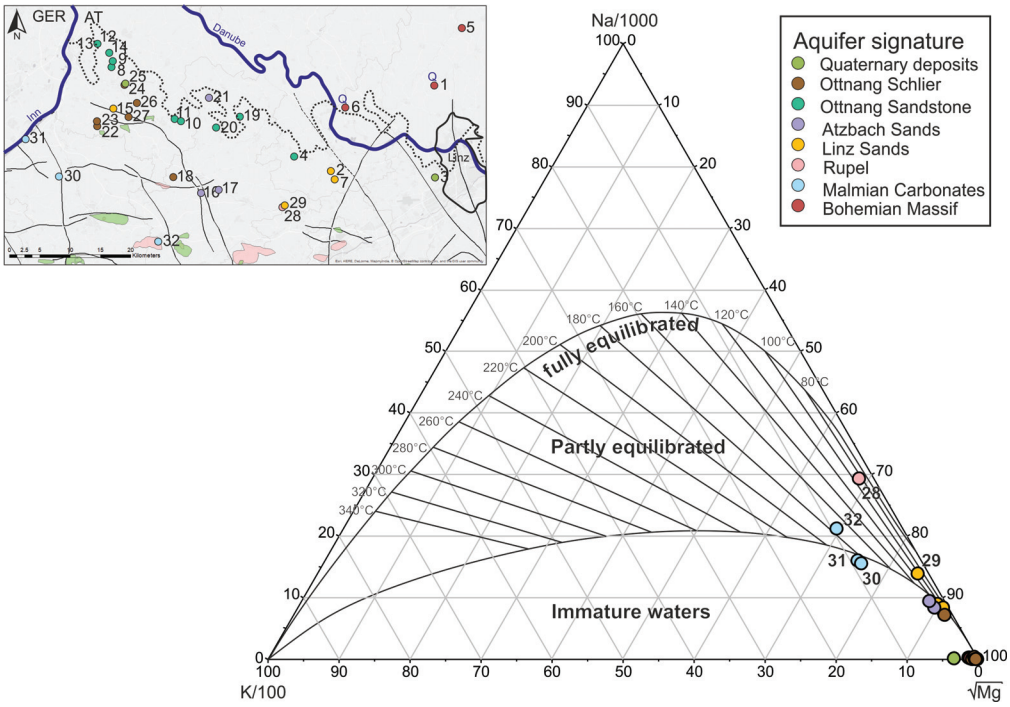

FIGURE 6.32: Ternary diagram with relative contents of Na, K and Mg in order to distinguish fully or partly equilibrated and immature waters, respectively (modified after Giggenbach, 1988); the samples for which cation-geothermometers have been calculated plot either in the partly equilibrated state area or close to the border of partial equilibrium and immature waters, the other groundwater samples located at the bottom right corner have been plotted for comparison, however, cation-geothermometers have not been calculated for these waters

6.6 Impact on the Hydrodynamic Concept of Upper Austria

The combination of the collected data and performed analyses of all samples reveals that the collected water samples can be categorised into different groups according to their hydrochemical signatures (Fig. 6.33). Four different groups can be distinguished among the sampled waters.

The first group (Group I) summarises waters originating from the Bohemian Massif and those, where the aquifer is recharged by waters from this crystalline formations, respectively (Fig. 6.33). This group contains samples 1, 5, 6 and 21. They are primarily characterised by their low amount of dissolved solids between 55-222 mg/l (on average 130 mg/l). According to the ion content, this group can be classified as Ca-Mg-HCO_3-type. The low total mineralisation is induced by the aquifer, a fractured aquifer like the Bohemian Massif shows a relatively small contact area of water and rock matrix, limiting the amount of possible water-rock interaction processes. As a result, the dissolved mineral content is reduced. Higher amounts of nitrate and sulfate in the samples are probably anthropogenically induced and not naturally obtained. The stable isotopic ratios of the waters suggest a recent infiltration (δ^2H-values between -72.2 and -75.1 ‰ and

δ^{18}O-values between -10.3 and -10.9 ‰).

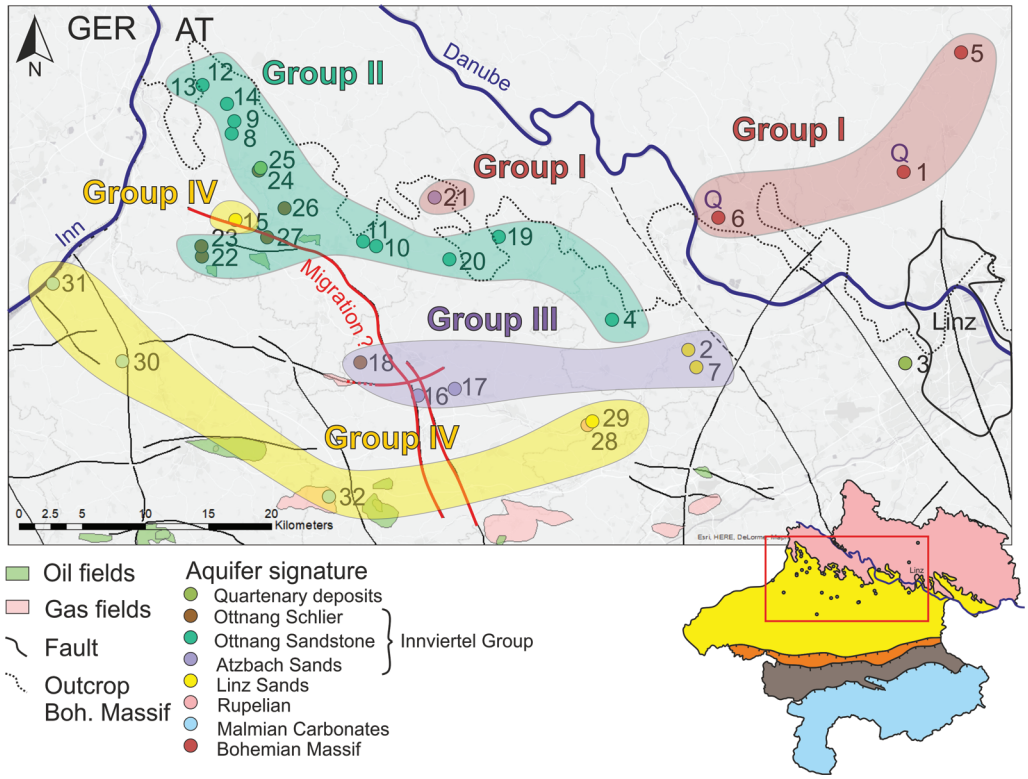

FIGURE 6.33: Map of collected samples with groups assigned to the waters according to their hydrochemical characteristics; sample 3 cannot be assigned to any group due to its anthropogenically induced distortions of the hydrochemical characteristics of the water; two faults (the Lindach Fault and its northwest trending conjugation are marked in red, these faults could serve as migration pathways for thermal waters from the south (Group IV)

A major share of the collected waters from shallow wells of the Inn and Hausruck region can be categorised as a second group (Group II, Fig. 6.33). Sample numbers 4, 8-14, 19, 20 and 22-27 form this group. Sample 3, taken south of Linz cannot be clearly categorised due to the influence of added substances changing the chemical characteristics of the water. Therefore, the composition of the pure water could not be investigated and assigned to a group. The amount of total dissolved solids ranges from 204-507 mg/l (on average 383 mg/l), which is significantly higher compared to the total mineralisation of waters from the Bohemian Massif. As already observed in Group I, these shallow wells also contain Ca-Mg-HCO_3-type waters. The aquifer properties are responsible for the increased mineralisation of Group II. Porous aquifers, like the Ottnangian Molasse strata provide a significantly increased internal surface enabling more contact between the formation and the contained water in comparison to the Bohemian Massif. Hence, more reactions between those components in the aquifer system occur. The ion composition varies slightly between the individual samples due to the large extent of the study area. These effects are probably caused by aquifer heterogeneities, e.g. facies variations

in the individual formation sections. Stable isotope results are in a similar range than the samples from Group I (δ^2H-values between -71.0 and -75.2 ‰ and δ^{18}O-values between -10.11 and -10.72 ‰; the values of sample 25 have been excluded due to a seasonal distortion), this leads to the assumption that the sampled waters entered the aquifer in recent times. Traces of methane have been detected in three headspace samples, free gas samples did not encounter any hydrocarbons, only nitrogen, oxygen and carbon dioxide were observed.

A previous study of water samples in the Innviertel Group classified three different types (Goldbrunner, 1988; Schubert, 2015). A few samples collected in the course of the recent project can be added to one of those three groups (Group 1, Group 2 and Group 3) defined by Goldbrunner (1988). Samples 8, 9 and 24 (Group II; Fig. 6.33) fulfill some of the criteria (Eh $>$ 72 mV, Cl $<$ 1 mg/l, pH between 6.90 and 7.80) in order to be classified as members of "Group 1" from this former publication. The collected waters from wells 12, 13, 14, 19, 22, 23 and 26 (Group II; Fig. 6.33) share characteristics of "Group 2" (Eh between -6 and 82 mV, Cl $\geq$ 1 mg/l, pH between 7.76 and 8.60) according to Goldbrunner (1988). Despite of their smaller redox values, many of the other defined features of this group were observed. Four of the samples from the current study cannot be clearly added to either "Group 1" or "Group 2" of Goldbrunner (1988), since they show characteristics from both groups. However, the measured redox potential in the current study is characterised by a greater instability than the chloride content and therefore, subjected to a higher variation of the measured values. Hence, the samples 10 and 11 (Group II; Fig. 6.33) would be assigned to "Group 1" due to their low chloride content and the samples 20 and 27 (Group II; Fig. 6.33) would belong to "Group 2" since their chloride values exceed the threshold value of 1 mg/l, defined by Goldbrunner (1988).

The samples 16, 17 and 18 as well as the waters from location 2 and 7 are summarised in Group III (Fig. 6.33). This group consists of cation exchange waters with a low amount of chloride in comparison to the thermal waters. As opposed to other samples from shallow aquifers, their water type can be defined as Na-HCO_3-type, with a total mineralisation ranging from 395-436 mg/l (on average 415 mg/l). Since samples 2 and 7 are located within the discharge area of the Upper Austrian and Bavarian thermal water aquifer (Fig. 3.1), a mixture of meteoric, shallow groundwater with deep thermal water is assumed (cf. Fig. 6.23). Increased water temperatures paired with a low ^{14}C content and a stable isotope signature (δ^2H-values between -82.1 and -90.7 ‰ and δ^{18}O-values between -11.74 and -12.87 ‰) suggesting a groundwater recharge during a glacial period give numerous indications for this theory. The waters from locations 16, 17 and 18 show similar features, but in contrast to the other two samples, their water temperatures are not increased. This does not exclude the possibility of a mixture with Malmian thermal waters, the groundwater residence time in the aquifer near those wells is increased, though. Elster et al. (2016) and Schubert (1996), however, stated that a reduced proportion of chloride in the samples disagrees with the mixing theory. They assume that no mixture of thermal and shallow groundwaters can be observed in the vicinity of the samples 2 and 7. Samples 16, 17 and 18 share some features with "Group 3" (Eh between -104

and 41 mV, Cl $>$ 1 mg/l, pH between 7.95 and 8.89), described by Goldbrunner (1988), thus these waters are comparable with waters from this group. The dissolved methane concentrations in the headspace samples yielded values between 0.06-2.35 mg/l. 0.3 % (sample 7) and 1.2 % (sample 2) of methane were detected in the free gas samples.
The amount of chloride contained in the deep geothermal waters is the major differentiation criterion for the last group of samples. This group (Group IV) contains six samples, 15, 28, 29, 30, 31 and 32 (Fig. 6.33). The waters of wells 30-32 are recovered from wells penetrating Malmian carbonates, the geothermal wells 28 and 29 bear thermal water which ascends from these carbonates into the Rupelian and Linz Sands, as already described in literature (e.g. Elster et al., 2016). The three Malmian waters are characterised by an amount of dissolved solids from 961-1409 mg/l (on average 1136 mg/l), the other three samples show values between 526-648 mg/l (on average 589 mg/l). The stable isotopes of the samples 15, 28 and 29 are depleted in ^{2}H and ^{18}O, which indicates a Pleistocene infiltration (δ^{2}H-values between -79.5 and -84.7 ‰ and δ^{18}O-values between -11.45 and -12.10 ‰). The stable isotopes of the Malmian samples plot on a separate trendline for waters from this aquifer (δ^{2}H-values between -76.5 and -79.5 ‰ and δ^{18}O-values between -9.84 and -10.57 ‰). The analyses of dissolved and free gases gave a significant amount of dissolved methane in the headspace samples (0.053-7.440 mg/l). Moreover, the free gas samples of the Malmian carbonates did not only detect methane, but also traces of higher hydrocarbons. The gaseous hydrocarbon content in the samples 30, 31 and 32 ranges between 35 and 60 %.
Although many of the obtained results have already been observed and described, sample 15 provides a new insight into the hydrodynamic characteristics of the thermal water aquifer. This water gives the first proof of thermal water mixture in the Innviertel region. The sample is recovered from the Linz Sands and documents the rise of water with chemical characteristics of Malmian thermal water in this area (approximately 30 % of thermal water; cf. Fig. 6.23). This assumption is supported by the investigation of free and dissolved gases, which detected a significant amount of methane measured in sample 15 (> 30 %). Furthermore, the stable isotopic composition suggest a Pleistocene infiltration of the water.
Due to these new findings and observations a revision of the hydrodynamic concept of the Malmian thermal water aquifer is suggested. According to this concept, the northern part of the Innviertel region is not solely recharged by meteoric waters from the Bohemian Massif (as shown in Fig. 3.1) but also experiences a northward movement of thermal water contradicting the established model (Bayerisches Landesamt für Wasserwirtschaft, 1999). These currents from south to north are coupled with an upward migration of thermal water from the Jurassic towards shallower Cenozoic formations, like the Linz Sands, as observed in the sampled well in Andorf. Hence, Fig. 6.34 shows an isopach map of the Malmian carbonates assigned with the corresponding water flow directions (red arrows; Bayerisches Landesamt für Wasserwirtschaft, 1999) and the new, revised flow directions in agreement with the results from this study (yellow arrows). According to the new suggestions, the water currents do not only reach the Linz Sands

south of Linz as observed in the samples 28 and 29, but also in the Inn- and Hausruckviertel area due to their migration parallel to the Malmian isolines. The area framed in red is enlarged in Fig. 6.35. This augmented area depicts two faults, the Lindach Fault and a conjugation of this fault with an elongation towards the north, in bold and red. These highlighted faults could deliver an explanation for the occurrence of Malmian water in shallower formations, otherwise a northward flow direction of the thermal water would contradict the assumed hydrodynamic potentials of the Malm (Fig. 6.35). Sample 15 is located in the vicinity of this conjugated fault (Fig. 1.1, Fig. 6.1). In samples 28 and 29, an ascension of thermal water via a normal fault is observed. Moreover, a cross section through the Upper Austrian Foreland Basin illustrates a movement along those fracture zones in the basin (Fig. 3.2). Likewise, the Lindach fault and its conjugation could provide pathways for the ascension of thermal waters. Unfortunately, no other wells penetrating the Linz Sands near these faults could be found to confirm this assumption.

Furthermore, this study provides investigations which show a significant amount of higher hydrocarbons contained in the free gas samples of thermal wells 30, 31 and 32. Since C_{2+} components are generated by thermal maturation of organic-rich sediments, this observation provides additional evidence for an interaction of the geothermal and the petroleum system in this basin and a transport of these gaseous phases with thermal water currents in the subsurface. Similar conclusions in a different area of the basin were already drawn by Pytlak et al. (2017). However, what remains unclear is the origin of these hydrocarbons found in the samples. Lower Oligocene source rocks beneath the Northern Calcareous Alps could have generated the thermogenic hydrocarbons either in Upper Austria or Bavaria. Bavarian hydrocarbons would have been transported to Upper Austria via water currents in the Malmian aquifer (Fig. 3.1, Fig. 6.34). Moreover, there are several options which could explain the occurrence of biogenic methane in thermal water samples. Microbial generation via degradation of organic matter or hydrocarbons provide an option. These processes could have either occurred in Bavaria coupled with a transport of the natural gas to Upper Austria, but an autochtonous formation in Upper Austria may be possible as well. A further investigation of the properties of these formations and undergone processes could lead to the solution of these open questions.

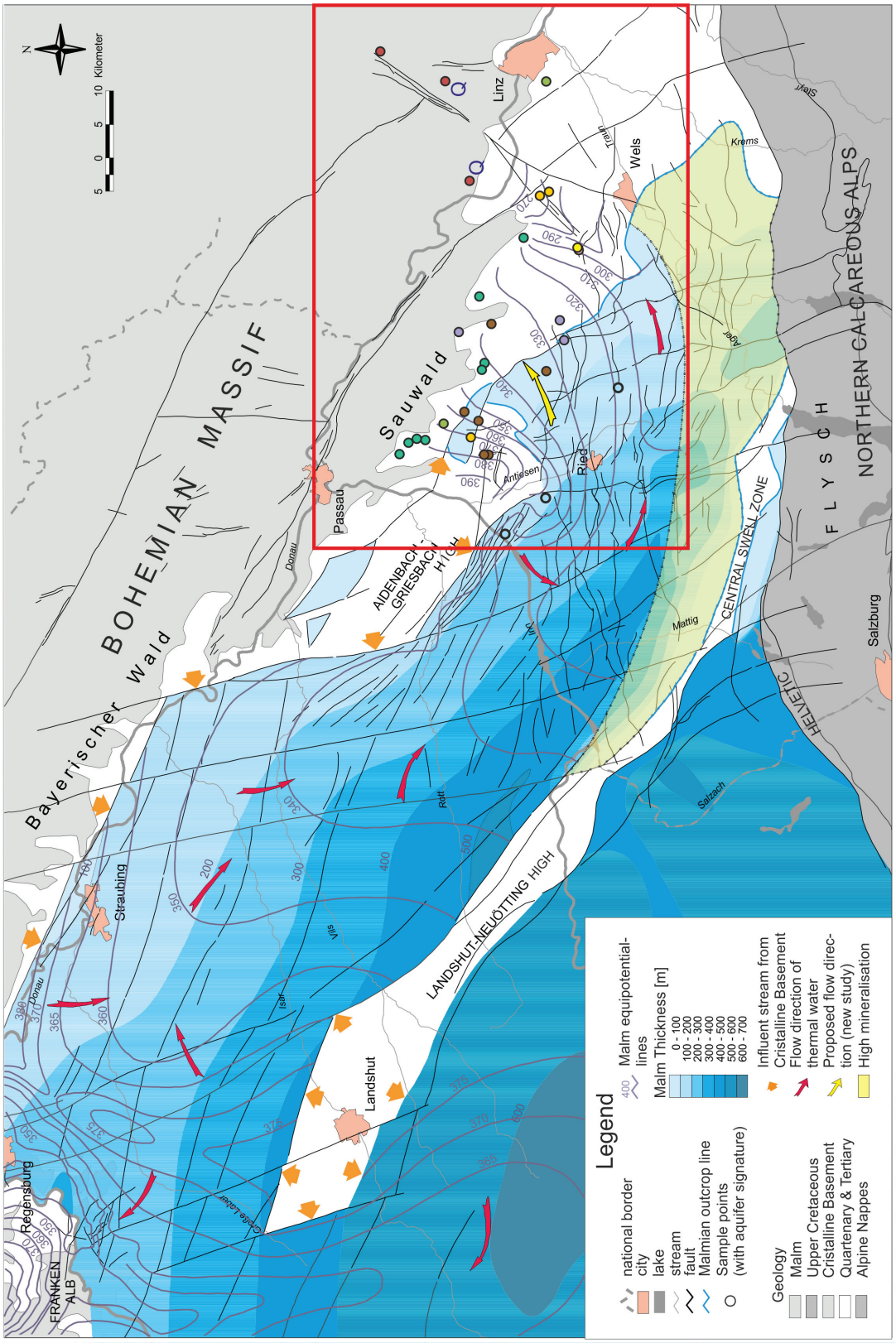

FIGURE 6.34: Malmian thickness map (modified after Bayerisches Landesamt für Wasserwirtschaft, 1999) with flow directions of the thermal waters within the aquifer (red arrows), the yellow arrows at the formation margins mark the recharge areas, the yellow arrows in Upper Austria mark the new, proposed flow direction of the thermal water. The area framed in red is enlarged in Fig. 6.35.

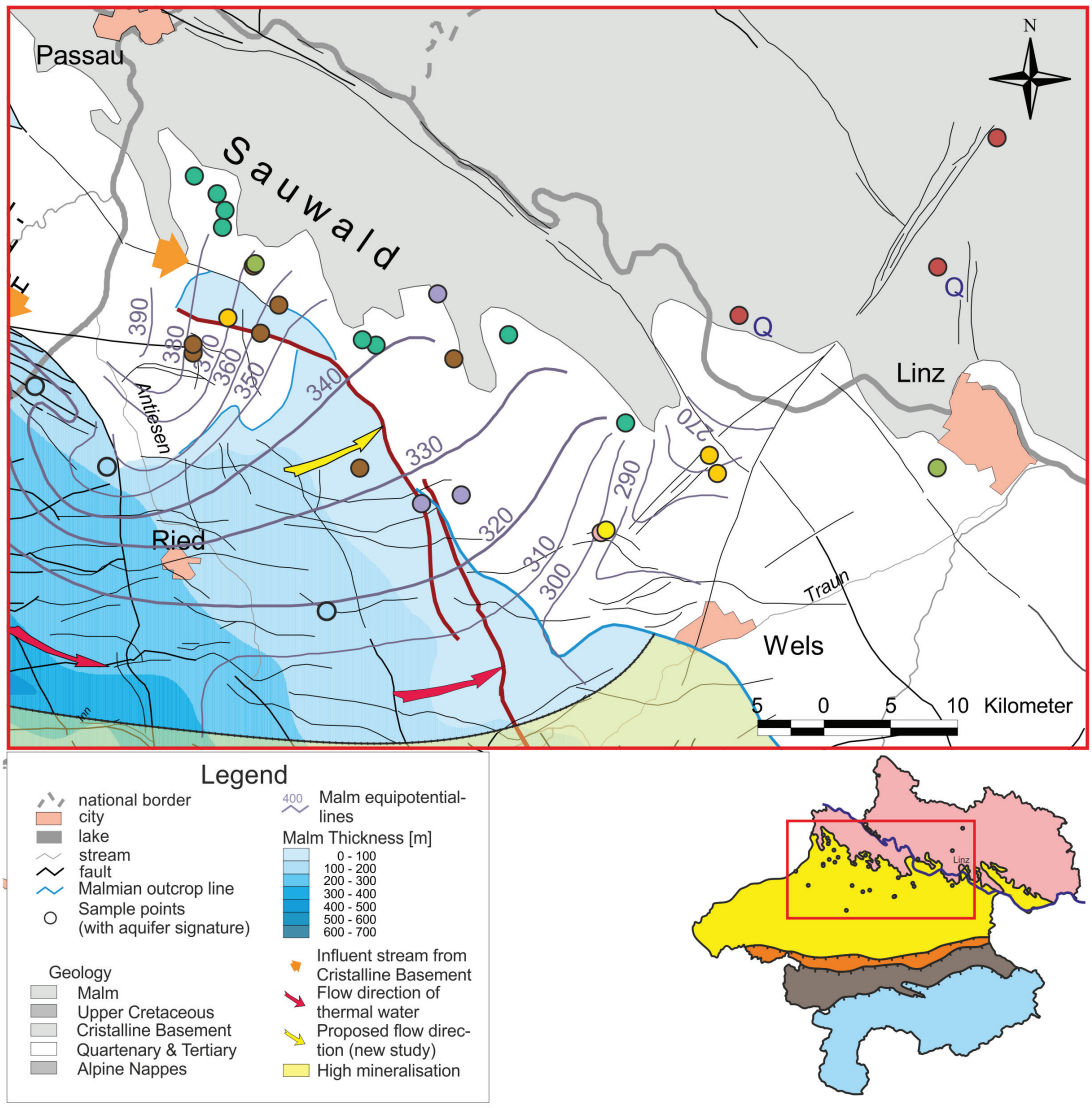

FIGURE 6.35: Close-up of the Malmian thickness map in Upper Austria (modified after Bayerisches Landesamt für Wasserwirtschaft, 1999), the red arrows mark the flow direction of the thermal waters within the aquifer, the yellow bold arrows outside of the Malmian outcrop mark recharge areas, the yellow arrows within the Malmian aquifer mark the new, proposed thermal water flow direction based on the outcome of this study. The Lindach fault and its conjugation towards the north and north-west is marked in red. This fault could act as a pathway for the ascension of thermal water into shallower strata

7 Conclusion

Based on the results and possible reasons for the data obtained from the sampled waters, which have been discussed in the previous chapter (chapter 6), the following conclusions can be drawn for the investigated samples.

- The samples can be categorised into four different groups (Group I-IV) according to their hydrochemical signatures.
- **Group I** includes the samples from the Bohemian Massif (samples 1, 5 and 6) and sample 21, for which a water supply from the Bohemian Massif is assumed. The total mineralisation of these Ca-Mg-HCO_3-type waters is between 55-222 mg/l (on average 130 mg/l). This low mineralisation is caused by the aquifer type, since the Bohemian Massif as a fractured aquifer only provides a small internal surface for interactions between the water and the host rock. The stable isotopic ratios of the samples suggest a recent infiltration of the aquifer. As far as the gas content of this group is concerned, only oxygen, nitrogen and carbon dioxide were detected.
- **Group II** comprises of a major part of the sampled wells (samples 4, 8-14, 19, 20 and 22-27). The water from these samples is assigned as Ca-Mg-HCO_3-type, the amount of dissolved solid varies between 204-507 mg/l (on average 383 mg/l). This increased total mineralisation is a characteristic which distinguishes the waters of Group II from Group I. Ottnangian sediments, which serve as a porous aquifer, enable a larger contact area for interactions between water and rock matrix due to the larger internal surface. This results in the augmented amount of dissolved solids in the water. An entry of these waters into the aquifer during recent times is derived from the stable isotopic ratios of the samples. An investigation of free and dissolved gases resulted in traces of methane, which could be detected in four headspace samples. However, free gas samples only contained oxygen, nitrogen and carbon dioxide.
- The samples 2, 7, 16, 17 and 18 are included in **Group III**. These waters are characterised by cation exchange and a low proportion in chloride. This feature separates the Na-HCO_3-type samples from the thermal waters. Total mineralisation lies between 395-436 mg/l (on average 415 mg/l). For the samples 2 and 7, a mixture with thermal water is assumed, since these wells are located within the discharge area of the Upper Austrian and Bavarian thermal water aquifer. Low ^{14}C contents and an increased water temperatures support this theory. Although this increased temperature is not observed in the samples 16, 17 and 18, an influence of thermal water

on these samples cannot be excluded. Stable isotopic ratios of the water show a depletion in ^{18}O and ^{2}H, suggesting a Pleistocene infiltration of the aquifer. Methane was detected in the headspace samples as well as in the free gas samples. However, these methane contents are significantly lower than those of the thermal waters.

- **Group IV** summarises the six samples 15 and 28-32. These waters originate from Malmian carbonates, the Rupelian and Linz Sands. The type assigned to these samples is the Na-HCO_3-(Cl)-type. A characteristic which distinguishes them from the waters of Group III is the higher amount of chloride contained in the waters. Malmian thermal waters hold between 961-1409 mg/l of total dissolved solids (on average 1136 mg/l), whereas the samples from the Linz Sands and the Rupelian show a mineralisation of 526-648 mg/l (on average 589 mg/l). The stable isotopic ratios of the six samples indicate a Pleistocene infiltration age, similar to the waters from Group III. However, the investigation of dissolved and free gases revealed a significant amount of methane associated with the water. Moreover, traces of higher hydrocarbons were detected.

- **Sample 15** is a 166 m deep water well in Andorf, recovering water from the Linz Sands. This well gives the first evidence of an occurrence of thermal water in the Innviertel region. The hydrochemical characteristics of this sample resemble the characteristics of the waters from geothermal wells, therefore, this sample was included in Group IV. The amount of total dissolved solids in this water is 594 mg/l, which is in a similar order of magnitude than the mineralisation of the samples 28 and 29. The amount of methane which was detected in the free gas sample is significant (> 30 %) and supports the conclusions drawn from the chemical investigations. These new findings suggest that the hydrodynamic concept of the Malmian thermal aquifer needs to be revised in the Upper Austrian area, considering the recently obtained new data. A northward conjugation of the Lindach fault could serve as a possible migration pathway against the hydraulic potential of the Malmian carbonates, enabling a rise of thermal water into shallower strata.

- **Methane** was detected in various samples from different aquifers. Whereas the Ottnangian strata contained only traces of dissolved methane (Group II and III), significant amounts of hydrocarbons were detected in the geothermal water samples (Group IV). Four samples contained higher hydrocarbons (samples 15, 30, 31 and 32). An investigation of the isotopic ratios of these gases yielded, that most of the methane included in the waters is of biogenic origin. However, due to the occurrence of $\mathbf{C_{2+}}$ **components**, a mixing of the biogenic methane with thermogenic natural gas is assumed. The origin of these thermogenic hydrocarbons is not clear yet. Two regions could serve as possible provenance areas for the thermogenic hydrocarbons. The first option suggests a formation from organic-rich strata in Bavaria coupled with a transport of the gas with water currents from Germany to Upper Austria. The second option considers a formation in Lower Oligocene

source rocks beneath the Northern Calcareous Alps and a northward migration of the thermogenic gas.

8 Recommendations and Outlook

The project outline aimed to create a thorough and holistic analytical program by using different methods and approaches to classify the water samples as good as possible. However, there are some additional procedures which could improve further investigations.

Firstly, a denser observation network of different aquifers in the basin would be of advantage for this project to delineate the proposed zones of shallow and deep groundwater mixture in more detail. However, since this is coupled to the number of water wells drilled in these aquifer horizons, this attempt may pose a challenge. Therefore, the number of water wells, which can be sampled, especially in the intermediate formations between the Malmian carbonates and the shallow Ottnangian strata, is probably limited. A solution to this problem is the incorporation of hydrocarbon wells in the Upper Austrian Molasse Basin. These wells mostly target the mentioned formations and could provide a significant amount of additional information for this project. Moreover, since the area east of Linz is hardly investigated in terms of deep groundwater flow paths, an expansion of the investigation area towards the east is highly recommended.

In terms of hydrochemical properties, the broad variety of measured parameters is well suitable to derive hydrochemical signatures and characteristics of aquifers. Nevertheless, a determination of the SiO_2-content of the samples taken up to now as well as samples of future campaigns could give supplementary information. Especially in order to distinguish waters hosted by siliciclastic or carbonate aquifers. Eventually, SiO_2 may enable the distinction of waters originating from the Bohemian Massif from waters from the North Alpine Foreland Basin. Additionally, this compound can be used to calculate SiO_2-geothermometers which are widely used in geothermal exploration. An advantage of these geothermometers in contrast to alkaline or earth-alkaline geothermometers is the applicable temperature range, which is significantly lower. Therefore, these calculations may provide more reliable and realistic results.

Furthermore, since most geothermal wells in the Malm do not host any ^{14}C anymore, another method to determine the age of water from this aquifer should be considered. The measurement of ^{81}Kr-decay is an alternative approach to investigate groundwater ages. Due to its half-life period of 229000 years (Audi et al., 2003) paired with its characteristic feature, that neither environmental sources in the subsurface nor anthropogenic contamination influence its content (Lehmann et al., 1993), it is a well-suitable isotope to identify groundwater residence times exceeding the detection limit of ^{14}C. Recently conducted ^{81}Kr-investigations of Malmian thermal wells the western part of the North Alpine Foreland Basin delivered results which fit to the assumed hydrodynamic characteristics of the

Jurassic formation in this part of the basin (Hydroisotop GmbH, 2017a). Therefore, this method could aid to clarify the hydrodynamic situation in the Upper Austrian part of the basin.

Regarding the content of free and dissolved gases in the water samples, the investigation procedure should be applied to more wells since this method seems to support the hydrochemical investigations by giving additional indications for mixture of deep and shallow groundwaters. To complete the assumptions from this investigation, free gas samples from the wells, where CH_4 was detected in the headspace sample should be taken, if this has not occurred yet. Especially the thermogenic origin of the free methane and the occurrence of higher hydrocarbons in the geothermal wells introduce a new field of research. In order to gain more data, gas from all geothermal wells in Upper Austria should be sampled and analysed regarding their molecular and isotopic composition. A comparison with gases sampled from Bavarian geothermal wells could unveil the origin and migration pathways of the thermogenic gaseous hydrocarbons and give new insights into the interaction of the petroleum systems in Upper Austria and, if present, Bavaria with the Malm aquifer.

Bibliography

Alcalá, F.J. and E. Custodio (2008). "Using the Cl/Br ratio as a tracer to identify the origin of salinity in aquifers in Spain and Portugal." In: *Journal of Hydrology* **359**, pp. 189–207.

Andres, G. (1983). "Untersuchungen zum Grundwasserhaushalt des jungtertiären Tiefenwassers mittels Grundwasseraltersbestimmungen." In: *Informationsbericht **2/83** des Bayerischen Landesamtes für Wasserwirtschaft*. München, pp. 45–57.

Andrews, J.N., J.E. Goldbrunner, W.G. Darling, P.J. Hooker, G.B. Wilson, M.J. Youngman, L. Eichinger, W. Rauert, and W. Stichler (1985). "A radiochemical, hydrochemical and dissolved gas study of groundwaters in the Molasse basin of Upper Austria." In: *Earth and Planetary Science Letters* **73**. Ed. by Elsevier Science Publishers B.V., pp. 317–332.

Andrews, J.N., M.J. Youngman, J.E. Goldbrunner, and W.G. Darling (1987). "The Geochemistry of Formation Waters in the Molasse Basin of Upper Austria." In: *Environmental Geology and Water Sciences* **10**, pp. 43–57.

Arnórsson, S., E. Gunnlaugsson, and H. Svavarsson (1983). "The chemistry of geothermal waters in Iceland. III. Chemical geothermometry in geothermal investigations." In: *Geochimica et Cosmochimica Acta* **47**, pp. 567–577.

Audi, G., O. Bersillon, J. Blachot, and A.H. Wapstra (2003). "The NUBASE evaluation of nuclear and decay properties." In: *Nuclear Physics A* **729**, pp. 3–128.

Bachmann, G.H., M. Müller, and K. Weggen (1987). "Evolution of the Molasse Basin (Germany, Switzerland)." In: *Tectonophysics* **137**, pp. 77–92.

Badecker, M.J. and W. Back (1979). "Hydrogeological processes and chemical reactions at a landfill." In: *Groundwater* **17**, pp. 429–437.

Barker, J.F. and P. Fritz (1981). "The occurrence and origin of methane in some groundwater flow systems." In: *Canadian Journal of Earth Sciences* **18**, pp. 1802–1816.

Bayerisches Landesamt für Wasserwirtschaft (1999). *Das Thermalwasservorkommen im niederbayerisch-oberösterreichischen Molassebecken - Hydrogeologisches Modell und Thermalwasser-Strömungsmodell im Auftrag des Freistaates Bayern und der Republik Österreich*. München: Kurzbericht.

Behne, W. (1953). "Untersuchungen zur Geochemie des Chlor und Brom." In: *Geochimica et Cosmochimica Acta* **3**, pp. 186–214.

Bernard, B.B., J.M. Brooks, and W.M. Sackett (1978). "Light hydrocarbons in recent Texas continental shelf and slope sediments." In: *Journal of Geophysical Research* **83**, pp. 4053–4406.

Berner, U. and E. Faber (1996). "Empirical carbon isotope/maturity relationships for gases from algal kerogens and terrigenous organic matter, based on dry, open-system pyrolysis." In: *Organic Geochemistry* **24**, pp. 947–955.

Bernhardt, A., L. Stright, and D.R. Lowe (2012). "Channelized debris-flow deposits and their impact on turbidity currents: The Puchkirchen axial channel belt in the Austrian Molasse Basin." In: *Sedimentology* **59**, pp. 2042–2070.

BGBl. II Nr. 309/1999 (1999). *Mineralwasser- und Quellwasserverordnung*. Bundesgesetzblatt für die Republik Österreich.

Can, I. (2002). "A new improved Na/K geothermometer by artificial neural networks." In: *Geothermics* **31**, pp. 751–760.

Capasso, G. and S. Inguaggiato (1998). "A simple method for the determination of dissolved gases in natural waters. An application to thermal waters from Vulcano Island." In: *Applied Geochemistry* **13**, pp. 631–642.

Caruso, A. and M. Santoro (2014). *Rapid and Reliable Detection of Dissolved Gases in Water*. Application Note 10405. Thermo Fisher Scientific. Milan.

Clark, I.D. and P.F. Fritz (1998). *Environmental Isotopes in Hydrology*. Lewis Publishers.

Coleman, D.D., C.-L. Liu, and K.M. Riley (1988). "Microbial methane in the shallow Paleozoic sediments and glacial deposits of Illinois." In: *Chemical Geology* **71**, pp. 23–40.

Craig, H. (1957). "Isotopic standards of carbon and oxygen and correction factors for mass-spektrometric analysis of carbondioxide." In: *Geochimica et Cosmochimica Acta* **12**, pp. 133–149.

Craig, H. (1961a). "Isotopic Variations in Meteoric Waters." In: *Science* **133**. Washington, D.C., pp. 1702–1703.

Craig, H. (1961b). "Standard for reporting concentrations of Deuterium and Oxygen-18 in natural waters." In: *Science* **133**. Washington, D.C., pp. 1833–1834.

D'Ans, J. and E. Lax (1967). *Taschenbuch für chemiker und Physiker*. Band I - Physikalisch chemische Daten. Berlin - Heidelberg - New York: Springer.

Davis, S.N. and R.J.M. de Wiest (1967). *Hydrogeology*. Second Edition. New York - London - Sydney: Wiley.

Davis, S.N., D.O. Whittemore, and J. Fabryka-Martin (1998). "Uses of Chloride/Bromide Ratios in Studies of Potable Water." In: *Groundwater* **36/2**, pp. 338–350.

de Ruig, M.J. (2003). "Deep Marine Sedimentation and Gas Reservoir Distribution in Upper Austria." In: *OIL GAS European Magazine*, pp. 64–73.

de Ruig, M.J. and S.M. Hubbard (2006). "Seismic facies and reservoir characteristics of a deep-marine channel belt in the Molasse foreland basin, Puchkirchen Formation, Austria." In: *AAPG Bulletin* **90**, pp. 735–752.

Drever, J.I. (2005). *Water, weathering, and soil*. Oxford: Elsevier.

Ehhalt, D. and K. Knott (1965). "Kinetische Isotopentrennung bei der Verdampfung von Wasser." In: *Tellus* **17**.3, pp. 389–397.

Elster, D., J. Goldbrunner, G. Wessely, P. Niederbacher, G. Schubert, R. Berka, R. Philippitsch, and T. Hörhan (2016). *Erläuterungen zur geologischen Themenkarte Thermalwässer in Österreich 1:500.000*. Wien: Geologische Bundesanstalt.

Enns, T., P.F. Scholander, and E.D. Bradstreet (1965). "Effect of Hydrostatic Pressure on Gases Dissolved in Water." In: *Journal of Physical Chemistry* **69/2**, pp. 389–391.

Faupl, P. and R. Roetzel (1987). "Gezeitenbeeinflußte Ablagerungen der Innviertler Gruppe (Ottnangien) in der oberösterreichischen Molassezone." In: *Jahrbuch der Geologischen Bundesanstalt* **130**, pp. 415–447.

Foster, M.D. (1950). "The origin of high sodium bicarbonate waters in the Atlantic and Gulf coastal plains." In: *Geochimica et Cosmochimica Acta* **1**, pp. 33–48.

Fournier, R.O. (1979). "A Revised Equation for the Na/K Geothermometer." In: *Geothermal Resources Council Transactions* **3**, pp. 221–224.

Fournier, R.O., D.E. White, and A.H. Truesdell (1974). "Geochemical indicators of subsurface temperature, part 1, basic assumptions." In: *Journal of Research of the U.S. Geological Survey* **2**, pp. 259–262.

Frape, S.K. and P. Fritz (1987). "Geochemical trends for groundwaters from the Canadian shield." In: *Saline Water and Gases in Crystalline Rocks*. Ed. by P. Fritz and S.K. Frape. Vol. **33**. St. John's, Newfoundland: Geological Association of Canada Special Paper, pp. 19–38.

Fresenius, W., K.H. Knoll, H.-W. Leonhardt, G. Matthess, H. Tangermann, and W. Schneider (1977). "Qualitative und quantitative Untersuchung des Sickerwassers einer Hausmülldeponie mit Basisabdichtung." In: *Müll und Abfall* **7**, pp. 190–206.

Fritz, P. and J.Ch. Fontes, eds. (1980). *Handbook of Environmental Isotope Geochemistry*. Vol. **1**. Amsterdam-Oxford-New York-Tokio: Elsevier.

Fuchs, G. and A. Matura (1976). "Zur Geologie des Kristallins der südlichen Böhmischen Masse." In: *Jahrbuch der Geologischen Bundesanstalt* **119**, pp. 1–43.

Fuchs, G. and A. Matura (1980). "Die Böhmische Masse in Österreich." In: *Der geologische Aufbau Österreichs*. Ed. by Geologische Bundesanstalt. Springer-Verlag Wien GmbH, pp. 121–143.

Furtak, H. and H.R. Langguth (1967). "Zur hydrochemischen Kennzeichnung von Grundwässern und Grundwassertypen mittels Kennzahlen." In: *Mem. IAH-Congress, 1965* **7**, pp. 89–96.

Gattinger, T.E. (1980). "Hydrogeologie." In: *Der geologische Aufbau Österreichs*. Ed. by Geologische Bundesanstalt. Springer-Verlag Wien GmbH, pp. 580–593.

GeoMol Team (2015). *GeoMol - Assessing subsurface potentials of the Alpine Foreland Basins for sustainable planning and use of natural resources*. Project Report. Augsburg: Bayerisches Landesamt für Umwelt (LfU).

Gerritse, R.G. and R.J. George (1988). "The role of soil and organic matter in the geochemical cycling of chloride and bromide." In: *Journal of Hydrology* **101**, pp. 83–95.

Geyh, M.A. (1970). "Carbon-14 concentration of lime in soils and aspects of the carbon-14 dating of groundwater." In: *Isotope Hydrology*. Wien (IAEA), pp. 215–223.

Giggenbach, W.F. (1988). "Geothermal solute equilibria. Derivation of Na–K–Mg–Ca geoindicators." In: *Geochimica et Cosmochimica Acta* **52**, pp. 2749–2765.

Ginsburg, I.I. (1963). *Grundlagen und Verfahren geochemischer Sucharbeiten auf Lagerstätten der Buntmetalle und seltenen Metalle*. Berlin: Akademie-Verlag.

Goldbrunner, J.E. (1984). "Zur Hydrogeologie des oberösterreichischen Molassebeckens." In: *Steirische Beträge zur Hydrogeologie* **36**, pp. 83–102.

Goldbrunner, J.E. (1988). "Tiefengrundwässer im Oberösterreichischen Molassebecken und im Steirischen Becken." In: *Steirische Beiträge zur Hydrogeologie* **39**, pp. 5–94.

Goldbrunner, J.E. (2000). "Hydrogeology of Deep Groundwaters in Austria." In: *Mitteilungen der Österreichischen Geologischen Gesellschaft* **92**, pp. 281–294.

Goldbrunner, J.E., B. Huber, T. Kohl, M. Gold, H.P. Heiss, A. Shirbaz, and C. Baujard (2007). *TAT. Thermische Auswirkungen von Thermalwassernutzungen im oberösterreichisch-niederbayerischen Innviertel. Endbericht*. Unpublished Report. Graz - Augsburg - Zürich: Geoteam GmbH - HydroConsult GmbH - Geowatt AG.

Golwer, A., K.H. Knoll, G. Matthess, W. Schneider, and K.H Wallhäusser (1976). "Belastung und Verunreinigung des Grundwassers durch feste Abfallstoffe." In: *Abhandlungen des Hessischen Landesamtes für Bodenforschung* **73**, p. 131.

Gooddy, D.C. and W.G. Darling (2005). "The potential for methane emissions from groundwaters of the UK." In: *Science of the Total Environment* **339**, pp. 117–126.

Gratzer, R., A. Bechtel, R.F. Sachsenhofer, H.-G. Linzer, D. Reischenbacher, and H.M. Schulz (2011). "Oil-oil and oil-source correlations in the Alpine Foreland Basin of Austria: Insights from biomarker and stable carbon isotope studies." In: *Marine and Petroleum Geology* **28**, pp. 1171–1186.

Groß, D., R. Sachsenhofer, A. Rech, S. Sageder, M. Geissler, S. Schnitzer, and W. Troiss (2015). "The Trattnach Oil Field in the North Alpine Foreland Basin (Austria)." In: *Austrian Journal of Earth Sciences* **108/2**, pp. 151–171.

Groß, D., R.F. Sachsenhofer, A. Bechtel, R. Gratzer, M.-L. Grundtner, H.-G. Linzer, D. Misch, Ł. Pytlak, and L. Scheucher (2018). "Petroleum systems in the Austrian sector of the North Alpine Foreland Basin: An Overview." In: *Journal of Petroleum Geology* **41/3**, pp. 299–318.

Grossman, E.L., B.K. Coffman, S.J. Fritz, and H. Wada (1989). "Bacterial production of methane and its influence on groundwater chemistry in east-central Texas aquifers." In: *Geological* **17**, pp. 495–499.

Grunert, P. (2011). "Integrated facies-analysis and stratigraphy of the early Miocene North Alpine Foreland Basin (Upper Austria)." Doctoral dissertation. Graz: Institute for Earth Sciences, Karl-Franzens-Universität Graz.

Grunert, P., R. Hinsch, R.F. Sachsenhofer, A. Bechtel, S. Ćorić, M. Harzhauser, W.E. Piller, and H. Sperl (2013). "Early Burdigalian infill of the Puchkirchen Trough (North Alpine Foreland Basin, Central Paratethys): Facies development and sequence stratigraphy." In: *Marine and Petroleum Geology* **39**, pp. 164–186.

Gundlach, H., G. Van der Boom, and W. Koch (1981). "Geochemische Untersuchungen." In: *Angewandte Geowissenschaften*. Ed. by F. Bender. Vol. **1**. Stuttgart: Enke, pp. 311–369.

Gusterhuber, J., I. Dunkl, R. Hinsch, H.-G. Linzer, and R.F. Sachsenhofer (2012). "Neogene uplift and erosion in the Alpine Foreland Basin (Upper Austria and Salzburg)." In: *Geologica Carpathica* **63**, pp. 295–305.

Gusterhuber, J., R. Hinsch, H.-G. Linzer, and R.F. Sachsenhofer (2013). "Hydrocarbon generation and migration from sub-thrust source rocks to foreland reservoirs: The Austrian Molasse Basin." In: *Austrian Journal of Earth Sciences* **106/2**, pp. 115–136.

Hahn-Weihnheimer, P., A. Hirner, and K. Lemcke (1979). "Zur Herkunft süddeutscher Erdöle: geochemische Ergebnisse und Versuch einer geologischen Interpretation." In: *Bulletin der Vereinigung Schweiz. Petroleum-Geologen und -Ingenieure* **45**.109, pp. 35–46.

Hem, J.D. (1985). "Study and interpretation of the chemical characteristics of natural water." In: *US Geological Survey Water Supply Paper* **2254**, p. 263.

Henry, W. (1803). "Experiments on the Quantity of Gases Absorbed by Water, at Different Temperatures, and under Different Pressures." In: *Philosophical Transactions of the Royal Society of London* **93**, 29–42 and 274–276.

Hoefs, J. (2009). *Stable Isotope Geochemistry*. Sixth Edition. Berlin - Heidelberg: Springer.

Hoth, P., A. Seibt, T. Kellner, and E. Huenges (1997). *Geowissenschaftliche Bewertungsgrundlagen zur Nutzung hydrogeothermaler Ressourcen in Norddeutschland*. Scientific Technical Report STR. Vol. **97/15**. Potsdam: GeoForschungsZentrum GFZ.

Humez, P., B. Mayer, J. Ing, M. Nightingale, V. Becker, A. Kingston, O. Akbilgic, and S. Taylor (2016). "Occurrence and origin of methane in groundwater in Alberta (Canada): Gas geochemical and isotopic approaches." In: *Science of the Total Environment* **541**, pp. 1253–1268.

Hydroisotop GmbH (2017a). *Machbarkeitsstudie - Bestimmung des Thermalwasseralters mittels Krypton-81-Untersuchung (Atom Trap Trace Analysis; ATTA)*. Unpublished Report. Schweitenkirchen.

Hydroisotop GmbH (2017b). *Physikalische und physikalisch-chemische Kontrolluntersuchungen des Thermalwassers der Tiefbohrung xxx TH 1 - 2017*. Unpublished Report. Schweitenkirchen.

IAEA (1981). "Stable isotope hydrology: Deuterium and oxygen-18 in the water cycle." In: *Technical Report Series* **210**. Vienna(IAEA), p. 339.

IAEA (1983). "Isotope techniques in the hydrogeological assessment of potential sites for the disposal of high-level radioactive wastes." In: *Technical Report Series* **228**. Vienna(IAEA), p. 151.

Jones, D.M., I.M. Head, N.D. Gray, J.J. Adams, A.K. Rowan, C.M. Aitken, B. Bennett, H. Huang, A. Brown, B.F.J. Bowler, T. Oldenburg, M. Erdmann, and S.R. Larter (2008). "Crude-oil biodegradation via methanogenesis in subsurface petroleum reservoirs." In: *Nature* **451**, pp. 176–181.

Jurek, A. (2015). *Automated Determination of Dissolved Gases in Water By Headspace Calibration of Mixed Gases*. EST analytical.

Kölbl, L. (1958). "Die Tiefenwässer des Erdölfeldes Matzen." In: *Erdöl-Zeitschrift* **74**, pp. 406–414.

Kolmer, C. (2011). "Hydrogeologie." In: *Erläuterungen - Geologische Karte von Oberösterreich 1:200000*. Ed. by C. Rupp, M. Linner, and G.W. Mandl. Wien: Geologische Bundesanstalt, pp. 175–182.

Kralik, M., I. Zieritz, J. Grath, G. Vincze, R. Philippitsch, and H. Pavlik (2005). *Hydrochemische Karte Österreichs - Oberflächennaher Grundwasserkörper und Fließgewässer*. Second Edition. Wien: Umweltbundesamt GmbH.

Krauskopf, K.B. (1956). "Factors controlling the concentrations of thirteen rare metals in sea-water." In: *Geochimica et Cosmochimica Acta* **9**, pp. 1–32.

Kuhlemann, J. and O. Kempf (2002). "Post-Eocene evolution of the North Alpine Foreland Basin and its response to Alpine tectonics." In: *Sedimentary Geology* 152, pp. 45–78.

Ladwein, W. and F. Schmidt (1993). "Die Entstehung von Kohlenwasserstoffen." In: *Erdöl und Erdgas in Österreich*. Ed. by F. Brix and O. Schultz. 2. Auflage. Wien: Naturhistorisches Museum Wien und F. Berger, Horn, pp. 14–18.

Lafargue, E. and C. Barker (1988). "Effect of Water Washing on Crude Oil Compositions." In: *AAPG Bulletin* **72(3)**, pp. 263–276.

Land Oberösterreich (2018). *DORIS interMAP*. `https://www.doris.at/viewer/(S(uw1ddvmhvqk3sdene52kk43h))/init.aspx?ks=alk&karte=wage`. Accessed: 2018-06-27.

Langmuir, D. (1997). *Aqueous Environmental Geochemistry*. Prentice-Hall, Inc.

Lehmann, B.E., S.N. Davis, and J.T. Fabryka-Martin (1993). "Atmospheric and Subsurface Sources of Stable and Radioactive Nuclides used for Groundwater Age Dating." In: *Water Resources Research* **29/7**, pp. 2027–2040.

Lemcke, K. (1981). "Das heutige geologische Bild des deutschen Alpenvorlandes nach drei Jahrzehnten Öl- und Gasexploration." In: *Eclogae Geologicae Helvetiae* **74/1**, pp. 1–18.

Lengauer, C., G. Tichy, and E. Enichlmayr (1987). "Beiträge zur paläogeographischen Entwicklung der Taufkirchner Bucht (Oberösterreich)." In: *Jahrbuch des Oberösterreichischen Musealvereines* **132**, pp. 165–210.

LGBl. OÖ Nr. 47/1961 (1961). *Gesetz vom 30. Juni 1961 über natürliche Heilvorkommen und Kurorte (O.ö. Heilvorkommen- und Kurortegesetz)*. Landesgesetzblatt für Oberösterreich.

Linzer, H.-G. and R.F. Sachsenhofer (2010). "Large Scale Mass Movements in the Deepwater Foreland Basin of the Alps - Implications to Hydrocarbon Generation and Distribution of Source and Reservoir Rocks." In: *AAPG Annual Convention and Exhibition*. 11-14 April.

Machel, H.G. (2001). "Bacterial and thermochemical sulfate reduction in diagenetic settings - old and new insights." In: *Sedimentary Geology* **140**, pp. 143–175.

Machel, H.G., H.R. Krouse, and R. Sassen (1995). "Products and distinguishing criteria of bacterial and thermochemical sulfate reduction." In: *Applied Geochemistry* **10**, pp. 373–389.

Matthess, G. (1990). *Die Beschaffenheit des Grundwassers*. Lehrbuch der Hydrogeologie Band 2. Berlin - Stuttgart: Borntraeger.

Mayrhofer, C., R. Niessner, and T. Baumann (2014). "Hydrochemistry and hydrogen sulfide generating processes in the Malm aquifer, Bavarian Molasse Basin, Germany." In: *Hydrogeology Journal* **22**, pp. 151–162.

Michard, G. (1979). "Geothermomètres chimiques." In: *Bulletin du Bureau de Recherches Géologiques et Minières (2. serie), Sect. III, Nr. 2*, pp. 183–189.

Michel, G. (1997). *Mineral- und Thermalwässer - Allgemeine Balneologie*. Lehrbuch der Hydrogeologie Band 7. Berlin - Stuttgart: Borntraeger.

Milkov, A.V. (2011). "Worldwide distribution and significance of secondary microbial methane formed during petroleum biodegradation in conventional reservoirs." In: *Organic Geochemistry* **42**, pp. 184–207.

Münnich, K.O., W. Roether, and L. Thilo (1967). "Dating of groundwater with tritium and ^{14}C." In: *Isotopes in Hydrology*. Wien (IAEA), pp. 305–320.

Muccio, Z. and G.P. Jackson (2009). "Isotope ratio mass spectrometry." In: *Analyst* **134**, pp. 213–222.

Nachtmann, W. (2001). "Vom Zufallsfund zum Wirtschaftsmotor - ein Jahrhundert Öl- und Gasgewinnung in Oberösterreich." In: *Berichte der Geologischen Bundesanstalt* **56**, pp. 81–82.

Nachtmann, W. and L. Wagner (1987). "Mesozoic and Early Tertiary evolution of the Alpine foreland in Upper Austria and Salzburg, Austria." In: *Compressional Intra-Plate Deformations in the Alpine Foreland*. Ed. by P.A. Ziegler. Vol. **137**. Tectonophysics, pp. 61–76.

Niebuhr, B., T. Pürner, and M. Wilmsen (2009). "Lithostratigraphie der außeralpinen Kreide Bayerns." In: *Schriftenreihe der Deutschen Gesellschaft für Geowissenschaften* **65**, pp. 7–58.

Nieva, D. and R. Nieva (1987). "Developments in geothermal energy in Mexico, part 12 - A cationic composition geothermometer for prospection of geothermal resources." In: *Heat recovery systems and CHP* **7**, pp. 243–258.

Nurmi, P.A., I.T. Kukkonen, and P.W. Lahermo (1988). "Geochemistry and origin of saline groundwaters in the Fennoscandian Shield." In: *Applied Geochemistry* **3**, pp. 185–203.

Orr, W.L. (1974). "Changes in Sulfur Content and Isotopic Ratios of Sulfur during Petroleum Maturation - Study of Big Horn Basin Paleozoic Oils." In: *AAPG Bulletin* **58**, pp. 2295–2318.

Orr, W.L. (1977). "Geologic and geochemical controls on the distribution of hydrogen sulfide in natural gases." In: *Advances in Organic Geochemistry*. Enadisma, Madrid, pp. 571–597.

Palmer, C. (1911). "The geochemical interpretation of water analyses." In: *United States Geological Survey Bulletin* **479**, p. 31.

Pearson, F.J. and B.B. Hanshaw (1970). "Sources of dissolved carbonate species in groundwater and their effects on carbon-14 dating." In: *Isotope Hydrology*. Wien (IAEA), pp. 271–286.

Pekdeger, A. and W. Balderer (1987). "The occurrence of saline groundwaters and gases in the cristalline rocks of northern Switzerland." In: *Saline Water and Gases in Crystalline Rocks*. Ed. by P. Fritz and S.K. Frape. Vol. **33**. St. John's, Newfoundland: Geological Association of Canada Special Paper, pp. 157–174.

Pfleiderer, S., G. Götzl, M. Bottig, A.K. Brüstle, C. Porpaczy, M. Schreilechner, C. Eichkitz, M. Jud, R. Sachsenhofer, K. Zosseder, S. Casper, J. Goldbrunner, C. Kriegl, C. Kolmer, and D.W. Diepolder (2016). "GeoMol - Geologische 3D-Modellierung des österreichischen Molassebeckens und Anwendungen in der Hydrogeologie und Geothermie im Grenzgebiet von Oberösterreich und Bayern." In: *Abhandlungen der Geologischen Bundesanstalt* **70**, pp. 1–88.

Piper, A. (1944). "A graphic procedure in the geochemical interpretation of water-analyses." In: *Eos, Transactions American Geophysical Union* **25**.6, pp. 914–928.

Polesny, H. (1983). "Verteilung der Öl- und Gasvorkommen in der oberösterreichischen Molassezone." In: *Erdöl-Erdgas-Zeitschrift* **90**, pp. 90–102.

Pytlak, Ł. (2017). "Origin, migration and alteration of hydrocarbons in the Austrian sector of the Alpine Foreland Basin." Doctoral dissertation. Department Applied Geosciences and Geophysics, Montanuniversität Leoben.

Pytlak, Ł., D. Gross, R.F. Sachsenhofer, A. Bechtel, and H.-G. Linzer (2016a). "Gas accumulations in Oligocene-Miocene reservoirs in the Alpine Foreland Basin (Austria): evidence for gas mixing and gas degradation." In: *International Journal of Earth Sciences*.

Pytlak, Ł., D. Gross, R.F. Sachsenhofer, A. Bechtel, R. Gratzer, and H.-G. Linzer (2016b). "Generation, mixing and alteration of thermogenic and microbial gas in oil deposits: The case of the Alpine Foreland Basin (Austria)." In: *Marine and Petroleum Geology* **78**, pp. 575–592.

Pytlak, Ł., A. Leis, W. Prochaska, R.F. Sachsenhofer, D. Gross, and H.-G. Linzer (2017). "Light Hydrocarbon Geochemistry of Oils in the Alpine Foreland Basin: Impact of Geothermal Fluids on the Petroleum System." In: *Geofluids* **2017**, p. 15.

Reardon, E.J. and P. Fritz (1978). "Computer modelling of groundwater ^{13}C and ^{14}C isotope compositions." In: *Journal of Hydrology* **36**, pp. 201–224.

Reischenbacher, D. and R.F. Sachsenhofer (2011). "Entstehung von Erdgas in der oberösterreichischen Molassezone: Daten und offene Fragen." In: *Berg- und Hüttenmännische Monatshefte* **156**, pp. 463–468.

Ricke, W. (1960). "Ein Beitrag zur Geochemie des Schwefels." In: *Geochimica et Cosmochimica Acta* **21**.1-2, pp. 35–80.

Roetzel, R., P. Hochuli, and F. Steininger (1983). "Die Faziesentwicklung des Oligozäns in der Molasse zwischen Krems und Wieselburg (Niederösterreich)." In: *Jahrbuch der Geologischen Bundesanstalt* 126, pp. 129–179.

Rogers, G.S. (1917). "Chemical relations of the oilfield waters in San Joaquin Valley, California." In: *US Geological Survey Bulletin* **653**, p. 110.

Rose, A.A., H.E. Hawkes, and J.S. Webb (1979). *Geochemistry in Mineral Exploration*. Second Edition. London - New York - Toronto - Sydney - San Francisco: Academic Press.

Sachsenhofer, R.F. and H.-M. Schulz (2006). "Architecture of Lower Oligocene source rocks in the Alpne Foreland Basin: a model for syn- and post-depositional source-rock features in the Paratethyan realm." In: *Petroleum Geoscience* **12**, pp. 363–377.

Sachsenhofer, R.F., B. Leitner, H.-G. Linzer, A. Bechtel, S. Ćorić, R. Gratzer, D. Reischenbacher, and A. Soliman (2010). "Deposition, Erosion and Hydrocarbon Source Potential of the Oligocene Eggerding Formation (Molasse Basin, Austria)." In: *Austrian Journal of Earth Sciences* **103**/1, pp. 76–99.

Schoell, M. (1988). "Multiple origins of methane in the Earth." In: *Chemical Geology* **71**, pp. 1–10.

Schoeller, H. (1956). "Géochemie des eaux souterraines. Application aux eaux de gesements de pétrole." In: *Rev. Inst. Pétrole et Ann. des Combustibles liquides, (1955)* **10**, pp. 181–213, 219–246, 507–552, 671–719, 823–874.

Schoeller, H. (1962). *Les Eaux Souterraines*. Paris: Masson.

Schröckenfuchs, G. (1975). "Hydrogeologie, Geochemie und Hydrodynamik der Formationswässer des Raumes Matzen-Schönkirchen Tief. Hydrogeology, geochemistry and hydrodynamics in the formation waters in the Matzen-Schönkirchen Tief area." In: *Erdöl-Erdgas Zeitschrift* **91**, pp. 299–321.

Schubert, A. (1996). "Tiefengrundwasseruntersuchungen im Molassebecken westlich von Linz." Doctoral dissertation. Berlin: Technische Universität Berlin.

Schubert, G. (2015). "Trinkbare Tiefengrundwässer in Österreich." In: *Abhandlungen der Geologischen Bundesanstalt* **64**. Wien, p. 179.

Schulz, H.-M. and W. van Berk (2009). "Bacterial methane in the Atzbach-Schwanenstadt gas field (Upper Austrian Molasse Basin), Part II: Retracing gas generation and filling history by mass balancing or organic carbon conversion applying hydrogeochemical modelling." In: *Marine and Petroleum Geology* **26**, pp. 1180–1189.

Schulz, H.-M., R.F. Sachsenhofer, A. Bechtel, H. Polesny, and L. Wagner (2002). "The origin of hydrocarbon source rocks in the Austrian Molasse Basin (Eocene-Oligocene transition)." In: *Marine and Petroleum Geology* **19**, pp. 683–709.

Schulz, H.-M., W. van Berk, A. Bechtel, U. Struck, and E. Faber (2009). "Bacterial methane in the Atzbach-Schwanenstadt gas field (Upper Austrian Molasse Basin), Part I: geology." In: *Marine and Petroleum Geology* **26**, pp. 1163–1179.

Schwedt, G. (1992). *Taschenatlas der Analytik*. Stuttgart - New York: Thieme.

Siegenthaler, U. (1979). "Stable hydrogen and oxygen isotopes in the water cycle." In: *Lectures in Isotope Geology*. Ed. by E. Jäger and J.C. Hunziker. Berlin - Heidelberg - New York: Springer, pp. 264–273.

Siegenthaler, U. (1980). "Herkunft und Verweildauer der Mineralwässer aufgrund von Isotopenmessungen." In: *Die Mineral- und Heilquellen der Schweiz*. Ed. by O. Högl. Bern - Stuttgart: Haupt, pp. 101–107.

Sigg, L. and W. Stumm (1989). *Aquatische Chemie: Eine Einführung in die Chemie wässriger Lösungen und natürlicher Gewässer*. Verlag der Fachvereine an den schweizerischen Hochschulen und Techniken AG, Zürich, und B.G. Teubner Verlag Stutt-gart.

Sissingh, W. (1997). "Tectonostratigraphy of the Northern Alpine Foreland Basin: Correlation fo Tertiary depositional cycles and orogenic phases." In: *Tectonophysics* **282**, pp. 223–256.

Stober, I. and K. Bucher (1999). "Origin of salinity of deep groundwater in crystalline rocks." In: *Terra Nova* **11**, pp. 181–185.

Thilo, L. and K.O. Münnich (1970). "Reliability of carbon-14 dating of groundwater: effect of carbonate exchange." In: *Isotope Hydrology*. Wien (IAEA), pp. 259–270.

Umweltbundesamt (2014). "Hygieneanforderungen an Bäder und deren Überwachung - Empfehlungen des Umweltbundesamtes (UBA) nach Anhörung der Schwimm- und Badebeckenwasserkommission des Bundesministeriums für Gesundheit (BMG) beim Umweltbundesamt." In: *Bundesgesundheitsblatt 2014* **57**, pp. 258–279.

Verma, S.P. and E. Santoyo (1997). "New improved equations for Na/K, Na/Li and SiO_2 geothermometers by outlier detection and rejection." In: *Journal of Volcanology and Geothermal Research* **79**, pp. 9–23.

Vohryzka, K., F. Weber, and F. Hame (1986). "Der Sulfatgehalt der oberösterreichischen Grundwässer." In: *Amtlicher oberösterreichischer Wassergüteatlas*. 13. Linz: Amt der o.ö. Landesregierung, pp. 1–23.

Wagner, L.R. (1996). "Stratigraphy and Hydrocarbons in upper Austrian Molasse Foredeep (active margin)." In: *Oil and Gas in Alpidic Thrustbelts and Basins of Central and Eastern Europe*. Ed. by G. Wessely and W. Liebl. Vol. **5**. European Association of Geoscientists and Engineers Special Publication, pp. 217–235.

Wagner, L.R. (1998). "Tectono-stratigraphy and hydrocarbons in the Molasse Foredeep of Salz-burg, Upper and Lower Austria." In: *Cenozoic Foreland Basins of Western Europe*. Ed. by A. Mascle, C. Puigdefàbregas, H.P. Luterbacher, and M. Fernàndez. Vol. **134**. Geological Society Special Publications, pp. 339–369.

Weber, F. (1980). *Zusammenfassende Beurteilung der geophysikalischen Messungen im Raum Geinberg und in der Tiefbohrung Geinberg 1*. Unpublished Report. Leoben.

Wehner, H. and K. Kuckelkorn (1995). "Zur Herkunft der Erdöle im nördlichen Alpen-/Karpatenvorland - Origin of Oils in the Alpine and Carpathian Foreland." In: *Erdöl Erdgas Kohle* **12**, pp. 508–514.

Wessely, G. (2006). *Geologie der Österreichischen Bundesländer*. Geologische Bundesanstalt.

Whiticar, M.J., E. Faber, and M. Schoell (1986). "Microbial methane formation in marine and freshwater environments: carbon dioxide reduction vs. acetate fermentation - isotope evidence." In: *Geochimica et Cosmochimica Acta* **50**, pp. 693–709.

Wishart, D.N. (2015). "Comparison of Silica and Cation Geothermometers of Bath Hot Springs, Jamaica WI." In: *Proceedings World Geothermal Congress 2015*. Melbourne, Australia, p. 13.

Wisotzky, F. (2012). *Angewandte Grundwasserchemie, Hydrogeologie und hydrogeochemische Modellierung: Grundlagen, Anwendungen und Problemlösungen*. Berlin - Heidelberg: Springer.

Wolfgramm, M., T. Bloch, J. Bartels, S. Heuberger, P. Kuhn, H. Naef, H.-D. Voigt, P. Seibt, M. Sonderegger, T. Steiger, and S. Uhlig (2015). "Reservoir-Geological Characterization of a Fractured Limestone: Results Obtained from the Geothermal Well St. Gallen GT-1 (Switzerland)." In: *Proceedings World Geothermal Congress 2015*. Melbourne, Australia, p. 12.

Zötl, J. and J.E. Goldbrunner (1993). *Die Mineral- und Heilwässer Österreichs*. Wien: Springer-Verlag Wien GmbH.

A Appendix

Wasseranalyse

Geologische Bundesanstalt
FA Geochemie
Leitung: HR Mag. Dr. Gerhard Hobiger

Probenahmepunkt:			1		
Koordinaten	**M** n.b.	**RW:** 14°15'10.32"E	**HW:** 48°24'9.96"N	**GOK (m ü. A.)**	n.b.
Bezeichnung:	1		**Geochemie-Nr.:**	**GCH-2017-061-001**	
Probenahmetiefe:	n.b.	**Probenehmer:**	Be/Pö		
Probenahmedatum und Uhrzeit:		05.09.2017 10:30	**Eingangsdatum:**	07.09.2017	

Feldparameter

		QZV *	MAP **	IP ***			
el. LF (µS/cm) (Gel.)	**75**	2250		2500	**Schüttung (l/s)**		n.b.
el. LF (µS/cm) (Labor)	70				**Redoxpotenzial (mV)**		306
					Temperatur (°C)		8
pH (Gel.)	**6.14**			6,5 - 9,5	**Sauerstoff (O_2)**	mg/l	8.8
pH (Labor)	5.82					(%)	81.9

Kationen (mg/l)

Ion	Messwert	QZV *	MAP **	IP ***
Calcium (Ca^{2+})	4.7			
Magnesium (Mg^{2+})	2.4			
Natrium (Na^{+})	5.0			200
Kalium (K^{+})	2.0			
Strontium (Sr^{2+})	0.0543			
Barium (Ba^{2+})	0.0107			
Lithium (Li^{+})	0.0023			
Rubidium (Rb^{+})	0.0006			
Cäsium (Cs^{+})	< 0,0001			
Ammonium (NH_4^{+})	n.b.	0.45		0.5
Eisen (Fe^{2+})	0.002			0.2
Mangan (Mn^{2+})	0.0005			0.05
Σ	14.1			

Anionen (mg/l)

Ion	Messwert	QZV *	MAP **	IP ***
Hydrogencarbonat (HCO_3^{-})	20.86			
Chlorid (Cl^{-})	1.6	180		200
Sulfat (SO_4^{2-})	8.4	225		250
Nitrat (NO_3^{-})	9.6	45	50	
Nitrit (NO_2^{-})	n.b.	0.09	0.1	
o- Phosphat (o-PO_4^{3-})	n.b.	0.3		
Sulfid (S^{2-})	n.b.			
Fluorid (F^{-})	<0,05		1.5	
Σ	40.4			

Ges. Ionengehalt	55 mg/l	**Ionenbilanz**
	1.1 mmol/l	*-1.8* %
Dichte	n.b. g/cm3	

Spezielle Parameter (mg/l)

Parameter	Messwert	QZV *	MAP **	IP ***
Kupfer (Cu)	0.0011	1.8	2	
Zink (Zn)	0.0101			
Blei (Pb)	< 0,0001	0.009	0.025	
Cadmium (Cd)	< 0,0001	0.0045	0.005	
Aluminium (Al)	0.0027			0.2
Arsen (As)	< 0,0001	0.009	0.01	
Antimon (Sb)	n.b.		0.005	
Chrom (Cr)	0.0002	0.045		
Nickel (Ni)	0.0013	0.018		
Quecksilber (Hg)	n.b.	0.0009	0.001	
Bor (B)	n.b.		1	
Uran (U)	< 0,0001		0.015	
Thorium (Th)	n.b.			
Cobalt (Co)	< 0,0001			
Molybdän (Mo)	< 0,0001			
Vanadium (V)	0.0004			
Selen (Se)	n.b.		0.01	
Tellur (Te)	n.b.			
Niob (Nb)	n.b.			
H_2SiO_3	n.b.			

Spezielle Parameter (mg/l)

Parameter	Messwert
Lanthan (La)	n.b.
Cer (Ce)	n.b.
Praseodym (Pr)	n.b.
Neodym (Nd)	n.b.
Samarium (Sm)	n.b.
Europium (Eu)	n.b.
Gadolimium (Gd)	n.b.
Terbium (Tb)	n.b.
Dysprosium (Dy)	n.b.
Holmium (Ho)	n.b.
Erbium (Er)	n.b.
Thulium (Tm)	n.b.
Ytterbium (Yb)	n.b.
Lutetium (Lu)	n.b.
Zinn (Sn)	n.b.
Thallium (Tl)	n.b.
Silber (Ag)	n.b.
Beryllium (Be)	n.b.
Bismut (Bi)	n.b.
Gallium (Ga)	n.b.

n.b. .. nicht bestimmt

* ... Qualitätszielverordnung Chemie Grundwasser QZV Chemie GW (BGBl. II 98/2010)

** ... Mindestanforderungsparameter aus der Trinkwasserverordnung - TWV (BGBl. II 304/2001)

*** ... Indikatorparameter aus der Trinkwasserverordnung - TWV (BGBl. II 304/2001)

Layout: G. Hobiger

Geologische Bundesanstalt
FA Geochemie
Leitung: HR Mag. Dr. Gerhard Hobiger

Berechnungen aus den Analysenwerten

Äquivalentanteile

Kationen				Anionen			
	Messwert				Messwert		
Ion	mg/l	meq/l	eq%	Ion	mg/l	meq/l	eq%
Ca^{2+}	4.72	0.24	33.55	HCO_3^-	20.86	0.34	47.8
Mg^{2+}	2.41	0.20	28.26	Cl^-	1.56	0.04	6.1
Na^+	4.95	0.22	30.68	SO_4^{2-}	8.39	0.17	24.4
K^+	1.99	0.05	7.25	NO_3^-	9.58	0.15	21.6
Sr^{2+}	0.05	0.00	0.18	NO_2^-	n.b.	n.b.	n.b.
Ba^{2+}	0.011	0.00	0.0	$o\text{-}PO_4^{3-}$	n.b.	n.b.	n.b.
Li^+	0.002	0.00	0.05	S^{2-}	n.b.	n.b.	n.b.
Rb^+	0.001	0.00	0.00	F^-	<0,05	0.00	0.0
Cs^+	< 0,0001	0.00	0.00	Σ	40.37	0.7	100.0
NH_4^+	n.b.	n.b.	n.b.				
Fe^{2+}	0.002	0.00	0.0				
Mn^{2+}	0.0005	0.00	0.0				
Σ	14.14	0.7	100.0				

Härten	
Gesamthärte (° dH)	1.2
Carbonathärte(° dH)	1.0
Nichtcarbonathärte (°dH)	0.3
Erdalkalien (mmol/l)	31.0

Berechnung des CO_2	
$lg(pCO_2)$	-1.90
freies CO_2 (mg/l)	31.99
freies CO_2 (mmol/l)	0.7268

Berechneter Ammoniakgehalt	
NH_3 (mg/l)	n.b.

Ges. Ionengehalt	55 mg/l	1.1 mmol/l

Ionenbilanz		
Σ Kationen (meq/l)	0.70	*-1.8 %*
Σ Anionen (meq/l)	0.71	

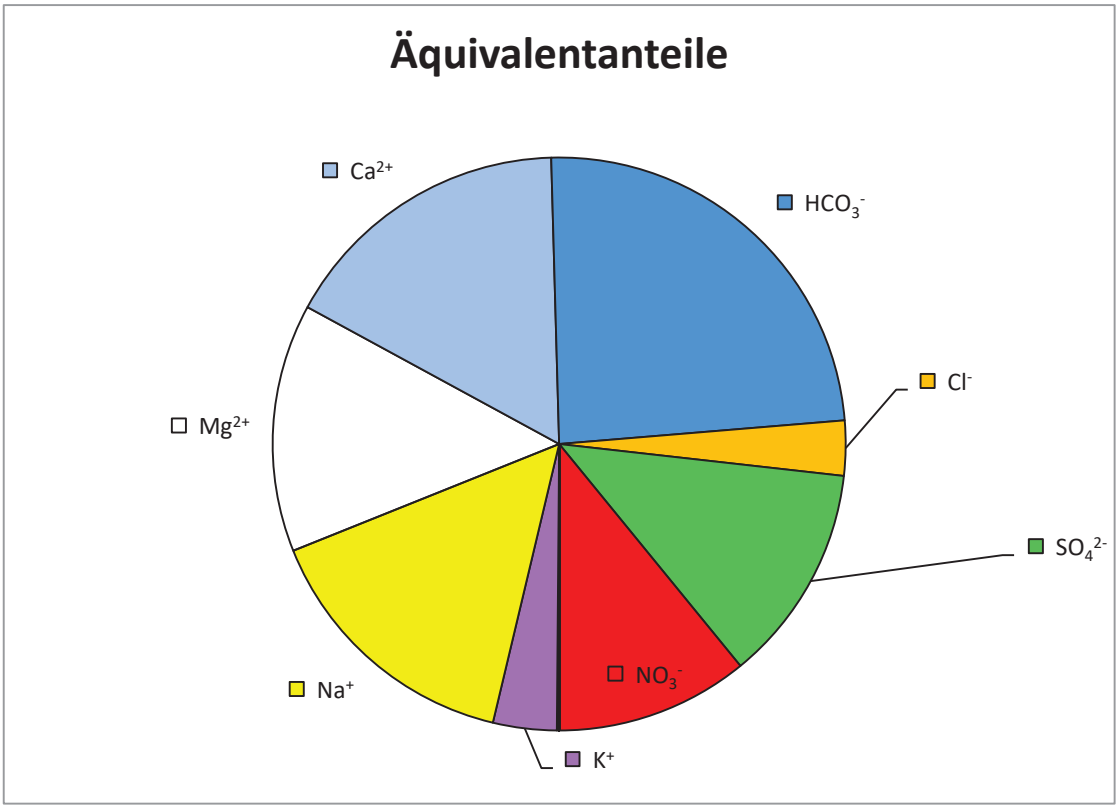

Wasseranalyse

Geologische Bundesanstalt
FA Geochemie
Leitung: HR Mag. Dr. Gerhard Hobiger

Probenahmepunkt:			**2**		
Koordinaten	**M** n.b.	**RW:** 14° 1'14.10"E	**HW:** 48°16'39.48"N	**GOK (m ü. A.)**	n.b.
Bezeichnung:	**2**		**Geochemie-Nr.:**	**GCH-2017-061-002**	
Probenahmetiefe:	**90**	**Probenehmer:**	**Be/Pö**		
Probenahmedatum und Uhrzeit:		**05.09.2017 12:45**	**Eingangsdatum:**	**07.09.2017**	

Feldparameter

		QZV *	MAP **	IP ***			
el. LF (µS/cm) (Gel.)	**460**	2250		2500	**Schüttung (l/s)**		**0.4**
el. LF (µS/cm) (Labor)	442				**Redoxpotenzial (mV)**		**-295**
					Temperatur (°C)		**16.4**
pH (Gel.)	**8.38**			6,5 - 9,5	**Sauerstoff (O_2)**	**mg/l**	**0.04**
pH (Labor)	7.98					**(%)**	**0.4**

Kationen (mg/l)

Ion	Messwert	QZV *	MAP **	IP ***
Calcium (Ca^{2+})	**5.7**			
Magnesium (Mg^{2+})	**1.1**			
Natrium (Na^{+})	**106.2**			200
Kalium (K^{+})	**1.5**			
Strontium (Sr^{2+})	**0.1026**			
Barium (Ba^{2+})	**0.0093**			
Lithium (Li^{+})	**0.0225**			
Rubidium (Rb^{+})	**0.0020**			
Cäsium (Cs^{+})	**< 0,0001**			
Ammonium (NH_4^{+})	**n.b.**	0.45		0.5
Eisen (Fe^{2+})	**0.000**			0.2
Mangan (Mn^{2+})	**0.0054**			0.05
Σ	**114.5**			

Anionen (mg/l)

Ion	Messwert	QZV *	MAP **	IP ***
Hydrogencarbonat (HCO_3^{-})	**284.95**			
Chlorid (Cl^{-})	**6.2**	180		200
Sulfat (SO_4^{2-})	**5.6**	225		250
Nitrat (NO_3^{-})	**0.0**	45	50	
Nitrit (NO_2^{-})	**n.b.**	0.09	0.1	
o- Phosphat (o-PO_4^{3-})	**n.b.**	0.3		
Sulfid (S^{2-})	**n.b.**			
Fluorid (F^{-})	**0.27**		1.5	
Σ	**297.0**			

Ges. Ionengehalt	**412 mg/l**	**Ionenbilanz**	
	9.8 mmol/l	***1.1***	**%**
Dichte	**n.b. g/cm3**		

Spezielle Parameter (mg/l)

Parameter	Messwert	QZV *	MAP **	IP ***
Kupfer (Cu)	**0.0002**	1.8	2	
Zink (Zn)	**< 0,0001**			
Blei (Pb)	**< 0,0001**	0.009	0.025	
Cadmium (Cd)	**< 0,0001**	0.0045	0.005	
Aluminium (Al)	**0.0019**			0.2
Arsen (As)	**< 0,0001**	0.009	0.01	
Antimon (Sb)	**n.b.**		0.005	
Chrom (Cr)	**< 0,0001**	0.045		
Nickel (Ni)	**< 0,0001**	0.018		
Quecksilber (Hg)	**n.b.**	0.0009	0.001	
Bor (B)	**n.b.**		1	
Uran (U)	**< 0,0001**		0.015	
Thorium (Th)	**n.b.**			
Cobalt (Co)	**< 0,0001**			
Molybdän (Mo)	**< 0,0001**			
Vanadium (V)	**< 0,0001**			
Selen (Se)	**n.b.**		0.01	
Tellur (Te)	**n.b.**			
Niob (Nb)	**n.b.**			
H_2SiO_3	**n.b.**			

Spezielle Parameter (mg/l)

Parameter	Messwert
Lanthan (La)	**n.b.**
Cer (Ce)	**n.b.**
Praseodym (Pr)	**n.b.**
Neodym (Nd)	**n.b.**
Samarium (Sm)	**n.b.**
Europium (Eu)	**n.b.**
Gadolimium (Gd)	**n.b.**
Terbium (Tb)	**n.b.**
Dysprosium (Dy)	**n.b.**
Holmium (Ho)	**n.b.**
Erbium (Er)	**n.b.**
Thulium (Tm)	**n.b.**
Ytterbium (Yb)	**n.b.**
Lutetium (Lu)	**n.b.**
Zinn (Sn)	**n.b.**
Thallium (Tl)	**n.b.**
Silber (Ag)	**n.b.**
Beryllium (Be)	**n.b.**
Bismut (Bi)	**n.b.**
Gallium (Ga)	**n.b.**

n.b. .. nicht bestimmt

* ... Qualitätszielverordnung Chemie Grundwasser QZV Chemie GW (BGBl. II 98/2010)

** ... Mindestanforderungsparameter aus der Trinkwasserverordnung - TWV (BGBl. II 304/2001)

*** ... Indikatorparameter aus der Trinkwasserverordnung - TWV (BGBl. II 304/2001)

Layout: G. Hobiger

Geologische Bundesanstalt
FA Geochemie
Leitung: HR Mag. Dr. Gerhard Hobiger

Berechnungen aus den Analysenwerten

Äquivalentanteile

Kationen				Anionen			
	Messwert				Messwert		
Ion	mg/l	meq/l	eq%	Ion	mg/l	meq/l	eq%
Ca^{2+}	5.68	0.28	5.64	HCO_3^-	284.95	4.67	93.9
Mg^{2+}	1.05	0.09	1.72	Cl^-	6.23	0.18	3.5
Na^+	106.19	4.62	91.78	SO_4^{2-}	5.56	0.12	2.3
K^+	1.45	0.04	0.74	NO_3^-	0.03	0.00	0.0
Sr^{2+}	0.10	0.00	0.05	NO_2^-	n.b.	n.b.	n.b.
Ba^{2+}	0.009	0.00	0.0	$o\text{-}PO_4^{3-}$	n.b.	n.b.	n.b.
Li^+	0.022	0.00	0.06	S^{2-}	n.b.	n.b.	n.b.
Rb^+	0.002	0.00	0.00	F^-	0.27	0.01	0.3
Cs^+	< 0,0001	0.00	0.00	Σ	297.03	5.0	100.0
NH_4^+	n.b.	n.b.	n.b.				
Fe^{2+}	0.000	0.00	0.0				
Mn^{2+}	0.0054	0.00	0.0				
Σ	114.52	5.0	100.0				

Härten	
Gesamthärte (° dH)	1.0
Carbonathärte(° dH)	1.0
Nichtcarbonathärte (°dH)	0.0
Erdalkalien (mmol/l)	3.7

Berechnung des CO_2	
lg(pCO_2)	-2.98
freies CO_2 (mg/l)	2.01
freies CO_2 (mmol/l)	0.0458

Berechneter Ammoniakgehalt	
NH_3 (mg/l)	n.b.

Ges. Ionengehalt	412 mg/l	9.8 mmol/l

Ionenbilanz		
Σ Kationen (meq/l)	5.03	*1.1 %*
Σ Anionen (meq/l)	4.98	

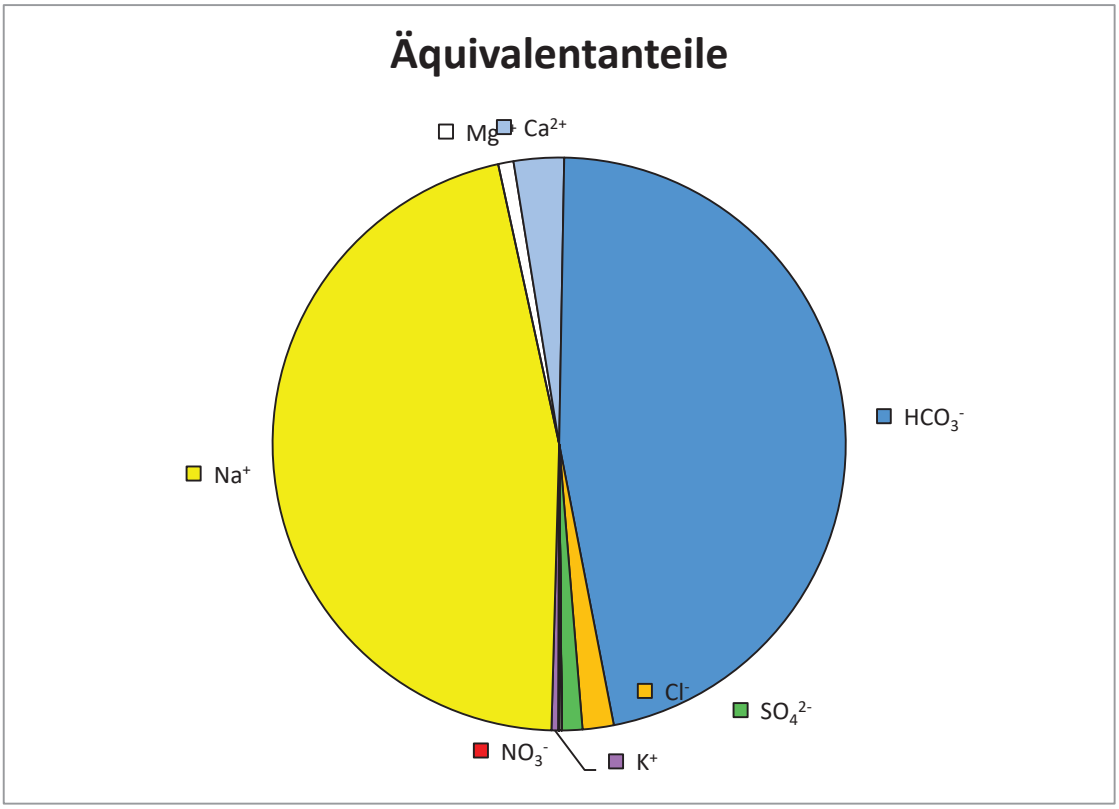

Wasseranalyse

Geologische Bundesanstalt
FA Geochemie
Leitung: HR Mag. Dr. Gerhard Hobiger

Probenahmepunkt:			3		
Koordinaten	**M** n.b.	**RW:** 14°15'8.55"E	**HW:** 48°16'0.04"N	**GOK (m ü. A.)**	n.b.
Bezeichnung:	3		**Geochemie-Nr.:**	**GCH-2017-061-003**	
Probenahmetiefe:	n.b.	**Probenehmer:**	Be/Pö		
Probenahmedatum und Uhrzeit:		05.09.2017 15:40	**Eingangsdatum:**	07.09.2017	

Feldparameter

		QZV *	MAP **	IP ***			
el. LF (µS/cm) (Gel.)	**867**	2250		2500	**Schüttung (l/s)**		n.b.
el. LF (µS/cm) (Labor)	843				**Redoxpotenzial (mV)**		270
					Temperatur (°C)		12.9
pH (Gel.)	**7.15**			6,5 - 9,5	**Sauerstoff (O_2)**	mg/l	11.25
pH (Labor)	7.07					(%)	109.6

Kationen (mg/l)

Ion	Messwert	QZV *	MAP **	IP ***
Calcium (Ca^{2+})	122.2			
Magnesium (Mg^{2+})	31.1			
Natrium (Na^{+})	13.8			200
Kalium (K^{+})	2.7			
Strontium (Sr^{2+})	0.2078			
Barium (Ba^{2+})	0.0750			
Lithium (Li^{+})	0.0027			
Rubidium (Rb^{+})	0.0007			
Cäsium (Cs^{+})	< 0,0001			
Ammonium (NH_4^{+})	n.b.	0.45		0.5
Eisen (Fe^{2+})	0.002			0.2
Mangan (Mn^{2+})	0.0017			0.05
Σ	170.1			

Anionen (mg/l)

Ion	Messwert	QZV *	MAP **	IP ***
Hydrogencarbonat (HCO_3^{-})	435.08			
Chlorid (Cl^{-})	39.4	180		200
Sulfat (SO_4^{2-})	36.1	225		250
Nitrat (NO_3^{-})	29.1	45	50	
Nitrit (NO_2^{-})	n.b.	0.09	0.1	
o- Phosphat (o-PO_4^{3-})	n.b.	0.3		
Sulfid (S^{2-})	n.b.			
Fluorid (F^{-})	0.12		1.5	
Σ	539.9			

Ges. Ionengehalt	710 mg/l	**Ionenbilanz**	
	14.1 mmol/l	*-1.5*	%
Dichte	n.b. g/cm3		

Spezielle Parameter (mg/l)

Parameter	Messwert	QZV *	MAP **	IP ***
Kupfer (Cu)	0.0024	1.8	2	
Zink (Zn)	0.0272			
Blei (Pb)	0.0002	0.009	0.025	
Cadmium (Cd)	< 0,0001	0.0045	0.005	
Aluminium (Al)	0.0017			0.2
Arsen (As)	0.0002	0.009	0.01	
Antimon (Sb)	n.b.		0.005	
Chrom (Cr)	0.0014	0.045		
Nickel (Ni)	0.0005	0.018		
Quecksilber (Hg)	n.b.	0.0009	0.001	
Bor (B)	n.b.		1	
Uran (U)	0.0012		0.015	
Thorium (Th)	n.b.			
Cobalt (Co)	< 0,0001			
Molybdän (Mo)	0.0002			
Vanadium (V)	0.0005			
Selen (Se)	n.b.		0.01	
Tellur (Te)	n.b.			
Niob (Nb)	n.b.			
H_2SiO_3	n.b.			

Spezielle Parameter (mg/l)

Parameter	Messwert
Lanthan (La)	n.b.
Cer (Ce)	n.b.
Praseodym (Pr)	n.b.
Neodym (Nd)	n.b.
Samarium (Sm)	n.b.
Europium (Eu)	n.b.
Gadolimium (Gd)	n.b.
Terbium (Tb)	n.b.
Dysprosium (Dy)	n.b.
Holmium (Ho)	n.b.
Erbium (Er)	n.b.
Thulium (Tm)	n.b.
Ytterbium (Yb)	n.b.
Lutetium (Lu)	n.b.
Zinn (Sn)	n.b.
Thallium (Tl)	n.b.
Silber (Ag)	n.b.
Beryllium (Be)	n.b.
Bismut (Bi)	n.b.
Gallium (Ga)	n.b.

n.b. .. nicht bestimmt

* ... Qualitätszielverordnung Chemie Grundwasser QZV Chemie GW (BGBl. II 98/2010)

** ... Mindestanforderungsparameter aus der Trinkwasserverordnung - TWV (BGBl. II 304/2001)

*** ... Indikatorparameter aus der Trinkwasserverordnung - TWV (BGBl. II 304/2001)

Layout: G. Hobiger

Geologische Bundesanstalt
FA Geochemie
Leitung: HR Mag. Dr. Gerhard Hobiger

Berechnungen aus den Analysenwerten

Äquivalentanteile

Kationen				Anionen			
	Messwert				Messwert		
Ion	mg/l	meq/l	eq%	Ion	mg/l	meq/l	eq%
Ca^{2+}	122.17	6.10	65.33	HCO_3^-	435.08	7.13	75.3
Mg^{2+}	31.10	2.56	27.42	Cl^-	39.43	1.11	11.7
Na^+	13.81	0.60	6.44	SO_4^{2-}	36.08	0.75	7.9
K^+	2.72	0.07	0.75	NO_3^-	29.15	0.47	5.0
Sr^{2+}	0.21	0.00	0.05	NO_2^-	n.b.	n.b.	n.b.
Ba^{2+}	0.075	0.00	0.0	o-PO_4^{3-}	n.b.	n.b.	n.b.
Li^+	0.003	0.00	0.00	S^{2-}	n.b.	n.b.	n.b.
Rb^+	0.001	0.00	0.00	F^-	0.12	0.01	0.1
Cs^+	< 0,0001	0.00	0.00	Σ	539.86	9.5	100.0
NH_4^+	n.b.	n.b.	n.b.				
Fe^{2+}	0.002	0.00	0.0				
Mn^{2+}	0.0017	0.00	0.0				
Σ	170.09	9.3	100.0				

Härten	
Gesamthärte (° dH)	24.3
Carbonathärte(° dH)	20.0
Nichtcarbonathärte (°dH)	4.3
Erdalkalien (mmol/l)	46.4

Berechnung des CO_2	
lg(pCO_2)	-1.61
freies CO_2 (mg/l)	52.99
freies CO_2 (mmol/l)	1.2040

Berechneter Ammoniakgehalt	
NH_3 (mg/l)	n.b.

Ges. Ionengehalt	710 mg/l	14.1 mmol/l

Ionenbilanz		
Σ Kationen (meq/l)	9.33	*-1.5 %*
Σ Anionen (meq/l)	9.47	

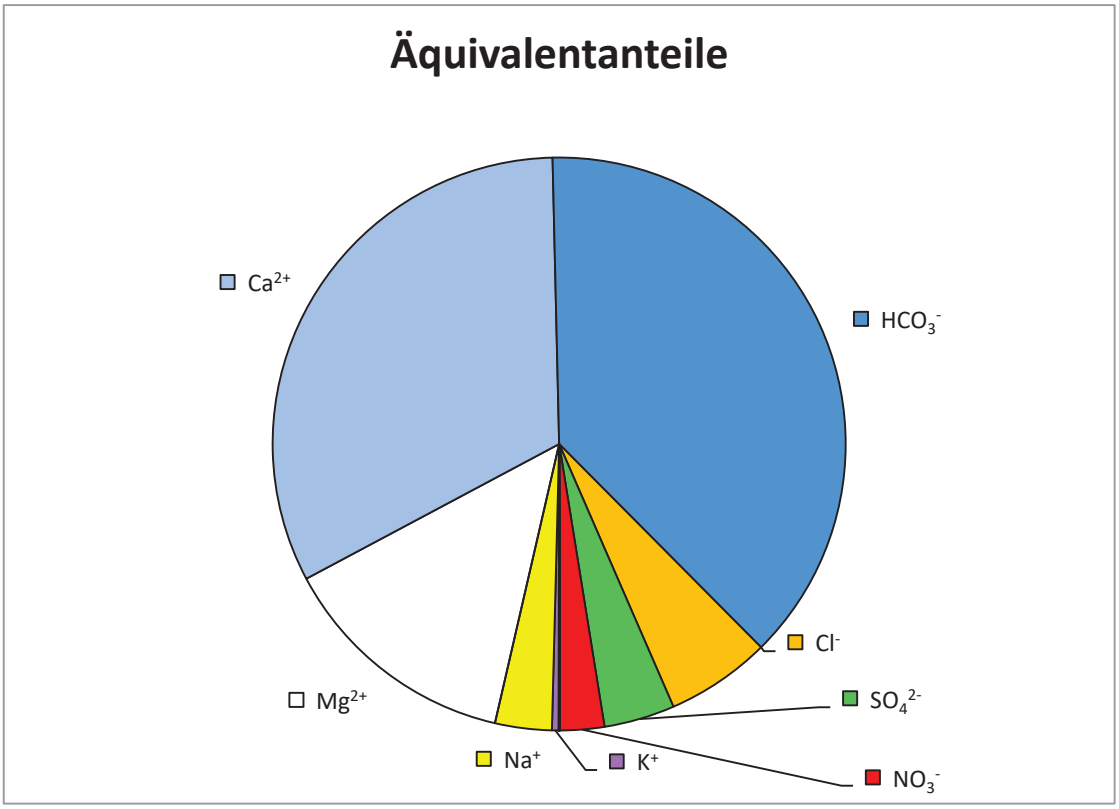

Wasseranalyse

Geologische Bundesanstalt
FA Geochemie
Leitung: HR Mag. Dr. Gerhard Hobiger

Probenahmepunkt:			**4**		
Koordinaten	**M** n.b.	**RW:** 13°56'20.94"E	**HW:** 48°18'0.66"N	**GOK (m ü. A.)**	n.b.
Bezeichnung:	**4**		**Geochemie-Nr.:**	**GCH-2017-061-004**	
Probenahmetiefe:	n.b.	**Probenehmer:**	**Be/Pö**		
Probenahmedatum und Uhrzeit:		**05.09.2017 17:00**	**Eingangsdatum:**	**07.09.2017**	

Feldparameter

		QZV *	MAP **	IP ***			
el. LF (µS/cm) (Gel.)	**360**	2250		2500	**Schüttung (l/s)**		**n.b.**
el. LF (µS/cm) (Labor)	351				**Redoxpotenzial (mV)**		**130**
					Temperatur (°C)		**11.7**
pH (Gel.)	**6.7**			6,5 - 9,5	**Sauerstoff (O_2)**	**mg/l**	**0.49**
pH (Labor)	6.57					**(%)**	**4.6**

Kationen (mg/l)

Ion	Messwert	QZV *	MAP **	IP ***
Calcium (Ca^{2+})	**45.0**			
Magnesium (Mg^{2+})	**12.6**			
Natrium (Na^{+})	**6.5**			200
Kalium (K^{+})	**1.4**			
Strontium (Sr^{2+})	**0.1225**			
Barium (Ba^{2+})	**0.0283**			
Lithium (Li^{+})	**0.0048**			
Rubidium (Rb^{+})	**0.0013**			
Cäsium (Cs^{+})	**< 0,0001**			
Ammonium (NH_4^{+})	**n.b.**	0.45		0.5
Eisen (Fe^{2+})	**0.047**			0.2
Mangan (Mn^{2+})	**0.0214**			0.05
Σ	**65.8**			

Anionen (mg/l)

Ion	Messwert	QZV *	MAP **	IP ***
Hydrogencarbonat (HCO_3^{-})	**137.84**			
Chlorid (Cl^{-})	**13.1**	180		200
Sulfat (SO_4^{2-})	**39.6**	225		250
Nitrat (NO_3^{-})	**13.4**	45	50	
Nitrit (NO_2^{-})	**n.b.**	0.09	0.1	
o- Phosphat (o-PO_4^{3-})	**n.b.**	0.3		
Sulfid (S^{2-})	**n.b.**			
Fluorid (F^{-})	**0.14**		1.5	
Σ	**204.1**			

Ges. Ionengehalt	**270 mg/l**	**Ionenbilanz**	
	5.2 mmol/l	***-1.8***	**%**
Dichte	**n.b. g/cm3**		

Spezielle Parameter (mg/l)

Parameter	Messwert	QZV *	MAP **	IP ***
Kupfer (Cu)	**0.0013**	1.8	2	
Zink (Zn)	**0.0181**			
Blei (Pb)	**< 0,0001**	0.009	0.025	
Cadmium (Cd)	**< 0,0001**	0.0045	0.005	
Aluminium (Al)	**0.0020**			0.2
Arsen (As)	**0.0009**	0.009	0.01	
Antimon (Sb)	**n.b.**		0.005	
Chrom (Cr)	**< 0,0001**	0.045		
Nickel (Ni)	**0.0009**	0.018		
Quecksilber (Hg)	**n.b.**	0.0009	0.001	
Bor (B)	**n.b.**		1	
Uran (U)	**0.0020**		0.015	
Thorium (Th)	**n.b.**			
Cobalt (Co)	**0.0001**			
Molybdän (Mo)	**0.0013**			
Vanadium (V)	**0.0003**			
Selen (Se)	**n.b.**		0.01	
Tellur (Te)	**n.b.**			
Niob (Nb)	**n.b.**			
H_2SiO_3	**n.b.**			

Spezielle Parameter (mg/l)

Parameter	Messwert	Parameter	Messwert
Lanthan (La)	**n.b.**	Ytterbium (Yb)	**n.b.**
Cer (Ce)	**n.b.**	Lutetium (Lu)	**n.b.**
Praseodym (Pr)	**n.b.**	Zinn (Sn)	**n.b.**
Neodym (Nd)	**n.b.**	Thallium (Tl)	**n.b.**
Samarium (Sm)	**n.b.**	Silber (Ag)	**n.b.**
Europium (Eu)	**n.b.**	Beryllium (Be)	**n.b.**
Gadolimium (Gd)	**n.b.**	Bismut (Bi)	**n.b.**
Terbium (Tb)	**n.b.**	Gallium (Ga)	**n.b.**
Dysprosium (Dy)	**n.b.**		
Holmium (Ho)	**n.b.**		
Erbium (Er)	**n.b.**		
Thulium (Tm)	**n.b.**		

n.b. .. nicht bestimmt

* ... Qualitätszielverordnung Chemie Grundwasser QZV Chemie GW (BGBl. II 98/2010)

** ... Mindestanforderungsparameter aus der Trinkwasserverordnung - TWV (BGBl. II 304/2001)

*** ... Indikatorparameter aus der Trinkwasserverordnung - TWV (BGBl. II 304/2001)

Layout: G. Hobiger

Geologische Bundesanstalt
FA Geochemie
Leitung: HR Mag. Dr. Gerhard Hobiger

Berechnungen aus den Analysenwerten

Äquivalentanteile

Kationen				Anionen			
	Messwert				Messwert		
Ion	mg/l	meq/l	eq%	Ion	mg/l	meq/l	eq%
Ca^{2+}	45.04	2.25	62.24	HCO_3^-	137.84	2.26	61.4
Mg^{2+}	12.62	1.04	28.76	Cl^-	13.11	0.37	10.1
Na^+	6.51	0.28	7.84	SO_4^{2-}	39.57	0.82	22.4
K^+	1.39	0.04	0.99	NO_3^-	13.41	0.22	5.9
Sr^{2+}	0.12	0.00	0.08	NO_2^-	n.b.	n.b.	n.b.
Ba^{2+}	0.028	0.00	0.0	o-PO_4^{3-}	n.b.	n.b.	n.b.
Li^+	0.005	0.00	0.02	S^{2-}	n.b.	n.b.	n.b.
Rb^+	0.001	0.00	0.00	F^-	0.14	0.01	0.2
Cs^+	< 0,0001	0.00	0.00	Σ	204.07	3.7	100.0
NH_4^+	n.b.	n.b.	n.b.				
Fe^{2+}	0.047	0.00	0.0				
Mn^{2+}	0.0214	0.00	0.0				
Σ	65.79	3.6	100.0				

Härten	
Gesamthärte (° dH)	9.2
Carbonathärte(° dH)	6.3
Nichtcarbonathärte (°dH)	2.9
Erdalkalien (mmol/l)	45.5

Berechnung des CO_2	
lg(pCO_2)	-1.64
freies CO_2 (mg/l)	50.94
freies CO_2 (mmol/l)	1.1574

Berechneter Ammoniakgehalt	
NH_3 (mg/l)	n.b.

Ges. Ionengehalt	270 mg/l	5.2 mmol/l

Ionenbilanz		
Σ Kationen (meq/l)	3.61	*-1.8 %*
Σ Anionen (meq/l)	3.68	

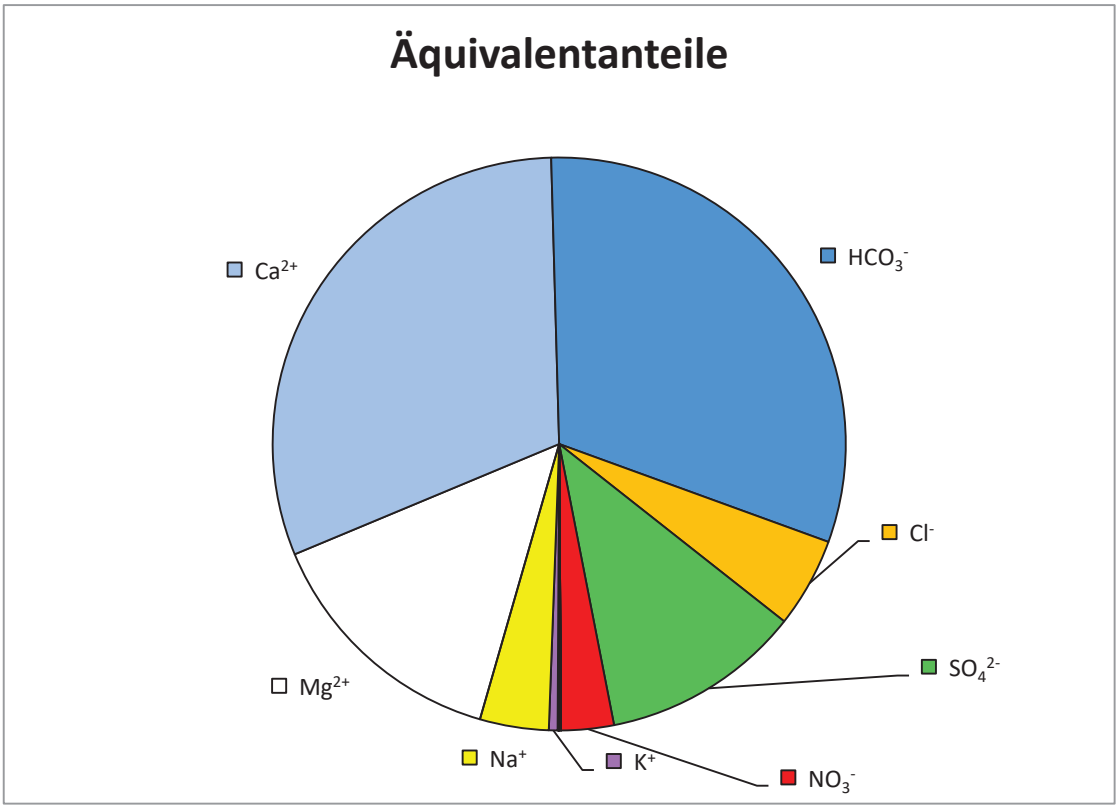

Wasseranalyse

Geologische Bundesanstalt
FA Geochemie
Leitung: HR Mag. Dr. Gerhard Hobiger

Probenahmepunkt:			5		
Koordinaten	**M** n.b.	**RW:** 14°18'54.00"E	**HW:** 48°29'16.08"N	**GOK (m ü. A.)**	n.b.
Bezeichnung:	5		**Geochemie-Nr.:**	**GCH-2017-061-005**	
Probenahmetiefe:	45	**Probenehmer:**	Be/Pö		
Probenahmedatum und Uhrzeit:	06.09.2017 11:00		**Eingangsdatum:**	07.09.2017	

Feldparameter

		QZV *	MAP **	IP ***			
el. LF (µS/cm) (Gel.)	**160**	2250		2500	**Schüttung (l/s)**		**0.5**
el. LF (µS/cm) (Labor)	149				**Redoxpotenzial (mV)**		**34**
					Temperatur (°C)		**8.1**
pH (Gel.)	**6.76**			6,5 - 9,5	**Sauerstoff (O_2)**	**mg/l**	**0.01**
pH (Labor)	6.5					**(%)**	**0.1**

Kationen (mg/l)

Ion	Messwert	QZV *	MAP **	IP ***
Calcium (Ca^{2+})	16.5			
Magnesium (Mg^{2+})	4.7			
Natrium (Na^{+})	6.6			200
Kalium (K^{+})	2.6			
Strontium (Sr^{2+})	0.1137			
Barium (Ba^{2+})	0.0473			
Lithium (Li^{+})	0.0099			
Rubidium (Rb^{+})	0.0010			
Cäsium (Cs^{+})	< 0,0001			
Ammonium (NH_4^{+})	n.b.	0.45		0.5
Eisen (Fe^{2+})	1.284			0.2
Mangan (Mn^{2+})	0.1178			0.05
Σ	32.0			

Anionen (mg/l)

Ion	Messwert	QZV *	MAP **	IP ***
Hydrogencarbonat (HCO_3^{-})	83.96			
Chlorid (Cl^{-})	1.1	180		200
Sulfat (SO_4^{2-})	9.8	225		250
Nitrat (NO_3^{-})	< 0,5	45	50	
Nitrit (NO_2^{-})	n.b.	0.09	0.1	
o- Phosphat (o-PO_4^{3-})	n.b.	0.3		
Sulfid (S^{2-})	n.b.			
Fluorid (F^{-})	0.07		1.5	
Σ	95.0			

Ges. Ionengehalt	**127** mg/l	**Ionenbilanz**	
	2.5 mmol/l	***0.2***	**%**
Dichte	n.b. g/cm3		

Spezielle Parameter (mg/l)

Parameter	Messwert	QZV *	MAP **	IP ***
Kupfer (Cu)	0.0013	1.8	2	
Zink (Zn)	0.0030			
Blei (Pb)	< 0,0001	0.009	0.025	
Cadmium (Cd)	< 0,0001	0.0045	0.005	
Aluminium (Al)	0.0019			0.2
Arsen (As)	< 0,0001	0.009	0.01	
Antimon (Sb)	n.b.		0.005	
Chrom (Cr)	< 0,0001	0.045		
Nickel (Ni)	< 0,0001	0.018		
Quecksilber (Hg)	n.b.	0.0009	0.001	
Bor (B)	n.b.		1	
Uran (U)	< 0,0001		0.015	
Thorium (Th)	n.b.			
Cobalt (Co)	< 0,0001			
Molybdän (Mo)	0.0004			
Vanadium (V)	< 0,0001			
Selen (Se)	n.b.		0.01	
Tellur (Te)	n.b.			
Niob (Nb)	n.b.			
H_2SiO_3	n.b.			

Spezielle Parameter (mg/l)

Parameter	Messwert
Lanthan (La)	n.b.
Cer (Ce)	n.b.
Praseodym (Pr)	n.b.
Neodym (Nd)	n.b.
Samarium (Sm)	n.b.
Europium (Eu)	n.b.
Gadolimium (Gd)	n.b.
Terbium (Tb)	n.b.
Dysprosium (Dy)	n.b.
Holmium (Ho)	n.b.
Erbium (Er)	n.b.
Thulium (Tm)	n.b.
Ytterbium (Yb)	n.b.
Lutetium (Lu)	n.b.
Zinn (Sn)	n.b.
Thallium (Tl)	n.b.
Silber (Ag)	n.b.
Beryllium (Be)	n.b.
Bismut (Bi)	n.b.
Gallium (Ga)	n.b.

n.b. .. nicht bestimmt

* ... Qualitätszielverordnung Chemie Grundwasser QZV Chemie GW (BGBl. II 98/2010)

** ... Mindestanforderungsparameter aus der Trinkwasserverordnung - TWV (BGBl. II 304/2001)

*** ... Indikatorparameter aus der Trinkwasserverordnung - TWV (BGBl. II 304/2001)

Layout: G. Hobiger

Geologische Bundesanstalt
FA Geochemie
Leitung: HR Mag. Dr. Gerhard Hobiger

Berechnungen aus den Analysenwerten

Äquivalentanteile

Kationen

Ion	Messwert mg/l	meq/l	eq%
Ca^{2+}	16.53	0.82	50.92
Mg^{2+}	4.67	0.38	23.74
Na^{+}	6.64	0.29	17.84
K^{+}	2.60	0.07	4.11
Sr^{2+}	0.11	0.00	0.16
Ba^{2+}	0.047	0.00	0.0
Li^{+}	0.010	0.00	0.09
Rb^{+}	0.001	0.00	0.00
Cs^{+}	< 0,0001	0.00	0.00
NH_4^{+}	n.b.	n.b.	n.b.
Fe^{2+}	1.284	0.05	2.8
Mn^{2+}	0.1178	0.00	0.3
Σ	32.01	1.6	100.0

Anionen

Ion	Messwert mg/l	meq/l	eq%
HCO_3^{-}	83.96	1.38	85.2
Cl^{-}	1.11	0.03	1.9
SO_4^{2-}	9.84	0.20	12.7
NO_3^{-}	< 0,5	0.00	0.0
NO_2^{-}	n.b.	n.b.	n.b.
$o\text{-}PO_4^{3-}$	n.b.	n.b.	n.b.
S^{2-}	n.b.	n.b.	n.b.
F^{-}	0.07	0.00	0.2
Σ	94.97	1.6	100.0

Härten

Gesamthärte (° dH)	3.4
Carbonathärte(° dH)	3.4
Nichtcarbonathärte (°dH)	0.0
Erdalkalien (mmol/l)	37.4

Berechnung des CO_2

$lg(pCO_2)$	-1.92
freies CO_2 (mg/l)	30.23
freies CO_2 (mmol/l)	0.6869

Berechneter Ammoniakgehalt

NH_3 (mg/l)	n.b.

Ges. Ionengehalt	127 mg/l	2.5 mmol/l

Ionenbilanz

Σ Kationen (meq/l)	1.62	*0.2 %*
Σ Anionen (meq/l)	1.62	

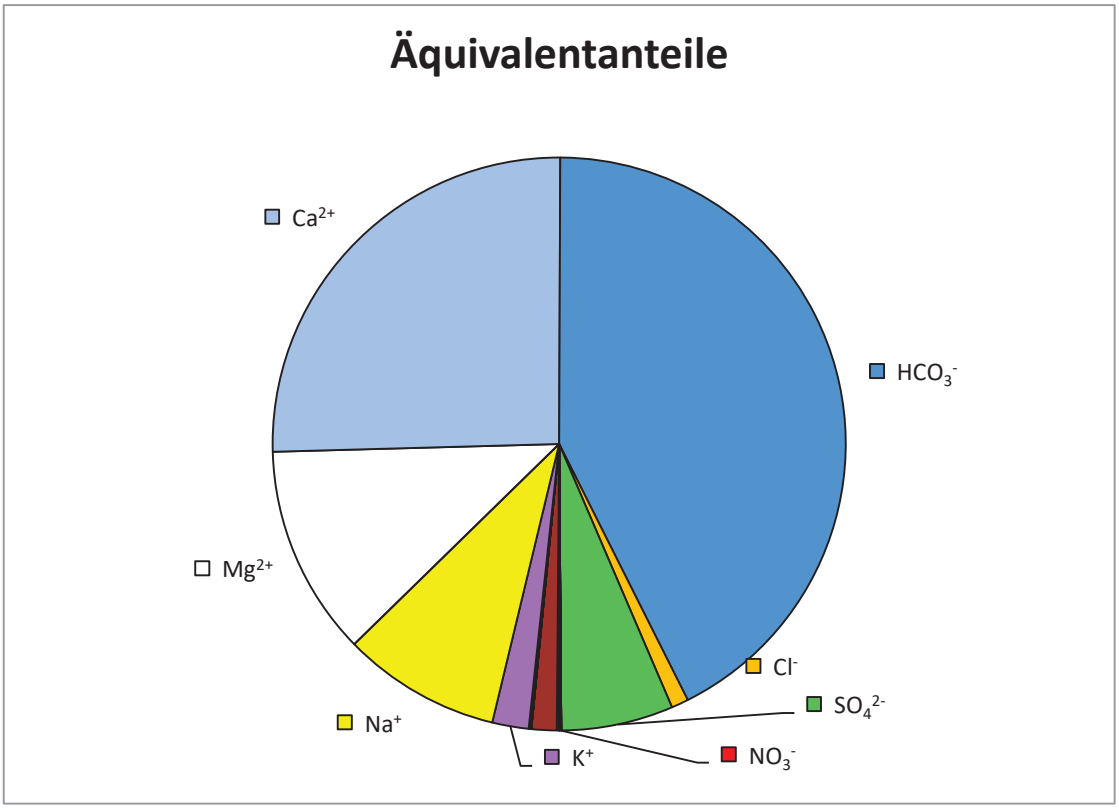

Wasseranalyse

Geologische Bundesanstalt
FA Geochemie
Leitung: HR Mag. Dr. Gerhard Hobiger

Probenahmepunkt:			**6**		
Koordinaten	**M** n.b.	**RW:** 14° 3'13.38"E	**HW:** 48°22'18.48"N	**GOK (m ü. A.)**	n.b.
Bezeichnung:	**6**		**Geochemie-Nr.:**	**GCH-2017-061-006**	
Probenahmetiefe:	n.b.	**Probenehmer:**	**Be/Pö**		
Probenahmedatum und Uhrzeit:		**06.09.2017 13:00**	**Eingangsdatum:**	**07.09.2017**	

Feldparameter

		QZV *	MAP **	IP ***			
el. LF (µS/cm) (Gel.)	**282**	2250		2500	**Schüttung (l/s)**		**0.96**
el. LF (µS/cm) (Labor)	269				**Redoxpotenzial (mV)**		**59**
					Temperatur (°C)		**11.4**
pH (Gel.)	**7.13**			6,5 - 9,5	**Sauerstoff (O_2)**	**mg/l**	**0.21**
pH (Labor)	6.75					**(%)**	**2**

Kationen (mg/l)

Ion	Messwert	QZV *	MAP **	IP ***
Calcium (Ca^{2+})	**32.1**			
Magnesium (Mg^{2+})	**9.3**			
Natrium (Na^{+})	**8.6**			200
Kalium (K^{+})	**3.4**			
Strontium (Sr^{2+})	**0.1209**			
Barium (Ba^{2+})	**0.1193**			
Lithium (Li^{+})	**0.0162**			
Rubidium (Rb^{+})	**0.0016**			
Cäsium (Cs^{+})	**< 0,0001**			
Ammonium (NH_4^{+})	**n.b.**	0.45		0.5
Eisen (Fe^{2+})	**0.670**			0.2
Mangan (Mn^{2+})	**0.0997**			0.05
Σ	**54.5**			

Anionen (mg/l)

Ion	Messwert	QZV *	MAP **	IP ***
Hydrogencarbonat (HCO_3^{-})	**142.05**			
Chlorid (Cl^{-})	**4.5**	180		200
Sulfat (SO_4^{2-})	**20.3**	225		250
Nitrat (NO_3^{-})	**0.6**	45	50	
Nitrit (NO_2^{-})	**n.b.**	0.09	0.1	
o- Phosphat (o-PO_4^{3-})	**n.b.**	0.3		
Sulfid (S^{2-})	**n.b.**			
Fluorid (F^{-})	**0.23**		1.5	
Σ	**167.6**			

Ges. Ionengehalt	**222 mg/l**	**Ionenbilanz**	
	4.4 mmol/l	***-1.1***	**%**
Dichte	**n.b. g/cm3**		

Spezielle Parameter (mg/l)

Parameter	Messwert	QZV *	MAP **	IP ***
Kupfer (Cu)	**0.0003**	1.8	2	
Zink (Zn)	**0.0016**			
Blei (Pb)	**< 0,0001**	0.009	0.025	
Cadmium (Cd)	**< 0,0001**	0.0045	0.005	
Aluminium (Al)	**0.0015**			0.2
Arsen (As)	**< 0,0001**	0.009	0.01	
Antimon (Sb)	**n.b.**		0.005	
Chrom (Cr)	**< 0,0001**	0.045		
Nickel (Ni)	**< 0,0001**	0.018		
Quecksilber (Hg)	**n.b.**	0.0009	0.001	
Bor (B)	**n.b.**		1	
Uran (U)	**< 0,0001**		0.015	
Thorium (Th)	**n.b.**			
Cobalt (Co)	**< 0,0001**			
Molybdän (Mo)	**0.0013**			
Vanadium (V)	**< 0,0001**			
Selen (Se)	**n.b.**		0.01	
Tellur (Te)	**n.b.**			
Niob (Nb)	**n.b.**			
H_2SiO_3	**n.b.**			

Spezielle Parameter (mg/l)

Parameter	Messwert
Lanthan (La)	**n.b.**
Cer (Ce)	**n.b.**
Praseodym (Pr)	**n.b.**
Neodym (Nd)	**n.b.**
Samarium (Sm)	**n.b.**
Europium (Eu)	**n.b.**
Gadolimium (Gd)	**n.b.**
Terbium (Tb)	**n.b.**
Dysprosium (Dy)	**n.b.**
Holmium (Ho)	**n.b.**
Erbium (Er)	**n.b.**
Thulium (Tm)	**n.b.**
Ytterbium (Yb)	**n.b.**
Lutetium (Lu)	**n.b.**
Zinn (Sn)	**n.b.**
Thallium (Tl)	**n.b.**
Silber (Ag)	**n.b.**
Beryllium (Be)	**n.b.**
Bismut (Bi)	**n.b.**
Gallium (Ga)	**n.b.**

n.b. .. nicht bestimmt

* ... Qualitätszielverordnung Chemie Grundwasser QZV Chemie GW (BGBl. II 98/2010)

** ... Mindestanforderungsparameter aus der Trinkwasserverordnung - TWV (BGBl. II 304/2001)

*** ... Indikatorparameter aus der Trinkwasserverordnung - TWV (BGBl. II 304/2001)

Layout: G. Hobiger

Geologische Bundesanstalt
FA Geochemie
Leitung: HR Mag. Dr. Gerhard Hobiger

Berechnungen aus den Analysenwerten

Äquivalentanteile

Kationen

Ion	Messwert mg/l	meq/l	eq%
Ca^{2+}	32.14	1.60	55.98
Mg^{2+}	9.28	0.76	26.65
Na^{+}	8.63	0.38	13.10
K^{+}	3.44	0.09	3.07
Sr^{2+}	0.12	0.00	0.10
Ba^{2+}	0.119	0.00	0.1
Li^{+}	0.016	0.00	0.08
Rb^{+}	0.002	0.00	0.00
Cs^{+}	< 0,0001	0.00	0.00
NH_4^{+}	n.b.	n.b.	n.b.
Fe^{2+}	0.670	0.02	0.8
Mn^{2+}	0.0997	0.00	0.1
Σ	54.51	2.9	100.0

Anionen

Ion	Messwert mg/l	meq/l	eq%
HCO_3^{-}	142.05	2.33	80.3
Cl^{-}	4.45	0.13	4.3
SO_4^{2-}	20.32	0.42	14.6
NO_3^{-}	0.55	0.01	0.3
NO_2^{-}	n.b.	n.b.	n.b.
$o\text{-}PO_4^{3-}$	n.b.	n.b.	n.b.
S^{2-}	n.b.	n.b.	n.b.
F^{-}	0.23	0.01	0.4
Σ	167.60	2.9	100.0

Härten

Gesamthärte (° dH)	6.6
Carbonathärte(° dH)	6.5
Nichtcarbonathärte (°dH)	0.1
Erdalkalien (mmol/l)	41.4

Berechnung des CO_2

$lg(pCO_2)$	-2.06
freies CO_2 (mg/l)	19.85
freies CO_2 (mmol/l)	0.4511

Berechneter Ammoniakgehalt

NH_3 (mg/l)	n.b.

Ges. Ionengehalt	222 mg/l	4.4 mmol/l

Ionenbilanz

Σ Kationen (meq/l)	2.87	*-1.1 %*
Σ Anionen (meq/l)	2.90	

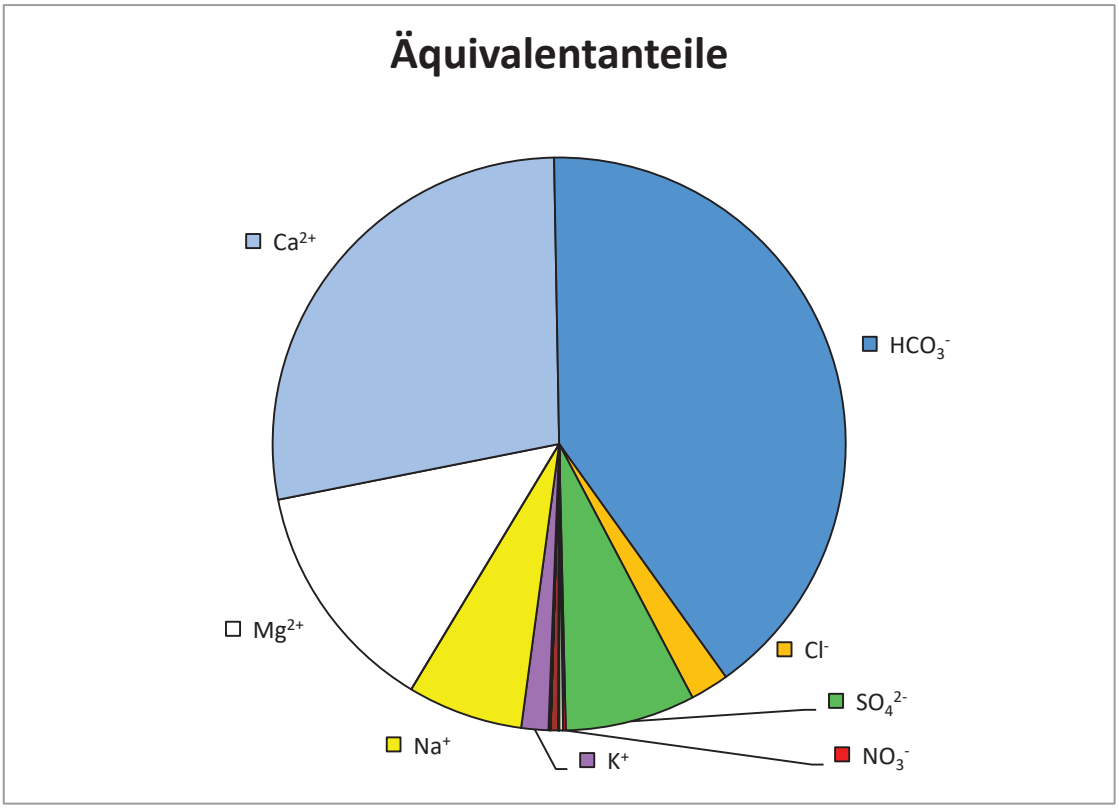

Wasseranalyse

Geologische Bundesanstalt
FA Geochemie
Leitung: HR Mag. Dr. Gerhard Hobiger

Probenahmepunkt:			**7**		
Koordinaten	**M** n.b.	**RW:** 14° 1'45.59"E	**HW:** 48°16'1.28"N	**GOK (m ü. A.)**	n.b.
Bezeichnung:	**7**		**Geochemie-Nr.:**	**GCH-2017-061-007**	
Probenahmetiefe:	n.b.	**Probenehmer:**	**Be/Pö**		
Probenahmedatum und Uhrzeit:		**06.09.2017 15:30**	**Eingangsdatum:**	**07.09.2017**	

Feldparameter

		QZV *	MAP **	IP ***			
el. LF (µS/cm) (Gel.)	**467**	2250		2500	**Schüttung (l/s)**		**n.b.**
el. LF (µS/cm) (Labor)	450				**Redoxpotenzial (mV)**		**-248**
					Temperatur (°C)		**19.7**
pH (Gel.)	**8.34**			6,5 - 9,5	**Sauerstoff (O_2)**	**mg/l**	**2.5**
pH (Labor)	8.18					**(%)**	**18.3**

Kationen (mg/l)

Ion	Messwert	QZV *	MAP **	IP ***
Calcium (Ca^{2+})	**9.3**			
Magnesium (Mg^{2+})	**1.4**			
Natrium (Na^{+})	**99.6**			200
Kalium (K^{+})	**1.3**			
Strontium (Sr^{2+})	**0.1458**			
Barium (Ba^{2+})	**0.0129**			
Lithium (Li^{+})	**0.0219**			
Rubidium (Rb^{+})	**0.0020**			
Cäsium (Cs^{+})	**< 0,0001**			
Ammonium (NH_4^{+})	**n.b.**	0.45		0.5
Eisen (Fe^{2+})	**0.013**			0.2
Mangan (Mn^{2+})	**0.0058**			0.05
Σ	**111.7**			

Anionen (mg/l)

Ion	Messwert	QZV *	MAP **	IP ***
Hydrogencarbonat (HCO_3^{-})	**285.36**			
Chlorid (Cl^{-})	**7.9**	180		200
Sulfat (SO_4^{2-})	**3.6**	225		250
Nitrat (NO_3^{-})	**n.b.**	45	50	
Nitrit (NO_2^{-})	**n.b.**	0.09	0.1	
o- Phosphat (o-PO_4^{3-})	**n.b.**	0.3		
Sulfid (S^{2-})	**n.b.**			
Fluorid (F^{-})	**0.25**		1.5	
Σ	**297.2**			

Ges. Ionengehalt	**409 mg/l**	**Ionenbilanz**	
	9.6 mmol/l	***-0.8***	**%**
Dichte	**n.b. g/cm3**		

Spezielle Parameter (mg/l)

Parameter	Messwert	QZV *	MAP **	IP ***
Kupfer (Cu)	**0.0003**	1.8	2	
Zink (Zn)	**< 0,0001**			
Blei (Pb)	**< 0,0001**	0.009	0.025	
Cadmium (Cd)	**< 0,0001**	0.0045	0.005	
Aluminium (Al)	**0.0022**			0.2
Arsen (As)	**< 0,0001**	0.009	0.01	
Antimon (Sb)	**n.b.**		0.005	
Chrom (Cr)	**< 0,0001**	0.045		
Nickel (Ni)	**0.0003**	0.018		
Quecksilber (Hg)	**n.b.**	0.0009	0.001	
Bor (B)	**n.b.**		1	
Uran (U)	**< 0,0001**		0.015	
Thorium (Th)	**n.b.**			
Cobalt (Co)	**< 0,0001**			
Molybdän (Mo)	**< 0,0001**			
Vanadium (V)	**< 0,0001**			
Selen (Se)	**n.b.**		0.01	
Tellur (Te)	**n.b.**			
Niob (Nb)	**n.b.**			
H_2SiO_3	**n.b.**			

Spezielle Parameter (mg/l)

Parameter	Messwert	Parameter	Messwert
Lanthan (La)	**n.b.**	Ytterbium (Yb)	**n.b.**
Cer (Ce)	**n.b.**	Lutetium (Lu)	**n.b.**
Praseodym (Pr)	**n.b.**	Zinn (Sn)	**n.b.**
Neodym (Nd)	**n.b.**	Thallium (Tl)	**n.b.**
Samarium (Sm)	**n.b.**	Silber (Ag)	**n.b.**
Europium (Eu)	**n.b.**	Beryllium (Be)	**n.b.**
Gadolimium (Gd)	**n.b.**	Bismut (Bi)	**n.b.**
Terbium (Tb)	**n.b.**	Gallium (Ga)	**n.b.**
Dysprosium (Dy)	**n.b.**		
Holmium (Ho)	**n.b.**		
Erbium (Er)	**n.b.**		
Thulium (Tm)	**n.b.**		

n.b. .. nicht bestimmt

* ... Qualitätszielverordnung Chemie Grundwasser QZV Chemie GW (BGBl. II 98/2010)

** ... Mindestanforderungsparameter aus der Trinkwasserverordnung - TWV (BGBl. II 304/2001)

*** ... Indikatorparameter aus der Trinkwasserverordnung - TWV (BGBl. II 304/2001)

Layout: G. Hobiger

Geologische Bundesanstalt
FA Geochemie
Leitung: HR Mag. Dr. Gerhard Hobiger

Berechnungen aus den Analysenwerten

Äquivalentanteile

Kationen

	Messwert		
Ion	mg/l	meq/l	eq%
Ca^{2+}	9.25	0.46	9.33
Mg^{2+}	1.38	0.11	2.29
Na^{+}	99.61	4.33	87.56
K^{+}	1.30	0.03	0.67
Sr^{2+}	0.15	0.00	0.07
Ba^{2+}	0.013	0.00	0.0
Li^{+}	0.022	0.00	0.06
Rb^{+}	0.002	0.00	0.00
Cs^{+}	< 0,0001	0.00	0.00
NH_4^{+}	n.b.	n.b.	n.b.
Fe^{2+}	0.013	0.00	0.0
Mn^{2+}	0.0058	0.00	0.0
Σ	111.74	4.9	100.0

Anionen

	Messwert		
Ion	mg/l	meq/l	eq%
HCO_3^{-}	285.36	4.68	93.7
Cl^{-}	7.91	0.22	4.5
SO_4^{2-}	3.65	0.08	1.5
NO_3^{-}	n.b.	n.b.	n.b.
NO_2^{-}	n.b.	n.b.	n.b.
o-PO_4^{3-}	n.b.	n.b.	n.b.
S^{2-}	n.b.	n.b.	n.b.
F^{-}	0.25	0.01	0.3
Σ	297.16	5.0	100.0

Härten

Gesamthärte (° dH)	1.6
Carbonathärte(° dH)	1.6
Nichtcarbonathärte (°dH)	0.0
Erdalkalien (mmol/l)	5.8

Berechnung des CO_2

lg(pCO_2)	-2.92
freies CO_2 (mg/l)	2.09
freies CO_2 (mmol/l)	0.0475

Berechneter Ammoniakgehalt

NH_3 (mg/l)	n.b.

Ges. Ionengehalt	**409 mg/l**	**9.6 mmol/l**

Ionenbilanz

Σ Kationen (meq/l)	4.95	*-0.8 %*
Σ Anionen (meq/l)	4.99	

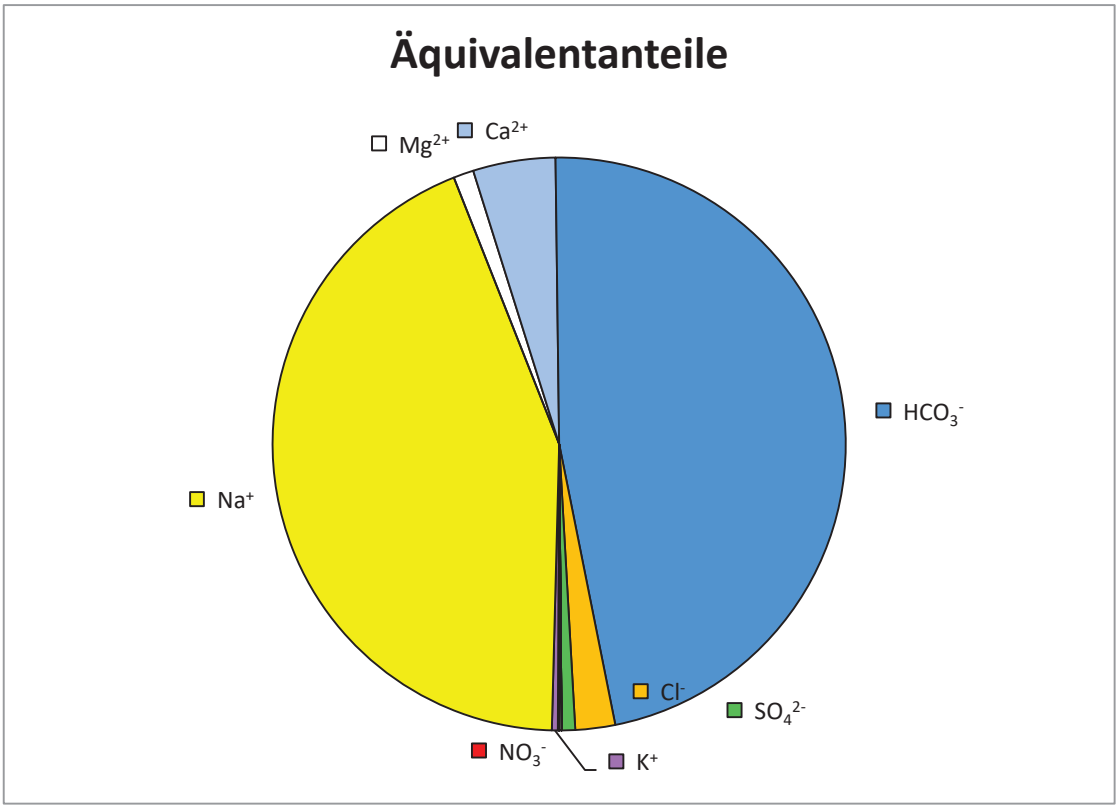

Wasseranalyse

Geologische Bundesanstalt
FA Geochemie
Leitung: HR Mag. Dr. Gerhard Hobiger

Probenahmepunkt:		**8**			
Koordinaten	**M** n.b.	**RW:** E13° 32.051'	**HW:** N48° 26.034'	**GOK (m ü. A.)**	n.b.
Bezeichnung:	**8**		**Geochemie-Nr.:**	**GCH-2017-071-001**	
Probenahmetiefe:	**197**	**Probenehmer:**	**Be/Pö**		
Probenahmedatum und Uhrzeit:		**12.10.2017 10:15**	**Eingangsdatum:**	**16.10.2017**	

Feldparameter

		QZV *	MAP **	IP ***			
el. LF (µS/cm) (Gel.)	**378**	2250		2500	**Schüttung (l/s)**		**n.b.**
el. LF (µS/cm) (Labor)	n.b.				**Redoxpotenzial (mV)**		**24**
					Temperatur (°C)		**13.8**
pH (Gel.)	**7.57**			6,5 - 9,5	**Sauerstoff (O_2)**	**mg/l**	**0.17**
pH (Labor)	n.b.					**(%)**	**1.7**

Kationen (mg/l)

Ion	Messwert	QZV *	MAP **	IP ***
Calcium (Ca^{2+})	**53.9**			
Magnesium (Mg^{2+})	**16.7**			
Natrium (Na^{+})	**4.8**			200
Kalium (K^{+})	**1.1**			
Strontium (Sr^{2+})	**0.3098**			
Barium (Ba^{2+})	**0.0262**			
Lithium (Li^{+})	**0.0161**			
Rubidium (Rb^{+})	**0.0015**			
Cäsium (Cs^{+})	**< 0,0001**			
Ammonium (NH_4^{+})	**n.b.**	0.45		0.5
Eisen (Fe^{2+})	**0.019**			0.2
Mangan (Mn^{2+})	**0.0055**			0.05
Σ	**76.9**			

Anionen (mg/l)

Ion	Messwert	QZV *	MAP **	IP ***
Hydrogencarbonat (HCO_3^{-})	**241.01**			
Chlorid (Cl^{-})	**0.8**	180		200
Sulfat (SO_4^{2-})	**15.6**	225		250
Nitrat (NO_3^{-})	**<0,5**	45	50	
Nitrit (NO_2^{-})	**n.b.**	0.09	0.1	
o- Phosphat (o-PO_4^{3-})	**n.b.**	0.3		
Sulfid (S^{2-})	**n.b.**			
Fluorid (F^{-})	**0.13**		1.5	
Σ	**257.6**			

Ges. Ionengehalt	**334 mg/l**	**Ionenbilanz**	
	6.4 mmol/l	***0.1***	**%**
Dichte	**n.b. g/cm3**		

Spezielle Parameter (mg/l)

Parameter	Messwert	QZV *	MAP **	IP ***
Kupfer (Cu)	**0.0011**	1.8	2	
Zink (Zn)	**< 0,0001**			
Blei (Pb)	**< 0,0001**	0.009	0.025	
Cadmium (Cd)	**< 0,0001**	0.0045	0.005	
Aluminium (Al)	**0.0014**			0.2
Arsen (As)	**0.0001**	0.009	0.01	
Antimon (Sb)	**n.b.**		0.005	
Chrom (Cr)	**< 0,0001**	0.045		
Nickel (Ni)	**0.0007**	0.018		
Quecksilber (Hg)	**n.b.**	0.0009	0.001	
Bor (B)	**n.b.**		1	
Uran (U)	**< 0,0001**		0.015	
Thorium (Th)	**n.b.**			
Cobalt (Co)	**< 0,0001**			
Molybdän (Mo)	**0.0011**			
Vanadium (V)	**< 0,0001**			
Selen (Se)	**n.b.**		0.01	
Tellur (Te)	**n.b.**			
Niob (Nb)	**n.b.**			
H_2SiO_3	**n.b.**			

Spezielle Parameter (mg/l)

Parameter	Messwert
Lanthan (La)	**n.b.**
Cer (Ce)	**n.b.**
Praseodym (Pr)	**n.b.**
Neodym (Nd)	**n.b.**
Samarium (Sm)	**n.b.**
Europium (Eu)	**n.b.**
Gadolimium (Gd)	**n.b.**
Terbium (Tb)	**n.b.**
Dysprosium (Dy)	**n.b.**
Holmium (Ho)	**n.b.**
Erbium (Er)	**n.b.**
Thulium (Tm)	**n.b.**
Ytterbium (Yb)	**n.b.**
Lutetium (Lu)	**n.b.**
Zinn (Sn)	**n.b.**
Thallium (Tl)	**n.b.**
Silber (Ag)	**n.b.**
Beryllium (Be)	**n.b.**
Bismut (Bi)	**n.b.**
Gallium (Ga)	**n.b.**

n.b. .. nicht bestimmt

* ... Qualitätszielverordnung Chemie Grundwasser QZV Chemie GW (BGBl. II 98/2010)

** ... Mindestanforderungsparameter aus der Trinkwasserverordnung - TWV (BGBl. II 304/2001)

*** ... Indikatorparameter aus der Trinkwasserverordnung - TWV (BGBl. II 304/2001)

Layout: G. Hobiger

Geologische Bundesanstalt
FA Geochemie
Leitung: HR Mag. Dr. Gerhard Hobiger

Berechnungen aus den Analysenwerten

Äquivalentanteile

Kationen

Ion	Messwert mg/l	meq/l	eq%
Ca^{2+}	53.88	2.69	62.37
Mg^{2+}	16.69	1.37	31.86
Na^{+}	4.84	0.21	4.89
K^{+}	1.07	0.03	0.63
Sr^{2+}	0.31	0.01	0.16
Ba^{2+}	0.026	0.00	0.0
Li^{+}	0.016	0.00	0.05
Rb^{+}	0.001	0.00	0.00
Cs^{+}	< 0,0001	0.00	0.00
NH_4^{+}	n.b.	n.b.	n.b.
Fe^{2+}	0.019	0.00	0.0
Mn^{2+}	0.0055	0.00	0.0
Σ	76.86	4.3	100.0

Anionen

Ion	Messwert mg/l	meq/l	eq%
HCO_3^{-}	241.01	3.95	91.8
Cl^{-}	0.81	0.02	0.5
SO_4^{2-}	15.65	0.33	7.6
NO_3^{-}	<0,5	0.00	0.0
NO_2^{-}	n.b.	n.b.	n.b.
$o\text{-}PO_4^{3-}$	n.b.	n.b.	n.b.
S^{2-}	n.b.	n.b.	n.b.
F^{-}	0.13	0.01	0.2
Σ	257.59	4.3	100.0

Härten

Gesamthärte (° dH)	11.4
Carbonathärte(° dH)	11.1
Nichtcarbonathärte (°dH)	0.3
Erdalkalien (mmol/l)	47.2

Berechnung des CO_2

$lg(pCO_2)$	-2.26
freies CO_2 (mg/l)	11.44
freies CO_2 (mmol/l)	0.2600

Berechneter Ammoniakgehalt

NH_3 (mg/l)	n.b.

Ges. Ionengehalt	334 mg/l	6.4 mmol/l

Ionenbilanz

Σ Kationen (meq/l)	4.31	*0.1 %*
Σ Anionen (meq/l)	4.31	

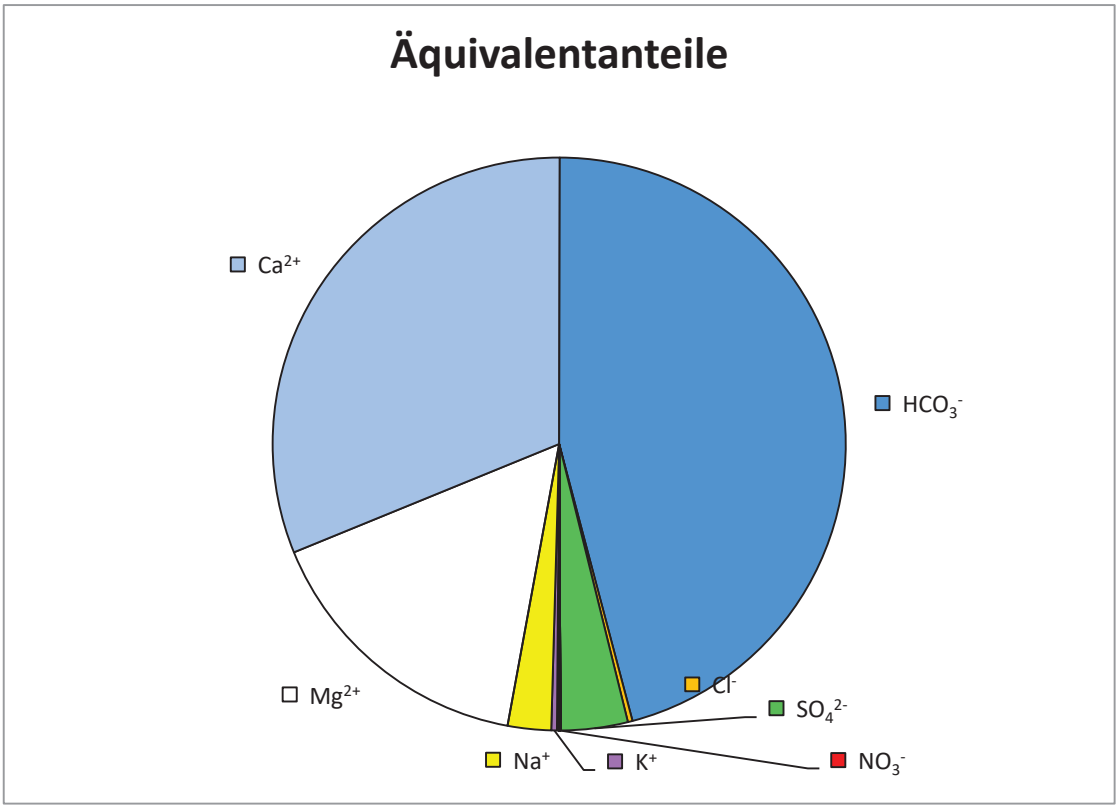

Wasseranalyse

Geologische Bundesanstalt
FA Geochemie
Leitung: HR Mag. Dr. Gerhard Hobiger

Probenahmepunkt:			9		
Koordinaten	**M** n.b.	**RW:** E13° 32.219'	**HW:** N48° 26.583'	**GOK (m ü. A.)**	n.b.
Bezeichnung:	9		**Geochemie-Nr.:**	GCH-2017-071-002	
Probenahmetiefe:	n.b.	**Probenehmer:**	Be/Pö		
Probenahmedatum und Uhrzeit:	12.10.2017 11:15		**Eingangsdatum:**	16.10.2017	

Feldparameter

		QZV *	MAP **	IP ***			
el. LF (µS/cm) (Gel.)	**534**	2250		2500	**Schüttung (l/s)**		**5.3**
el. LF (µS/cm) (Labor)	n.b.				**Redoxpotenzial (mV)**		**45**
					Temperatur (°C)		**10.8**
pH (Gel.)	**7.53**			6,5 - 9,5	**Sauerstoff (O_2)**	**mg/l**	**6.3**
pH (Labor)	n.b.					**(%)**	**59.2**

Kationen (mg/l)

Ion	Messwert	QZV *	MAP **	IP ***
Calcium (Ca^{2+})	**87.5**			
Magnesium (Mg^{2+})	**19.8**			
Natrium (Na^{+})	**3.1**			200
Kalium (K^{+})	**1.3**			
Strontium (Sr^{2+})	**0.3268**			
Barium (Ba^{2+})	**0.0182**			
Lithium (Li^{+})	**0.0189**			
Rubidium (Rb^{+})	**0.0015**			
Cäsium (Cs^{+})	**< 0,0001**			
Ammonium (NH_4^{+})	**n.b.**	0.45		0.5
Eisen (Fe^{2+})	**0.112**			0.2
Mangan (Mn^{2+})	**0.0266**			0.05
Σ	**112.2**			

Anionen (mg/l)

Ion	Messwert	QZV *	MAP **	IP ***
Hydrogencarbonat (HCO_3^{-})	**341.69**			
Chlorid (Cl^{-})	**0.9**	180		200
Sulfat (SO_4^{2-})	**24.2**	225		250
Nitrat (NO_3^{-})	**<0,5**	45	50	
Nitrit (NO_2^{-})	**n.b.**	0.09	0.1	
o- Phosphat (o-PO_4^{3-})	**n.b.**	0.3		
Sulfid (S^{2-})	**n.b.**			
Fluorid (F^{-})	**0.23**		1.5	
Σ	**367.0**			

Ges. Ionengehalt	**479 mg/l**	**Ionenbilanz**	
	9.1 mmol/l	***0.6***	**%**
Dichte	**n.b. g/cm3**		

Spezielle Parameter (mg/l)

Parameter	Messwert	QZV *	MAP **	IP ***
Kupfer (Cu)	**0.0005**	1.8	2	
Zink (Zn)	**< 0,0001**			
Blei (Pb)	**< 0,0001**	0.009	0.025	
Cadmium (Cd)	**< 0,0001**	0.0045	0.005	
Aluminium (Al)	**0.0015**			0.2
Arsen (As)	**0.0002**	0.009	0.01	
Antimon (Sb)	**n.b.**		0.005	
Chrom (Cr)	**< 0,0001**	0.045		
Nickel (Ni)	**< 0,0001**	0.018		
Quecksilber (Hg)	**n.b.**	0.0009	0.001	
Bor (B)	**n.b.**		1	
Uran (U)	**< 0,0001**		0.015	
Thorium (Th)	**n.b.**			
Cobalt (Co)	**< 0,0001**			
Molybdän (Mo)	**0.0006**			
Vanadium (V)	**< 0,0001**			
Selen (Se)	**n.b.**		0.01	
Tellur (Te)	**n.b.**			
Niob (Nb)	**n.b.**			
H_2SiO_3	**n.b.**			

Spezielle Parameter (mg/l)

Parameter	Messwert
Lanthan (La)	**n.b.**
Cer (Ce)	**n.b.**
Praseodym (Pr)	**n.b.**
Neodym (Nd)	**n.b.**
Samarium (Sm)	**n.b.**
Europium (Eu)	**n.b.**
Gadolimium (Gd)	**n.b.**
Terbium (Tb)	**n.b.**
Dysprosium (Dy)	**n.b.**
Holmium (Ho)	**n.b.**
Erbium (Er)	**n.b.**
Thulium (Tm)	**n.b.**
Ytterbium (Yb)	**n.b.**
Lutetium (Lu)	**n.b.**
Zinn (Sn)	**n.b.**
Thallium (Tl)	**n.b.**
Silber (Ag)	**n.b.**
Beryllium (Be)	**n.b.**
Bismut (Bi)	**n.b.**
Gallium (Ga)	**n.b.**

n.b. .. nicht bestimmt

* ... Qualitätszielverordnung Chemie Grundwasser QZV Chemie GW (BGBl. II 98/2010)

** ... Mindestanforderungsparameter aus der Trinkwasserverordnung - TWV (BGBl. II 304/2001)

*** ... Indikatorparameter aus der Trinkwasserverordnung - TWV (BGBl. II 304/2001)

Layout: G. Hobiger

Geologische Bundesanstalt
FA Geochemie
Leitung: HR Mag. Dr. Gerhard Hobiger

Berechnungen aus den Analysenwerten

Äquivalentanteile

Kationen

Ion	Messwert mg/l	meq/l	eq%
Ca^{2+}	87.48	4.37	70.66
Mg^{2+}	19.79	1.63	26.36
Na^{+}	3.11	0.14	2.19
K^{+}	1.29	0.03	0.54
Sr^{2+}	0.33	0.01	0.12
Ba^{2+}	0.018	0.00	0.0
Li^{+}	0.019	0.00	0.04
Rb^{+}	0.001	0.00	0.00
Cs^{+}	< 0,0001	0.00	0.00
NH_4^{+}	n.b.	n.b.	n.b.
Fe^{2+}	0.112	0.00	0.1
Mn^{2+}	0.0266	0.00	0.0
Σ	112.18	6.2	100.0

Anionen

Ion	Messwert mg/l	meq/l	eq%
HCO_3^{-}	341.69	5.60	91.2
Cl^{-}	0.92	0.03	0.4
SO_4^{2-}	24.15	0.50	8.2
NO_3^{-}	<0,5	0.00	0.0
NO_2^{-}	n.b.	n.b.	n.b.
$o\text{-}PO_4^{3-}$	n.b.	n.b.	n.b.
S^{2-}	n.b.	n.b.	n.b.
F^{-}	0.23	0.01	0.2
Σ	366.99	6.1	100.0

Härten

Gesamthärte (° dH)	16.8
Carbonathärte(° dH)	15.7
Nichtcarbonathärte (°dH)	1.1
Erdalkalien (mmol/l)	48.6

Berechnung des CO_2

lg(pCO_2)	-2.09
freies CO_2 (mg/l)	18.58
freies CO_2 (mmol/l)	0.4223

Berechneter Ammoniakgehalt

NH_3 (mg/l)	n.b.

Ges. Ionengehalt	479 mg/l	9.1 mmol/l

Ionenbilanz

Σ Kationen (meq/l)	6.18	*0.6 %*
Σ Anionen (meq/l)	6.14	

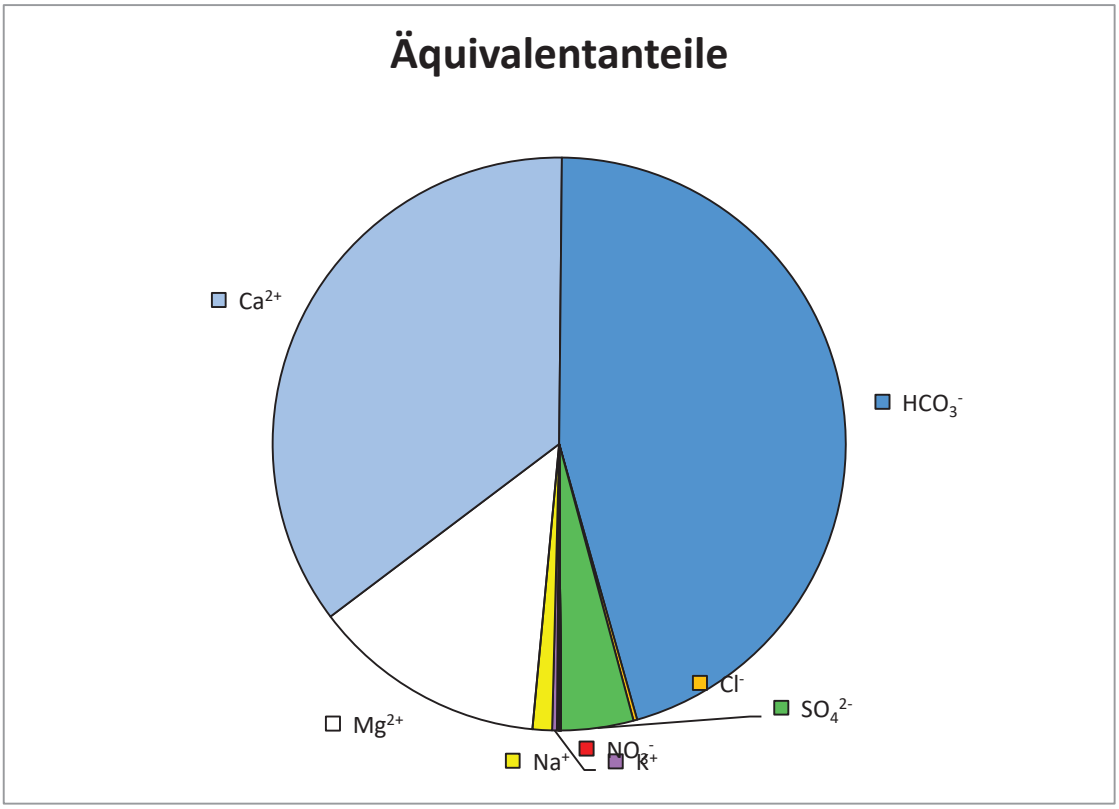

Wasseranalyse

Geologische Bundesanstalt
FA Geochemie
Leitung: HR Mag. Dr. Gerhard Hobiger

Probenahmepunkt:		**10**		
Koordinaten	**M** n.b.	**RW:** E13° 41.279'	**HW:** N48° 21.228'	**GOK (m ü. A.)** n.b.
Bezeichnung:	**10**		**Geochemie-Nr.:**	**GCH-2017-071-003**
Probenahmetiefe:	**n.b.**	**Probenehmer:**	**Be/Pö**	
Probenahmedatum und Uhrzeit:		**12.10.2017 14:00**	**Eingangsdatum:**	**16.10.2017**

Feldparameter

		QZV *	MAP **	IP ***			
el. LF (µS/cm) (Gel.)	**322**	2250		2500	**Schüttung (l/s)**		**n.b.**
el. LF (µS/cm) (Labor)	n.b.				**Redoxpotenzial (mV)**		**-124**
					Temperatur (°C)		**10.9**
pH (Gel.)	**7.75**			6,5 - 9,5	**Sauerstoff (O_2)**	**mg/l**	**0.01**
pH (Labor)	n.b.					**(%)**	**0.1**

Kationen (mg/l)

Ion	Messwert	QZV *	MAP **	IP ***
Calcium (Ca^{2+})	**47.3**			
Magnesium (Mg^{2+})	**11.9**			
Natrium (Na^{+})	**4.0**			200
Kalium (K^{+})	**1.0**			
Strontium (Sr^{2+})	**0.1093**			
Barium (Ba^{2+})	**0.0091**			
Lithium (Li^{+})	**0.0071**			
Rubidium (Rb^{+})	**0.0011**			
Cäsium (Cs^{+})	**< 0,0001**			
Ammonium (NH_4^{+})	**n.b.**	0.45		0.5
Eisen (Fe^{2+})	**0.312**			0.2
Mangan (Mn^{2+})	**0.0384**			0.05
Σ	**64.7**			

Anionen (mg/l)

Ion	Messwert	QZV *	MAP **	IP ***
Hydrogencarbonat (HCO_3^{-})	**213.56**			
Chlorid (Cl^{-})	**0.7**	180		200
Sulfat (SO_4^{2-})	**6.3**	225		250
Nitrat (NO_3^{-})	**<0,5**	45	50	
Nitrit (NO_2^{-})	**n.b.**	0.09	0.1	
o- Phosphat (o-PO_4^{3-})	**n.b.**	0.3		
Sulfid (S^{2-})	**n.b.**			
Fluorid (F^{-})	**0.15**		1.5	
Σ	**220.7**			

Ges. Ionengehalt	**285 mg/l**	**Ionenbilanz**	
	5.5 mmol/l	***-2.8***	**%**
Dichte	**n.b. g/cm3**		

Spezielle Parameter (mg/l)

Parameter	Messwert	QZV *	MAP **	IP ***
Kupfer (Cu)	**0.0013**	1.8	2	
Zink (Zn)	**< 0,0001**			
Blei (Pb)	**< 0,0001**	0.009	0.025	
Cadmium (Cd)	**< 0,0001**	0.0045	0.005	
Aluminium (Al)	**0.0022**			0.2
Arsen (As)	**0.0015**	0.009	0.01	
Antimon (Sb)	**n.b.**		0.005	
Chrom (Cr)	**< 0,0001**	0.045		
Nickel (Ni)	**0.0003**	0.018		
Quecksilber (Hg)	**n.b.**	0.0009	0.001	
Bor (B)	**n.b.**		1	
Uran (U)	**< 0,0001**		0.015	
Thorium (Th)	**n.b.**			
Cobalt (Co)	**< 0,0001**			
Molybdän (Mo)	**0.0004**			
Vanadium (V)	**< 0,0001**			
Selen (Se)	**n.b.**		0.01	
Tellur (Te)	**n.b.**			
Niob (Nb)	**n.b.**			
H_2SiO_3	**n.b.**			

Spezielle Parameter (mg/l)

Parameter	Messwert
Lanthan (La)	**n.b.**
Cer (Ce)	**n.b.**
Praseodym (Pr)	**n.b.**
Neodym (Nd)	**n.b.**
Samarium (Sm)	**n.b.**
Europium (Eu)	**n.b.**
Gadolimium (Gd)	**n.b.**
Terbium (Tb)	**n.b.**
Dysprosium (Dy)	**n.b.**
Holmium (Ho)	**n.b.**
Erbium (Er)	**n.b.**
Thulium (Tm)	**n.b.**
Ytterbium (Yb)	**n.b.**
Lutetium (Lu)	**n.b.**
Zinn (Sn)	**n.b.**
Thallium (Tl)	**n.b.**
Silber (Ag)	**n.b.**
Beryllium (Be)	**n.b.**
Bismut (Bi)	**n.b.**
Gallium (Ga)	**n.b.**

n.b. .. nicht bestimmt

* ... Qualitätszielverordnung Chemie Grundwasser QZV Chemie GW (BGBl. II 98/2010)

** ... Mindestanforderungsparameter aus der Trinkwasserverordnung - TWV (BGBl. II 304/2001)

*** ... Indikatorparameter aus der Trinkwasserverordnung - TWV (BGBl. II 304/2001)

Layout: G. Hobiger

Geologische Bundesanstalt
FA Geochemie
Leitung: HR Mag. Dr. Gerhard Hobiger

Berechnungen aus den Analysenwerten

Äquivalentanteile

Kationen				Anionen			
	Messwert				Messwert		
Ion	mg/l	meq/l	eq%	Ion	mg/l	meq/l	eq%
Ca^{2+}	47.32	2.36	66.40	HCO_3^-	213.56	3.50	95.7
Mg^{2+}	11.88	0.98	27.48	Cl^-	0.70	0.02	0.5
Na^+	4.02	0.18	4.92	SO_4^{2-}	6.31	0.13	3.6
K^+	1.03	0.03	0.74	NO_3^-	<0,5	0.00	0.0
Sr^{2+}	0.11	0.00	0.07	NO_2^-	n.b.	n.b.	n.b.
Ba^{2+}	0.009	0.00	0.0	o-PO_4^{3-}	n.b.	n.b.	n.b.
Li^+	0.007	0.00	0.03	S^{2-}	n.b.	n.b.	n.b.
Rb^+	0.001	0.00	0.00	F^-	0.15	0.01	0.2
Cs^+	< 0,0001	0.00	0.00	Σ	220.71	3.7	100.0
NH_4^+	n.b.	n.b.	n.b.				
Fe^{2+}	0.312	0.01	0.3				
Mn^{2+}	0.0384	0.00	0.0				
Σ	64.72	3.6	100.0				

Härten	
Gesamthärte (° dH)	9.4
Carbonathärte(° dH)	9.4
Nichtcarbonathärte (°dH)	0.0
Erdalkalien (mmol/l)	47.0

Berechnung des CO_2	
lg(pCO_2)	-2.51
freies CO_2 (mg/l)	7.17
freies CO_2 (mmol/l)	0.1630

Berechneter Ammoniakgehalt	
NH_3 (mg/l)	n.b.

Ges. Ionengehalt	285 mg/l	5.5 mmol/l

Ionenbilanz		
Σ Kationen (meq/l)	3.56	*-2.8 %*
Σ Anionen (meq/l)	3.66	

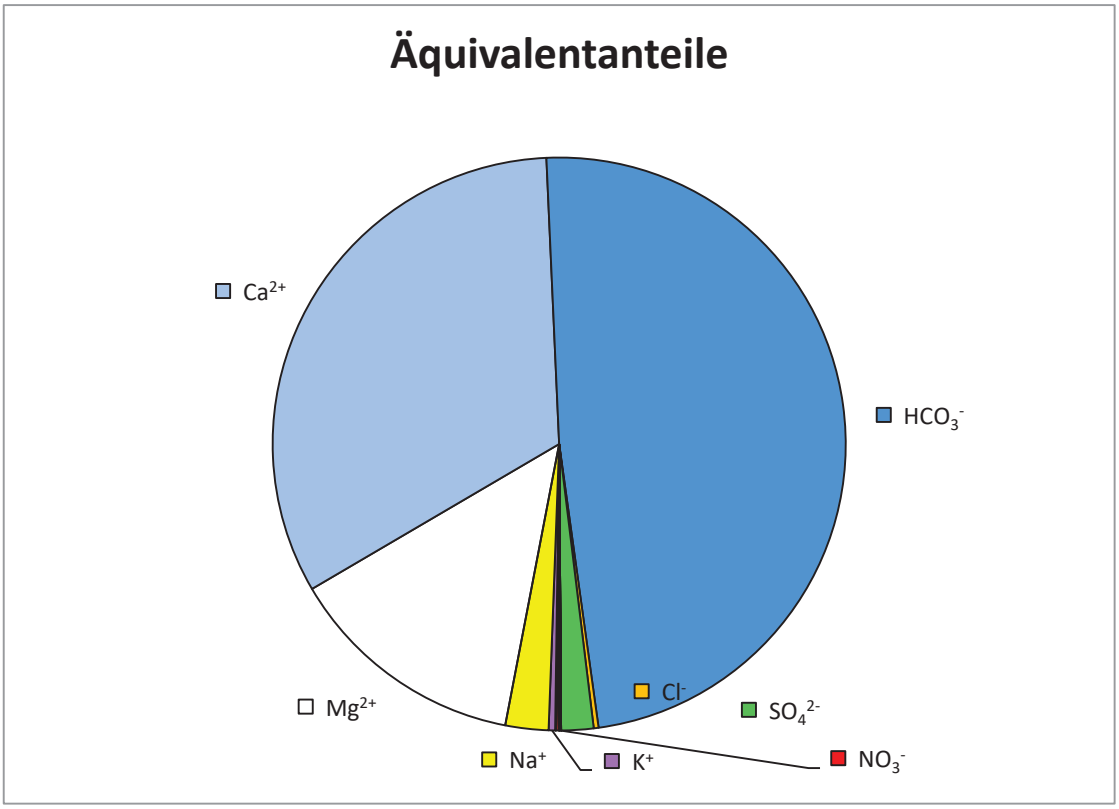

Wasseranalyse

Geologische Bundesanstalt
FA Geochemie
Leitung: HR Mag. Dr. Gerhard Hobiger

Probenahmepunkt:		**11**			
Koordinaten	**M** n.b.	**RW:** E13° 40.379'	**HW:** N48° 21.426'	**GOK (m ü. A.)**	n.b.
Bezeichnung:	**11**		**Geochemie-Nr.:**	**GCH-2017-071-004**	
Probenahmetiefe:	n.b.	**Probenehmer:**	**Be/Pö**		
Probenahmedatum und Uhrzeit:		**12.10.2017 14:45**	**Eingangsdatum:**	**16.10.2017**	

Feldparameter

		QZV *	MAP **	IP ***			
el. LF (µS/cm) (Gel.)	**317**	2250		2500	**Schüttung (l/s)**		**n.b.**
el. LF (µS/cm) (Labor)	n.b.				**Redoxpotenzial (mV)**		**-85**
					Temperatur (°C)		**11.8**
pH (Gel.)	**7.68**			6,5 - 9,5	**Sauerstoff (O_2)**	**mg/l**	**0.02**
pH (Labor)	n.b.					**(%)**	**0.2**

Kationen (mg/l)

Ion	Messwert	QZV *	MAP **	IP ***
Calcium (Ca^{2+})	**46.4**			
Magnesium (Mg^{2+})	**10.0**			
Natrium (Na^{+})	**4.0**			200
Kalium (K^{+})	**0.7**			
Strontium (Sr^{2+})	**0.1240**			
Barium (Ba^{2+})	**0.0070**			
Lithium (Li^{+})	**0.0055**			
Rubidium (Rb^{+})	**0.0008**			
Cäsium (Cs^{+})	**< 0,0001**			
Ammonium (NH_4^{+})	**n.b.**	0.45		0.5
Eisen (Fe^{2+})	**0.425**			0.2
Mangan (Mn^{2+})	**0.0490**			0.05
Σ	**61.7**			

Anionen (mg/l)

Ion	Messwert	QZV *	MAP **	IP ***
Hydrogencarbonat (HCO_3^{-})	**207.45**			
Chlorid (Cl^{-})	**0.8**	180		200
Sulfat (SO_4^{2-})	**6.4**	225		250
Nitrat (NO_3^{-})	**<0,5**	45	50	
Nitrit (NO_2^{-})	**n.b.**	0.09	0.1	
o- Phosphat (o-PO_4^{3-})	**n.b.**	0.3		
Sulfid (S^{2-})	**n.b.**			
Fluorid (F^{-})	**0.14**		1.5	
Σ	**214.8**			

Ges. Ionengehalt	**277 mg/l**	**Ionenbilanz**	
	5.3 mmol/l	***-6.0***	**%**
Dichte	**n.b. g/cm3**		

Spezielle Parameter (mg/l)

Parameter	Messwert	QZV *	MAP **	IP ***
Kupfer (Cu)	**< 0,0001**	1.8	2	
Zink (Zn)	**< 0,0001**			
Blei (Pb)	**< 0,0001**	0.009	0.025	
Cadmium (Cd)	**< 0,0001**	0.0045	0.005	
Aluminium (Al)	**0.0010**			0.2
Arsen (As)	**0.0000**	0.009	0.01	
Antimon (Sb)	**n.b.**		0.005	
Chrom (Cr)	**< 0,0001**	0.045		
Nickel (Ni)	**< 0,0001**	0.018		
Quecksilber (Hg)	**n.b.**	0.0009	0.001	
Bor (B)	**n.b.**		1	
Uran (U)	**< 0,0001**		0.015	
Thorium (Th)	**n.b.**			
Cobalt (Co)	**< 0,0001**			
Molybdän (Mo)	**0.0004**			
Vanadium (V)	**< 0,0001**			
Selen (Se)	**n.b.**		0.01	
Tellur (Te)	**n.b.**			
Niob (Nb)	**n.b.**			
H_2SiO_3	**n.b.**			

Spezielle Parameter (mg/l)

Parameter	Messwert
Lanthan (La)	**n.b.**
Cer (Ce)	**n.b.**
Praseodym (Pr)	**n.b.**
Neodym (Nd)	**n.b.**
Samarium (Sm)	**n.b.**
Europium (Eu)	**n.b.**
Gadolimium (Gd)	**n.b.**
Terbium (Tb)	**n.b.**
Dysprosium (Dy)	**n.b.**
Holmium (Ho)	**n.b.**
Erbium (Er)	**n.b.**
Thulium (Tm)	**n.b.**
Ytterbium (Yb)	**n.b.**
Lutetium (Lu)	**n.b.**
Zinn (Sn)	**n.b.**
Thallium (Tl)	**n.b.**
Silber (Ag)	**n.b.**
Beryllium (Be)	**n.b.**
Bismut (Bi)	**n.b.**
Gallium (Ga)	**n.b.**

n.b. .. nicht bestimmt

* ... Qualitätszielverordnung Chemie Grundwasser QZV Chemie GW (BGBl. II 98/2010)

** ... Mindestanforderungsparameter aus der Trinkwasserverordnung - TWV (BGBl. II 304/2001)

*** ... Indikatorparameter aus der Trinkwasserverordnung - TWV (BGBl. II 304/2001)

Layout: G. Hobiger

Geologische Bundesanstalt
FA Geochemie
Leitung: HR Mag. Dr. Gerhard Hobiger

Berechnungen aus den Analysenwerten

Äquivalentanteile

Kationen

Ion	Messwert mg/l	meq/l	eq%
Ca^{2+}	46.39	2.31	69.02
Mg^{2+}	10.05	0.83	24.65
Na^{+}	3.98	0.17	5.16
K^{+}	0.72	0.02	0.55
Sr^{2+}	0.12	0.00	0.08
Ba^{2+}	0.007	0.00	0.0
Li^{+}	0.006	0.00	0.02
Rb^{+}	0.001	0.00	0.00
Cs^{+}	< 0,0001	0.00	0.00
NH_4^{+}	n.b.	n.b.	n.b.
Fe^{2+}	0.425	0.02	0.5
Mn^{2+}	0.0490	0.00	0.1
Σ	61.75	3.4	100.0

Anionen

Ion	Messwert mg/l	meq/l	eq%
HCO_3^{-}	207.45	3.40	95.4
Cl^{-}	0.76	0.02	0.6
SO_4^{2-}	6.42	0.13	3.8
NO_3^{-}	<0,5	0.00	0.0
NO_2^{-}	n.b.	n.b.	n.b.
$o\text{-}PO_4^{3-}$	n.b.	n.b.	n.b.
S^{2-}	n.b.	n.b.	n.b.
F^{-}	0.14	0.01	0.2
Σ	214.77	3.6	100.0

Härten

Gesamthärte (° dH)	8.8
Carbonathärte(° dH)	8.8
Nichtcarbonathärte (°dH)	0.0
Erdalkalien (mmol/l)	46.9

Berechnung des CO_2

lg(pCO_2)	-2.44
freies CO_2 (mg/l)	8.05
freies CO_2 (mmol/l)	0.1829

Berechneter Ammoniakgehalt

NH_3 (mg/l)	n.b.

Ges. Ionengehalt	277 mg/l	5.3 mmol/l

Ionenbilanz

Σ Kationen (meq/l)	3.35	*-6.0 %*
Σ Anionen (meq/l)	3.56	

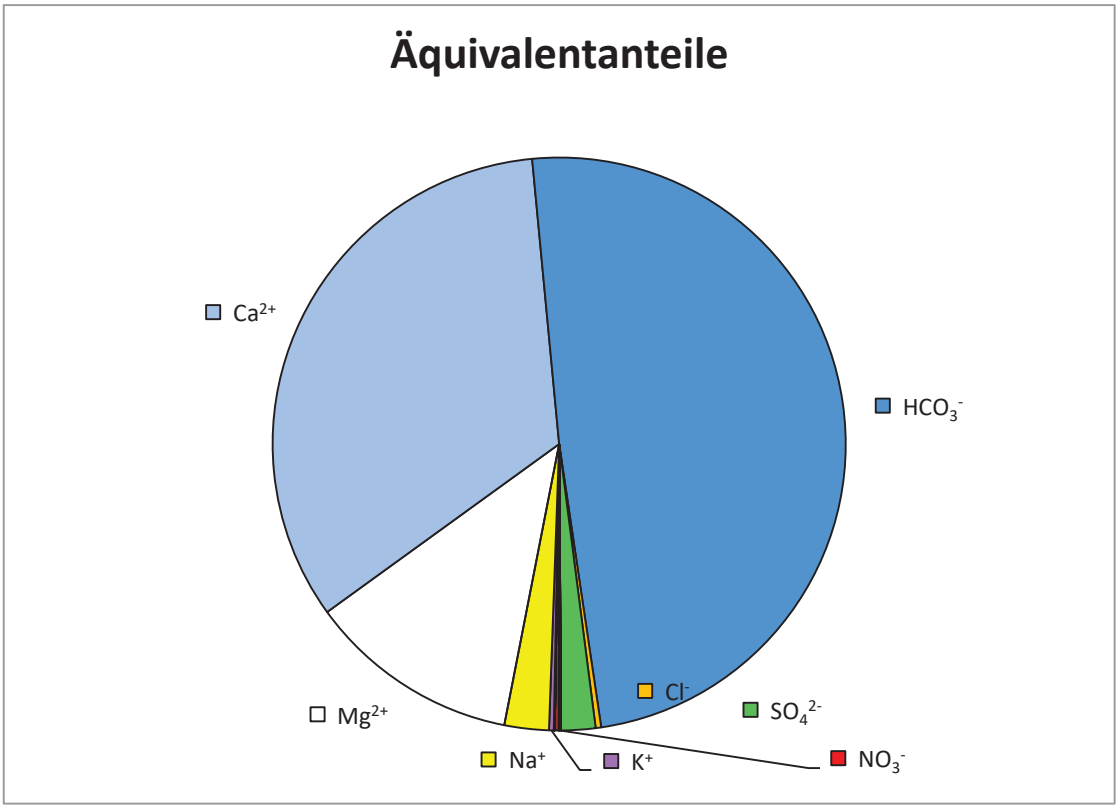

Wasseranalyse

Geologische Bundesanstalt
FA Geochemie
Leitung: HR Mag. Dr. Gerhard Hobiger

Probenahmepunkt:		**12**			
Koordinaten	**M** n.b.	**RW:** E13° 30.211'	**HW:** N48° 28.077'	**GOK (m ü. A.)**	n.b.
Bezeichnung:	**12**		**Geochemie-Nr.:**	**GCH-2017-071-005**	
Probenahmetiefe:	n.b.	**Probenehmer:**	**Be/Pö**		
Probenahmedatum und Uhrzeit:		**12.10.2017 16:00**	**Eingangsdatum:**	**16.10.2017**	

Feldparameter

		QZV *	MAP **	IP ***			
el. LF (µS/cm) (Gel.)	**468**	2250		2500	**Schüttung (l/s)**		**n.b.**
el. LF (µS/cm) (Labor)	n.b.				**Redoxpotenzial (mV)**		**-98**
					Temperatur (°C)		**10.8**
pH (Gel.)	**7.56**			6,5 - 9,5	**Sauerstoff (O_2)**	**mg/l**	**0.16**
pH (Labor)	n.b.					**(%)**	**1.7**

Kationen (mg/l)

Ion	Messwert	QZV *	MAP **	IP ***
Calcium (Ca^{2+})	**74.9**			
Magnesium (Mg^{2+})	**13.5**			
Natrium (Na^{+})	**3.1**			200
Kalium (K^{+})	**0.8**			
Strontium (Sr^{2+})	**0.2224**			
Barium (Ba^{2+})	**0.0087**			
Lithium (Li^{+})	**0.0102**			
Rubidium (Rb^{+})	**0.0017**			
Cäsium (Cs^{+})	**< 0,0001**			
Ammonium (NH_4^{+})	**n.b.**	0.45		0.5
Eisen (Fe^{2+})	**0.029**			0.2
Mangan (Mn^{2+})	**0.0040**			0.05
Σ	**92.5**			

Anionen (mg/l)

Ion	Messwert	QZV *	MAP **	IP ***
Hydrogencarbonat (HCO_3^{-})	**247.11**			
Chlorid (Cl^{-})	**5.4**	180		200
Sulfat (SO_4^{2-})	**45.7**	225		250
Nitrat (NO_3^{-})	**<0,5**	45	50	
Nitrit (NO_2^{-})	**n.b.**	0.09	0.1	
o- Phosphat (o-PO_4^{3-})	**n.b.**	0.3		
Sulfid (S^{2-})	**n.b.**			
Fluorid (F^{-})	**0.11**		1.5	
Σ	**298.3**			

Ges. Ionengehalt	**391 mg/l**	**Ionenbilanz**	
	7.3 mmol/l	***-3.0***	**%**
Dichte	**n.b. g/cm3**		

Spezielle Parameter (mg/l)

Parameter	Messwert	QZV *	MAP **	IP ***
Kupfer (Cu)	**0.0003**	1.8	2	
Zink (Zn)	**< 0,0001**			
Blei (Pb)	**< 0,0001**	0.009	0.025	
Cadmium (Cd)	**< 0,0001**	0.0045	0.005	
Aluminium (Al)	**0.0011**			0.2
Arsen (As)	**0.0005**	0.009	0.01	
Antimon (Sb)	**n.b.**		0.005	
Chrom (Cr)	**< 0,0001**	0.045		
Nickel (Ni)	**< 0,0001**	0.018		
Quecksilber (Hg)	**n.b.**	0.0009	0.001	
Bor (B)	**n.b.**		1	
Uran (U)	**< 0,0001**		0.015	
Thorium (Th)	**n.b.**			
Cobalt (Co)	**< 0,0001**			
Molybdän (Mo)	**0.0010**			
Vanadium (V)	**< 0,0001**			
Selen (Se)	**n.b.**		0.01	
Tellur (Te)	**n.b.**			
Niob (Nb)	**n.b.**			
H_2SiO_3	**n.b.**			

Spezielle Parameter (mg/l)

Parameter	Messwert
Lanthan (La)	**n.b.**
Cer (Ce)	**n.b.**
Praseodym (Pr)	**n.b.**
Neodym (Nd)	**n.b.**
Samarium (Sm)	**n.b.**
Europium (Eu)	**n.b.**
Gadolimium (Gd)	**n.b.**
Terbium (Tb)	**n.b.**
Dysprosium (Dy)	**n.b.**
Holmium (Ho)	**n.b.**
Erbium (Er)	**n.b.**
Thulium (Tm)	**n.b.**
Ytterbium (Yb)	**n.b.**
Lutetium (Lu)	**n.b.**
Zinn (Sn)	**n.b.**
Thallium (Tl)	**n.b.**
Silber (Ag)	**n.b.**
Beryllium (Be)	**n.b.**
Bismut (Bi)	**n.b.**
Gallium (Ga)	**n.b.**

n.b. .. nicht bestimmt

* ... Qualitätszielverordnung Chemie Grundwasser QZV Chemie GW (BGBl. II 98/2010)

** ... Mindestanforderungsparameter aus der Trinkwasserverordnung - TWV (BGBl. II 304/2001)

*** ... Indikatorparameter aus der Trinkwasserverordnung - TWV (BGBl. II 304/2001)

Layout: G. Hobiger

Geologische Bundesanstalt
FA Geochemie
Leitung: HR Mag. Dr. Gerhard Hobiger

Berechnungen aus den Analysenwerten

Äquivalentanteile

Kationen				Anionen			
	Messwert				Messwert		
Ion	mg/l	meq/l	eq%	Ion	mg/l	meq/l	eq%
Ca^{2+}	74.86	3.74	74.62	HCO_3^-	247.11	4.05	78.5
Mg^{2+}	13.47	1.11	22.14	Cl^-	5.38	0.15	2.9
Na^+	3.11	0.14	2.70	SO_4^{2-}	45.69	0.95	18.4
K^+	0.75	0.02	0.38	NO_3^-	<0,5	0.00	0.0
Sr^{2+}	0.22	0.01	0.10	NO_2^-	n.b.	n.b.	n.b.
Ba^{2+}	0.009	0.00	0.0	o-PO_4^{3-}	n.b.	n.b.	n.b.
Li^+	0.010	0.00	0.03	S^{2-}	n.b.	n.b.	n.b.
Rb^+	0.002	0.00	0.00	F^-	0.11	0.01	0.1
Cs^+	< 0,0001	0.00	0.00	Σ	298.29	5.2	100.0
NH_4^+	n.b.	n.b.	n.b.				
Fe^{2+}	0.029	0.00	0.0				
Mn^{2+}	0.0040	0.00	0.0				
Σ	92.47	5.0	100.0				

Härten	
Gesamthärte (° dH)	13.6
Carbonathärte(° dH)	11.4
Nichtcarbonathärte (°dH)	2.2
Erdalkalien (mmol/l)	48.4

Berechnung des CO_2	
lg(pCO_2)	-2.26
freies CO_2 (mg/l)	12.65
freies CO_2 (mmol/l)	0.2875

Berechneter Ammoniakgehalt	
NH_3 (mg/l)	n.b.

Ges. Ionengehalt	391 mg/l	7.3 mmol/l

Ionenbilanz		
Σ Kationen (meq/l)	5.01	*-3.0 %*
Σ Anionen (meq/l)	5.16	

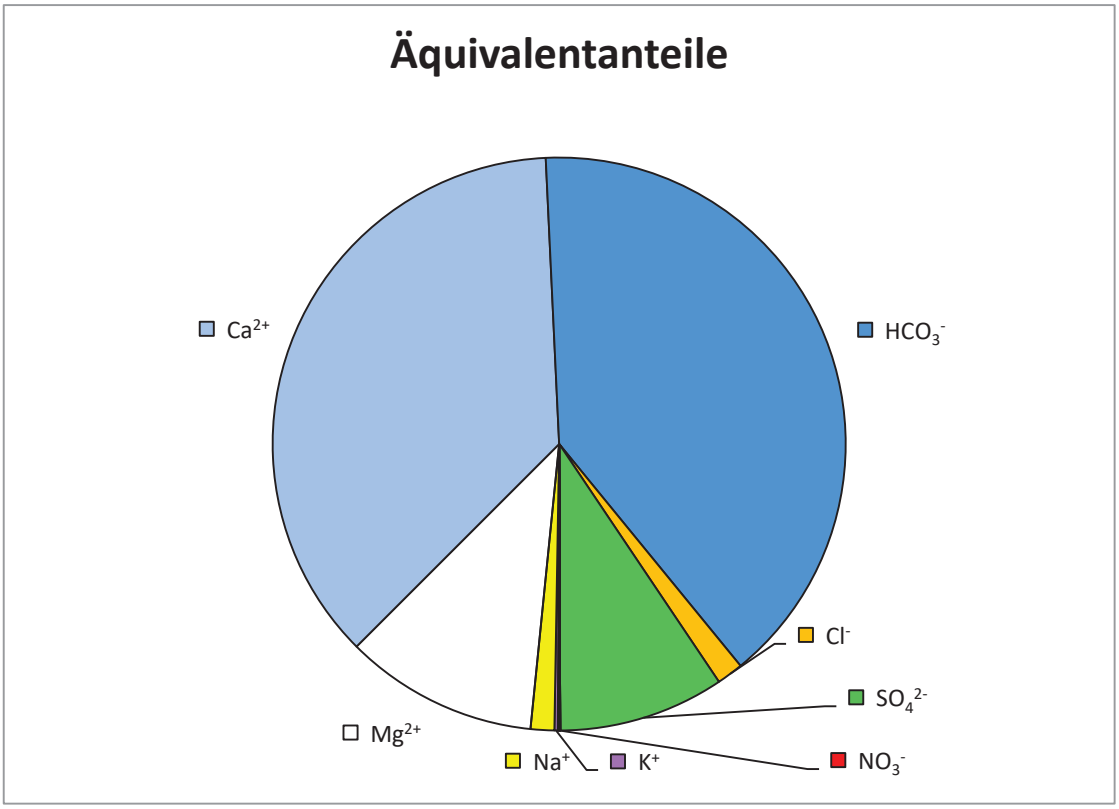

Wasseranalyse

Geologische Bundesanstalt
FA Geochemie
Leitung: HR Mag. Dr. Gerhard Hobiger

Probenahmepunkt:		**13**			
Koordinaten	**M** n.b.	**RW:** E13° 30.214'	**HW:** N48° 28.083'	**GOK (m ü. A.)**	n.b.
Bezeichnung:	**13**		**Geochemie-Nr.:**	**GCH-2017-071-006**	
Probenahmetiefe:	n.b.	**Probenehmer:**	**Be/Pö**		
Probenahmedatum und Uhrzeit:		**12.10.2017**	**Eingangsdatum:**	**16.10.2017**	

Feldparameter

		QZV *	MAP **	IP ***			
el. LF (µS/cm) (Gel.)	**476**	2250		2500	**Schüttung (l/s)**		**7.8**
el. LF (µS/cm) (Labor)	n.b.				**Redoxpotenzial (mV)**		**-150**
					Temperatur (°C)		**10.6**
pH (Gel.)	**7.53**			6,5 - 9,5	**Sauerstoff (O_2)**	**mg/l**	**0.01**
pH (Labor)	n.b.					**(%)**	**0**

Kationen (mg/l)

Ion	Messwert	QZV *	MAP **	IP ***
Calcium (Ca^{2+})	**79.5**			
Magnesium (Mg^{2+})	**13.3**			
Natrium (Na^{+})	**2.7**			200
Kalium (K^{+})	**0.7**			
Strontium (Sr^{2+})	**0.2291**			
Barium (Ba^{2+})	**0.0063**			
Lithium (Li^{+})	**0.0100**			
Rubidium (Rb^{+})	**0.0020**			
Cäsium (Cs^{+})	**< 0,0001**			
Ammonium (NH_4^{+})	**n.b.**	0.45		0.5
Eisen (Fe^{2+})	**0.027**			0.2
Mangan (Mn^{2+})	**0.0029**			0.05
Σ	**96.5**			

Anionen (mg/l)

Ion	Messwert	QZV *	MAP **	IP ***
Hydrogencarbonat (HCO_3^{-})	**253.22**			
Chlorid (Cl^{-})	**5.7**	180		200
Sulfat (SO_4^{2-})	**47.8**	225		250
Nitrat (NO_3^{-})	**<0,5**	45	50	
Nitrit (NO_2^{-})	**n.b.**	0.09	0.1	
o- Phosphat (o-PO_4^{3-})	**n.b.**	0.3		
Sulfid (S^{2-})	**n.b.**			
Fluorid (F^{-})	**0.08**		1.5	
Σ	**306.8**			

Ges. Ionengehalt	**403 mg/l**	**Ionenbilanz**	
	7.5 mmol/l	***-1.9***	**%**
Dichte	**n.b. g/cm3**		

Spezielle Parameter (mg/l)

Parameter	Messwert	QZV *	MAP **	IP ***
Kupfer (Cu)	**0.0005**	1.8	2	
Zink (Zn)	**< 0,0001**			
Blei (Pb)	**< 0,0001**	0.009	0.025	
Cadmium (Cd)	**< 0,0001**	0.0045	0.005	
Aluminium (Al)	**0.0013**			0.2
Arsen (As)	**0.0004**	0.009	0.01	
Antimon (Sb)	**n.b.**		0.005	
Chrom (Cr)	**< 0,0001**	0.045		
Nickel (Ni)	**0.0008**	0.018		
Quecksilber (Hg)	**n.b.**	0.0009	0.001	
Bor (B)	**n.b.**		1	
Uran (U)	**< 0,0001**		0.015	
Thorium (Th)	**n.b.**			
Cobalt (Co)	**< 0,0001**			
Molybdän (Mo)	**0.0010**			
Vanadium (V)	**< 0,0001**			
Selen (Se)	**n.b.**		0.01	
Tellur (Te)	**n.b.**			
Niob (Nb)	**n.b.**			
H_2SiO_3	**n.b.**			

Spezielle Parameter (mg/l)

Parameter	Messwert
Lanthan (La)	**n.b.**
Cer (Ce)	**n.b.**
Praseodym (Pr)	**n.b.**
Neodym (Nd)	**n.b.**
Samarium (Sm)	**n.b.**
Europium (Eu)	**n.b.**
Gadolimium (Gd)	**n.b.**
Terbium (Tb)	**n.b.**
Dysprosium (Dy)	**n.b.**
Holmium (Ho)	**n.b.**
Erbium (Er)	**n.b.**
Thulium (Tm)	**n.b.**
Ytterbium (Yb)	**n.b.**
Lutetium (Lu)	**n.b.**
Zinn (Sn)	**n.b.**
Thallium (Tl)	**n.b.**
Silber (Ag)	**n.b.**
Beryllium (Be)	**n.b.**
Bismut (Bi)	**n.b.**
Gallium (Ga)	**n.b.**

n.b. .. nicht bestimmt

* ... Qualitätszielverordnung Chemie Grundwasser QZV Chemie GW (BGBl. II 98/2010)

** ... Mindestanforderungsparameter aus der Trinkwasserverordnung - TWV (BGBl. II 304/2001)

*** ... Indikatorparameter aus der Trinkwasserverordnung - TWV (BGBl. II 304/2001)

Layout: G. Hobiger

Geologische Bundesanstalt
FA Geochemie
Leitung: HR Mag. Dr. Gerhard Hobiger

Berechnungen aus den Analysenwerten

Äquivalentanteile

Kationen

Ion	Messwert mg/l	meq/l	eq%
Ca^{2+}	79.48	3.97	76.15
Mg^{2+}	13.34	1.10	21.08
Na^{+}	2.71	0.12	2.26
K^{+}	0.73	0.02	0.36
Sr^{2+}	0.23	0.01	0.10
Ba^{2+}	0.006	0.00	0.0
Li^{+}	0.010	0.00	0.03
Rb^{+}	0.002	0.00	0.00
Cs^{+}	< 0,0001	0.00	0.00
NH_4^{+}	n.b.	n.b.	n.b.
Fe^{2+}	0.027	0.00	0.0
Mn^{2+}	0.0029	0.00	0.0
Σ	96.53	5.2	100.0

Anionen

Ion	Messwert mg/l	meq/l	eq%
HCO_3^{-}	253.22	4.15	78.2
Cl^{-}	5.70	0.16	3.0
SO_4^{2-}	47.77	0.99	18.7
NO_3^{-}	<0,5	0.00	0.0
NO_2^{-}	n.b.	n.b.	n.b.
$o\text{-}PO_4^{3-}$	n.b.	n.b.	n.b.
S^{2-}	n.b.	n.b.	n.b.
F^{-}	0.08	0.00	0.1
Σ	306.77	5.3	100.0

Härten

Gesamthärte (° dH)	14.2
Carbonathärte(° dH)	11.6
Nichtcarbonathärte (°dH)	2.6
Erdalkalien (mmol/l)	48.7

Berechnung des CO_2

lg(pCO_2)	-2.22
freies CO_2 (mg/l)	13.93
freies CO_2 (mmol/l)	0.3164

Berechneter Ammoniakgehalt

NH_3 (mg/l)	n.b.

Ges. Ionengehalt	403 mg/l	7.5 mmol/l

Ionenbilanz

Σ Kationen (meq/l)	5.21	*-1.9 %*
Σ Anionen (meq/l)	5.31	

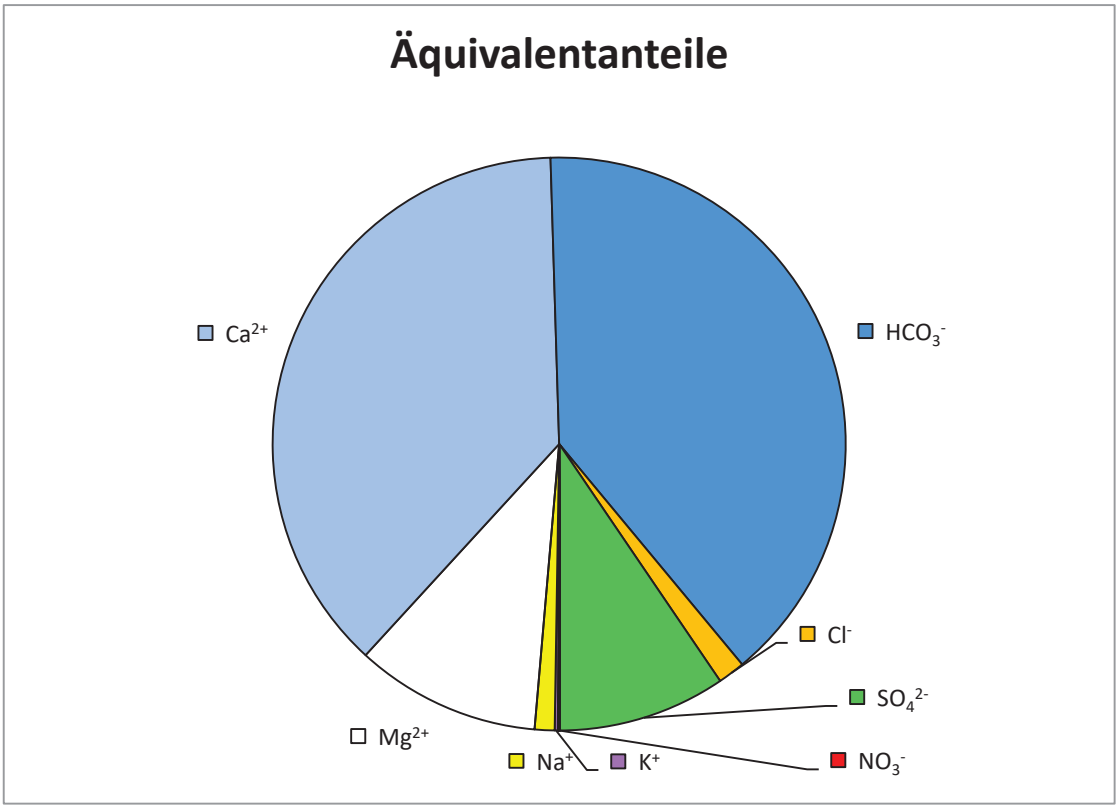

Wasseranalyse

Geologische Bundesanstalt
FA Geochemie
Leitung: HR Mag. Dr. Gerhard Hobiger

Probenahmepunkt:			**14**		
Koordinaten	**M** n.b.	**RW:** E13° 31.706'	**HW:** N48° 27.328'	**GOK (m ü. A.)**	n.b.
Bezeichnung:	**14**		**Geochemie-Nr.:**	**GCH-2017-071-007**	
Probenahmetiefe:	n.b.	**Probenehmer:**	**Be/Pö**		
Probenahmedatum und Uhrzeit:		**13.10.2017 08:50**	**Eingangsdatum:**	**16.10.2017**	

Feldparameter

		QZV *	MAP **	IP ***			
el. LF (µS/cm) (Gel.)	**410**	2250		2500	**Schüttung (l/s)**		**n.b.**
el. LF (µS/cm) (Labor)	n.b.				**Redoxpotenzial (mV)**		**-133**
					Temperatur (°C)		**11.4**
pH (Gel.)	**7.6**			6,5 - 9,5	**Sauerstoff (O_2)**	**mg/l**	**0.1**
pH (Labor)	n.b.					**(%)**	**0.7**

Kationen (mg/l)

Ion	Messwert	QZV *	MAP **	IP ***
Calcium (Ca^{2+})	**60.1**			
Magnesium (Mg^{2+})	**16.0**			
Natrium (Na^{+})	**3.3**			200
Kalium (K^{+})	**0.8**			
Strontium (Sr^{2+})	**0.2507**			
Barium (Ba^{2+})	**0.0174**			
Lithium (Li^{+})	**0.0124**			
Rubidium (Rb^{+})	**0.0014**			
Cäsium (Cs^{+})	**< 0,0001**			
Ammonium (NH_4^{+})	**n.b.**	0.45		0.5
Eisen (Fe^{2+})	**0.083**			0.2
Mangan (Mn^{2+})	**0.0048**			0.05
Σ	**80.6**			

Anionen (mg/l)

Ion	Messwert	QZV *	MAP **	IP ***
Hydrogencarbonat (HCO_3^{-})	**241.01**			
Chlorid (Cl^{-})	**2.1**	180		200
Sulfat (SO_4^{2-})	**29.6**	225		250
Nitrat (NO_3^{-})	**<0,5**	45	50	
Nitrit (NO_2^{-})	**n.b.**	0.09	0.1	
o- Phosphat (o-PO_4^{3-})	**n.b.**	0.3		
Sulfid (S^{2-})	**n.b.**			
Fluorid (F^{-})	**0.13**		1.5	
Σ	**272.8**			

Ges. Ionengehalt	**353 mg/l**	**Ionenbilanz**	
	6.7 mmol/l	***-3.0***	**%**
Dichte	**n.b. g/cm3**		

Spezielle Parameter (mg/l)

Parameter	Messwert	QZV *	MAP **	IP ***
Kupfer (Cu)	**0.0002**	1.8	2	
Zink (Zn)	**< 0,0001**			
Blei (Pb)	**< 0,0001**	0.009	0.025	
Cadmium (Cd)	**< 0,0001**	0.0045	0.005	
Aluminium (Al)	**0.0010**			0.2
Arsen (As)	**0.0002**	0.009	0.01	
Antimon (Sb)	**n.b.**		0.005	
Chrom (Cr)	**< 0,0001**	0.045		
Nickel (Ni)	**< 0,0001**	0.018		
Quecksilber (Hg)	**n.b.**	0.0009	0.001	
Bor (B)	**n.b.**		1	
Uran (U)	**< 0,0001**		0.015	
Thorium (Th)	**n.b.**			
Cobalt (Co)	**< 0,0001**			
Molybdän (Mo)	**0.0009**			
Vanadium (V)	**< 0,0001**			
Selen (Se)	**n.b.**		0.01	
Tellur (Te)	**n.b.**			
Niob (Nb)	**n.b.**			
H_2SiO_3	**n.b.**			

Spezielle Parameter (mg/l)

Parameter	Messwert
Lanthan (La)	**n.b.**
Cer (Ce)	**n.b.**
Praseodym (Pr)	**n.b.**
Neodym (Nd)	**n.b.**
Samarium (Sm)	**n.b.**
Europium (Eu)	**n.b.**
Gadolimium (Gd)	**n.b.**
Terbium (Tb)	**n.b.**
Dysprosium (Dy)	**n.b.**
Holmium (Ho)	**n.b.**
Erbium (Er)	**n.b.**
Thulium (Tm)	**n.b.**
Ytterbium (Yb)	**n.b.**
Lutetium (Lu)	**n.b.**
Zinn (Sn)	**n.b.**
Thallium (Tl)	**n.b.**
Silber (Ag)	**n.b.**
Beryllium (Be)	**n.b.**
Bismut (Bi)	**n.b.**
Gallium (Ga)	**n.b.**

n.b. .. nicht bestimmt

* ... Qualitätszielverordnung Chemie Grundwasser QZV Chemie GW (BGBl. II 98/2010)

** ... Mindestanforderungsparameter aus der Trinkwasserverordnung - TWV (BGBl. II 304/2001)

*** ... Indikatorparameter aus der Trinkwasserverordnung - TWV (BGBl. II 304/2001)

Layout: G. Hobiger

Geologische Bundesanstalt
FA Geochemie
Leitung: HR Mag. Dr. Gerhard Hobiger

Berechnungen aus den Analysenwerten

Äquivalentanteile

Kationen

	Messwert		
Ion	mg/l	meq/l	eq%
Ca^{2+}	60.10	3.00	66.73
Mg^{2+}	16.04	1.32	29.37
Na^{+}	3.30	0.14	3.19
K^{+}	0.81	0.02	0.46
Sr^{2+}	0.25	0.01	0.13
Ba^{2+}	0.017	0.00	0.0
Li^{+}	0.012	0.00	0.04
Rb^{+}	0.001	0.00	0.00
Cs^{+}	< 0,0001	0.00	0.00
NH_4^{+}	n.b.	n.b.	n.b.
Fe^{2+}	0.083	0.00	0.1
Mn^{2+}	0.0048	0.00	0.0
Σ	80.63	4.5	100.0

Anionen

	Messwert		
Ion	mg/l	meq/l	eq%
HCO_3^{-}	241.01	3.95	85.3
Cl^{-}	2.10	0.06	1.3
SO_4^{2-}	29.58	0.62	13.3
NO_3^{-}	<0,5	0.00	0.0
NO_2^{-}	n.b.	n.b.	n.b.
$o\text{-}PO_4^{3-}$	n.b.	n.b.	n.b.
S^{2-}	n.b.	n.b.	n.b.
F^{-}	0.13	0.01	0.2
Σ	272.83	4.6	100.0

Härten

Gesamthärte (° dH)	12.1
Carbonathärte(° dH)	11.1
Nichtcarbonathärte (°dH)	1.0
Erdalkalien (mmol/l)	48.1

Berechnung des CO_2

lg(pCO_2)	-2.31
freies CO_2 (mg/l)	11.18
freies CO_2 (mmol/l)	0.2540

Berechneter Ammoniakgehalt

NH_3 (mg/l)	n.b.

Ges. Ionengehalt	353 mg/l	6.7 mmol/l

Ionenbilanz

Σ Kationen (meq/l)	4.49	*-3.0 %*
Σ Anionen (meq/l)	4.63	

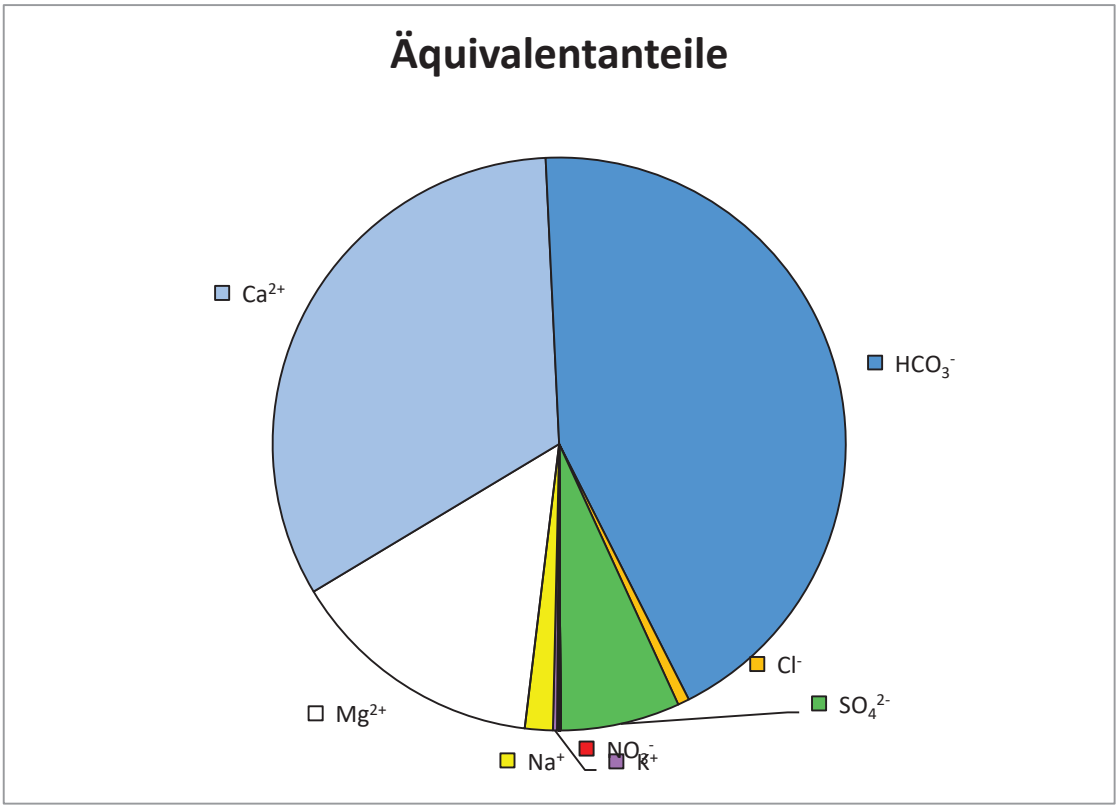

Wasseranalyse

Geologische Bundesanstalt
FA Geochemie
Leitung: HR Mag. Dr. Gerhard Hobiger

Probenahmepunkt:		**15**			
Koordinaten	**M** n.b.	**RW:** E13° 32.257'	**HW:** N48° 22.336'	**GOK (m ü. A.)**	n.b.
Bezeichnung:	**15**		**Geochemie-Nr.:**	**GCH-2017-071-008**	
Probenahmetiefe:	n.b.	**Probenehmer:**	**Be/Pö**		
Probenahmedatum und Uhrzeit:		**13.10.2017 10:00**	**Eingangsdatum:**	**16.10.2017**	

Feldparameter

		QZV *	MAP **	IP ***			
el. LF (µS/cm) (Gel.)	**703**	2250		2500	**Schüttung (l/s)**		**n.b.**
el. LF (µS/cm) (Labor)	n.b.				**Redoxpotenzial (mV)**		**93**
					Temperatur (°C)		**13.2**
pH (Gel.)	**8.29**			6,5 - 9,5	**Sauerstoff (O_2)**	**mg/l**	**2.5**
pH (Labor)	n.b.					**(%)**	**26**

Kationen (mg/l)

Ion	Messwert	QZV *	MAP **	IP ***
Calcium (Ca^{2+})	6.4			
Magnesium (Mg^{2+})	3.0			
Natrium (Na^{+})	160.5			200
Kalium (K^{+})	1.5			
Strontium (Sr^{2+})	0.1426			
Barium (Ba^{2+})	0.0113			
Lithium (Li^{+})	0.0559			
Rubidium (Rb^{+})	0.0015			
Cäsium (Cs^{+})	< 0,0001			
Ammonium (NH_4^{+})	n.b.	0.45		0.5
Eisen (Fe^{2+})	0.014			0.2
Mangan (Mn^{2+})	0.0039			0.05
Σ	171.6			

Anionen (mg/l)

Ion	Messwert	QZV *	MAP **	IP ***
Hydrogencarbonat (HCO_3^{-})	375.25			
Chlorid (Cl^{-})	46.7	180		200
Sulfat (SO_4^{2-})	<0,5	225		250
Nitrat (NO_3^{-})	<0,5	45	50	
Nitrit (NO_2^{-})	n.b.	0.09	0.1	
o- Phosphat (o-PO_4^{3-})	n.b.	0.3		
Sulfid (S^{2-})	n.b.			
Fluorid (F^{-})	0.58		1.5	
Σ	422.5			

Ges. Ionengehalt	**594 mg/l**	**Ionenbilanz**	
	14.8 mmol/l	***1.3***	**%**
Dichte	**n.b. g/cm3**		

Spezielle Parameter (mg/l)

Parameter	Messwert	QZV *	MAP **	IP ***
Kupfer (Cu)	0.0016	1.8	2	
Zink (Zn)	0.0747			
Blei (Pb)	< 0,0001	0.009	0.025	
Cadmium (Cd)	< 0,0001	0.0045	0.005	
Aluminium (Al)	0.0014			0.2
Arsen (As)	0.0000	0.009	0.01	
Antimon (Sb)	n.b.		0.005	
Chrom (Cr)	< 0,0001	0.045		
Nickel (Ni)	< 0,0001	0.018		
Quecksilber (Hg)	n.b.	0.0009	0.001	
Bor (B)	n.b.		1	
Uran (U)	< 0,0001		0.015	
Thorium (Th)	n.b.			
Cobalt (Co)	< 0,0001			
Molybdän (Mo)	0.0005			
Vanadium (V)	< 0,0001			
Selen (Se)	n.b.		0.01	
Tellur (Te)	n.b.			
Niob (Nb)	n.b.			
H_2SiO_3	n.b.			

Spezielle Parameter (mg/l)

Parameter	Messwert
Lanthan (La)	n.b.
Cer (Ce)	n.b.
Praseodym (Pr)	n.b.
Neodym (Nd)	n.b.
Samarium (Sm)	n.b.
Europium (Eu)	n.b.
Gadolimium (Gd)	n.b.
Terbium (Tb)	n.b.
Dysprosium (Dy)	n.b.
Holmium (Ho)	n.b.
Erbium (Er)	n.b.
Thulium (Tm)	n.b.
Ytterbium (Yb)	n.b.
Lutetium (Lu)	n.b.
Zinn (Sn)	n.b.
Thallium (Tl)	n.b.
Silber (Ag)	n.b.
Beryllium (Be)	n.b.
Bismut (Bi)	n.b.
Gallium (Ga)	n.b.

n.b. .. nicht bestimmt

* ... Qualitätszielverordnung Chemie Grundwasser QZV Chemie GW (BGBl. II 98/2010)

** ... Mindestanforderungsparameter aus der Trinkwasserverordnung - TWV (BGBl. II 304/2001)

*** ... Indikatorparameter aus der Trinkwasserverordnung - TWV (BGBl. II 304/2001)

Layout: G. Hobiger

Geologische Bundesanstalt
FA Geochemie
Leitung: HR Mag. Dr. Gerhard Hobiger

Berechnungen aus den Analysenwerten

Äquivalentanteile

Kationen

	Messwert		
Ion	mg/l	meq/l	eq%
Ca^{2+}	6.44	0.32	4.23
Mg^{2+}	2.98	0.25	3.23
Na^{+}	160.51	6.98	91.89
K^{+}	1.46	0.04	0.49
Sr^{2+}	0.14	0.00	0.04
Ba^{2+}	0.011	0.00	0.0
Li^{+}	0.056	0.01	0.11
Rb^{+}	0.001	0.00	0.00
Cs^{+}	< 0,0001	0.00	0.00
NH_4^{+}	n.b.	n.b.	n.b.
Fe^{2+}	0.014	0.00	0.0
Mn^{2+}	0.0039	0.00	0.0
Σ	171.62	7.6	100.0

Anionen

	Messwert		
Ion	mg/l	meq/l	eq%
HCO_3^{-}	375.25	6.15	82.0
Cl^{-}	46.69	1.32	17.6
SO_4^{2-}	<0,5	0.00	0.0
NO_3^{-}	<0,5	0.00	0.0
NO_2^{-}	n.b.	n.b.	n.b.
$o\text{-}PO_4^{3-}$	n.b.	n.b.	n.b.
S^{2-}	n.b.	n.b.	n.b.
F^{-}	0.58	0.03	0.4
Σ	422.51	7.5	100.0

Härten

Gesamthärte (° dH)	1.6
Carbonathärte(° dH)	1.6
Nichtcarbonathärte (°dH)	0.0
Erdalkalien (mmol/l)	3.8

Berechnung des CO_2

lg(pCO_2)	-2.80
freies CO_2 (mg/l)	3.40
freies CO_2 (mmol/l)	0.0774

Berechneter Ammoniakgehalt

NH_3 (mg/l)	n.b.

Ges. Ionengehalt	594 mg/l	14.8 mmol/l

Ionenbilanz

Σ Kationen (meq/l)	7.60	*1.3 %*
Σ Anionen (meq/l)	7.50	

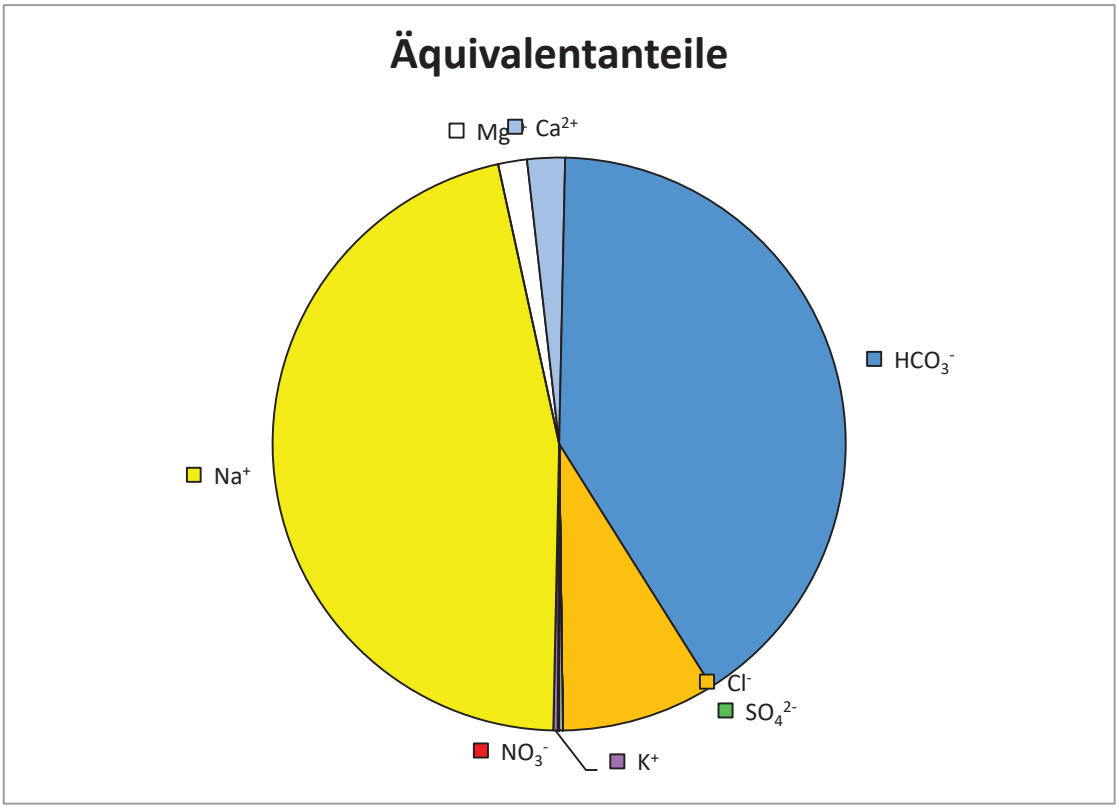

Wasseranalyse

Geologische Bundesanstalt
FA Geochemie
Leitung: HR Mag. Dr. Gerhard Hobiger

Probenahmepunkt:		**16**		
Koordinaten	**M** n.b.	**RW:** E13° 43.871'	**HW:** N48° 14.806'	**GOK (m ü. A.)** n.b.
Bezeichnung:	**16**		**Geochemie-Nr.:**	**GCH-2017-078-001**
Probenahmetiefe (m):	**220**	**Probenehmer:**	**Be/Pö**	
Probenahmedatum und Uhrzeit:		**09.11.2017 09:00**	**Eingangsdatum:**	**10.11.2017**

Feldparameter

		QZV *	MAP **	IP ***			
el. LF (µS/cm) (Gel.)	**460**	2250		2500	**Schüttung (l/s)**		**n.b.**
el. LF (µS/cm) (Labor)	n.b.				**Redoxpotenzial (mV)**		**-173**
					Temperatur (°C)		**12.2**
pH (Gel.)	**8.76**			6,5 - 9,5	**Sauerstoff (O_2)**	**mg/l**	**0.04**
pH (Labor)	n.b.					**(%)**	**0.4**

Kationen (mg/l)

Ion	Messwert	QZV *	MAP **	IP ***
Calcium (Ca^{2+})	3.3			
Magnesium (Mg^{2+})	1.1			
Natrium (Na^{+})	100.3			200
Kalium (K^{+})	2.4			
Strontium (Sr^{2+})	0.0848			
Barium (Ba^{2+})	0.0295			
Lithium (Li^{+})	0.0839			
Rubidium (Rb^{+})	0.0011			
Cäsium (Cs^{+})	< 0,0001			
Ammonium (NH_4^{+})	n.b.	0.45		0.5
Eisen (Fe^{2+})	0.003			0.2
Mangan (Mn^{2+})	0.0018			0.05
Σ	107.3			

Anionen (mg/l)

Ion	Messwert	QZV *	MAP **	IP ***
Hydrogencarbonat (HCO_3^{-})	268.47			
Chlorid (Cl^{-})	5.6	180		200
Sulfat (SO_4^{2-})	13.6	225		250
Nitrat (NO_3^{-})	<0,5	45	50	
Nitrit (NO_2^{-})	n.b.	0.09	0.1	
o- Phosphat (o-PO_4^{3-})	n.b.	0.3		
Sulfid (S^{2-})	n.b.			
Fluorid (F^{-})	0.16		1.5	
Σ	287.7			

Ges. Ionengehalt	**395 mg/l**	**Ionenbilanz**	
	9.3 mmol/l	***-3.2***	**%**
Dichte	**n.b. g/cm3**		

Spezielle Parameter (mg/l)

Parameter	Messwert	QZV *	MAP **	IP ***
Kupfer (Cu)	0.0005	1.8	2	
Zink (Zn)	0.0070			
Blei (Pb)	< 0,0001	0.009	0.025	
Cadmium (Cd)	< 0,0001	0.0045	0.005	
Aluminium (Al)	0.0019			0.2
Arsen (As)	< 0,0001	0.009	0.01	
Antimon (Sb)	n.b.		0.005	
Chrom (Cr)	0.0002	0.045		
Nickel (Ni)	< 0,0001	0.018		
Quecksilber (Hg)	n.b.	0.0009	0.001	
Bor (B)	n.b.		1	
Uran (U)	< 0,0001		0.015	
Thorium (Th)	n.b.			
Cobalt (Co)	< 0,0001			
Molybdän (Mo)	0.0003			
Vanadium (V)	< 0,0001			
Selen (Se)	n.b.		0.01	
Tellur (Te)	n.b.			
Niob (Nb)	n.b.			
H_2SiO_3	n.b.			

Spezielle Parameter (mg/l)

Parameter	Messwert
Lanthan (La)	n.b.
Cer (Ce)	n.b.
Praseodym (Pr)	n.b.
Neodym (Nd)	n.b.
Samarium (Sm)	n.b.
Europium (Eu)	n.b.
Gadolimium (Gd)	n.b.
Terbium (Tb)	n.b.
Dysprosium (Dy)	n.b.
Holmium (Ho)	n.b.
Erbium (Er)	n.b.
Thulium (Tm)	n.b.
Ytterbium (Yb)	n.b.
Lutetium (Lu)	n.b.
Zinn (Sn)	n.b.
Thallium (Tl)	n.b.
Silber (Ag)	n.b.
Beryllium (Be)	n.b.
Bismut (Bi)	n.b.
Gallium (Ga)	n.b.

n.b. .. nicht bestimmt

* ... Qualitätszielverordnung Chemie Grundwasser QZV Chemie GW (BGBl. II 98/2010)

** ... Mindestanforderungsparameter aus der Trinkwasserverordnung - TWV (BGBl. II 304/2001)

*** ... Indikatorparameter aus der Trinkwasserverordnung - TWV (BGBl. II 304/2001)

Layout: G. Hobiger

Geologische Bundesanstalt
FA Geochemie
Leitung: HR Mag. Dr. Gerhard Hobiger

Berechnungen aus den Analysenwerten

Äquivalentanteile

Kationen

Ion	Messwert mg/l	meq/l	eq%
Ca^{2+}	3.29	0.16	3.50
Mg^{2+}	1.12	0.09	1.97
Na^{+}	100.25	4.36	92.92
K^{+}	2.38	0.06	1.30
Sr^{2+}	0.08	0.00	0.04
Ba^{2+}	0.030	0.00	0.0
Li^{+}	0.084	0.01	0.26
Rb^{+}	0.001	0.00	0.00
Cs^{+}	< 0,0001	0.00	0.00
NH_4^{+}	n.b.	n.b.	n.b.
Fe^{2+}	0.003	0.00	0.0
Mn^{2+}	0.0018	0.00	0.0
Σ	107.26	4.7	100.0

Anionen

Ion	Messwert mg/l	meq/l	eq%
HCO_3^{-}	268.47	4.40	90.8
Cl^{-}	5.57	0.16	3.2
SO_4^{2-}	13.55	0.28	5.8
NO_3^{-}	<0,5	0.00	0.0
NO_2^{-}	n.b.	n.b.	n.b.
$o\text{-}PO_4^{3-}$	n.b.	n.b.	n.b.
S^{2-}	n.b.	n.b.	n.b.
F^{-}	0.16	0.01	0.2
Σ	287.74	4.8	100.0

Härten

Gesamthärte (° dH)	0.7
Carbonathärte(° dH)	0.7
Nichtcarbonathärte (°dH)	0.0
Erdalkalien (mmol/l)	2.8

Berechnung des CO_2

$lg(pCO_2)$	-3.41
freies CO_2 (mg/l)	0.86
freies CO_2 (mmol/l)	0.0195

Berechneter Ammoniakgehalt

NH_3 (mg/l)	n.b.

Ges. Ionengehalt	395 mg/l	9.3 mmol/l

Ionenbilanz

Σ Kationen (meq/l)	4.69	-3.2 %
Σ Anionen (meq/l)	4.85	

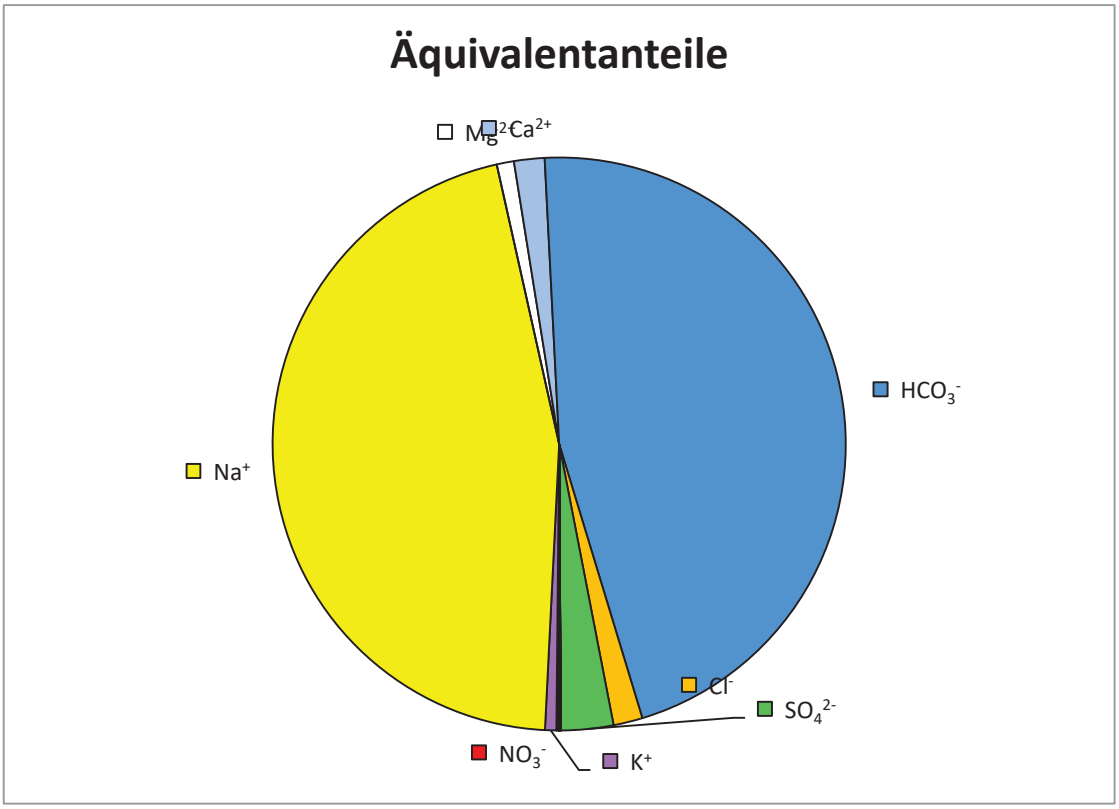

Wasseranalyse

Geologische Bundesanstalt
FA Geochemie
Leitung: HR Mag. Dr. Gerhard Hobiger

Probenahmepunkt:		**17**		
Koordinaten	**M** n.b.	**RW:** E13° 46.301'	**HW:** N48° 15.153'	**GOK (m ü. A.)** n.b.
Bezeichnung:	**17**		**Geochemie-Nr.:**	**GCH-2017-078-002**
Probenahmetiefe (m):	n.b.	**Probenehmer:**	**Be/Pö**	
Probenahmedatum und Uhrzeit:		**09.11.2017 10:30**	**Eingangsdatum:**	**10.11.2017**

Feldparameter

		QZV *	MAP **	IP ***			
el. LF (µS/cm) (Gel.)	**480**	2250		2500	**Schüttung (l/s)**		**n.b.**
el. LF (µS/cm) (Labor)	n.b.				**Redoxpotenzial (mV)**		**-213**
					Temperatur (°C)		**12.5**
pH (Gel.)	**8.64**			6,5 - 9,5	**Sauerstoff (O_2)**	**mg/l**	**0.03**
pH (Labor)	n.b.					**(%)**	**0.4**

Kationen (mg/l)

Ion	Messwert	QZV *	MAP **	IP ***
Calcium (Ca^{2+})	3.1			
Magnesium (Mg^{2+})	1.0			
Natrium (Na^{+})	107.4			200
Kalium (K^{+})	2.4			
Strontium (Sr^{2+})	0.0602			
Barium (Ba^{2+})	0.0390			
Lithium (Li^{+})	0.0838			
Rubidium (Rb^{+})	0.0014			
Cäsium (Cs^{+})	< 0,0001			
Ammonium (NH_4^{+})	n.b.	0.45		0.5
Eisen (Fe^{2+})	0.013			0.2
Mangan (Mn^{2+})	0.0036			0.05
Σ	114.2			

Anionen (mg/l)

Ion	Messwert	QZV *	MAP **	IP ***
Hydrogencarbonat (HCO_3^{-})	286.78			
Chlorid (Cl^{-})	2.5	180		200
Sulfat (SO_4^{2-})	18.3	225		250
Nitrat (NO_3^{-})	<0,5	45	50	
Nitrit (NO_2^{-})	n.b.	0.09	0.1	
o- Phosphat (o-PO_4^{3-})	n.b.	0.3		
Sulfid (S^{2-})	n.b.			
Fluorid (F^{-})	0.13		1.5	
Σ	307.7			

Ges. Ionengehalt	**422 mg/l**	**Ionenbilanz**	
	9.8 mmol/l	***-3.3***	**%**
Dichte	**n.b. g/cm3**		

Spezielle Parameter (mg/l)

Parameter	Messwert	QZV *	MAP **	IP ***
Kupfer (Cu)	0.0017	1.8	2	
Zink (Zn)	0.0163			
Blei (Pb)	< 0,0001	0.009	0.025	
Cadmium (Cd)	< 0,0001	0.0045	0.005	
Aluminium (Al)	0.0027			0.2
Arsen (As)	< 0,0001	0.009	0.01	
Antimon (Sb)	n.b.		0.005	
Chrom (Cr)	0.0002	0.045		
Nickel (Ni)	0.0002	0.018		
Quecksilber (Hg)	n.b.	0.0009	0.001	
Bor (B)	n.b.		1	
Uran (U)	< 0,0001		0.015	
Thorium (Th)	n.b.			
Cobalt (Co)	< 0,0001			
Molybdän (Mo)	0.0003			
Vanadium (V)	< 0,0001			
Selen (Se)	n.b.		0.01	
Tellur (Te)	n.b.			
Niob (Nb)	n.b.			
H_2SiO_3	n.b.			

Spezielle Parameter (mg/l)

Parameter	Messwert
Lanthan (La)	n.b.
Cer (Ce)	n.b.
Praseodym (Pr)	n.b.
Neodym (Nd)	n.b.
Samarium (Sm)	n.b.
Europium (Eu)	n.b.
Gadolimium (Gd)	n.b.
Terbium (Tb)	n.b.
Dysprosium (Dy)	n.b.
Holmium (Ho)	n.b.
Erbium (Er)	n.b.
Thulium (Tm)	n.b.
Ytterbium (Yb)	n.b.
Lutetium (Lu)	n.b.
Zinn (Sn)	n.b.
Thallium (Tl)	n.b.
Silber (Ag)	n.b.
Beryllium (Be)	n.b.
Bismut (Bi)	n.b.
Gallium (Ga)	n.b.

n.b. .. nicht bestimmt

* ... Qualitätszielverordnung Chemie Grundwasser QZV Chemie GW (BGBl. II 98/2010)

** ... Mindestanforderungsparameter aus der Trinkwasserverordnung - TWV (BGBl. II 304/2001)

*** ... Indikatorparameter aus der Trinkwasserverordnung - TWV (BGBl. II 304/2001)

Layout: G. Hobiger

Geologische Bundesanstalt
FA Geochemie
Leitung: HR Mag. Dr. Gerhard Hobiger

Berechnungen aus den Analysenwerten

Äquivalentanteile

Kationen

Ion	Messwert mg/l	meq/l	eq%
Ca^{2+}	3.15	0.16	3.15
Mg^{2+}	1.00	0.08	1.65
Na^{+}	107.43	4.67	93.67
K^{+}	2.42	0.06	1.24
Sr^{2+}	0.06	0.00	0.03
Ba^{2+}	0.039	0.00	0.0
Li^{+}	0.084	0.01	0.24
Rb^{+}	0.001	0.00	0.00
Cs^{+}	< 0,0001	0.00	0.00
NH_4^{+}	n.b.	n.b.	n.b.
Fe^{2+}	0.013	0.00	0.0
Mn^{2+}	0.0036	0.00	0.0
Σ	114.19	5.0	100.0

Anionen

Ion	Messwert mg/l	meq/l	eq%
HCO_3^{-}	286.78	4.70	91.1
Cl^{-}	2.48	0.07	1.4
SO_4^{2-}	18.32	0.38	7.4
NO_3^{-}	<0,5	0.00	0.0
NO_2^{-}	n.b.	n.b.	n.b.
$o\text{-}PO_4^{3-}$	n.b.	n.b.	n.b.
S^{2-}	n.b.	n.b.	n.b.
F^{-}	0.13	0.01	0.1
Σ	307.70	5.2	100.0

Härten

Gesamthärte (° dH)	0.7
Carbonathärte(° dH)	0.7
Nichtcarbonathärte (°dH)	0.0
Erdalkalien (mmol/l)	2.4

Berechnung des CO_2

$lg(pCO_2)$	-3.26
freies CO_2 (mg/l)	1.20
freies CO_2 (mmol/l)	0.0273

Berechneter Ammoniakgehalt

NH_3 (mg/l)	n.b.

Ges. Ionengehalt	422 mg/l	9.8 mmol/l

Ionenbilanz

Σ Kationen (meq/l)	4.99	-3.3 %
Σ Anionen (meq/l)	5.16	

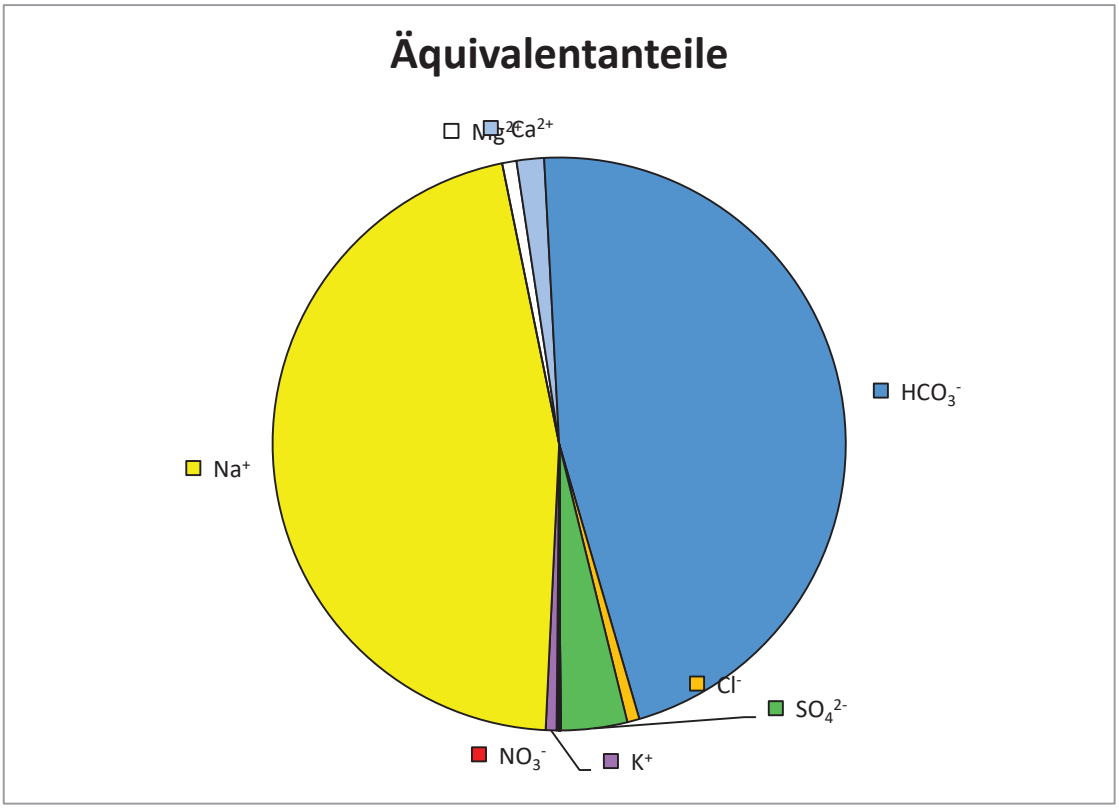

Wasseranalyse

Geologische Bundesanstalt
FA Geochemie
Leitung: HR Mag. Dr. Gerhard Hobiger

Probenahmepunkt:		**18**		
Koordinaten	**M** n.b.	**RW:** E13° 40.239'	**HW:** N48° 16.225'	**GOK (m ü. A.)** n.b.
Bezeichnung:	**18**		**Geochemie-Nr.:**	**GCH-2017-078-003**
Probenahmetiefe (m):	**180**	**Probenehmer:**	**Be/Pö**	
Probenahmedatum und Uhrzeit:		**09.11.2017 11:30**	**Eingangsdatum:**	**10.11.2017**

Feldparameter

		QZV *	MAP **	IP ***			
el. LF (µS/cm) (Gel.)	**471**	2250		2500	**Schüttung (l/s)**		**n.b.**
el. LF (µS/cm) (Labor)	n.b.				**Redoxpotenzial (mV)**		**-149**
					Temperatur (°C)		**11.4**
pH (Gel.)	**8.61**			6,5 - 9,5	**Sauerstoff (O_2)**	**mg/l**	**0.06**
pH (Labor)	n.b.					**(%)**	**0.6**

Kationen (mg/l)

Ion	Messwert	QZV *	MAP **	IP ***
Calcium (Ca^{2+})	3.7			
Magnesium (Mg^{2+})	1.9			
Natrium (Na^{+})	110.5			200
Kalium (K^{+})	1.8			
Strontium (Sr^{2+})	0.1071			
Barium (Ba^{2+})	0.0116			
Lithium (Li^{+})	0.0756			
Rubidium (Rb^{+})	0.0005			
Cäsium (Cs^{+})	< 0,0001			
Ammonium (NH_4^{+})	n.b.	0.45		0.5
Eisen (Fe^{2+})	0.010			0.2
Mangan (Mn^{2+})	0.0030			0.05
Σ	118.1			

Anionen (mg/l)

Ion	Messwert	QZV *	MAP **	IP ***
Hydrogencarbonat (HCO_3^{-})	317.28			
Chlorid (Cl^{-})	0.5	180		200
Sulfat (SO_4^{2-})	0.3	225		250
Nitrat (NO_3^{-})	<0,5	45	50	
Nitrit (NO_2^{-})	n.b.	0.09	0.1	
o- Phosphat (o-PO_4^{3-})	n.b.	0.3		
Sulfid (S^{2-})	n.b.			
Fluorid (F^{-})	0.33		1.5	
Σ	318.3			

Ges. Ionengehalt	**436 mg/l**	**Ionenbilanz**
	10.3 mmol/l	***-0.5*** **%**
Dichte	**n.b. g/cm3**	

Spezielle Parameter (mg/l)

Parameter	Messwert	QZV *	MAP **	IP ***
Kupfer (Cu)	0.0003	1.8	2	
Zink (Zn)	0.0274			
Blei (Pb)	< 0,0001	0.009	0.025	
Cadmium (Cd)	< 0,0001	0.0045	0.005	
Aluminium (Al)	0.0015			0.2
Arsen (As)	< 0,0001	0.009	0.01	
Antimon (Sb)	n.b.		0.005	
Chrom (Cr)	0.0002	0.045		
Nickel (Ni)	< 0,0001	0.018		
Quecksilber (Hg)	n.b.	0.0009	0.001	
Bor (B)	n.b.		1	
Uran (U)	< 0,0001		0.015	
Thorium (Th)	n.b.			
Cobalt (Co)	< 0,0001			
Molybdän (Mo)	0.0002			
Vanadium (V)	< 0,0001			
Selen (Se)	n.b.		0.01	
Tellur (Te)	n.b.			
Niob (Nb)	n.b.			
H_2SiO_3	n.b.			

Spezielle Parameter (mg/l)

Parameter	Messwert
Lanthan (La)	n.b.
Cer (Ce)	n.b.
Praseodym (Pr)	n.b.
Neodym (Nd)	n.b.
Samarium (Sm)	n.b.
Europium (Eu)	n.b.
Gadolimium (Gd)	n.b.
Terbium (Tb)	n.b.
Dysprosium (Dy)	n.b.
Holmium (Ho)	n.b.
Erbium (Er)	n.b.
Thulium (Tm)	n.b.
Ytterbium (Yb)	n.b.
Lutetium (Lu)	n.b.
Zinn (Sn)	n.b.
Thallium (Tl)	n.b.
Silber (Ag)	n.b.
Beryllium (Be)	n.b.
Bismut (Bi)	n.b.
Gallium (Ga)	n.b.

n.b. .. nicht bestimmt

* ... Qualitätszielverordnung Chemie Grundwasser QZV Chemie GW (BGBl. II 98/2010)

** ... Mindestanforderungsparameter aus der Trinkwasserverordnung - TWV (BGBl. II 304/2001)

*** ... Indikatorparameter aus der Trinkwasserverordnung - TWV (BGBl. II 304/2001)

Layout: G. Hobiger

Geologische Bundesanstalt
FA Geochemie
Leitung: HR Mag. Dr. Gerhard Hobiger

Berechnungen aus den Analysenwerten

Äquivalentanteile

Kationen

	Messwert		
Ion	mg/l	meq/l	eq%
Ca^{2+}	3.73	0.19	3.58
Mg^{2+}	1.93	0.16	3.04
Na^{+}	110.51	4.81	92.25
K^{+}	1.75	0.04	0.86
Sr^{2+}	0.11	0.00	0.05
Ba^{2+}	0.012	0.00	0.0
Li^{+}	0.076	0.01	0.21
Rb^{+}	0.000	0.00	0.00
Cs^{+}	< 0,0001	0.00	0.00
NH_4^{+}	n.b.	n.b.	n.b.
Fe^{2+}	0.010	0.00	0.0
Mn^{2+}	0.0030	0.00	0.0
Σ	118.13	5.2	100.0

Anionen

	Messwert		
Ion	mg/l	meq/l	eq%
HCO_3^{-}	317.28	5.20	99.3
Cl^{-}	0.47	0.01	0.3
SO_4^{2-}	0.26	0.01	0.1
NO_3^{-}	<0,5	0.00	0.0
NO_2^{-}	n.b.	n.b.	n.b.
$o\text{-}PO_4^{3-}$	n.b.	n.b.	n.b.
S^{2-}	n.b.	n.b.	n.b.
F^{-}	0.33	0.02	0.3
Σ	318.33	5.2	100.0

Härten

Gesamthärte (° dH)	1.0
Carbonathärte(° dH)	1.0
Nichtcarbonathärte (°dH)	0.0
Erdalkalien (mmol/l)	3.3

Berechnung des CO_2

lg(pCO_2)	-3.19
freies CO_2 (mg/l)	1.46
freies CO_2 (mmol/l)	0.0331

Berechneter Ammoniakgehalt

NH_3 (mg/l)	n.b.

Ges. Ionengehalt	436 mg/l	10.3 mmol/l

Ionenbilanz

Σ Kationen (meq/l)	5.21	*-0.5 %*
Σ Anionen (meq/l)	5.24	

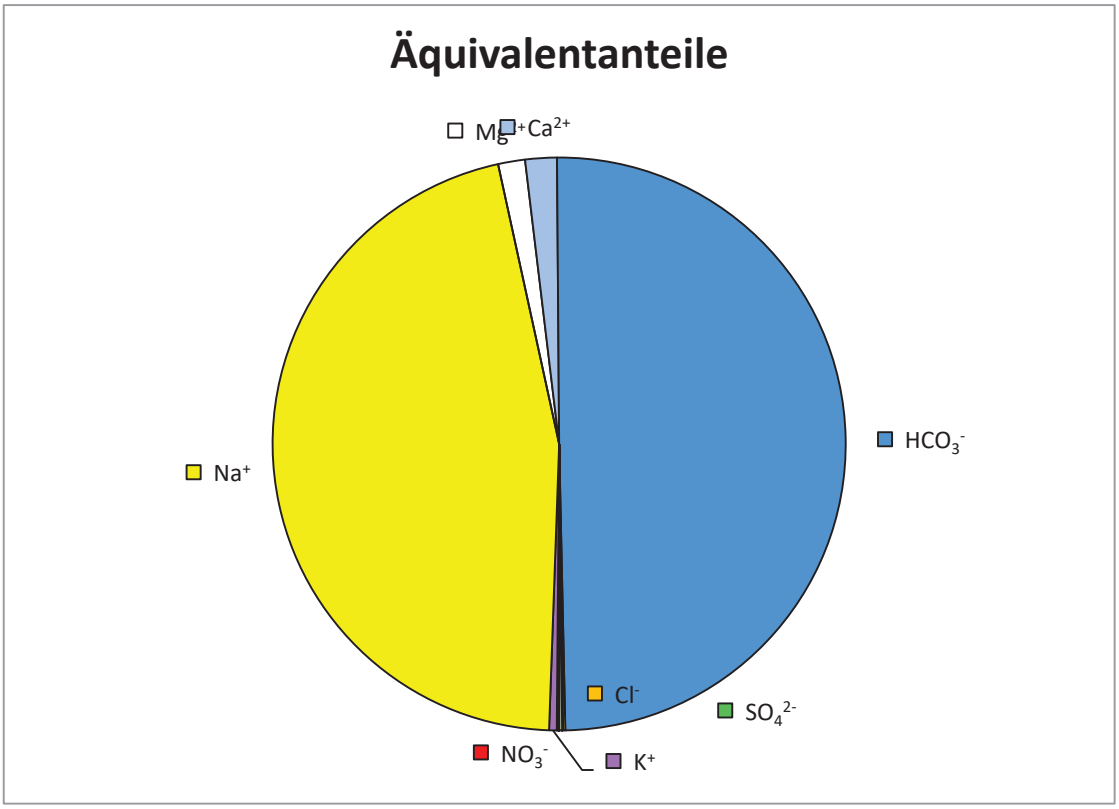

Wasseranalyse

Geologische Bundesanstalt
FA Geochemie
Leitung: HR Mag. Dr. Gerhard Hobiger

Probenahmepunkt:		**19**		
Koordinaten	**M** n.b.	**RW:** E13° 49.150'	**HW:** N48° 21.584'	**GOK (m ü. A.)** n.b.
Bezeichnung:	**19**		**Geochemie-Nr.:**	**GCH-2017-078-004**
Probenahmetiefe (m):	**50**	**Probenehmer:**	**Be/Pö**	
Probenahmedatum und Uhrzeit:		**09.11.2017 13:30**	**Eingangsdatum:**	**10.11.2017**

Feldparameter

		QZV *	MAP **	IP ***			
el. LF (µS/cm) (Gel.)	**544**	2250		2500	**Schüttung (l/s)**		**n.b.**
el. LF (µS/cm) (Labor)	n.b.				**Redoxpotenzial (mV)**		**-18**
					Temperatur (°C)		**10.1**
pH (Gel.)	**7.38**			6,5 - 9,5	**Sauerstoff (O_2)**	**mg/l**	**0.27**
pH (Labor)	n.b.					**(%)**	**2.6**

Kationen (mg/l)

Ion	Messwert	QZV *	MAP **	IP ***
Calcium (Ca^{2+})	**86.8**			
Magnesium (Mg^{2+})	**21.1**			
Natrium (Na^{+})	**3.6**			200
Kalium (K^{+})	**1.3**			
Strontium (Sr^{2+})	**0.2215**			
Barium (Ba^{2+})	**0.0164**			
Lithium (Li^{+})	**0.0160**			
Rubidium (Rb^{+})	**0.0004**			
Cäsium (Cs^{+})	**< 0,0001**			
Ammonium (NH_4^{+})	**n.b.**	0.45		0.5
Eisen (Fe^{2+})	**0.231**			0.2
Mangan (Mn^{2+})	**0.0315**			0.05
Σ	**113.3**			

Anionen (mg/l)

Ion	Messwert	QZV *	MAP **	IP ***
Hydrogencarbonat (HCO_3^{-})	**347.79**			
Chlorid (Cl^{-})	**3.0**	180		200
Sulfat (SO_4^{2-})	**25.1**	225		250
Nitrat (NO_3^{-})	**1.6**	45	50	
Nitrit (NO_2^{-})	**n.b.**	0.09	0.1	
o- Phosphat (o-PO_4^{3-})	**n.b.**	0.3		
Sulfid (S^{2-})	**n.b.**			
Fluorid (F^{-})	**0.09**		1.5	
Σ	**377.5**			

Ges. Ionengehalt	**491 mg/l**	**Ionenbilanz**	
	9.3 mmol/l	***-0.9***	**%**
Dichte	**n.b. g/cm3**		

Spezielle Parameter (mg/l)

Parameter	Messwert	QZV *	MAP **	IP ***
Kupfer (Cu)	**0.0007**	1.8	2	
Zink (Zn)	**0.0073**			
Blei (Pb)	**< 0,0001**	0.009	0.025	
Cadmium (Cd)	**< 0,0001**	0.0045	0.005	
Aluminium (Al)	**0.0016**			0.2
Arsen (As)	**0.0010**	0.009	0.01	
Antimon (Sb)	**n.b.**		0.005	
Chrom (Cr)	**0.0002**	0.045		
Nickel (Ni)	**0.0001**	0.018		
Quecksilber (Hg)	**n.b.**	0.0009	0.001	
Bor (B)	**n.b.**		1	
Uran (U)	**0.0009**		0.015	
Thorium (Th)	**n.b.**			
Cobalt (Co)	**0.0002**			
Molybdän (Mo)	**0.0006**			
Vanadium (V)	**< 0,0001**			
Selen (Se)	**n.b.**		0.01	
Tellur (Te)	**n.b.**			
Niob (Nb)	**n.b.**			
H_2SiO_3	**n.b.**			

Spezielle Parameter (mg/l)

Parameter	Messwert
Lanthan (La)	**n.b.**
Cer (Ce)	**n.b.**
Praseodym (Pr)	**n.b.**
Neodym (Nd)	**n.b.**
Samarium (Sm)	**n.b.**
Europium (Eu)	**n.b.**
Gadolimium (Gd)	**n.b.**
Terbium (Tb)	**n.b.**
Dysprosium (Dy)	**n.b.**
Holmium (Ho)	**n.b.**
Erbium (Er)	**n.b.**
Thulium (Tm)	**n.b.**
Ytterbium (Yb)	**n.b.**
Lutetium (Lu)	**n.b.**
Zinn (Sn)	**n.b.**
Thallium (Tl)	**n.b.**
Silber (Ag)	**n.b.**
Beryllium (Be)	**n.b.**
Bismut (Bi)	**n.b.**
Gallium (Ga)	**n.b.**

n.b. .. nicht bestimmt

* ... Qualitätszielverordnung Chemie Grundwasser QZV Chemie GW (BGBl. II 98/2010)

** ... Mindestanforderungsparameter aus der Trinkwasserverordnung - TWV (BGBl. II 304/2001)

*** ... Indikatorparameter aus der Trinkwasserverordnung - TWV (BGBl. II 304/2001)

Layout: G. Hobiger

Geologische Bundesanstalt
FA Geochemie
Leitung: HR Mag. Dr. Gerhard Hobiger

Berechnungen aus den Analysenwerten

Äquivalentanteile

Kationen

Ion	Messwert mg/l	meq/l	eq%
Ca^{2+}	86.79	4.33	69.00
Mg^{2+}	21.15	1.74	27.72
Na^{+}	3.61	0.16	2.50
K^{+}	1.26	0.03	0.51
Sr^{2+}	0.22	0.01	0.08
Ba^{2+}	0.016	0.00	0.0
Li^{+}	0.016	0.00	0.04
Rb^{+}	0.000	0.00	0.00
Cs^{+}	< 0,0001	0.00	0.00
NH_4^{+}	n.b.	n.b.	n.b.
Fe^{2+}	0.231	0.01	0.1
Mn^{2+}	0.0315	0.00	0.0
Σ	113.33	6.3	100.0

Anionen

Ion	Messwert mg/l	meq/l	eq%
HCO_3^{-}	347.79	5.70	90.0
Cl^{-}	2.99	0.08	1.3
SO_4^{2-}	25.08	0.52	8.2
NO_3^{-}	1.58	0.03	0.4
NO_2^{-}	n.b.	n.b.	n.b.
$o\text{-}PO_4^{3-}$	n.b.	n.b.	n.b.
S^{2-}	n.b.	n.b.	n.b.
F^{-}	0.09	0.00	0.1
Σ	377.53	6.3	100.0

Härten

Gesamthärte (° dH)	17.0
Carbonathärte(° dH)	16.0
Nichtcarbonathärte (°dH)	1.0
Erdalkalien (mmol/l)	48.4

Berechnung des CO_2

$lg(pCO_2)$	-1.94
freies CO_2 (mg/l)	27.11
freies CO_2 (mmol/l)	0.6159

Berechneter Ammoniakgehalt

NH_3 (mg/l)	n.b.

Ges. Ionengehalt	491 mg/l	9.3 mmol/l

Ionenbilanz

Σ Kationen (meq/l)	6.28	*-0.9 %*
Σ Anionen (meq/l)	6.34	

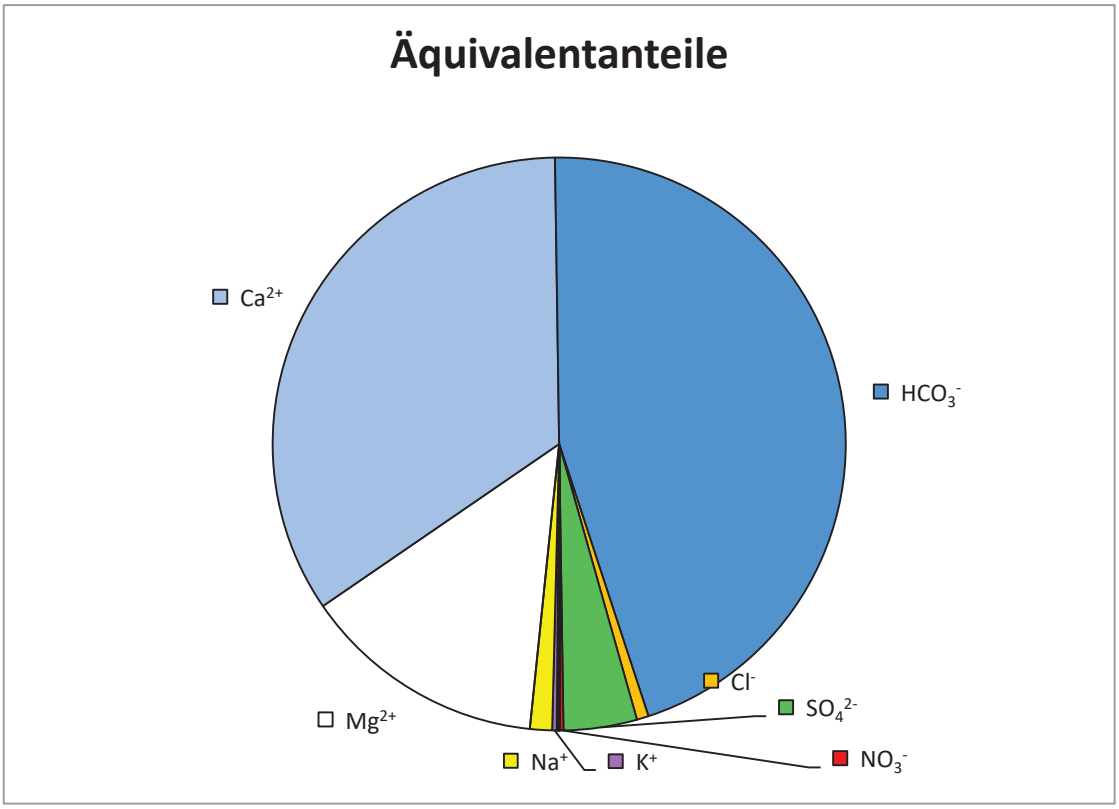

Wasseranalyse

Geologische Bundesanstalt
FA Geochemie
Leitung: HR Mag. Dr. Gerhard Hobiger

Probenahmepunkt:		**20**		
Koordinaten	**M** n.b.	**RW:** E13° 45.937'	**HW:** N48° 20.635'	**GOK (m ü. A.)** n.b.
Bezeichnung:	**20**		**Geochemie-Nr.:**	**GCH-2017-078-005**
Probenahmetiefe:	**n.b.**	**Probenehmer:**	**Be/Pö**	
Probenahmedatum und Uhrzeit:		**09.11.2017 14:15**	**Eingangsdatum:**	**10.11.2017**

Feldparameter

		QZV *	MAP **	IP ***			
el. LF (µS/cm) (Gel.)	**511**	2250		2500	**Schüttung (l/s)**		**n.b.**
el. LF (µS/cm) (Labor)	n.b.				**Redoxpotenzial (mV)**		**75**
					Temperatur (°C)		**10.7**
pH (Gel.)	**6.59**			6,5 - 9,5	**Sauerstoff (O_2)**	**mg/l**	**0.07**
pH (Labor)	n.b.					**(%)**	**0.7**

Kationen (mg/l)

Ion	Messwert	QZV *	MAP **	IP ***
Calcium (Ca^{2+})	**61.3**			
Magnesium (Mg^{2+})	**17.6**			
Natrium (Na^{+})	**20.9**			200
Kalium (K^{+})	**1.8**			
Strontium (Sr^{2+})	**0.2039**			
Barium (Ba^{2+})	**0.0273**			
Lithium (Li^{+})	**0.0173**			
Rubidium (Rb^{+})	**0.0025**			
Cäsium (Cs^{+})	**< 0,0001**			
Ammonium (NH_4^{+})	**n.b.**	0.45		0.5
Eisen (Fe^{2+})	**0.138**			0.2
Mangan (Mn^{2+})	**0.8829**			0.05
Σ	**102.9**			

Anionen (mg/l)

Ion	Messwert	QZV *	MAP **	IP ***
Hydrogencarbonat (HCO_3^{-})	**244.06**			
Chlorid (Cl^{-})	**19.1**	180		200
Sulfat (SO_4^{2-})	**44.4**	225		250
Nitrat (NO_3^{-})	**<0,5**	45	50	
Nitrit (NO_2^{-})	**n.b.**	0.09	0.1	
o- Phosphat (o-PO_4^{3-})	**n.b.**	0.3		
Sulfid (S^{2-})	**n.b.**			
Fluorid (F^{-})	**0.11**		1.5	
Σ	**307.7**			

Ges. Ionengehalt	**411 mg/l**	**Ionenbilanz**	
	8.2 mmol/l	***0.7***	**%**
Dichte	**n.b. g/cm3**		

Spezielle Parameter (mg/l)

Parameter	Messwert	QZV *	MAP **	IP ***
Kupfer (Cu)	**0.0015**	1.8	2	
Zink (Zn)	**0.0199**			
Blei (Pb)	**< 0,0001**	0.009	0.025	
Cadmium (Cd)	**< 0,0001**	0.0045	0.005	
Aluminium (Al)	**0.0028**			0.2
Arsen (As)	**0.0014**	0.009	0.01	
Antimon (Sb)	**n.b.**		0.005	
Chrom (Cr)	**0.0003**	0.045		
Nickel (Ni)	**0.0024**	0.018		
Quecksilber (Hg)	**n.b.**	0.0009	0.001	
Bor (B)	**n.b.**		1	
Uran (U)	**0.0004**		0.015	
Thorium (Th)	**n.b.**			
Cobalt (Co)	**0.0006**			
Molybdän (Mo)	**0.0023**			
Vanadium (V)	**0.0002**			
Selen (Se)	**n.b.**		0.01	
Tellur (Te)	**n.b.**			
Niob (Nb)	**n.b.**			
H_2SiO_3	**n.b.**			

Spezielle Parameter (mg/l)

Parameter	Messwert
Lanthan (La)	**n.b.**
Cer (Ce)	**n.b.**
Praseodym (Pr)	**n.b.**
Neodym (Nd)	**n.b.**
Samarium (Sm)	**n.b.**
Europium (Eu)	**n.b.**
Gadolimium (Gd)	**n.b.**
Terbium (Tb)	**n.b.**
Dysprosium (Dy)	**n.b.**
Holmium (Ho)	**n.b.**
Erbium (Er)	**n.b.**
Thulium (Tm)	**n.b.**
Ytterbium (Yb)	**n.b.**
Lutetium (Lu)	**n.b.**
Zinn (Sn)	**n.b.**
Thallium (Tl)	**n.b.**
Silber (Ag)	**n.b.**
Beryllium (Be)	**n.b.**
Bismut (Bi)	**n.b.**
Gallium (Ga)	**n.b.**

n.b. .. nicht bestimmt

* ... Qualitätszielverordnung Chemie Grundwasser QZV Chemie GW (BGBl. II 98/2010)

** ... Mindestanforderungsparameter aus der Trinkwasserverordnung - TWV (BGBl. II 304/2001)

*** ... Indikatorparameter aus der Trinkwasserverordnung - TWV (BGBl. II 304/2001)

Layout: G. Hobiger

Geologische Bundesanstalt
FA Geochemie
Leitung: HR Mag. Dr. Gerhard Hobiger

Berechnungen aus den Analysenwerten

Äquivalentanteile

Kationen

Ion	Messwert mg/l	meq/l	eq%
Ca^{2+}	61.34	3.06	55.54
Mg^{2+}	17.64	1.45	26.33
Na^{+}	20.90	0.91	16.49
K^{+}	1.79	0.05	0.83
Sr^{2+}	0.20	0.00	0.08
Ba^{2+}	0.027	0.00	0.0
Li^{+}	0.017	0.00	0.05
Rb^{+}	0.003	0.00	0.00
Cs^{+}	< 0,0001	0.00	0.00
NH_4^{+}	n.b.	n.b.	n.b.
Fe^{2+}	0.138	0.00	0.1
Mn^{2+}	0.8829	0.03	0.6
Σ	102.93	5.5	100.0

Anionen

Ion	Messwert mg/l	meq/l	eq%
HCO_3^{-}	244.06	4.00	73.1
Cl^{-}	19.14	0.54	9.9
SO_4^{2-}	44.43	0.93	16.9
NO_3^{-}	<0,5	0.00	0.0
NO_2^{-}	n.b.	n.b.	n.b.
$o\text{-}PO_4^{3-}$	n.b.	n.b.	n.b.
S^{2-}	n.b.	n.b.	n.b.
F^{-}	0.11	0.01	0.1
Σ	307.75	5.5	100.0

Härten

Gesamthärte (° dH)	12.7
Carbonathärte(° dH)	11.2
Nichtcarbonathärte (°dH)	1.4
Erdalkalien (mmol/l)	41.0

Berechnung des CO_2

lg(pCO_2)	-1.30
freies CO_2 (mg/l)	116.69
freies CO_2 (mmol/l)	2.6515

Berechneter Ammoniakgehalt

NH_3 (mg/l)	n.b.

Ges. Ionengehalt	411 mg/l	8.2 mmol/l

Ionenbilanz

Σ Kationen (meq/l)	5.51	*0.7 %*
Σ Anionen (meq/l)	5.47	

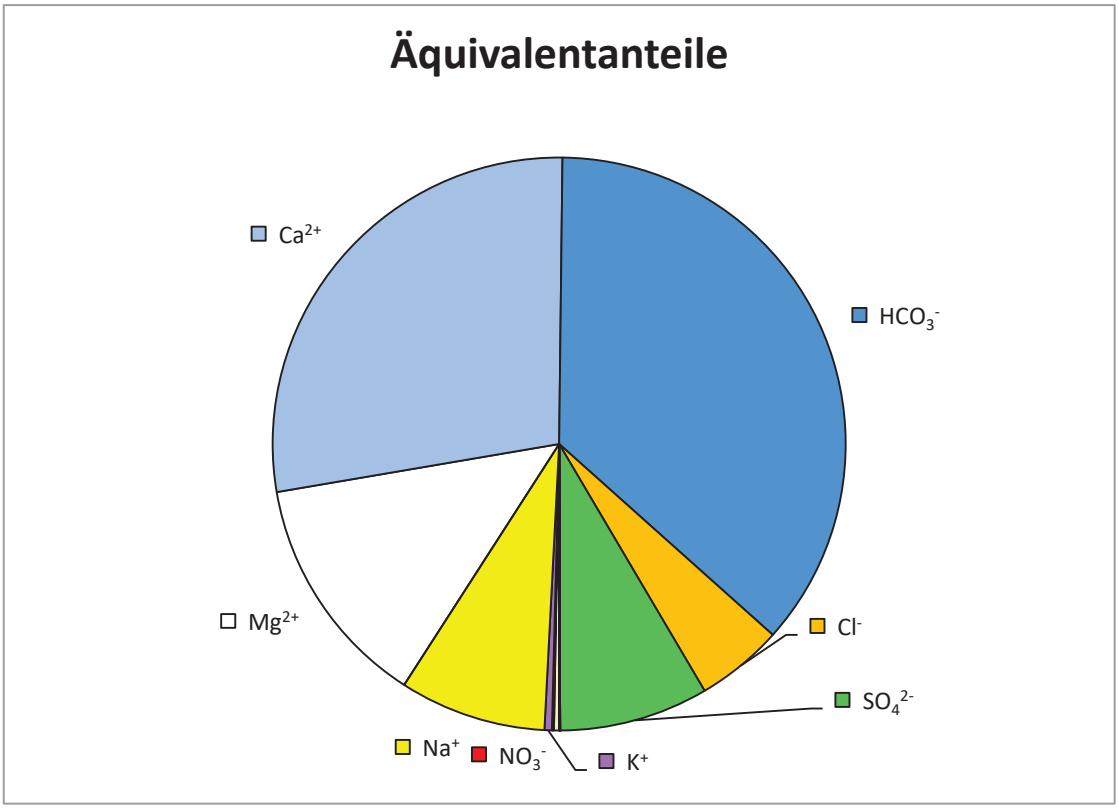

Wasseranalyse

Geologische Bundesanstalt
FA Geochemie
Leitung: HR Mag. Dr. Gerhard Hobiger

Probenahmepunkt:		**21**		
Koordinaten	**M** n.b.	**RW:** E13° 45.018'	**HW:** N48° 23.280'	**GOK (m ü. A.)** n.b.
Bezeichnung:	**21**		**Geochemie-Nr.:**	**GCH-2017-078-006**
Probenahmetiefe (m):	**55**	**Probenehmer:**	**Be/Pö**	
Probenahmedatum und Uhrzeit:		**09.11.2017 15:30**	**Eingangsdatum:**	**10.11.2017**

Feldparameter

		QZV *	MAP **	IP ***			
el. LF (µS/cm) (Gel.)	**154**	2250		2500	**Schüttung (l/s)**		**n.b.**
el. LF (µS/cm) (Labor)	n.b.				**Redoxpotenzial (mV)**		**175**
					Temperatur (°C)		**10.5**
pH (Gel.)	**6.44**			6,5 - 9,5	**Sauerstoff (O_2)**	**mg/l**	**8.39**
pH (Labor)	n.b.					**(%)**	**79**

Kationen (mg/l)

Ion	Messwert	QZV *	MAP **	IP ***
Calcium (Ca^{2+})	**20.5**			
Magnesium (Mg^{2+})	**3.0**			
Natrium (Na^{+})	**4.2**			200
Kalium (K^{+})	**0.7**			
Strontium (Sr^{2+})	**0.0365**			
Barium (Ba^{2+})	**0.0353**			
Lithium (Li^{+})	**0.0026**			
Rubidium (Rb^{+})	**0.0001**			
Cäsium (Cs^{+})	**< 0,0001**			
Ammonium (NH_4^{+})	**n.b.**	0.45		0.5
Eisen (Fe^{2+})	**0.001**			0.2
Mangan (Mn^{2+})	**0.0038**			0.05
Σ	**28.5**			

Anionen (mg/l)

Ion	Messwert	QZV *	MAP **	IP ***
Hydrogencarbonat (HCO_3^{-})	**67.12**			
Chlorid (Cl^{-})	**1.8**	180		200
Sulfat (SO_4^{2-})	**3.8**	225		250
Nitrat (NO_3^{-})	**15.5**	45	50	
Nitrit (NO_2^{-})	**n.b.**	0.09	0.1	
o- Phosphat (o-PO_4^{3-})	**n.b.**	0.3		
Sulfid (S^{2-})	**n.b.**			
Fluorid (F^{-})	**0.07**		1.5	
Σ	**88.3**			

Ges. Ionengehalt	**117 mg/l**	**Ionenbilanz**	
	2.3 mmol/l	***-0.7***	**%**
Dichte	**n.b. g/cm3**		

Spezielle Parameter (mg/l)

Parameter	Messwert	QZV *	MAP **	IP ***
Kupfer (Cu)	**0.0007**	1.8	2	
Zink (Zn)	**0.0119**			
Blei (Pb)	**< 0,0001**	0.009	0.025	
Cadmium (Cd)	**< 0,0001**	0.0045	0.005	
Aluminium (Al)	**0.0021**			0.2
Arsen (As)	**0.0002**	0.009	0.01	
Antimon (Sb)	**n.b.**		0.005	
Chrom (Cr)	**0.0009**	0.045		
Nickel (Ni)	**< 0,0001**	0.018		
Quecksilber (Hg)	**n.b.**	0.0009	0.001	
Bor (B)	**n.b.**		1	
Uran (U)	**< 0,0001**		0.015	
Thorium (Th)	**n.b.**			
Cobalt (Co)	**< 0,0001**			
Molybdän (Mo)	**< 0,0001**			
Vanadium (V)	**0.0003**			
Selen (Se)	**n.b.**		0.01	
Tellur (Te)	**n.b.**			
Niob (Nb)	**n.b.**			
H_2SiO_3	**n.b.**			

Spezielle Parameter (mg/l)

Parameter	Messwert
Lanthan (La)	**n.b.**
Cer (Ce)	**n.b.**
Praseodym (Pr)	**n.b.**
Neodym (Nd)	**n.b.**
Samarium (Sm)	**n.b.**
Europium (Eu)	**n.b.**
Gadolimium (Gd)	**n.b.**
Terbium (Tb)	**n.b.**
Dysprosium (Dy)	**n.b.**
Holmium (Ho)	**n.b.**
Erbium (Er)	**n.b.**
Thulium (Tm)	**n.b.**
Ytterbium (Yb)	**n.b.**
Lutetium (Lu)	**n.b.**
Zinn (Sn)	**n.b.**
Thallium (Tl)	**n.b.**
Silber (Ag)	**n.b.**
Beryllium (Be)	**n.b.**
Bismut (Bi)	**n.b.**
Gallium (Ga)	**n.b.**

n.b. .. nicht bestimmt

* ... Qualitätszielverordnung Chemie Grundwasser QZV Chemie GW (BGBl. II 98/2010)

** ... Mindestanforderungsparameter aus der Trinkwasserverordnung - TWV (BGBl. II 304/2001)

*** ... Indikatorparameter aus der Trinkwasserverordnung - TWV (BGBl. II 304/2001)

Layout: G. Hobiger

Geologische Bundesanstalt
FA Geochemie
Leitung: HR Mag. Dr. Gerhard Hobiger

Berechnungen aus den Analysenwerten

Äquivalentanteile

Kationen

Ion	Messwert mg/l	meq/l	eq%
Ca^{2+}	20.53	1.02	69.53
Mg^{2+}	2.97	0.24	16.57
Na^{+}	4.24	0.18	12.53
K^{+}	0.72	0.02	1.24
Sr^{2+}	0.04	0.00	0.06
Ba^{2+}	0.035	0.00	0.0
Li^{+}	0.003	0.00	0.03
Rb^{+}	0.000	0.00	0.00
Cs^{+}	< 0,0001	0.00	0.00
NH_4^{+}	n.b.	n.b.	n.b.
Fe^{2+}	0.001	0.00	0.0
Mn^{2+}	0.0038	0.00	0.0
Σ	28.53	1.5	100.0

Anionen

Ion	Messwert mg/l	meq/l	eq%
HCO_3^{-}	67.12	1.10	74.1
Cl^{-}	1.79	0.05	3.4
SO_4^{2-}	3.80	0.08	5.3
NO_3^{-}	15.54	0.25	16.9
NO_2^{-}	n.b.	n.b.	n.b.
$o\text{-}PO_4^{3-}$	n.b.	n.b.	n.b.
S^{2-}	n.b.	n.b.	n.b.
F^{-}	0.07	0.00	0.2
Σ	88.31	1.5	100.0

Härten

Gesamthärte (° dH)	3.6
Carbonathärte(° dH)	3.1
Nichtcarbonathärte (°dH)	0.5
Erdalkalien (mmol/l)	43.1

Berechnung des CO_2

lg(pCO_2)	-1.69
freies CO_2 (mg/l)	47.89
freies CO_2 (mmol/l)	1.0882

Berechneter Ammoniakgehalt

NH_3 (mg/l)	n.b.

Ges. Ionengehalt	117 mg/l	2.3 mmol/l

Ionenbilanz

Σ Kationen (meq/l)	1.47	-0.7 %
Σ Anionen (meq/l)	1.48	

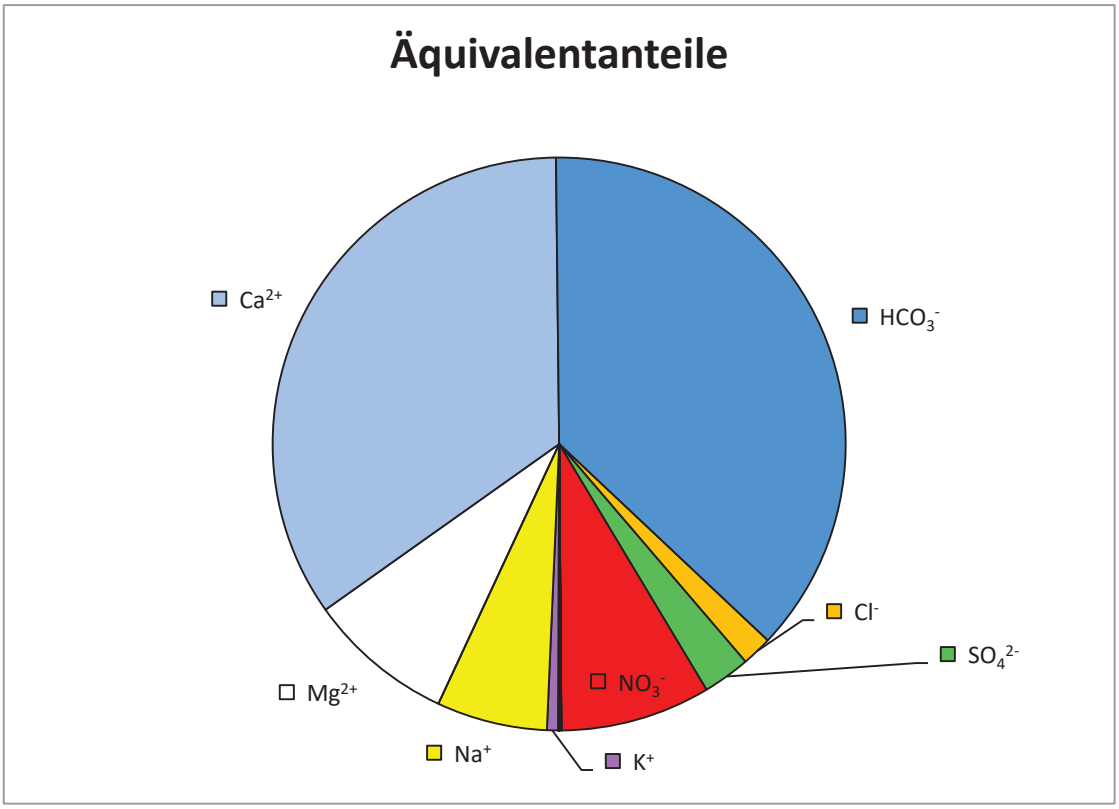

Wasseranalyse

Geologische Bundesanstalt
FA Geochemie
Leitung: HR Mag. Dr. Gerhard Hobiger

Probenahmepunkt:			**22**		
Koordinaten	**M** n.b.	**RW:** N48° 20.817'	**HW:** E13° 30.098'	**GOK (m ü. A.)**	n.b.
Bezeichnung:	**22**		**Geochemie-Nr.:**	**GCH-2018-006-001**	
Probenahmetiefe:	n.b.	**Probenehmer:**	**Pö/Be**		
Probenahmedatum und Uhrzeit:		**22.01.2018 09:30**	**Eingangsdatum:**	**24.01.2018**	

Feldparameter

		QZV *	MAP **	IP ***			
el. LF (µS/cm) (Gel.)	**571**	2250		2500	**Schüttung (l/s)**		n.b.
el. LF (µS/cm) (Labor)	n.b.				**Redoxpotenzial (mV)**		n.b.
					Temperatur (°C)		10
pH (Gel.)	**7.44**			6,5 - 9,5	**Sauerstoff (O_2)**	mg/l	n.b.
pH (Labor)	n.b.					(%)	n.b.

Kationen (mg/l)

Ion	Messwert	QZV *	MAP **	IP ***
Calcium (Ca^{2+})	70.6			
Magnesium (Mg^{2+})	26.0			
Natrium (Na^{+})	6.6			200
Kalium (K^{+})	1.8			
Strontium (Sr^{2+})	0.3750			
Barium (Ba^{2+})	0.0388			
Lithium (Li^{+})	0.0298			
Rubidium (Rb^{+})	0.0009			
Cäsium (Cs^{+})	< 0,0001			
Ammonium (NH_4^{+})	n.b.	0.45		0.5
Eisen (Fe^{2+})	1.857			0.2
Mangan (Mn^{2+})	0.0659			0.05
Σ	107.4			

Anionen (mg/l)

Ion	Messwert	QZV *	MAP **	IP ***
Hydrogencarbonat (HCO_3^{-})	335.59			
Chlorid (Cl^{-})	7.3	180		200
Sulfat (SO_4^{2-})	21.8	225		250
Nitrat (NO_3^{-})	<0,5	45	50	
Nitrit (NO_2^{-})	n.b.	0.09	0.1	
o- Phosphat (o-PO_4^{3-})	n.b.	0.3		
Sulfid (S^{2-})	n.b.			
Fluorid (F^{-})	0.10		1.5	
Σ	364.8			

Ges. Ionengehalt	**472** mg/l	**Ionenbilanz**	
	9.1 mmol/l	***-1.4***	**%**
Dichte	n.b. g/cm3		

Spezielle Parameter (mg/l)

Parameter	Messwert	QZV *	MAP **	IP ***
Kupfer (Cu)	< 0,0001	1.8	2	
Zink (Zn)	0.0404			
Blei (Pb)	< 0,0001	0.009	0.025	
Cadmium (Cd)	< 0,0001	0.0045	0.005	
Aluminium (Al)	0.0008			0.2
Arsen (As)	0.0001	0.009	0.01	
Antimon (Sb)	n.b.		0.005	
Chrom (Cr)	< 0,0001	0.045		
Nickel (Ni)	< 0,0001	0.018		
Quecksilber (Hg)	n.b.	0.0009	0.001	
Bor (B)	n.b.		1	
Uran (U)	< 0,0001		0.015	
Thorium (Th)	n.b.			
Cobalt (Co)	< 0,0001			
Molybdän (Mo)	0.0008			
Vanadium (V)	< 0,0001			
Selen (Se)	n.b.		0.01	
Tellur (Te)	n.b.			
Niob (Nb)	n.b.			
Silicium (Si)	n.b.			

Spezielle Parameter (mg/l)

Parameter	Messwert
Lanthan (La)	n.b.
Cer (Ce)	n.b.
Praseodym (Pr)	n.b.
Neodym (Nd)	n.b.
Samarium (Sm)	n.b.
Europium (Eu)	n.b.
Gadolimium (Gd)	n.b.
Terbium (Tb)	n.b.
Dysprosium (Dy)	n.b.
Holmium (Ho)	n.b.
Erbium (Er)	n.b.
Thulium (Tm)	n.b.
Ytterbium (Yb)	n.b.
Lutetium (Lu)	n.b.
Zinn (Sn)	n.b.
Thallium (Tl)	n.b.
Silber (Ag)	n.b.
Beryllium (Be)	n.b.
Bismut (Bi)	n.b.
Gallium (Ga)	n.b.

Die HCO3- Konzentration wurde berechnet

n.b. .. nicht bestimmt

* ... Qualitätszielverordnung Chemie Grundwasser QZV Chemie GW (BGBl. II 98/2010)

** ... Mindestanforderungsparameter aus der Trinkwasserverordnung - TWV (BGBl. II 304/2001)

*** ... Indikatorparameter aus der Trinkwasserverordnung - TWV (BGBl. II 304/2001)

Layout: G. Hobiger

Geologische Bundesanstalt
FA Geochemie
Leitung: HR Mag. Dr. Gerhard Hobiger

Berechnungen aus den Analysenwerten

Äquivalentanteile

Kationen

Ion	Messwert mg/l	meq/l	eq%
Ca^{2+}	70.59	3.52	57.96
Mg^{2+}	25.99	2.14	35.19
Na^{+}	6.61	0.29	4.73
K^{+}	1.80	0.05	0.76
Sr^{2+}	0.37	0.01	0.14
Ba^{2+}	0.039	0.00	0.0
Li^{+}	0.030	0.00	0.07
Rb^{+}	0.001	0.00	0.00
Cs^{+}	< 0,0001	0.00	0.00
NH_4^{+}	n.b.	n.b.	n.b.
Fe^{2+}	1.857	0.07	1.1
Mn^{2+}	0.0659	0.00	0.0
Σ	107.36	6.1	100.0

Anionen

Ion	Messwert mg/l	meq/l	eq%
HCO_3^{-}	335.59	5.50	89.2
Cl^{-}	7.35	0.21	3.4
SO_4^{2-}	21.78	0.45	7.4
NO_3^{-}	<0,5	0.00	0.0
NO_2^{-}	n.b.	n.b.	n.b.
$o\text{-}PO_4^{3-}$	n.b.	n.b.	n.b.
S^{2-}	n.b.	n.b.	n.b.
F^{-}	0.10	0.01	0.1
Σ	364.82	6.2	100.0

Härten

Gesamthärte (° dH)	15.9
Carbonathärte(° dH)	15.4
Nichtcarbonathärte (°dH)	0.5
Erdalkalien (mmol/l)	46.7

Berechnung des CO_2

$lg(pCO_2)$	-2.01
freies CO_2 (mg/l)	22.88
freies CO_2 (mmol/l)	0.5200

Berechneter Ammoniakgehalt

NH_3 (mg/l)	n.b.

Ges. Ionengehalt	472 mg/l	9.1 mmol/l

Ionenbilanz

Σ Kationen (meq/l)	6.08	*-1.4 %*
Σ Anionen (meq/l)	6.17	

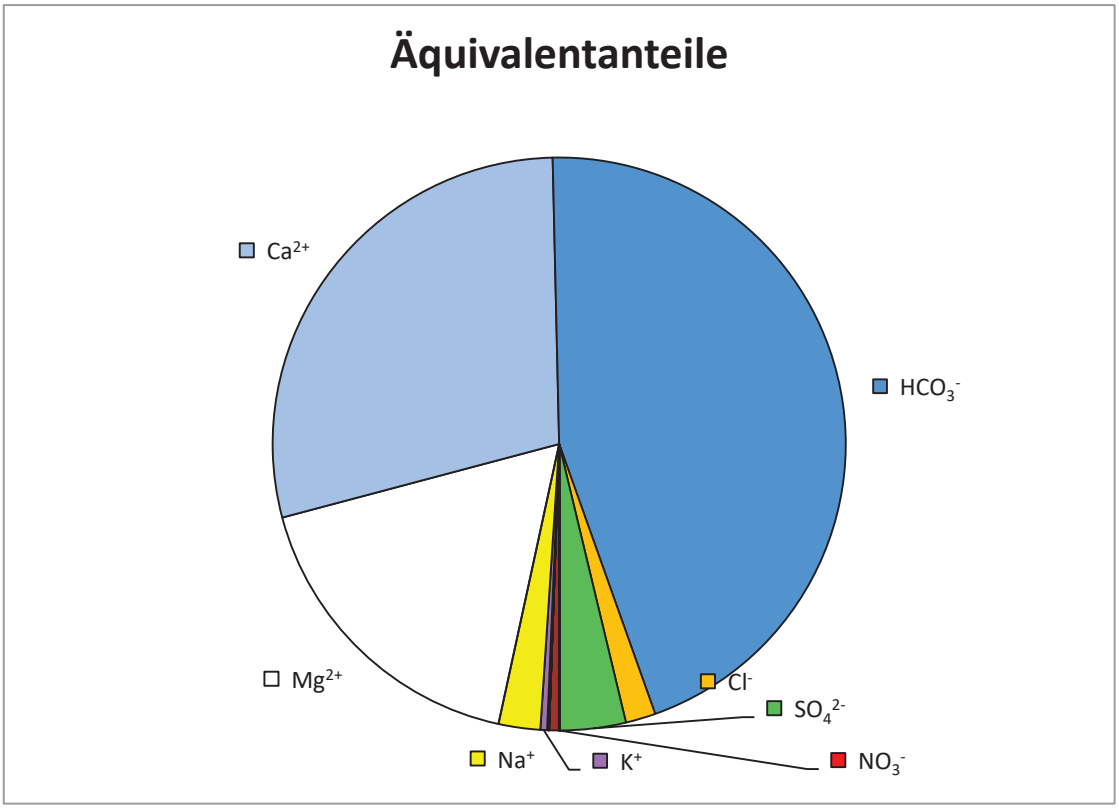

Wasseranalyse

Geologische Bundesanstalt
FA Geochemie
Leitung: HR Mag. Dr. Gerhard Hobiger

Probenahmepunkt:			**23**		
Koordinaten	**M** n.b.	**RW:** N48° 21.195'	**HW:** E13° 30.135'	**GOK (m ü. A.)**	n.b.
Bezeichnung:	**23**		**Geochemie-Nr.:**	**GCH-2018-006-002**	
Probenahmetiefe:	n.b.	**Probenehmer:**	**Pö/Be**		
Probenahmedatum und Uhrzeit:		**22.01.2018 10:45**	**Eingangsdatum:**	**24.01.2018**	

Feldparameter

		QZV *	MAP **	IP ***			
el. LF (µS/cm) (Gel.)	**605**	2250		2500	**Schüttung (l/s)**		**n.b.**
el. LF (µS/cm) (Labor)	n.b.				**Redoxpotenzial (mV)**		**-168**
					Temperatur (°C)		**9.7**
pH (Gel.)	**7.48**			6,5 - 9,5	**Sauerstoff (O_2)**	**mg/l**	**0.5**
pH (Labor)	n.b.					**(%)**	**0.4**

Kationen (mg/l)

Ion	Messwert	QZV *	MAP **	IP ***
Calcium (Ca^{2+})	74.7			
Magnesium (Mg^{2+})	28.4			
Natrium (Na^{+})	6.7			200
Kalium (K^{+})	4.8			
Strontium (Sr^{2+})	0.6474			
Barium (Ba^{2+})	0.0554			
Lithium (Li^{+})	0.0316			
Rubidium (Rb^{+})	0.0012			
Cäsium (Cs^{+})	< 0,0001			
Ammonium (NH_4^{+})	n.b.	0.45		0.5
Eisen (Fe^{2+})	0.677			0.2
Mangan (Mn^{2+})	0.0357			0.05
Σ	116.2			

Anionen (mg/l)

Ion	Messwert	QZV *	MAP **	IP ***
Hydrogencarbonat (HCO_3^{-})	356.9			
Chlorid (Cl^{-})	6.3	180		200
Sulfat (SO_4^{2-})	27.8	225		250
Nitrat (NO_3^{-})	<0,5	45	50	
Nitrit (NO_2^{-})	n.b.	0.09	0.1	
o- Phosphat (o-PO_4^{3-})	n.b.	0.3		
Sulfid (S^{2-})	n.b.			
Fluorid (F^{-})	0.11		1.5	
Σ	391.2			

Ges. Ionengehalt	**507** mg/l	**Ionenbilanz**	
	9.8 mmol/l	***-1.2***	**%**
Dichte	n.b. g/cm3		

Spezielle Parameter (mg/l)

Parameter	Messwert	QZV *	MAP **	IP ***
Kupfer (Cu)	0.0004	1.8	2	
Zink (Zn)	0.0055			
Blei (Pb)	< 0,0001	0.009	0.025	
Cadmium (Cd)	< 0,0001	0.0045	0.005	
Aluminium (Al)	0.0385			0.2
Arsen (As)	< 0,0001	0.009	0.01	
Antimon (Sb)	n.b.		0.005	
Chrom (Cr)	< 0,0001	0.045		
Nickel (Ni)	< 0,0001	0.018		
Quecksilber (Hg)	n.b.	0.0009	0.001	
Bor (B)	n.b.		1	
Uran (U)	< 0,0001		0.015	
Thorium (Th)	n.b.			
Cobalt (Co)	< 0,0001			
Molybdän (Mo)	0.0008			
Vanadium (V)	< 0,0001			
Selen (Se)	n.b.		0.01	
Tellur (Te)	n.b.			
Niob (Nb)	n.b.			
Silicium (Si)	n.b.			

Spezielle Parameter (mg/l)

Parameter	Messwert
Lanthan (La)	n.b.
Cer (Ce)	n.b.
Praseodym (Pr)	n.b.
Neodym (Nd)	n.b.
Samarium (Sm)	n.b.
Europium (Eu)	n.b.
Gadolimium (Gd)	n.b.
Terbium (Tb)	n.b.
Dysprosium (Dy)	n.b.
Holmium (Ho)	n.b.
Erbium (Er)	n.b.
Thulium (Tm)	n.b.
Ytterbium (Yb)	n.b.
Lutetium (Lu)	n.b.
Zinn (Sn)	n.b.
Thallium (Tl)	n.b.
Silber (Ag)	n.b.
Beryllium (Be)	n.b.
Bismut (Bi)	n.b.
Gallium (Ga)	n.b.

n.b. .. nicht bestimmt

* ... Qualitätszielverordnung Chemie Grundwasser QZV Chemie GW (BGBl. II 98/2010)

** ... Mindestanforderungsparameter aus der Trinkwasserverordnung - TWV (BGBl. II 304/2001)

*** ... Indikatorparameter aus der Trinkwasserverordnung - TWV (BGBl. II 304/2001)

Layout: G. Hobiger

Geologische Bundesanstalt
FA Geochemie
Leitung: HR Mag. Dr. Gerhard Hobiger

Berechnungen aus den Analysenwerten

Äquivalentanteile

Kationen

Ion	Messwert mg/l	meq/l	eq%
Ca^{2+}	74.70	3.73	57.08
Mg^{2+}	28.44	2.34	35.84
Na^{+}	6.74	0.29	4.49
K^{+}	4.84	0.12	1.90
Sr^{2+}	0.65	0.01	0.23
Ba^{2+}	0.055	0.00	0.0
Li^{+}	0.032	0.00	0.07
Rb^{+}	0.001	0.00	0.00
Cs^{+}	< 0,0001	0.00	0.00
NH_4^{+}	n.b.	n.b.	n.b.
Fe^{2+}	0.677	0.02	0.4
Mn^{2+}	0.0357	0.00	0.0
Σ	116.18	6.5	100.0

Anionen

Ion	Messwert mg/l	meq/l	eq%
HCO_3^{-}	356.9	5.85	88.5
Cl^{-}	6.32	0.18	2.7
SO_4^{2-}	27.79	0.58	8.7
NO_3^{-}	<0,5	0.00	0.0
NO_2^{-}	n.b.	n.b.	n.b.
$o\text{-}PO_4^{3-}$	n.b.	n.b.	n.b.
S^{2-}	n.b.	n.b.	n.b.
F^{-}	0.11	0.01	0.1
Σ	391.16	6.6	100.0

Härten

Gesamthärte (° dH)	17.0
Carbonathärte(° dH)	16.4
Nichtcarbonathärte (°dH)	0.6
Erdalkalien (mmol/l)	46.6

Berechnung des CO_2

$lg(pCO_2)$	-2.03
freies CO_2 (mg/l)	22.26
freies CO_2 (mmol/l)	0.5058

Berechneter Ammoniakgehalt

NH_3 (mg/l)	n.b.

Ges. Ionengehalt	507 mg/l	9.8 mmol/l

Ionenbilanz

Σ Kationen (meq/l)	6.53	*-1.2 %*
Σ Anionen (meq/l)	6.61	

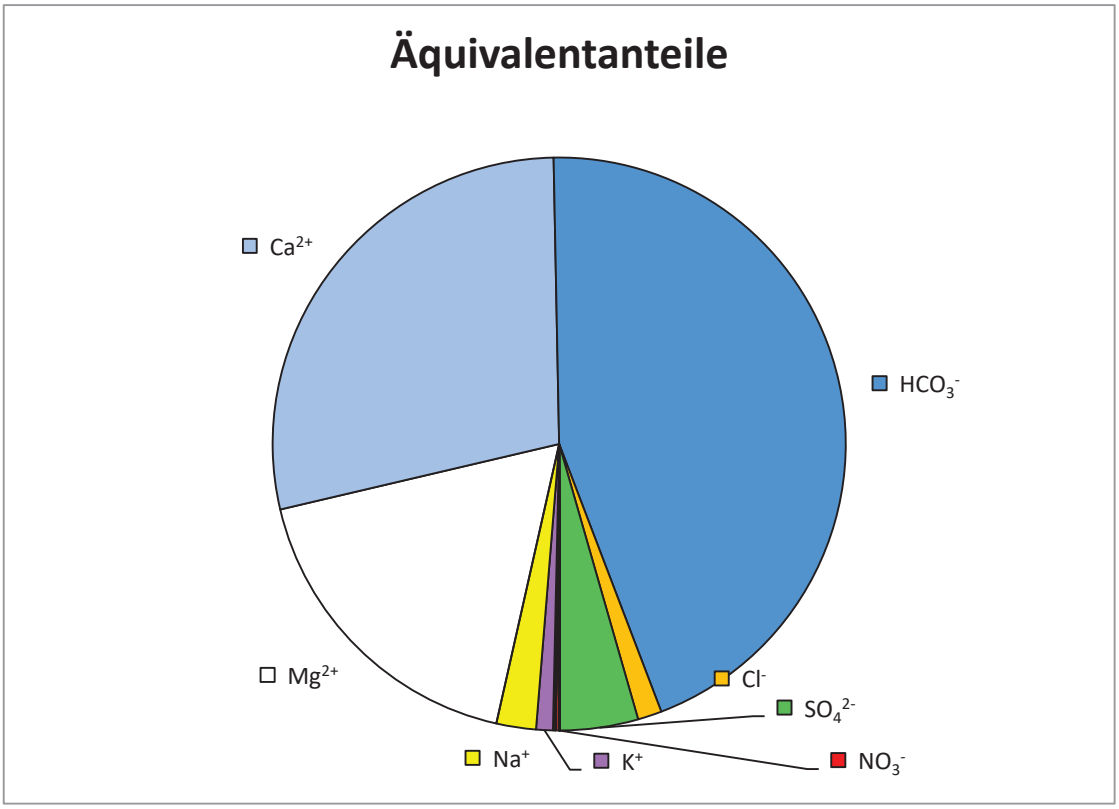

Wasseranalyse

Geologische Bundesanstalt
FA Geochemie
Leitung: HR Mag. Dr. Gerhard Hobiger

Probenahmepunkt:		**24**		
Koordinaten	**M** n.b.	**RW:** N48° 24.431'	**HW:** E13° 33.875'	**GOK (m ü. A.)** n.b.
Bezeichnung:	**24**		**Geochemie-Nr.:**	**GCH-2018-006-003**
Probenahmetiefe:	n.b.	**Probenehmer:**	**Pö/Be**	
Probenahmedatum und Uhrzeit:		**22.01.2018 11:35**	**Eingangsdatum:**	**24.01.2018**

Feldparameter

		QZV *	MAP **	IP ***			
el. LF (µS/cm) (Gel.)	**440**	2250		2500	**Schüttung (l/s)**		**n.b.**
el. LF (µS/cm) (Labor)	n.b.				**Redoxpotenzial (mV)**		**16.00**
					Temperatur (°C)		**12**
pH (Gel.)	**7.89**			6,5 - 9,5	**Sauerstoff (O_2)**	**mg/l**	**5.17**
pH (Labor)	n.b.					**(%)**	**50**

Kationen (mg/l)

Ion	Messwert	QZV *	MAP **	IP ***
Calcium (Ca^{2+})	**55.8**			
Magnesium (Mg^{2+})	**18.6**			
Natrium (Na^{+})	**20.7**			200
Kalium (K^{+})	**1.6**			
Strontium (Sr^{2+})	**0.9441**			
Barium (Ba^{2+})	**0.0462**			
Lithium (Li^{+})	**0.0362**			
Rubidium (Rb^{+})	**0.0024**			
Cäsium (Cs^{+})	**< 0,0001**			
Ammonium (NH_4^{+})	**n.b.**	0.45		0.5
Eisen (Fe^{2+})	**0.268**			0.2
Mangan (Mn^{2+})	**0.0044**			0.05
Σ	**98.0**			

Anionen (mg/l)

Ion	Messwert	QZV *	MAP **	IP ***
Hydrogencarbonat (HCO_3^{-})	**298**			
Chlorid (Cl^{-})	**0.6**	180		200
Sulfat (SO_4^{2-})	**17.8**	225		250
Nitrat (NO_3^{-})	**<0,5**	45	50	
Nitrit (NO_2^{-})	**n.b.**	0.09	0.1	
o- Phosphat (o-PO_4^{3-})	**n.b.**	0.3		
Sulfid (S^{2-})	**n.b.**			
Fluorid (F^{-})	**0.53**		1.5	
Σ	**316.9**			

Ges. Ionengehalt	**415 mg/l**	**Ionenbilanz**
	8.2 mmol/l	***-0.1*** **%**
Dichte	**n.b.** g/cm3	

Spezielle Parameter (mg/l)

Parameter	Messwert	QZV *	MAP **	IP ***
Kupfer (Cu)	**0.0010**	1.8	2	
Zink (Zn)	**0.0326**			
Blei (Pb)	**< 0,0001**	0.009	0.025	
Cadmium (Cd)	**< 0,0001**	0.0045	0.005	
Aluminium (Al)	**0.0049**			0.2
Arsen (As)	**< 0,0001**	0.009	0.01	
Antimon (Sb)	**n.b.**		0.005	
Chrom (Cr)	**< 0,0001**	0.045		
Nickel (Ni)	**< 0,0001**	0.018		
Quecksilber (Hg)	**n.b.**	0.0009	0.001	
Bor (B)	**n.b.**		1	
Uran (U)	**< 0,0001**		0.015	
Thorium (Th)	**n.b.**			
Cobalt (Co)	**< 0,0001**			
Molybdän (Mo)	**0.0002**			
Vanadium (V)	**< 0,0001**			
Selen (Se)	**n.b.**		0.01	
Tellur (Te)	**n.b.**			
Niob (Nb)	**n.b.**			
Silicium (Si)	**n.b.**			

Spezielle Parameter (mg/l)

Parameter	Messwert
Lanthan (La)	**n.b.**
Cer (Ce)	**n.b.**
Praseodym (Pr)	**n.b.**
Neodym (Nd)	**n.b.**
Samarium (Sm)	**n.b.**
Europium (Eu)	**n.b.**
Gadolimium (Gd)	**n.b.**
Terbium (Tb)	**n.b.**
Dysprosium (Dy)	**n.b.**
Holmium (Ho)	**n.b.**
Erbium (Er)	**n.b.**
Thulium (Tm)	**n.b.**
Ytterbium (Yb)	**n.b.**
Lutetium (Lu)	**n.b.**
Zinn (Sn)	**n.b.**
Thallium (Tl)	**n.b.**
Silber (Ag)	**n.b.**
Beryllium (Be)	**n.b.**
Bismut (Bi)	**n.b.**
Gallium (Ga)	**n.b.**

Die HCO3- Konzentration wurde berechnet

n.b. .. nicht bestimmt

* ... Qualitätszielverordnung Chemie Grundwasser QZV Chemie GW (BGBl. II 98/2010)

** ... Mindestanforderungsparameter aus der Trinkwasserverordnung - TWV (BGBl. II 304/2001)

*** ... Indikatorparameter aus der Trinkwasserverordnung - TWV (BGBl. II 304/2001)

Layout: G. Hobiger

Geologische Bundesanstalt
FA Geochemie
Leitung: HR Mag. Dr. Gerhard Hobiger

Berechnungen aus den Analysenwerten

Äquivalentanteile

Kationen				Anionen			
	Messwert				Messwert		
Ion	mg/l	meq/l	eq%	Ion	mg/l	meq/l	eq%
Ca^{2+}	55.85	2.79	52.66	HCO_3^-	298	4.88	92.2
Mg^{2+}	18.56	1.53	28.86	Cl^-	0.60	0.02	0.3
Na^+	20.71	0.90	17.03	SO_4^{2-}	17.78	0.37	7.0
K^+	1.56	0.04	0.75	NO_3^-	<0,5	0.00	0.0
Sr^{2+}	0.94	0.02	0.41	NO_2^-	n.b.	n.b.	n.b.
Ba^{2+}	0.046	0.00	0.0	$o\text{-}PO_4^{3-}$	n.b.	n.b.	n.b.
Li^+	0.036	0.01	0.10	S^{2-}	n.b.	n.b.	n.b.
Rb^+	0.002	0.00	0.00	F^-	0.53	0.03	0.5
Cs^+	< 0,0001	0.00	0.00	Σ	316.90	5.3	100.0
NH_4^+	n.b.	n.b.	n.b.				
Fe^{2+}	0.268	0.01	0.2				
Mn^{2+}	0.0044	0.00	0.0				
Σ	97.98	5.3	100.0				

Die HCO3- Konzentration wurde berechnet

Ionenbilanz		
Σ Kationen (meq/l)	5.29	*-0.1 %*
Σ Anionen (meq/l)	5.30	

Härten	
Gesamthärte (° dH)	12.1
Carbonathärte(° dH)	12.1
Nichtcarbonathärte (°dH)	0.0
Erdalkalien (mmol/l)	41.0

Berechnung des CO_2	
lg(pCO_2)	-2.50
freies CO_2 (mg/l)	6.97
freies CO_2 (mmol/l)	0.1584

Berechneter Ammoniakgehalt	
NH_3 (mg/l)	n.b.

Ges. Ionengehalt	415 mg/l	8.2 mmol/l

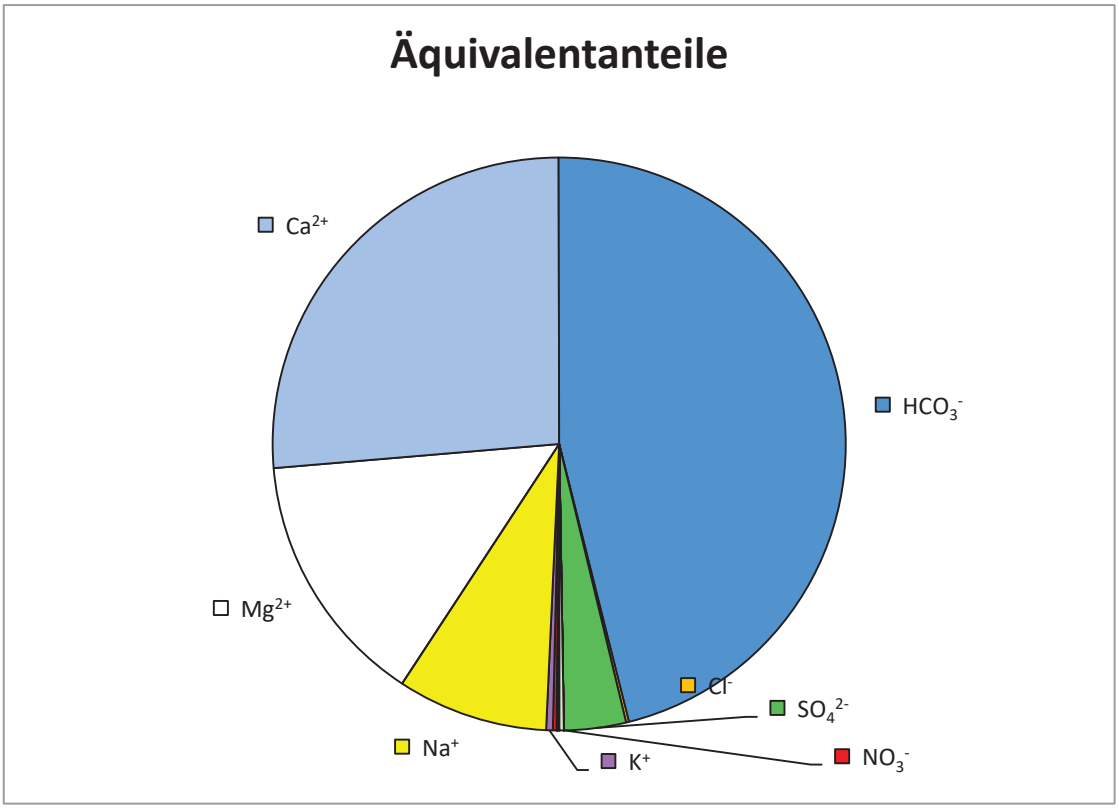

Wasseranalyse

Geologische Bundesanstalt
FA Geochemie
Leitung: HR Mag. Dr. Gerhard Hobiger

Probenahmepunkt:			**25**		
Koordinaten	**M** n.b.	**RW:** N48° 24.432'	**HW:** E13° 33.881'	**GOK (m ü. A.)**	n.b.
Bezeichnung:	**25**		**Geochemie-Nr.:**	**GCH-2018-006-004**	
Probenahmetiefe:	n.b.	**Probenehmer:**	**Pö/Be**		
Probenahmedatum und Uhrzeit:		**22.01.2018 12:15**	**Eingangsdatum:**	**24.01.2018**	

Feldparameter

		QZV *	MAP **	IP ***			
el. LF (µS/cm) (Gel.)	**254**	2250		2500	**Schüttung (l/s)**		n.b.
el. LF (µS/cm) (Labor)	n.b.				**Redoxpotenzial (mV)**		141.00
					Temperatur (°C)		8.8
pH (Gel.)	**7.29**			6,5 - 9,5	**Sauerstoff (O_2)**	mg/l	10.25
pH (Labor)	n.b.					(%)	91.8

Kationen (mg/l)

Ion	Messwert	QZV *	MAP **	IP ***
Calcium (Ca^{2+})	33.3			
Magnesium (Mg^{2+})	5.3			
Natrium (Na^{+})	4.7			200
Kalium (K^{+})	8.0			
Strontium (Sr^{2+})	0.1297			
Barium (Ba^{2+})	0.0075			
Lithium (Li^{+})	0.0018			
Rubidium (Rb^{+})	0.0017			
Cäsium (Cs^{+})	< 0,0001			
Ammonium (NH_4^{+})	n.b.	0.45		0.5
Eisen (Fe^{2+})	0.101			0.2
Mangan (Mn^{2+})	0.0029			0.05
Σ	51.5			

Anionen (mg/l)

Ion	Messwert	QZV *	MAP **	IP ***
Hydrogencarbonat (HCO_3^{-})	134.24			
Chlorid (Cl^{-})	2.3	180		200
Sulfat (SO_4^{2-})	4.4	225		250
Nitrat (NO_3^{-})	11.2	45	50	
Nitrit (NO_2^{-})	n.b.	0.09	0.1	
o- Phosphat (o-PO_4^{3-})	n.b.	0.3		
Sulfid (S^{2-})	n.b.			
Fluorid (F^{-})	0.10		1.5	
Σ	152.2			

Ges. Ionengehalt	204 mg/l	**Ionenbilanz**
	4.0 mmol/l	*-1.2* %
Dichte	n.b. g/cm3	

Spezielle Parameter (mg/l)

Parameter	Messwert	QZV *	MAP **	IP ***
Kupfer (Cu)	0.0095	1.8	2	
Zink (Zn)	0.1303			
Blei (Pb)	0.0002	0.009	0.025	
Cadmium (Cd)	< 0,0001	0.0045	0.005	
Aluminium (Al)	0.0251			0.2
Arsen (As)	0.0015	0.009	0.01	
Antimon (Sb)	n.b.		0.005	
Chrom (Cr)	0.0009	0.045		
Nickel (Ni)	< 0,0001	0.018		
Quecksilber (Hg)	n.b.	0.0009	0.001	
Bor (B)	n.b.		1	
Uran (U)	0.0003		0.015	
Thorium (Th)	n.b.			
Cobalt (Co)	< 0,0001			
Molybdän (Mo)	0.0005			
Vanadium (V)	0.0013			
Selen (Se)	n.b.		0.01	
Tellur (Te)	n.b.			
Niob (Nb)	n.b.			
Silicium (Si)	n.b.			

Spezielle Parameter (mg/l)

Parameter	Messwert
Lanthan (La)	n.b.
Cer (Ce)	n.b.
Praseodym (Pr)	n.b.
Neodym (Nd)	n.b.
Samarium (Sm)	n.b.
Europium (Eu)	n.b.
Gadolimium (Gd)	n.b.
Terbium (Tb)	n.b.
Dysprosium (Dy)	n.b.
Holmium (Ho)	n.b.
Erbium (Er)	n.b.
Thulium (Tm)	n.b.
Ytterbium (Yb)	n.b.
Lutetium (Lu)	n.b.
Zinn (Sn)	n.b.
Thallium (Tl)	n.b.
Silber (Ag)	n.b.
Beryllium (Be)	n.b.
Bismut (Bi)	n.b.
Gallium (Ga)	n.b.

n.b. .. nicht bestimmt

* ... Qualitätszielverordnung Chemie Grundwasser QZV Chemie GW (BGBl. II 98/2010)

** ... Mindestanforderungsparameter aus der Trinkwasserverordnung - TWV (BGBl. II 304/2001)

*** ... Indikatorparameter aus der Trinkwasserverordnung - TWV (BGBl. II 304/2001)

Layout: G. Hobiger

Geologische Bundesanstalt
FA Geochemie
Leitung: HR Mag. Dr. Gerhard Hobiger

Berechnungen aus den Analysenwerten

Äquivalentanteile

Kationen

Ion	Messwert mg/l	meq/l	eq%
Ca^{2+}	33.25	1.66	66.10
Mg^{2+}	5.28	0.43	17.30
Na^{+}	4.73	0.21	8.20
K^{+}	7.97	0.20	8.12
Sr^{2+}	0.13	0.00	0.12
Ba^{2+}	0.007	0.00	0.0
Li^{+}	0.002	0.00	0.01
Rb^{+}	0.002	0.00	0.00
Cs^{+}	< 0,0001	0.00	0.00
NH_4^{+}	n.b.	n.b.	n.b.
Fe^{2+}	0.101	0.00	0.1
Mn^{2+}	0.0029	0.00	0.0
Σ	51.48	2.5	100.0

Anionen

Ion	Messwert mg/l	meq/l	eq%
HCO_3^{-}	134.24	2.20	86.5
Cl^{-}	2.30	0.06	2.6
SO_4^{2-}	4.41	0.09	3.6
NO_3^{-}	11.16	0.18	7.1
NO_2^{-}	n.b.	n.b.	n.b.
$o\text{-}PO_4^{3-}$	n.b.	n.b.	n.b.
S^{2-}	n.b.	n.b.	n.b.
F^{-}	0.10	0.01	0.2
Σ	152.20	2.5	100.0

Härten

Gesamthärte (° dH)	5.9
Carbonathärte(° dH)	5.9
Nichtcarbonathärte (°dH)	0.0
Erdalkalien (mmol/l)	41.8

Berechnung des CO_2

$lg(pCO_2)$	-2.25
freies CO_2 (mg/l)	13.84
freies CO_2 (mmol/l)	0.3145

Berechneter Ammoniakgehalt

NH_3 (mg/l)	n.b.

Ges. Ionengehalt	204 mg/l	4.0 mmol/l

Ionenbilanz

Σ Kationen (meq/l)	2.51	*-1.2 %*
Σ Anionen (meq/l)	2.54	

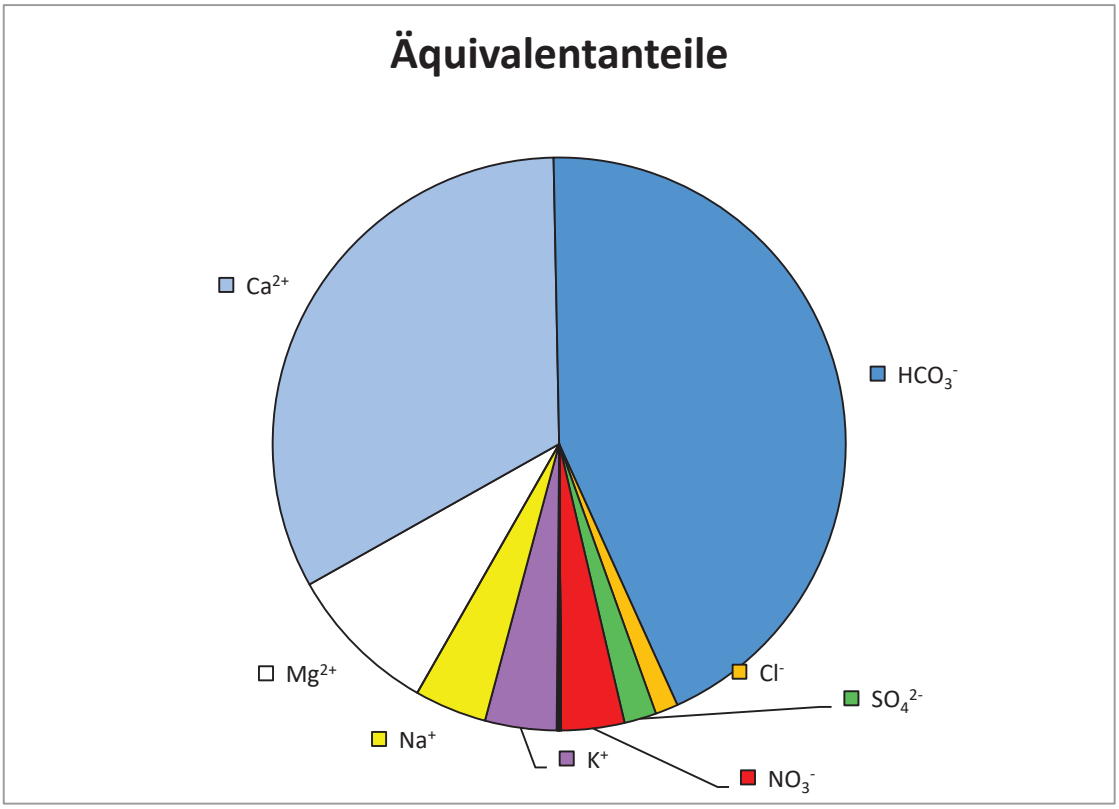

Wasseranalyse

Geologische Bundesanstalt
FA Geochemie
Leitung: HR Mag. Dr. Gerhard Hobiger

Probenahmepunkt:		**26**		
Koordinaten	**M n.b.**	**RW: N48° 21.612'**	**HW: E13° 34.291'**	**GOK (m ü. A.) n.b.**
Bezeichnung:	**26**		**Geochemie-Nr.:**	**GCH-2018-006-005**
Probenahmetiefe:	**n.b.**	**Probenehmer:**	**Pö/Be**	
Probenahmedatum und Uhrzeit:		**22.01.2018 13:15**	**Eingangsdatum:**	**24.01.2018**

Feldparameter

		QZV *	MAP **	IP ***			
el. LF (µS/cm) (Gel.)	**577**	2250		2500	**Schüttung (l/s)**		**n.b.**
el. LF (µS/cm) (Labor)	n.b.				**Redoxpotenzial (mV)**		**20.00**
					Temperatur (°C)		**11**
pH (Gel.)	**7.41**			6,5 - 9,5	**Sauerstoff (O_2)**	**mg/l**	**2.47**
pH (Labor)	n.b.					**(%)**	**23.5**

Kationen (mg/l)

Ion	Messwert	QZV *	MAP **	IP ***
Calcium (Ca^{2+})	**78.5**			
Magnesium (Mg^{2+})	**21.3**			
Natrium (Na^{+})	**6.7**			200
Kalium (K^{+})	**1.8**			
Strontium (Sr^{2+})	**0.2948**			
Barium (Ba^{2+})	**0.0261**			
Lithium (Li^{+})	**0.0158**			
Rubidium (Rb^{+})	**0.0011**			
Cäsium (Cs^{+})	**< 0,0001**			
Ammonium (NH_4^{+})	**n.b.**	0.45		0.5
Eisen (Fe^{2+})	**0.069**			0.2
Mangan (Mn^{2+})	**0.0258**			0.05
Σ	**108.8**			

Anionen (mg/l)

Ion	Messwert	QZV *	MAP **	IP ***
Hydrogencarbonat (HCO_3^{-})	**323.38**			
Chlorid (Cl^{-})	**4.1**	180		200
Sulfat (SO_4^{2-})	**28.8**	225		250
Nitrat (NO_3^{-})	**<0,5**	45	50	
Nitrit (NO_2^{-})	**n.b.**	0.09	0.1	
o- Phosphat (o-PO_4^{3-})	**n.b.**	0.3		
Sulfid (S^{2-})	**n.b.**			
Fluorid (F^{-})	**0.19**		1.5	
Σ	**356.5**			

Ges. Ionengehalt	**465 mg/l**	**Ionenbilanz**
	8.9 mmol/l	***-0.1*** **%**
Dichte	**n.b. g/cm3**	

Spezielle Parameter (mg/l)

Parameter	Messwert	QZV *	MAP **	IP ***
Kupfer (Cu)	**0.0015**	1.8	2	
Zink (Zn)	**0.1147**			
Blei (Pb)	**< 0,0001**	0.009	0.025	
Cadmium (Cd)	**< 0,0001**	0.0045	0.005	
Aluminium (Al)	**0.0040**			0.2
Arsen (As)	**0.0003**	0.009	0.01	
Antimon (Sb)	**n.b.**		0.005	
Chrom (Cr)	**< 0,0001**	0.045		
Nickel (Ni)	**0.0013**	0.018		
Quecksilber (Hg)	**n.b.**	0.0009	0.001	
Bor (B)	**n.b.**		1	
Uran (U)	**< 0,0001**		0.015	
Thorium (Th)	**n.b.**			
Cobalt (Co)	**< 0,0001**			
Molybdän (Mo)	**0.0005**			
Vanadium (V)	**< 0,0001**			
Selen (Se)	**n.b.**		0.01	
Tellur (Te)	**n.b.**			
Niob (Nb)	**n.b.**			
Silicium (Si)	**n.b.**			

Spezielle Parameter (mg/l)

Parameter	Messwert
Lanthan (La)	**n.b.**
Cer (Ce)	**n.b.**
Praseodym (Pr)	**n.b.**
Neodym (Nd)	**n.b.**
Samarium (Sm)	**n.b.**
Europium (Eu)	**n.b.**
Gadolimium (Gd)	**n.b.**
Terbium (Tb)	**n.b.**
Dysprosium (Dy)	**n.b.**
Holmium (Ho)	**n.b.**
Erbium (Er)	**n.b.**
Thulium (Tm)	**n.b.**
Ytterbium (Yb)	**n.b.**
Lutetium (Lu)	**n.b.**
Zinn (Sn)	**n.b.**
Thallium (Tl)	**n.b.**
Silber (Ag)	**n.b.**
Beryllium (Be)	**n.b.**
Bismut (Bi)	**n.b.**
Gallium (Ga)	**n.b.**

n.b. .. nicht bestimmt

* ... Qualitätszielverordnung Chemie Grundwasser QZV Chemie GW (BGBl. II 98/2010)

** ... Mindestanforderungsparameter aus der Trinkwasserverordnung - TWV (BGBl. II 304/2001)

*** ... Indikatorparameter aus der Trinkwasserverordnung - TWV (BGBl. II 304/2001)

Layout: G. Hobiger

Geologische Bundesanstalt
FA Geochemie
Leitung: HR Mag. Dr. Gerhard Hobiger

Berechnungen aus den Analysenwerten

Äquivalentanteile

Kationen

Ion	Messwert mg/l	meq/l	eq%
Ca^{2+}	78.50	3.92	65.06
Mg^{2+}	21.29	1.75	29.09
Na^{+}	6.73	0.29	4.86
K^{+}	1.83	0.05	0.78
Sr^{2+}	0.29	0.01	0.11
Ba^{2+}	0.026	0.00	0.0
Li^{+}	0.016	0.00	0.04
Rb^{+}	0.001	0.00	0.00
Cs^{+}	< 0,0001	0.00	0.00
NH_4^{+}	n.b.	n.b.	n.b.
Fe^{2+}	0.069	0.00	0.0
Mn^{2+}	0.0258	0.00	0.0
Σ	108.77	6.0	100.0

Anionen

Ion	Messwert mg/l	meq/l	eq%
HCO_3^{-}	323.38	5.30	87.9
Cl^{-}	4.13	0.12	1.9
SO_4^{2-}	28.84	0.60	10.0
NO_3^{-}	<0,5	0.00	0.0
NO_2^{-}	n.b.	n.b.	n.b.
$o\text{-}PO_4^{3-}$	n.b.	n.b.	n.b.
S^{2-}	n.b.	n.b.	n.b.
F^{-}	0.19	0.01	0.2
Σ	356.54	6.0	100.0

Härten

Gesamthärte (° dH)	15.9
Carbonathärte(° dH)	14.9
Nichtcarbonathärte (°dH)	1.0
Erdalkalien (mmol/l)	47.1

Berechnung des CO_2

lg(pCO_2)	-2.00
freies CO_2 (mg/l)	23.12
freies CO_2 (mmol/l)	0.5253

Berechneter Ammoniakgehalt

NH_3 (mg/l)	n.b.

Ges. Ionengehalt	465 mg/l	8.9 mmol/l

Ionenbilanz

Σ Kationen (meq/l)	6.02	*-0.1 %*
Σ Anionen (meq/l)	6.03	

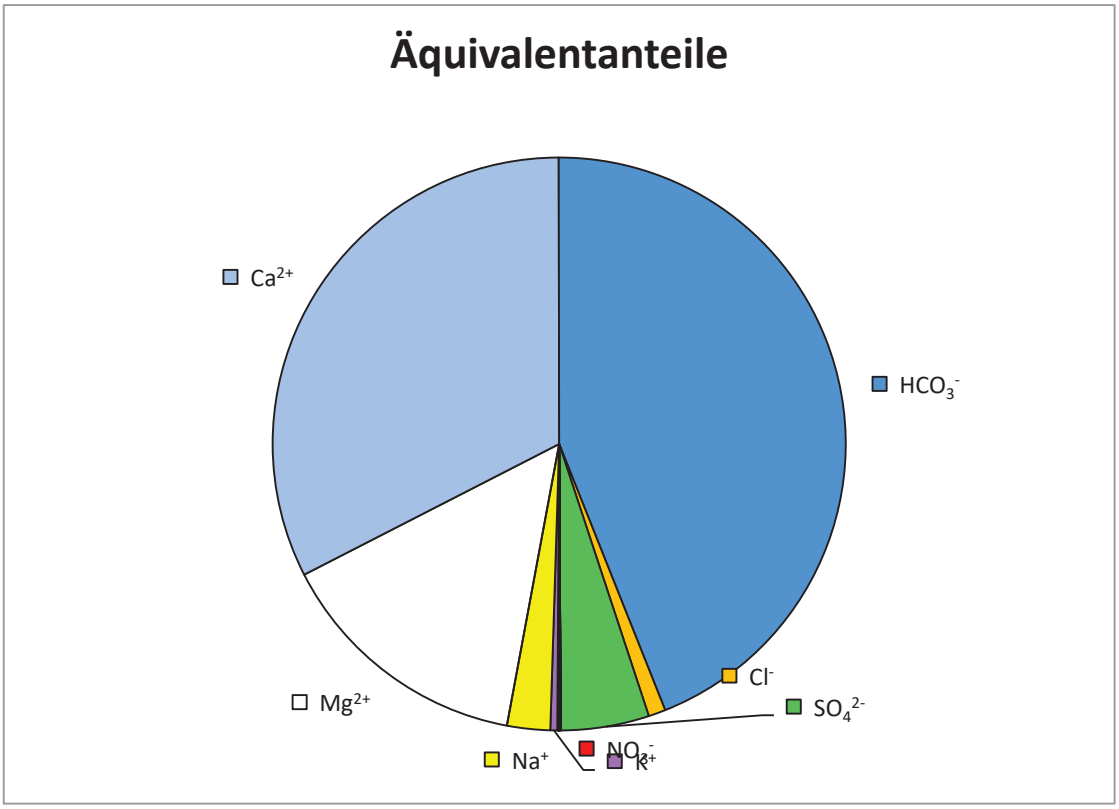

Wasseranalyse

Geologische Bundesanstalt
FA Geochemie
Leitung: HR Mag. Dr. Gerhard Hobiger

Probenahmepunkt:		**27**		
Koordinaten	**M n.b.**	**RW: N48° 22.847'**	**HW: E13° 35.418'**	**GOK (m ü. A.) n.b.**
Bezeichnung:	**27**		**Geochemie-Nr.:**	**GCH-2018-006-006**
Probenahmetiefe:	**n.b.**	**Probenehmer:**	**Pö/Be**	
Probenahmedatum und Uhrzeit:		**22.01.2018 14:50**	**Eingangsdatum:**	**24.01.2018**

Feldparameter

		QZV *	MAP **	IP ***			
el. LF (µS/cm) (Gel.)	**460**	2250		2500	**Schüttung (l/s)**		**n.b.**
el. LF (µS/cm) (Labor)	n.b.				**Redoxpotenzial (mV)**		**-57.00**
					Temperatur (°C)		**9.1**
pH (Gel.)	**7.77**			6,5 - 9,5	**Sauerstoff (O_2)**	**mg/l**	**2.55**
pH (Labor)	n.b.					**(%)**	**23.8**

Kationen (mg/l)

Ion	Messwert	QZV *	MAP **	IP ***
Calcium (Ca^{2+})	63.4			
Magnesium (Mg^{2+})	16.8			
Natrium (Na^{+})	3.3			200
Kalium (K^{+})	1.2			
Strontium (Sr^{2+})	0.1900			
Barium (Ba^{2+})	0.0083			
Lithium (Li^{+})	0.0108			
Rubidium (Rb^{+})	0.0019			
Cäsium (Cs^{+})	< 0,0001			
Ammonium (NH_4^{+})	n.b.	0.45		0.5
Eisen (Fe^{2+})	0.250			0.2
Mangan (Mn^{2+})	0.0546			0.05
Σ	85.1			

Anionen (mg/l)

Ion	Messwert	QZV *	MAP **	IP ***
Hydrogencarbonat (HCO_3^{-})	259.32			
Chlorid (Cl^{-})	2.6	180		200
Sulfat (SO_4^{2-})	21.4	225		250
Nitrat (NO_3^{-})	<0,5	45	50	
Nitrit (NO_2^{-})	n.b.	0.09	0.1	
o- Phosphat (o-PO_4^{3-})	n.b.	0.3		
Sulfid (S^{2-})	n.b.			
Fluorid (F^{-})	0.13		1.5	
Σ	283.5			

Ges. Ionengehalt	**369 mg/l**	**Ionenbilanz**
	7.0 mmol/l	***-0.9*** **%**
Dichte	**n.b. g/cm3**	

Spezielle Parameter (mg/l)

Parameter	Messwert	QZV *	MAP **	IP ***
Kupfer (Cu)	0.0015	1.8	2	
Zink (Zn)	0.6885			
Blei (Pb)	0.0004	0.009	0.025	
Cadmium (Cd)	< 0,0001	0.0045	0.005	
Aluminium (Al)	0.0049			0.2
Arsen (As)	0.0032	0.009	0.01	
Antimon (Sb)	n.b.		0.005	
Chrom (Cr)	< 0,0001	0.045		
Nickel (Ni)	< 0,0001	0.018		
Quecksilber (Hg)	n.b.	0.0009	0.001	
Bor (B)	n.b.		1	
Uran (U)	< 0,0001		0.015	
Thorium (Th)	n.b.			
Cobalt (Co)	< 0,0001			
Molybdän (Mo)	0.0004			
Vanadium (V)	< 0,0001			
Selen (Se)	n.b.		0.01	
Tellur (Te)	n.b.			
Niob (Nb)	n.b.			
Silicium (Si)	n.b.			

Spezielle Parameter (mg/l)

Parameter	Messwert
Lanthan (La)	n.b.
Cer (Ce)	n.b.
Praseodym (Pr)	n.b.
Neodym (Nd)	n.b.
Samarium (Sm)	n.b.
Europium (Eu)	n.b.
Gadolimium (Gd)	n.b.
Terbium (Tb)	n.b.
Dysprosium (Dy)	n.b.
Holmium (Ho)	n.b.
Erbium (Er)	n.b.
Thulium (Tm)	n.b.
Ytterbium (Yb)	n.b.
Lutetium (Lu)	n.b.
Zinn (Sn)	n.b.
Thallium (Tl)	n.b.
Silber (Ag)	n.b.
Beryllium (Be)	n.b.
Bismut (Bi)	n.b.
Gallium (Ga)	n.b.

n.b. .. nicht bestimmt

* ... Qualitätszielverordnung Chemie Grundwasser QZV Chemie GW (BGBl. II 98/2010)

** ... Mindestanforderungsparameter aus der Trinkwasserverordnung - TWV (BGBl. II 304/2001)

*** ... Indikatorparameter aus der Trinkwasserverordnung - TWV (BGBl. II 304/2001)

Layout: G. Hobiger

Geologische Bundesanstalt
FA Geochemie
Leitung: HR Mag. Dr. Gerhard Hobiger

Berechnungen aus den Analysenwerten

Äquivalentanteile

Kationen

Ion	Messwert mg/l	meq/l	eq%
Ca^{2+}	63.36	3.16	66.81
Mg^{2+}	16.76	1.38	29.14
Na^{+}	3.32	0.14	3.05
K^{+}	1.19	0.03	0.64
Sr^{2+}	0.19	0.00	0.09
Ba^{2+}	0.008	0.00	0.0
Li^{+}	0.011	0.00	0.03
Rb^{+}	0.002	0.00	0.00
Cs^{+}	< 0,0001	0.00	0.00
NH_4^{+}	n.b.	n.b.	n.b.
Fe^{2+}	0.250	0.01	0.2
Mn^{2+}	0.0546	0.00	0.0
Σ	85.14	4.7	100.0

Anionen

Ion	Messwert mg/l	meq/l	eq%
HCO_3^{-}	259.32	4.25	89.0
Cl^{-}	2.63	0.07	1.5
SO_4^{2-}	21.45	0.45	9.3
NO_3^{-}	<0,5	0.00	0.0
NO_2^{-}	n.b.	n.b.	n.b.
$o\text{-}PO_4^{3-}$	n.b.	n.b.	n.b.
S^{2-}	n.b.	n.b.	n.b.
F^{-}	0.13	0.01	0.1
Σ	283.52	4.8	100.0

Härten

Gesamthärte (° dH)	12.7
Carbonathärte(° dH)	11.9
Nichtcarbonathärte (°dH)	0.8
Erdalkalien (mmol/l)	48.0

Berechnung des CO_2

$lg(pCO_2)$	-2.46
freies CO_2 (mg/l)	8.55
freies CO_2 (mmol/l)	0.1942

Berechneter Ammoniakgehalt

NH_3 (mg/l)	n.b.

Ges. Ionengehalt	369 mg/l	7.0 mmol/l

Ionenbilanz

Σ Kationen (meq/l)	4.73	*-0.9 %*
Σ Anionen (meq/l)	4.78	

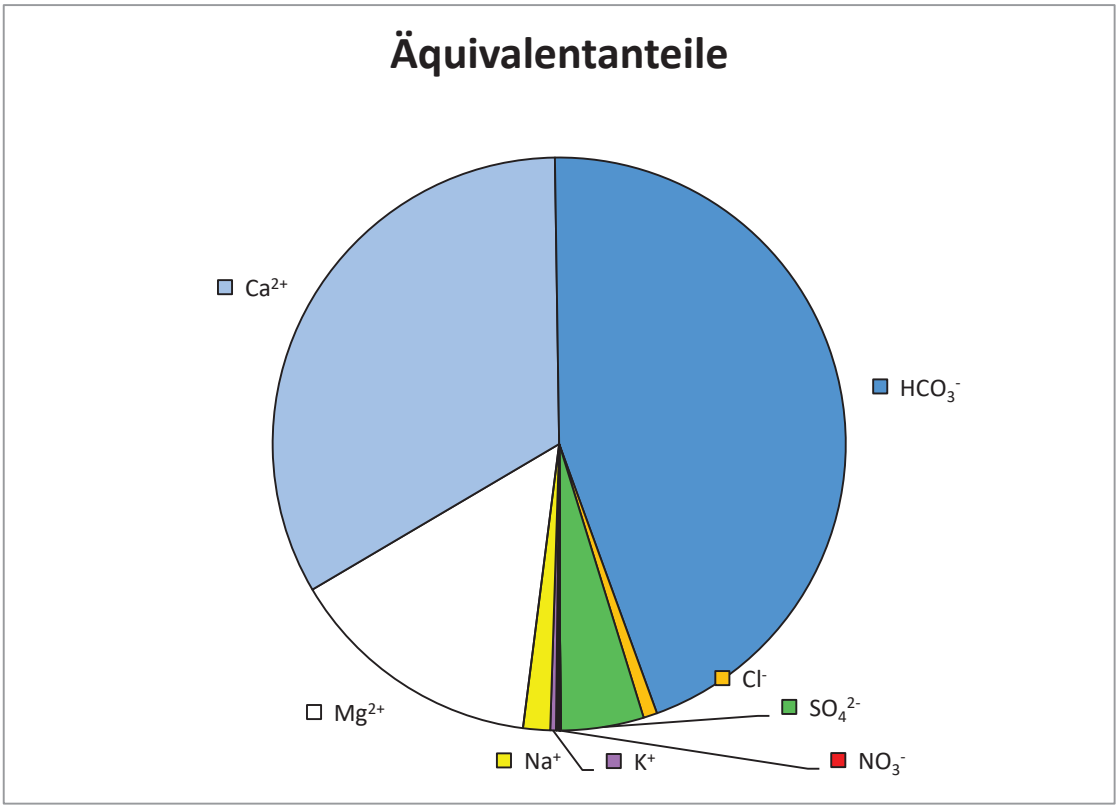

Wasseranalyse

Geologische Bundesanstalt
FA Geochemie
Leitung: HR Mag. Dr. Gerhard Hobiger

Probenahmepunkt:		**28**		
Koordinaten	**M n.b.**	**RW: N48° 13.678'**	**HW: E13° 55.056'**	**GOK (m ü. A.) n.b.**
Bezeichnung:	**28**		**Geochemie-Nr.:**	**GCH-2018-006-008**
Probenahmetiefe:	**n.b.**	**Probenehmer:**	**Pö/Be**	
Probenahmedatum und Uhrzeit:		**22.01.2018 16:15**	**Eingangsdatum:**	**24.01.2018**

Feldparameter

		QZV *	MAP **	IP ***			
el. LF (µS/cm) (Gel.)	**827**	2250		2500	**Schüttung (l/s)**		**n.b.**
el. LF (µS/cm) (Labor)	n.b.				**Redoxpotenzial (mV)**		**-303.00**
					Temperatur (°C)		**38.3**
pH (Gel.)	**8.59**			6,5 - 9,5	**Sauerstoff (O_2)**	**mg/l**	**0.01**
pH (Labor)	n.b.					**(%)**	**0.2**

Kationen (mg/l)

Ion	Messwert	QZV *	MAP **	IP ***
Calcium (Ca^{2+})	**0.9**			
Magnesium (Mg^{2+})	**0.2**			
Natrium (Na^{+})	**192.3**			200
Kalium (K^{+})	**1.4**			
Strontium (Sr^{2+})	**0.0172**			
Barium (Ba^{2+})	**0.0022**			
Lithium (Li^{+})	**0.0306**			
Rubidium (Rb^{+})	**0.0021**			
Cäsium (Cs^{+})	**< 0,0001**			
Ammonium (NH_4^{+})	**n.b.**	0.45		0.5
Eisen (Fe^{2+})	**0.021**			0.2
Mangan (Mn^{2+})	**0.0019**			0.05
Σ	**194.9**			

Anionen (mg/l)

Ion	Messwert	QZV *	MAP **	IP ***
Hydrogencarbonat (HCO_3^{-})	**369.15**			
Chlorid (Cl^{-})	**76.9**	180		200
Sulfat (SO_4^{2-})	**6.4**	225		250
Nitrat (NO_3^{-})	**<0,5**	45	50	
Nitrit (NO_2^{-})	**n.b.**	0.09	0.1	
o- Phosphat (o-PO_4^{3-})	**n.b.**	0.3		
Sulfid (S^{2-})	**n.b.**			
Fluorid (F^{-})	**0.92**		1.5	
Σ	**453.4**			

Ges. Ionengehalt	**648 mg/l**	**Ionenbilanz**	
	16.8 mmol/l	***0.8***	**%**
Dichte	**n.b. g/cm3**		

Spezielle Parameter (mg/l)

Parameter	Messwert	QZV *	MAP **	IP ***
Kupfer (Cu)	**0.0014**	1.8	2	
Zink (Zn)	**0.0132**			
Blei (Pb)	**0.0001**	0.009	0.025	
Cadmium (Cd)	**< 0,0001**	0.0045	0.005	
Aluminium (Al)	**0.0242**			0.2
Arsen (As)	**< 0,0001**	0.009	0.01	
Antimon (Sb)	**n.b.**		0.005	
Chrom (Cr)	**< 0,0001**	0.045		
Nickel (Ni)	**< 0,0001**	0.018		
Quecksilber (Hg)	**n.b.**	0.0009	0.001	
Bor (B)	**n.b.**		1	
Uran (U)	**< 0,0001**		0.015	
Thorium (Th)	**n.b.**			
Cobalt (Co)	**< 0,0001**			
Molybdän (Mo)	**< 0,0001**			
Vanadium (V)	**< 0,0001**			
Selen (Se)	**n.b.**		0.01	
Tellur (Te)	**n.b.**			
Niob (Nb)	**n.b.**			
Silicium (Si)	**n.b.**			

Spezielle Parameter (mg/l)

Parameter	Messwert
Lanthan (La)	**n.b.**
Cer (Ce)	**n.b.**
Praseodym (Pr)	**n.b.**
Neodym (Nd)	**n.b.**
Samarium (Sm)	**n.b.**
Europium (Eu)	**n.b.**
Gadolimium (Gd)	**n.b.**
Terbium (Tb)	**n.b.**
Dysprosium (Dy)	**n.b.**
Holmium (Ho)	**n.b.**
Erbium (Er)	**n.b.**
Thulium (Tm)	**n.b.**
Ytterbium (Yb)	**n.b.**
Lutetium (Lu)	**n.b.**
Zinn (Sn)	**n.b.**
Thallium (Tl)	**n.b.**
Silber (Ag)	**n.b.**
Beryllium (Be)	**n.b.**
Bismut (Bi)	**n.b.**
Gallium (Ga)	**n.b.**

n.b. .. nicht bestimmt

* ... Qualitätszielverordnung Chemie Grundwasser QZV Chemie GW (BGBl. II 98/2010)

** ... Mindestanforderungsparameter aus der Trinkwasserverordnung - TWV (BGBl. II 304/2001)

*** ... Indikatorparameter aus der Trinkwasserverordnung - TWV (BGBl. II 304/2001)

Layout: G. Hobiger

Geologische Bundesanstalt
FA Geochemie
Leitung: HR Mag. Dr. Gerhard Hobiger

Berechnungen aus den Analysenwerten

Äquivalentanteile

Kationen

Ion	Messwert mg/l	meq/l	eq%
Ca^{2+}	0.94	0.05	0.55
Mg^{2+}	0.24	0.02	0.23
Na^{+}	192.29	8.36	98.74
K^{+}	1.36	0.03	0.41
Sr^{2+}	0.02	0.00	0.00
Ba^{2+}	0.002	0.00	0.0
Li^{+}	0.031	0.00	0.05
Rb^{+}	0.002	0.00	0.00
Cs^{+}	< 0,0001	0.00	0.00
NH_4^{+}	n.b.	n.b.	n.b.
Fe^{2+}	0.021	0.00	0.0
Mn^{2+}	0.0019	0.00	0.0
Σ	194.90	8.5	100.0

Anionen

Ion	Messwert mg/l	meq/l	eq%
HCO_3^{-}	369.15	6.05	72.0
Cl^{-}	76.93	2.17	25.8
SO_4^{2-}	6.43	0.13	1.6
NO_3^{-}	<0,5	0.00	0.0
NO_2^{-}	n.b.	n.b.	n.b.
$o\text{-}PO_4^{3-}$	n.b.	n.b.	n.b.
S^{2-}	n.b.	n.b.	n.b.
F^{-}	0.92	0.05	0.6
Σ	453.43	8.4	100.0

Härten

Gesamthärte (° dH)	0.2
Carbonathärte(° dH)	0.2
Nichtcarbonathärte (°dH)	0.0
Erdalkalien (mmol/l)	0.4

Berechnung des CO_2

lg(pCO_2)	-2.95
freies CO_2 (mg/l)	1.23
freies CO_2 (mmol/l)	0.0279

Berechneter Ammoniakgehalt

NH_3 (mg/l)	n.b.

Ges. Ionengehalt	648 mg/l	16.8 mmol/l

Ionenbilanz

Σ Kationen (meq/l)	8.47	*0.8 %*
Σ Anionen (meq/l)	8.40	

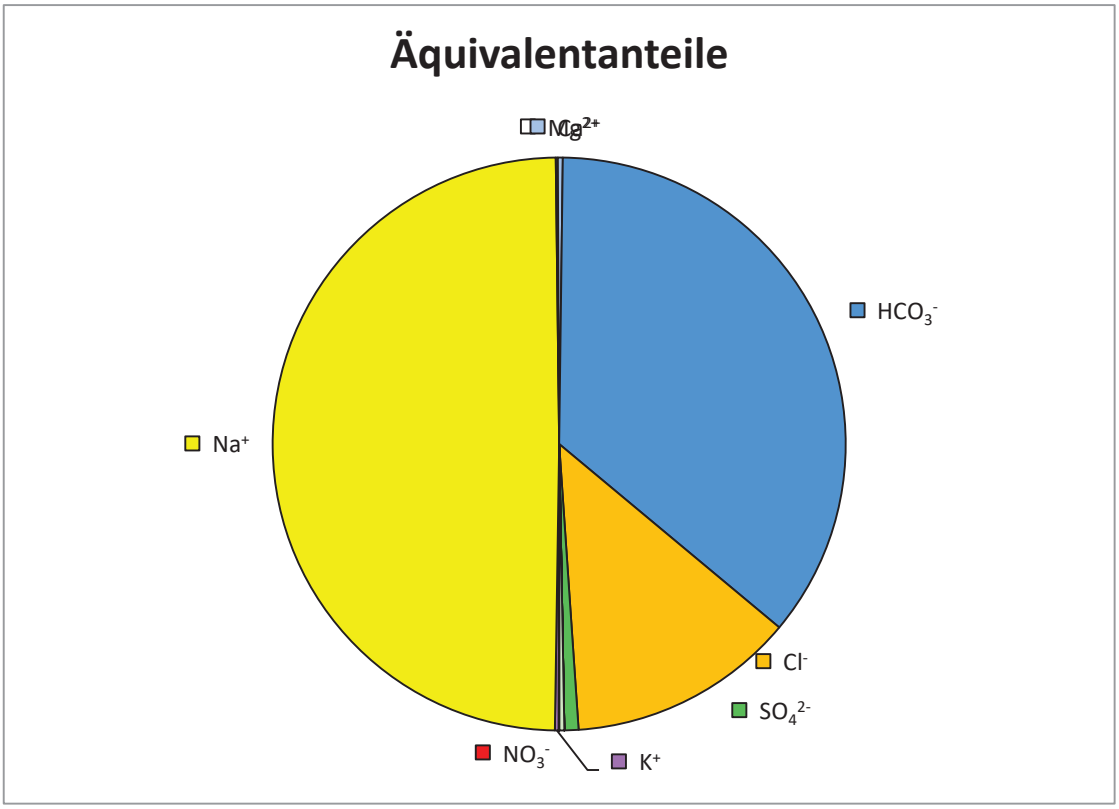

Wasseranalyse

Geologische Bundesanstalt
FA Geochemie
Leitung: HR Mag. Dr. Gerhard Hobiger

Probenahmepunkt:			**29**		
Koordinaten	**M** n.b.	**RW:** N48° 13.534'	**HW:** E13° 54.734'	**GOK (m ü. A.)**	n.b.
Bezeichnung:	**29**		**Geochemie-Nr.:**	**GCH-2018-006-007**	
Probenahmetiefe:	n.b.	**Probenehmer:**	**Pö/Be**		
Probenahmedatum und Uhrzeit:		**22.01.2018 17:20**	**Eingangsdatum:**	**24.01.2018**	

Feldparameter

		QZV *	MAP **	IP ***			
el. LF (µS/cm) (Gel.)	**558**	2250		2500	**Schüttung (l/s)**		**n.b.**
el. LF (µS/cm) (Labor)	n.b.				**Redoxpotenzial (mV)**		**-315.00**
					Temperatur (°C)		**36.6**
pH (Gel.)	**8.34**			6,5 - 9,5	**Sauerstoff (O_2)**	**mg/l**	**0.01**
pH (Labor)	n.b.					**(%)**	**0.2**

Kationen (mg/l)

Ion	Messwert	QZV *	MAP **	IP ***
Calcium (Ca^{2+})	**2.9**			
Magnesium (Mg^{2+})	**0.7**			
Natrium (Na^{+})	**139.1**			200
Kalium (K^{+})	**1.5**			
Strontium (Sr^{2+})	**0.0498**			
Barium (Ba^{2+})	**0.0055**			
Lithium (Li^{+})	**0.0268**			
Rubidium (Rb^{+})	**0.0022**			
Cäsium (Cs^{+})	**< 0,0001**			
Ammonium (NH_4^{+})	**n.b.**	0.45		0.5
Eisen (Fe^{2+})	**0.005**			0.2
Mangan (Mn^{2+})	**0.0063**			0.05
Σ	**144.3**			

Anionen (mg/l)

Ion	Messwert	QZV *	MAP **	IP ***
Hydrogencarbonat (HCO_3^{-})	**353.89**			
Chlorid (Cl^{-})	**21.1**	180		200
Sulfat (SO_4^{2-})	**6.3**	225		250
Nitrat (NO_3^{-})	**<0,5**	45	50	
Nitrit (NO_2^{-})	**n.b.**	0.09	0.1	
o- Phosphat (o-PO_4^{3-})	**n.b.**	0.3		
Sulfid (S^{2-})	**n.b.**			
Fluorid (F^{-})	**0.49**		1.5	
Σ	**381.8**			

Ges. Ionengehalt	**526 mg/l**	**Ionenbilanz**	
	12.7 mmol/l	***-3.9***	**%**
Dichte	**n.b. g/cm3**		

Spezielle Parameter (mg/l)

Parameter	Messwert	QZV *	MAP **	IP ***
Kupfer (Cu)	**0.0007**	1.8	2	
Zink (Zn)	**0.0012**			
Blei (Pb)	**< 0,0001**	0.009	0.025	
Cadmium (Cd)	**< 0,0001**	0.0045	0.005	
Aluminium (Al)	**0.0079**			0.2
Arsen (As)	**< 0,0001**	0.009	0.01	
Antimon (Sb)	**n.b.**		0.005	
Chrom (Cr)	**< 0,0001**	0.045		
Nickel (Ni)	**< 0,0001**	0.018		
Quecksilber (Hg)	**n.b.**	0.0009	0.001	
Bor (B)	**n.b.**		1	
Uran (U)	**< 0,0001**		0.015	
Thorium (Th)	**n.b.**			
Cobalt (Co)	**< 0,0001**			
Molybdän (Mo)	**< 0,0001**			
Vanadium (V)	**< 0,0001**			
Selen (Se)	**n.b.**		0.01	
Tellur (Te)	**n.b.**			
Niob (Nb)	**n.b.**			
Silicium (Si)	**n.b.**			

Spezielle Parameter (mg/l)

Parameter	Messwert
Lanthan (La)	**n.b.**
Cer (Ce)	**n.b.**
Praseodym (Pr)	**n.b.**
Neodym (Nd)	**n.b.**
Samarium (Sm)	**n.b.**
Europium (Eu)	**n.b.**
Gadolimium (Gd)	**n.b.**
Terbium (Tb)	**n.b.**
Dysprosium (Dy)	**n.b.**
Holmium (Ho)	**n.b.**
Erbium (Er)	**n.b.**
Thulium (Tm)	**n.b.**
Ytterbium (Yb)	**n.b.**
Lutetium (Lu)	**n.b.**
Zinn (Sn)	**n.b.**
Thallium (Tl)	**n.b.**
Silber (Ag)	**n.b.**
Beryllium (Be)	**n.b.**
Bismut (Bi)	**n.b.**
Gallium (Ga)	**n.b.**

n.b. .. nicht bestimmt

* ... Qualitätszielverordnung Chemie Grundwasser QZV Chemie GW (BGBl. II 98/2010)

** ... Mindestanforderungsparameter aus der Trinkwasserverordnung - TWV (BGBl. II 304/2001)

*** ... Indikatorparameter aus der Trinkwasserverordnung - TWV (BGBl. II 304/2001)

Layout: G. Hobiger

Geologische Bundesanstalt
FA Geochemie
Leitung: HR Mag. Dr. Gerhard Hobiger

Berechnungen aus den Analysenwerten

Äquivalentanteile

Kationen

Ion	Messwert mg/l	meq/l	eq%
Ca^{2+}	2.93	0.15	2.32
Mg^{2+}	0.75	0.06	0.97
Na^{+}	139.11	6.05	96.03
K^{+}	1.46	0.04	0.59
Sr^{2+}	0.05	0.00	0.02
Ba^{2+}	0.006	0.00	0.0
Li^{+}	0.027	0.00	0.06
Rb^{+}	0.002	0.00	0.00
Cs^{+}	< 0,0001	0.00	0.00
NH_4^{+}	n.b.	n.b.	n.b.
Fe^{2+}	0.005	0.00	0.0
Mn^{2+}	0.0063	0.00	0.0
Σ	144.35	6.3	100.0

Anionen

Ion	Messwert mg/l	meq/l	eq%
HCO_3^{-}	353.89	5.80	88.5
Cl^{-}	21.08	0.59	9.1
SO_4^{2-}	6.34	0.13	2.0
NO_3^{-}	<0,5	0.00	0.0
NO_2^{-}	n.b.	n.b.	n.b.
$o\text{-}PO_4^{3-}$	n.b.	n.b.	n.b.
S^{2-}	n.b.	n.b.	n.b.
F^{-}	0.49	0.03	0.4
Σ	381.81	6.6	100.0

Härten

Gesamthärte (° dH)	0.6
Carbonathärte(° dH)	0.6
Nichtcarbonathärte (°dH)	0.0
Erdalkalien (mmol/l)	1.7

Berechnung des CO_2

$lg(pCO_2)$	-2.72
freies CO_2 (mg/l)	2.14
freies CO_2 (mmol/l)	0.0486

Berechneter Ammoniakgehalt

NH_3 (mg/l)	n.b.

Ges. Ionengehalt	526 mg/l	12.7 mmol/l

Ionenbilanz

Σ Kationen (meq/l)	6.30	*-3.9 %*
Σ Anionen (meq/l)	6.55	

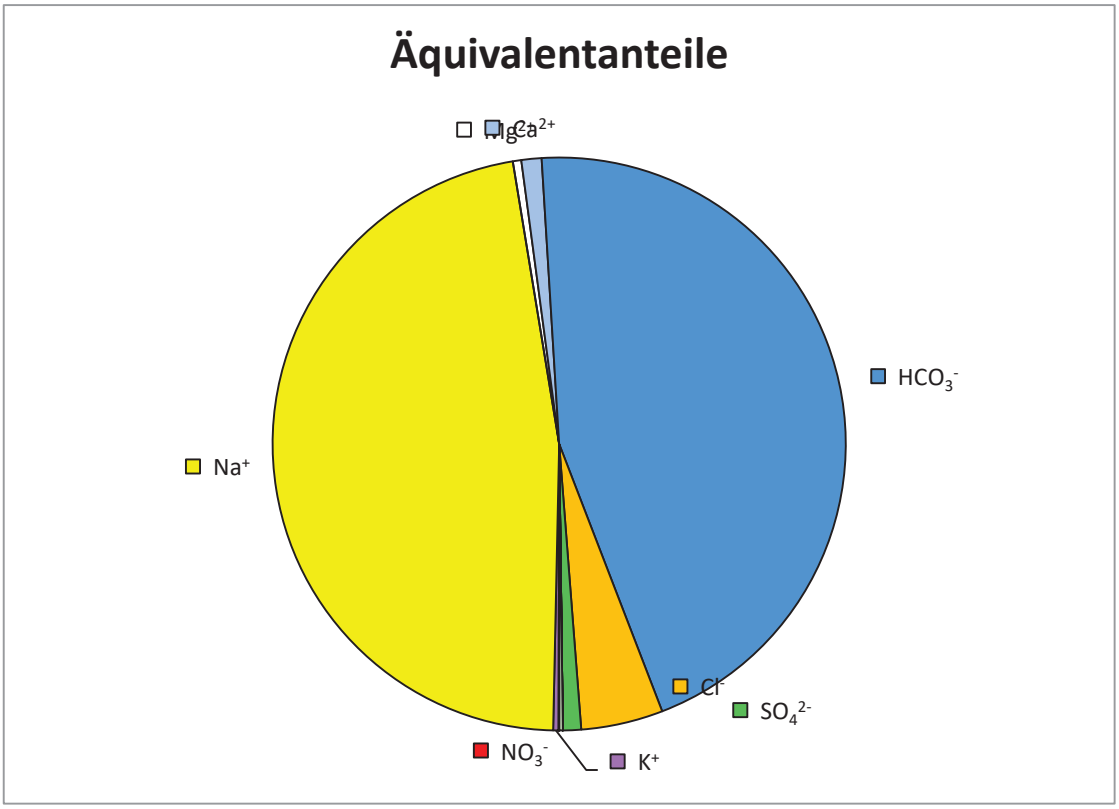

Wasseranalyse

Geologische Bundesanstalt
FA Geochemie
Leitung: HR Mag. Dr. Gerhard Hobiger

Probenahmepunkt:		**30**		
Koordinaten	**M** n.b.	**RW:** N48° 16.308'	**HW:** E13° 25.003'	**GOK (m ü. A.)** n.b.
Bezeichnung:	**30**		**Geochemie-Nr.:**	**GCH-2018-009-001**
Probenahmetiefe:	**n.b.**	**Probenehmer:**	**Pö/Be**	
Probenahmedatum und Uhrzeit:		**25.01.2018 09:15**	**Eingangsdatum:**	**26.01.2018**

Feldparameter

		QZV *	MAP **	IP ***			
el. LF (µS/cm) (Gel.)	**1428**	2250		2500	**Schüttung (l/s)**		**n.b.**
el. LF (µS/cm) (Labor)	n.b.				**Redoxpotenzial (mV)**		**-190.00**
					Temperatur (°C)		**27.1**
pH (Gel.)	**7.25**			6,5 - 9,5	**Sauerstoff (O_2)**	**mg/l**	**1.92**
pH (Labor)	n.b.					**(%)**	**23.6**

Kationen (mg/l)

Ion	Messwert	QZV *	MAP **	IP ***
Calcium (Ca^{2+})	9.9			
Magnesium (Mg^{2+})	1.5			
Natrium (Na^{+})	263.5			200
Kalium (K^{+})	14.7			
Strontium (Sr^{2+})	0.3687			
Barium (Ba^{2+})	0.0626			
Lithium (Li^{+})	0.2465			
Rubidium (Rb^{+})	0.0339			
Cäsium (Cs^{+})	0.0016			
Ammonium (NH_4^{+})	n.b.	0.45		0.5
Eisen (Fe^{2+})	0.014			0.2
Mangan (Mn^{2+})	0.0011			0.05
Σ	290.4			

Anionen (mg/l)

Ion	Messwert	QZV *	MAP **	IP ***
Hydrogencarbonat (HCO_3^{-})	524.74			
Chlorid (Cl^{-})	134.4	180		200
Sulfat (SO_4^{2-})	5.9	225		250
Nitrat (NO_3^{-})	<0,5	45	50	
Nitrit (NO_2^{-})	n.b.	0.09	0.1	
o- Phosphat (o-PO_4^{3-})	n.b.	0.3		
Sulfid (S^{2-})	n.b.			
Fluorid (F^{-})	5.61		1.5	
Σ	670.6			

Ges. Ionengehalt	**961 mg/l**	**Ionenbilanz**
	24.9 mmol/l	***-2.4*** **%**
Dichte	**n.b.** g/cm3	

Spezielle Parameter (mg/l)

Parameter	Messwert	QZV *	MAP **	IP ***
Kupfer (Cu)	0.0013	1.8	2	
Zink (Zn)	0.0096			
Blei (Pb)	< 0,0001	0.009	0.025	
Cadmium (Cd)	< 0,0001	0.0045	0.005	
Aluminium (Al)	0.0135			0.2
Arsen (As)	0.0003	0.009	0.01	
Antimon (Sb)	n.b.		0.005	
Chrom (Cr)	< 0,0001	0.045		
Nickel (Ni)	0.0006	0.018		
Quecksilber (Hg)	n.b.	0.0009	0.001	
Bor (B)	n.b.		1	
Uran (U)	< 0,0001		0.015	
Thorium (Th)	n.b.			
Cobalt (Co)	< 0,0001			
Molybdän (Mo)	< 0,0001			
Vanadium (V)	< 0,0001			
Selen (Se)	n.b.		0.01	
Tellur (Te)	n.b.			
Niob (Nb)	n.b.			
Silicium (Si)	n.b.			

Spezielle Parameter (mg/l)

Parameter	Messwert
Lanthan (La)	n.b.
Cer (Ce)	n.b.
Praseodym (Pr)	n.b.
Neodym (Nd)	n.b.
Samarium (Sm)	n.b.
Europium (Eu)	n.b.
Gadolimium (Gd)	n.b.
Terbium (Tb)	n.b.
Dysprosium (Dy)	n.b.
Holmium (Ho)	n.b.
Erbium (Er)	n.b.
Thulium (Tm)	n.b.
Ytterbium (Yb)	n.b.
Lutetium (Lu)	n.b.
Zinn (Sn)	n.b.
Thallium (Tl)	n.b.
Silber (Ag)	n.b.
Beryllium (Be)	n.b.
Bismut (Bi)	n.b.
Gallium (Ga)	n.b.

n.b. .. nicht bestimmt

* ... Qualitätszielverordnung Chemie Grundwasser QZV Chemie GW (BGBl. II 98/2010)

** ... Mindestanforderungsparameter aus der Trinkwasserverordnung - TWV (BGBl. II 304/2001)

*** ... Indikatorparameter aus der Trinkwasserverordnung - TWV (BGBl. II 304/2001)

Layout: G. Hobiger

Geologische Bundesanstalt
FA Geochemie
Leitung: HR Mag. Dr. Gerhard Hobiger

Berechnungen aus den Analysenwerten

Äquivalentanteile

Kationen

Ion	Messwert mg/l	meq/l	eq%
Ca^{2+}	9.86	0.49	3.93
Mg^{2+}	1.55	0.13	1.02
Na^{+}	263.54	11.46	91.67
K^{+}	14.71	0.38	3.01
Sr^{2+}	0.37	0.01	0.07
Ba^{2+}	0.063	0.00	0.0
Li^{+}	0.247	0.04	0.28
Rb^{+}	0.034	0.00	0.00
Cs^{+}	0.002	0.00	0.00
NH_4^{+}	n.b.	n.b.	n.b.
Fe^{2+}	0.014	0.00	0.0
Mn^{2+}	0.0011	0.00	0.0
Σ	290.39	12.5	100.0

Anionen

Ion	Messwert mg/l	meq/l	eq%
HCO_3^{-}	524.74	8.60	67.1
Cl^{-}	134.38	3.79	29.6
SO_4^{2-}	5.91	0.12	1.0
NO_3^{-}	<0,5	0.00	0.0
NO_2^{-}	n.b.	n.b.	n.b.
$o\text{-}PO_4^{3-}$	n.b.	n.b.	n.b.
S^{2-}	n.b.	n.b.	n.b.
F^{-}	5.61	0.30	2.3
Σ	670.64	12.8	100.0

Härten

Gesamthärte (° dH)	1.7
Carbonathärte(° dH)	1.7
Nichtcarbonathärte (°dH)	0.0
Erdalkalien (mmol/l)	2.5

Berechnung des CO_2

lg(pCO_2)	-1.54
freies CO_2 (mg/l)	40.85
freies CO_2 (mmol/l)	0.9282

Berechneter Ammoniakgehalt

NH_3 (mg/l)	n.b.

Ges. Ionengehalt	961 mg/l	24.9 mmol/l

Ionenbilanz

Σ Kationen (meq/l)	12.50	-2.4 %
Σ Anionen (meq/l)	12.81	

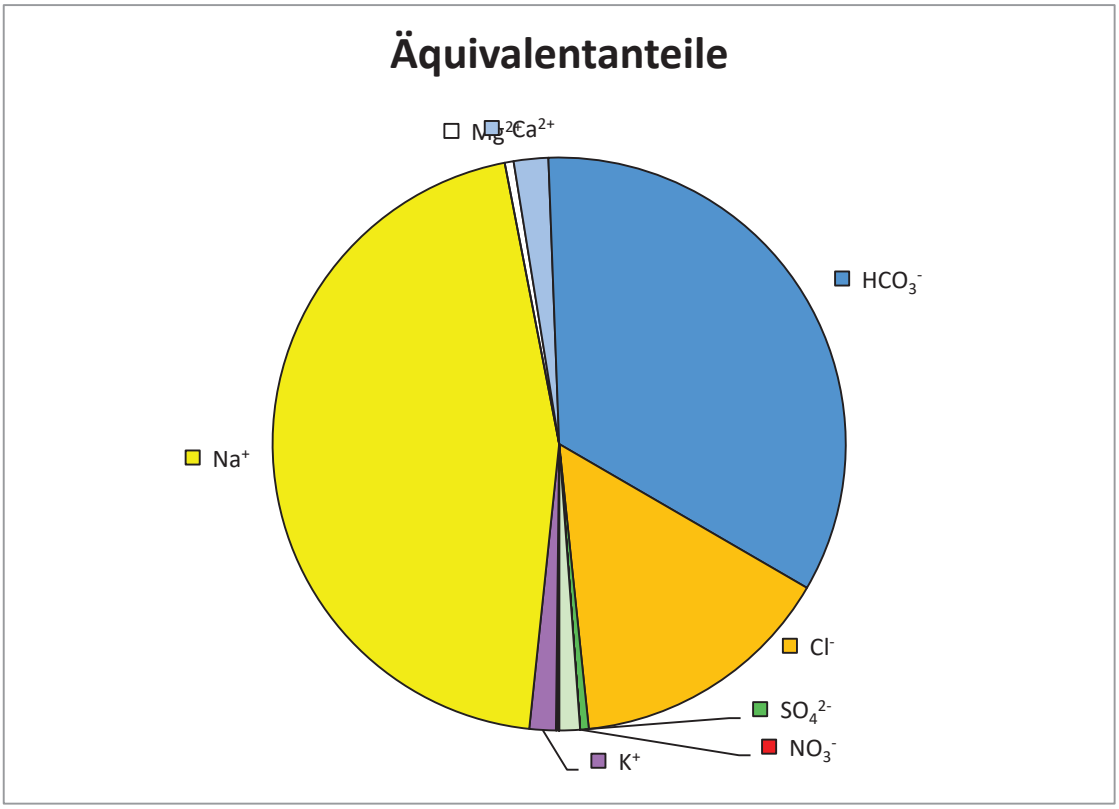

Wasseranalyse

Geologische Bundesanstalt
FA Geochemie
Leitung: HR Mag. Dr. Gerhard Hobiger

Probenahmepunkt:		**31**		
Koordinaten	**M n.b.**	**RW: N48° 19.639'**	**HW: E13° 20.549'**	**GOK (m ü. A.) n.b.**
Bezeichnung:	**31**		**Geochemie-Nr.:**	**GCH-2018-009-002**
Probenahmetiefe:	**n.b.**	**Probenehmer:**	**Pö/Be**	
Probenahmedatum und Uhrzeit:		**25.01.2018 11:30**	**Eingangsdatum:**	**26.01.2018**

Feldparameter

		QZV *	MAP **	IP ***			
el. LF (µS/cm) (Gel.)	**1431**	2250		2500	**Schüttung (l/s)**		**n.b.**
el. LF (µS/cm) (Labor)	n.b.				**Redoxpotenzial (mV)**		**-310.00**
					Temperatur (°C)		**51.4**
pH (Gel.)	**6.93**			6,5 - 9,5	**Sauerstoff (O_2)**	**mg/l**	**0.04**
pH (Labor)	n.b.					**(%)**	**0.9**

Kationen (mg/l)

Ion	Messwert	QZV *	MAP **	IP ***
Calcium (Ca^{2+})	**12.5**			
Magnesium (Mg^{2+})	**2.0**			
Natrium (Na^{+})	**292.2**			200
Kalium (K^{+})	**16.3**			
Strontium (Sr^{2+})	**0.4083**			
Barium (Ba^{2+})	**0.0622**			
Lithium (Li^{+})	**0.2433**			
Rubidium (Rb^{+})	**0.0377**			
Cäsium (Cs^{+})	**0.0017**			
Ammonium (NH_4^{+})	**n.b.**	0.45		0.5
Eisen (Fe^{2+})	**0.013**			0.2
Mangan (Mn^{2+})	**0.0035**			0.05
Σ	**323.7**			

Anionen (mg/l)

Ion	Messwert	QZV *	MAP **	IP ***
Hydrogencarbonat (HCO_3^{-})	**533.04**			
Chlorid (Cl^{-})	**169.8**	180		200
Sulfat (SO_4^{2-})	**4.5**	225		250
Nitrat (NO_3^{-})	**<0,5**	45	50	
Nitrit (NO_2^{-})	**n.b.**	0.09	0.1	
o- Phosphat (o-PO_4^{3-})	**n.b.**	0.3		
Sulfid (S^{2-})	**n.b.**			
Fluorid (F^{-})	**6.01**		1.5	
Σ	**713.3**			

Ges. Ionengehalt	**1037 mg/l**	**Ionenbilanz**	
	27.4 mmol/l	***0.2***	**%**
Dichte	**n.b. g/cm3**		

Spezielle Parameter (mg/l)

Parameter	Messwert	QZV *	MAP **	IP ***
Kupfer (Cu)	**0.0003**	1.8	2	
Zink (Zn)	**0.0070**			
Blei (Pb)	**0.0001**	0.009	0.025	
Cadmium (Cd)	**< 0,0001**	0.0045	0.005	
Aluminium (Al)	**0.0090**			0.2
Arsen (As)	**0.0002**	0.009	0.01	
Antimon (Sb)	**n.b.**		0.005	
Chrom (Cr)	**< 0,0001**	0.045		
Nickel (Ni)	**0.0001**	0.018		
Quecksilber (Hg)	**n.b.**	0.0009	0.001	
Bor (B)	**n.b.**		1	
Uran (U)	**< 0,0001**		0.015	
Thorium (Th)	**n.b.**			
Cobalt (Co)	**< 0,0001**			
Molybdän (Mo)	**< 0,0001**			
Vanadium (V)	**< 0,0001**			
Selen (Se)	**n.b.**		0.01	
Tellur (Te)	**n.b.**			
Niob (Nb)	**n.b.**			
Silicium (Si)	**n.b.**			

Spezielle Parameter (mg/l)

Parameter	Messwert
Lanthan (La)	**n.b.**
Cer (Ce)	**n.b.**
Praseodym (Pr)	**n.b.**
Neodym (Nd)	**n.b.**
Samarium (Sm)	**n.b.**
Europium (Eu)	**n.b.**
Gadolimium (Gd)	**n.b.**
Terbium (Tb)	**n.b.**
Dysprosium (Dy)	**n.b.**
Holmium (Ho)	**n.b.**
Erbium (Er)	**n.b.**
Thulium (Tm)	**n.b.**
Ytterbium (Yb)	**n.b.**
Lutetium (Lu)	**n.b.**
Zinn (Sn)	**n.b.**
Thallium (Tl)	**n.b.**
Silber (Ag)	**n.b.**
Beryllium (Be)	**n.b.**
Bismut (Bi)	**n.b.**
Gallium (Ga)	**n.b.**

n.b. .. nicht bestimmt

* ... Qualitätszielverordnung Chemie Grundwasser QZV Chemie GW (BGBl. II 98/2010)

** ... Mindestanforderungsparameter aus der Trinkwasserverordnung - TWV (BGBl. II 304/2001)

*** ... Indikatorparameter aus der Trinkwasserverordnung - TWV (BGBl. II 304/2001)

Layout: G. Hobiger

Geologische Bundesanstalt
FA Geochemie
Leitung: HR Mag. Dr. Gerhard Hobiger

Berechnungen aus den Analysenwerten

Äquivalentanteile

Kationen				Anionen			
	Messwert				Messwert		
Ion	mg/l	meq/l	eq%	Ion	mg/l	meq/l	eq%
Ca^{2+}	12.50	0.62	4.47	HCO_3^-	533.04	8.74	62.7
Mg^{2+}	1.96	0.16	1.16	Cl^-	169.78	4.79	34.4
Na^+	292.22	12.71	91.06	SO_4^{2-}	4.48	0.09	0.7
K^+	16.28	0.42	2.98	NO_3^-	<0,5	0.00	0.0
Sr^{2+}	0.41	0.01	0.07	NO_2^-	n.b.	n.b.	n.b.
Ba^{2+}	0.062	0.00	0.0	$o\text{-}PO_4^{3-}$	n.b.	n.b.	n.b.
Li^+	0.243	0.04	0.25	S^{2-}	n.b.	n.b.	n.b.
Rb^+	0.038	0.00	0.00	F^-	6.01	0.32	2.3
Cs^+	0.002	0.00	0.00	Σ	713.30	13.9	100.0
NH_4^+	n.b.	n.b.	n.b.				
Fe^{2+}	0.013	0.00	0.0				
Mn^{2+}	0.0035	0.00	0.0				
Σ	323.73	14.0	100.0				

Härten	
Gesamthärte (° dH)	2.2
Carbonathärte(° dH)	2.2
Nichtcarbonathärte (°dH)	0.0
Erdalkalien (mmol/l)	2.8

Berechnung des CO_2	
lg(pCO_2)	-1.04
freies CO_2 (mg/l)	75.31
freies CO_2 (mmol/l)	1.7113

Berechneter Ammoniakgehalt	
NH_3 (mg/l)	n.b.

Ges. Ionengehalt	1037 mg/l	27.4 mmol/l

Ionenbilanz		
Σ Kationen (meq/l)	13.96	*0.2 %*
Σ Anionen (meq/l)	13.93	

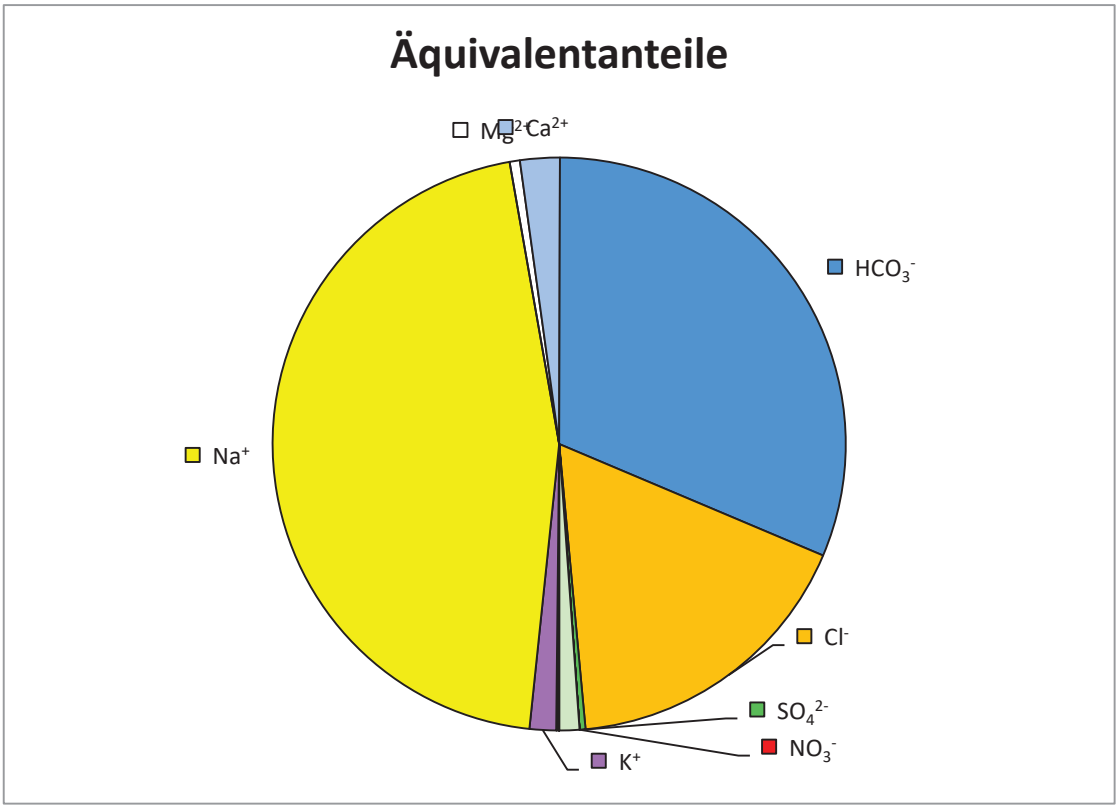

Wasseranalyse

Geologische Bundesanstalt
FA Geochemie
Leitung: HR Mag. Dr. Gerhard Hobiger

Probenahmepunkt:		**32**		
Koordinaten	**M n.b.**	**RW: N48° 10.519'**	**HW: E13° 38.215'**	**GOK (m ü. A.) n.b.**
Bezeichnung:	**32**		**Geochemie-Nr.:**	**GCH-2018-009-003**
Probenahmetiefe:	**n.b.**	**Probenehmer:**	**Pö/Be**	
Probenahmedatum und Uhrzeit:		**25.01.2018 14:30**	**Eingangsdatum:**	**26.01.2018**

Feldparameter

		QZV *	MAP **	IP ***			
el. LF (µS/cm) (Gel.)	**2010**	2250		2500	**Schüttung (l/s)**		**n.b.**
el. LF (µS/cm) (Labor)	n.b.				**Redoxpotenzial (mV)**		**-80.00**
					Temperatur (°C)		**49.2**
pH (Gel.)	**7.72**			6,5 - 9,5	**Sauerstoff (O_2)**	**mg/l**	**2.29**
pH (Labor)	n.b.					**(%)**	**42.8**

Kationen (mg/l)

Ion	Messwert	QZV *	MAP **	IP ***
Calcium (Ca^{2+})	**9.6**			
Magnesium (Mg^{2+})	**1.7**			
Natrium (Na^{+})	**399.6**			200
Kalium (K^{+})	**17.6**			
Strontium (Sr^{2+})	**0.3811**			
Barium (Ba^{2+})	**0.3944**			
Lithium (Li^{+})	**0.2722**			
Rubidium (Rb^{+})	**0.0351**			
Cäsium (Cs^{+})	**0.0024**			
Ammonium (NH_4^{+})	**n.b.**	0.45		0.5
Eisen (Fe^{2+})	**0.039**			0.2
Mangan (Mn^{2+})	**0.0026**			0.05
Σ	**429.7**			

Anionen (mg/l)

Ion	Messwert	QZV *	MAP **	IP ***
Hydrogencarbonat (HCO_3^{-})	**676.06**			
Chlorid (Cl^{-})	**252.2**	180		200
Sulfat (SO_4^{2-})	**43.6**	225		250
Nitrat (NO_3^{-})	**<0,5**	45	50	
Nitrit (NO_2^{-})	**n.b.**	0.09	0.1	
o- Phosphat (o-PO_4^{3-})	**n.b.**	0.3		
Sulfid (S^{2-})	**n.b.**			
Fluorid (F^{-})	**7.24**		1.5	
Σ	**979.0**			

Ges. Ionengehalt	**1409 mg/l**	**Ionenbilanz**
	37.2 mmol/l	***-5.1*** **%**
Dichte	**n.b. g/cm3**	

Spezielle Parameter (mg/l)

Parameter	Messwert	QZV *	MAP **	IP ***
Kupfer (Cu)	**0.0010**	1.8	2	
Zink (Zn)	**0.0049**			
Blei (Pb)	**< 0,0001**	0.009	0.025	
Cadmium (Cd)	**< 0,0001**	0.0045	0.005	
Aluminium (Al)	**0.0130**			0.2
Arsen (As)	**0.0001**	0.009	0.01	
Antimon (Sb)	**n.b.**		0.005	
Chrom (Cr)	**< 0,0001**	0.045		
Nickel (Ni)	**0.0002**	0.018		
Quecksilber (Hg)	**n.b.**	0.0009	0.001	
Bor (B)	**n.b.**		1	
Uran (U)	**< 0,0001**		0.015	
Thorium (Th)	**n.b.**			
Cobalt (Co)	**< 0,0001**			
Molybdän (Mo)	**< 0,0001**			
Vanadium (V)	**< 0,0001**			
Selen (Se)	**n.b.**		0.01	
Tellur (Te)	**n.b.**			
Niob (Nb)	**n.b.**			
Silicium (Si)	**n.b.**			

Spezielle Parameter (mg/l)

Parameter	Messwert
Lanthan (La)	**n.b.**
Cer (Ce)	**n.b.**
Praseodym (Pr)	**n.b.**
Neodym (Nd)	**n.b.**
Samarium (Sm)	**n.b.**
Europium (Eu)	**n.b.**
Gadolimium (Gd)	**n.b.**
Terbium (Tb)	**n.b.**
Dysprosium (Dy)	**n.b.**
Holmium (Ho)	**n.b.**
Erbium (Er)	**n.b.**
Thulium (Tm)	**n.b.**
Ytterbium (Yb)	**n.b.**
Lutetium (Lu)	**n.b.**
Zinn (Sn)	**n.b.**
Thallium (Tl)	**n.b.**
Silber (Ag)	**n.b.**
Beryllium (Be)	**n.b.**
Bismut (Bi)	**n.b.**
Gallium (Ga)	**n.b.**

n.b. .. nicht bestimmt

* ... Qualitätszielverordnung Chemie Grundwasser QZV Chemie GW (BGBl. II 98/2010)

** ... Mindestanforderungsparameter aus der Trinkwasserverordnung - TWV (BGBl. II 304/2001)

*** ... Indikatorparameter aus der Trinkwasserverordnung - TWV (BGBl. II 304/2001)

Layout: G. Hobiger

Geologische Bundesanstalt
FA Geochemie
Leitung: HR Mag. Dr. Gerhard Hobiger

Berechnungen aus den Analysenwerten

Äquivalentanteile

Kationen

	Messwert		
Ion	mg/l	meq/l	eq%
Ca^{2+}	9.62	0.48	2.59
Mg^{2+}	1.75	0.14	0.78
Na^{+}	399.58	17.38	93.90
K^{+}	17.59	0.45	2.43
Sr^{2+}	0.38	0.01	0.05
Ba^{2+}	0.394	0.01	0.0
Li^{+}	0.272	0.04	0.21
Rb^{+}	0.035	0.00	0.00
Cs^{+}	0.002	0.00	0.00
NH_4^{+}	n.b.	n.b.	n.b.
Fe^{2+}	0.039	0.00	0.0
Mn^{2+}	0.0026	0.00	0.0
Σ	429.66	18.5	100.0

Anionen

	Messwert		
Ion	mg/l	meq/l	eq%
HCO_3^{-}	676.06	11.08	56.9
Cl^{-}	252.17	7.11	36.5
SO_4^{2-}	43.57	0.91	4.7
NO_3^{-}	<0,5	0.00	0.0
NO_2^{-}	n.b.	n.b.	n.b.
$o\text{-}PO_4^{3-}$	n.b.	n.b.	n.b.
S^{2-}	n.b.	n.b.	n.b.
F^{-}	7.24	0.38	2.0
Σ	979.02	19.5	100.0

Härten

Gesamthärte (° dH)	1.7
Carbonathärte(° dH)	1.7
Nichtcarbonathärte (°dH)	0.0
Erdalkalien (mmol/l)	1.7

Berechnung des CO_2

lg(pCO_2)	-1.76
freies CO_2 (mg/l)	15.15
freies CO_2 (mmol/l)	0.3443

Berechneter Ammoniakgehalt

NH_3 (mg/l)	n.b.

Ges. Ionengehalt	1409 mg/l	37.2 mmol/l

Ionenbilanz

Σ Kationen (meq/l)	18.51	*-5.1 %*
Σ Anionen (meq/l)	19.48